Phytoplankton of the Southern Agulhas Large Marine Ecosystem (sACLME)

by

Martinus Jakobus Sonnekus

Submitted in fulfilment of the requirements for the degree of

Doctor of Philosophy

in the Department of Botany, Faculty of Science,

Nelson Mandela University

April 2020

Promoter: Prof. Thomas G. Bornman

Co-promoter: Prof. Eileen E. Campbell

Co-promoter: Dr Derek R. du Preez

Declaration by Candidate

Name: Martinus J. Sonnekus

Student number: 203005902

Qualification: Philosophiae Doctor (Botany)

Title of project: Phytoplankton of the southern Agulhas Large Marine Ecosystem

DECLARATION:

In accordance with Rule G5.6.3, I hereby declare that the above-mentioned thesis is my own work and that it has not previously been submitted for assessment to another University or for another qualification.

Signature: 

Date: 26/02/2020

Declaration - Publications

The following publications/manuscripts form part and/or include research presented in this thesis:

Sonnekus, M.J., Bornman, T.G., Campbell, E.E., 2017. Phytoplankton and nutrient dynamics of six South West Indian Ocean seamounts. Deep Sea Research Part II: Topical Studies in Oceanography 136, 59-72.

Signature: 

Date: 26/02/2020

Abstract

The southern Agulhas Large Marine Ecosystem (sACLME) consists of the greater Agulhas Current system, including the areas influenced by the Agulhas Current, the Agulhas Shelf, Agulhas Bank, Agulhas Retroflection as well as the Agulhas Return Current. Four biogeographical regions were identified within the sACLME and the composition of the phytoplankton communities and the associated physico-chemical variables in each were investigated. Water temperature and nitrate concentration were found to be the main drivers of the sACLME phytoplankton community. A total of 215 phytoplankton taxa were identified that were separated into two groups: the Agulhas Current group and the Southwest Indian Ocean Ridge group. The structure of the phytoplankton community was consistently homogeneous throughout the sACLME. Nutrient concentrations of the water varied, but nitrate was the most abundant source of nitrogen, especially in regions that were subjected to the upwelling of cold nutrient-rich water. The phytoplankton communities were significantly influenced by the availability and stoichiometry of the macronutrients nitrogen; phosphorus and silicon. The low mean N:P ratio of 5.5 is an indication that the waters of the sACLME are generally nitrogen limited, as is typical of oceanic systems. There is a change in phytoplankton cell size and functional groups within in the various water masses that are specific to certain biogeographical regions within the Agulhas Current system. It is clear that frontal systems may form barriers between phytoplankton communities

Keywords: Subsurface Chlorophyll Maximum, Euphotic zone, Southwest Indian Ridge, Agulhas Shelf, Agulhas Bank, Agulhas Retroflection, Agulhas Return Current.

Acknowledgements

First and foremost, I am sincerely thankful to my promoter Prof. Tommy Bornman, for his continuous support and guidance through this project. Thank you, Tommy, for giving me the opportunity to undertake this study, always having an open-door policy and for your willingness and enthusiasm to help with my work. The knowledge and work ethic I gained from you will always be valued. To my two co-promoters; Prof. Eileen Campbell and Dr. Derek du Preez, a note of thanks for giving me the opportunity to undertake this study and your valued inputs. To “tannie” Pat Smailes, your passion and love for phytoplankton, especially diatoms, is just overwhelming. Five minutes with you, and you will want to study phytoplankton! Look at me, I did. I thank you for the hours and hours that I could spend in your company, for your patience, love and wisdom. It is much appreciated, valued and treasured.

To my colleagues at STEM in ACTION, I say thank you all for the continuous encouragement and support: Isabel van Gend, Tarin Roberts, Vee Ntungela, Vicki Guyan, JP Stofberg, Clibert Mukasvanga and Tandi Mjungulu.

The following entities are thanked for funding the project and contributing to the research cruises: The Agulhas and Somali Currents Large Marine Ecosystem (ASCLME) Project and the African Coelacanth Ecosystem Programme (ACEP) of the Department of Science and Technology (DST). Our appreciation also goes to the officers and crew of the R/V *Dr Fridtjof Nansen* (Seamounts cruise), FRS *Algoa* (Agulhas Shelf and Bank cruise) and FRS *Africana* (Agulhas Retroflection cruise). We are also grateful to the Botany Department and Centre for High Resolution Transmission Electron Microscopy of the Nelson Mandela University, and the South African Institute for Aquatic Biodiversity (SAIAB) for the use of their facilities. The National Research Foundation (NRF) is acknowledged for providing South Africa / Poland bilateral collaborative research funding (Grant UID 72338) to visit the Department of Paleoceanography at the University of Szczecin. The assistance provided by Prof Andrzej Witkowski and Dr Przemek Dąbek in the identification of the diatoms is especially appreciated.

Last, but not least, to my parents, sister, brother-in-law, Merika and her family and friends, thank you for the encouragement and support. To Merika, you are my rock. Your support, encouragement and love have kept me through the years and for that I will always be grateful.

I dedicate this thesis to “tannie” Pat;

Your love for diatoms is contagious.

Table of Contents

List of Figures

List of Tables

1 General Introduction

The western Indian Ocean, especially the southwest Indian Ocean, is one of the least explored regions of the world's ocean (Vousden *et al.*, 2008). However, the Agulhas Current has been well documented (Bang, 1970; Pearce and Gründlingh, 1982; Olson and Evans, 1986; Lutjeharms and Van Ballegooyen, 1988; Valentine *et al.*, 1993; Beal and Bryden, 1999; Lutjeharms, 2006; Lutjeharms, 2007; Lutjeharms and Bornman, 2010; Goschen *et al.*, 2015). By contrast; phytoplankton research within the greater Agulhas Current system is limited and, where available, is confined to specific regions of this large marine ecosystem: the Mozambican coast and the source waters of the Agulhas Current (Barlow *et al.*, 2008; Sá *et al.*, 2013), Natal Bight (Lutjeharms *et al.*, 1989b; Lutjeharms *et al.*, 2000b; Barlow *et al.*, 2008), KwaZulu Natal coast (Thorrington-Smith, 1969), Agulhas Bank (Carter *et al.*, 1987; McMurray *et al.*, 1993) and the Agulhas Return Current (ARC) with its associated fronts (Froneman *et al.*, 1999; Read *et al.*, 2000; Froneman *et al.*, 2007). Most of the phytoplankton studies focused on aspects such as pigments, biomass and cell sizes (Froneman *et al.*, 1999; Barlow *et al.*, 2002; Barlow *et al.*, 2008; Barlow *et al.*, 2010). Very few studies (Froneman *et al.*, 1998; Froneman *et al.*, 1999) considered the composition of phytoplankton communities and the associated environmental variables that drive community structure and species distribution.

The Agulhas Current Large Marine Ecosystem (ACLME) is located in the southwest Indian Ocean and includes the continental shelves and coastal waters of eastern South Africa, Mozambique, the island of Madagascar, as well as the archipelagos of the Comoros, the Seychelles, Mauritius and the French overseas department of La Reunion (Heileman *et al.*, 2008). The dominant oceanographic feature within the ACLME is the Agulhas Current (Fig. 1.1), which forms part of the anticyclonic gyre of the South Indian Ocean (Beckley, 1998; Lutjeharms, 2006). Four geographical regions within the southern ACLME (sACLME) are based on the characteristics of the continental shelf and water masses: the Agulhas Shelf, the Agulhas Bank, the Agulhas Retroflection and the ARC (Fig. 1.1). The Agulhas Shelf is characterised by the fast-flowing Agulhas Current and narrow continental shelf and the Natal Bight. The widening of the continental shelf forms the Agulhas Bank on which the Agulhas

Current starts to meander. The Agulhas Retroflection forms towards the southern end of the Agulhas Bank where the Agulhas Current makes a 180° turn and flows eastwards as the ARC along the Subtropical Front (STF). The ARC terminates around 60°E (Lutjeharms and Ansorge, 2001) in the Southwest Indian Ocean Ridge (Pollard and Read, 2017; Read and Pollard, 2017; Sonnekus *et al.*, 2017). It is thought that the Southwest Indian Ocean Ridge directs some of the ARC northwards towards the equator (Lutjeharms and Ansorge, 2001) thereby closing the anticyclonic gyre (Lutjeharms, 2006).

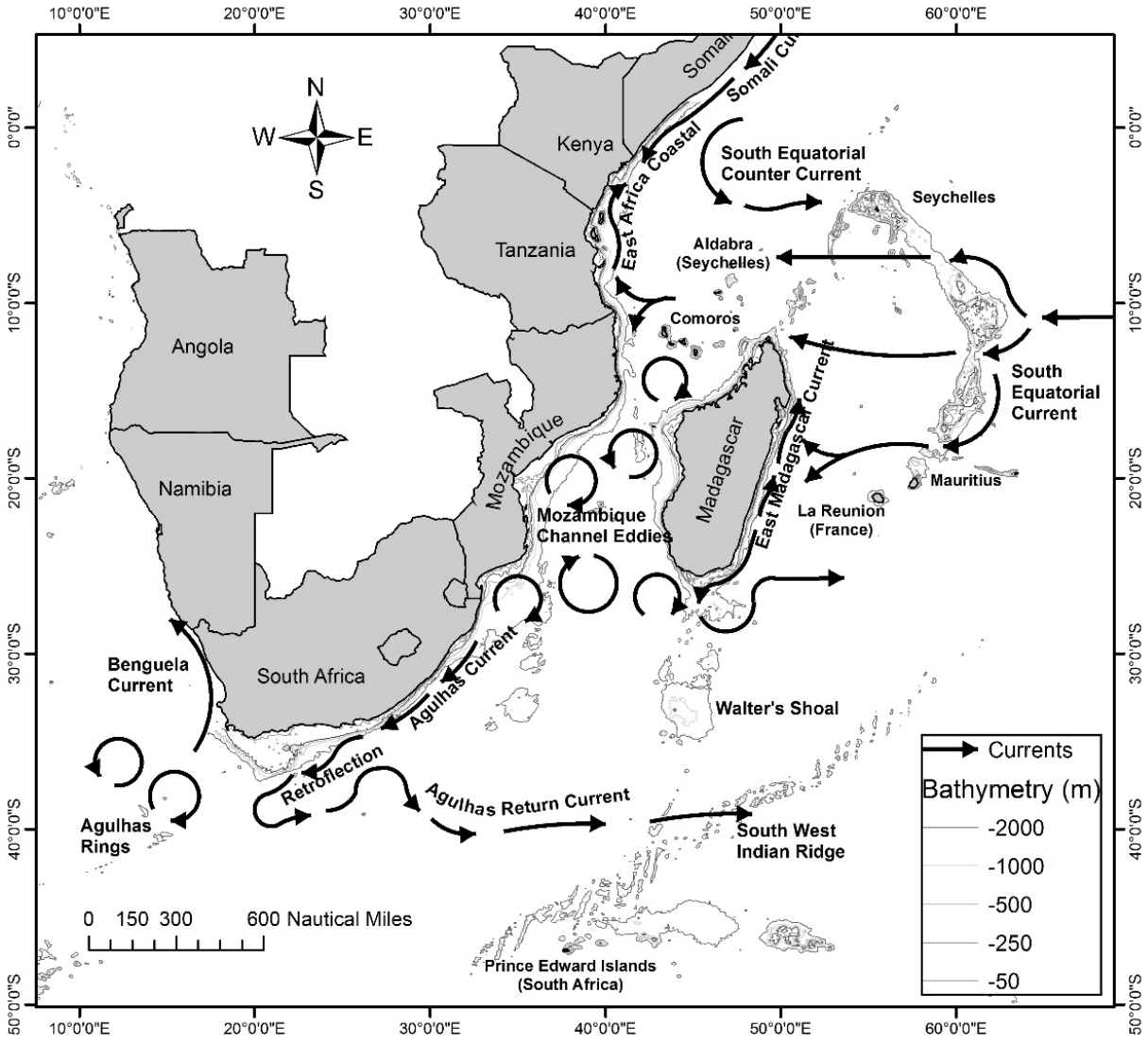

Fig. 1.1 An overview of the oceanography associated with the Agulhas Current Large Marine Ecosystem.

This study investigates the southern section of the ACLME including the ARC at about 39°S (Lutjeharms and Ansorge, 2001; Dencausse *et al.*, 2010), as this forms the southern boundary of the sACLME or the greater Agulhas Current system (Lutjeharms and Ansorge, 2001). The northern section (north of 24°S), including the waters off Mozambique, the island of Madagascar, the Comoros, the Seychelles, Mauritius and the French overseas department of La Reunion of the ACLME were excluded.

The warming of large marine ecosystems (Belkin (2009) through global climate change is expected to lead to a change in phytoplankton communities (Morán *et al.*, 2010) and may, in turn, have a significant influence on primary productivity (Thomas *et al.*, 2012). It is estimated that marine phytoplankton are responsible for ~50% of global primary productivity (Field *et al.*, 1998). Phytoplankton productivity forms the base of large marine ecosystems food webs and determines energy flow to higher trophic levels such as fish, shellfish, seabirds and marine mammals. In marine ecosystems they have important roles in primary production, biogeochemical cycles and regulating the global carbon budgets of the world's oceans (Redfield, 1958; Falkowski *et al.*, 1998; Thomas *et al.*, 2012). Phytoplankton communities are highly dynamic and may vary in time and space (Barlow *et al.*, 2010) as a result of the complex hydrological environment in which they occur. The expected rise in ocean temperature will interrupt the supply of nutrients to surface waters as a direct consequence of increased ocean stratification (Bopp *et al.*, 2005; Doney, 2006; Thomas *et al.*, 2012). Barlow *et al.* (2010) report that the phytoplankton communities on the Agulhas Shelf are highly adaptable to changing environmental conditions and are able to change their physiological mechanisms accordingly. The question is whether they are adaptable to short environmental cycles only or will they be successful over longer time periods? Which species or communities will be the most affected? Deutsch *et al.* (2008) and Thomas *et al.* (2012) postulate that tropical phytoplankton communities may be the most vulnerable to environmental change, estimating that a one-third of all tropical species may be lost if ocean temperature rises. Thomas *et al.* (2012) also predict that tropical communities will shift towards the poles with polar communities remaining range bound. For the ACLME, as a tropical to subtropical large marine ecosystem, ocean warming could have a

profound impact on the phytoplankton communities. Cardinale *et al.* (2012) anticipates that the loss of biodiversity will have a destabilizing effect on ecosystem functions and services - productivity will decrease (diverse communities tend to be more productive) and resource capturing will become less effective.

The initial loss of a few species within a community might not have a large impact on ecosystem functions but increasing losses will scale the impact on ecosystem functions (Cardinale *et al.*, 2011; Cardinale *et al.*, 2012). It is therefore of interest to study what phytoplankton communities occur in the sACLME and which of the environmental drivers influence their productivity and distribution.

The objective of this study was to describe the phytoplankton community structure of the sACLME by characterising species composition and biomass (using chlorophyll *a*) and also to evaluate the community in relation to the physico-chemical conditions. The information obtained from this study contributes to our knowledge of the sACLME, forming a baseline against which future changes can be compared. This will result in a more effective ecosystem-based management plan for the ACLME.

The objective was addressed testing the following hypotheses:

1. The sACLME can be divided into biogeographical regions based on the phytoplankton community with their unique sets of environmental drivers (Chapters 3 – 6).
2. The distribution of phytoplankton changes from a low-biomass, flagellate-dominated community in the oligotrophic subtropical open waters on the northern Shelf to a biomass-rich, diatom-dominated community in the cooler mesotrophic waters of the Agulhas Bank and ARC (Chapter 7).
3. Species richness decreases from the oligotrophic north to the mesotrophic southern region of the sACLME (Chapter 7).
4. The phytoplankton community of the Agulhas Shelf is different to that of the cooler ARC and there is a progressive change along the path of the Agulhas Current.

The thesis is structured to follow the path of the Agulhas Current from its origin, on the South African/Mozambican border, to its termination in the Southern Indian Ocean around 60°E as follows:

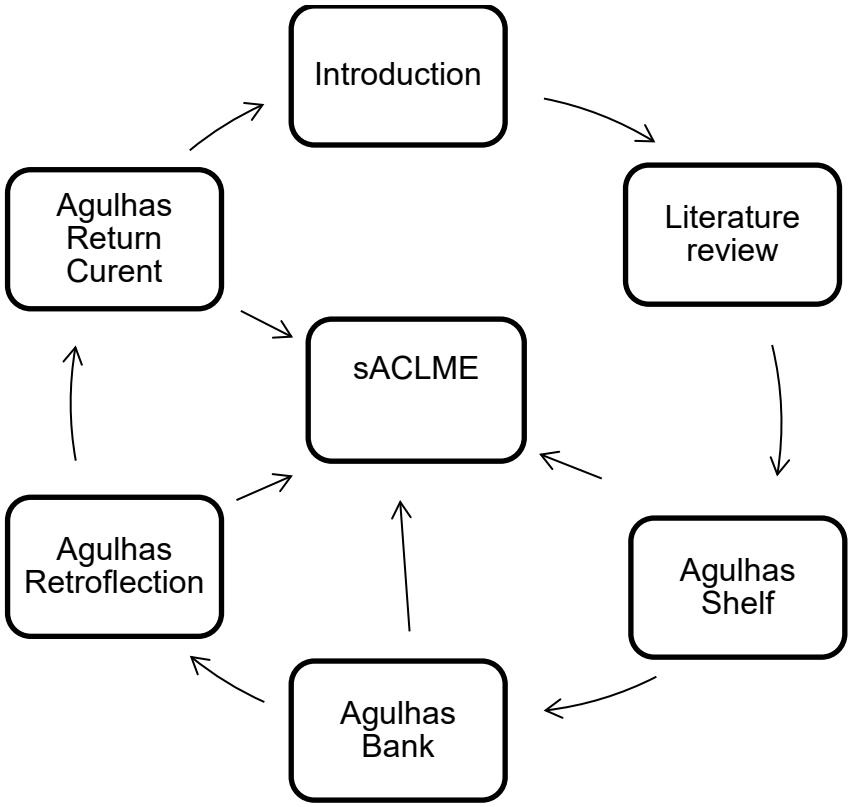

Fig. 1.2 Schematic layout of the thesis.

Definitions used in the thesis

Both the epipelagic and euphotic zone refers to the upper part of the ocean that receives sufficient light for photosynthesis. However, in this thesis the terms refer to slightly different parts of the water column, defined as follows:

Epipelagic – The upper 200 m of the water column that may receive enough sunlight to allow for photosynthesis. Light limitation may occur.

Euphotic – The upper part of the water column located between the surface and the chlorophyll *a* maximum that receives enough sunlight to allow for photosynthesis.

2 Literature Review

2.1 Large Marine Ecosystems

In July 1992 the United Nations Conference on Environment and Development (UNCED) developed declarations on the ocean that recommended the following: "That nations of the globe, 1) prevent, reduce, and control degradation of the marine environment to maintain and improve its life-support and productive capacities; 2) develop and increase the potential of marine living resources to meet human nutritional needs and social, economic, and development goals; and 3) promote the integrated management and sustainable development of coastal areas and the marine environment" (Sherman *et al.*, 1998). The large marine ecosystems concept provides an "ecological framework that may be helpful in achieving the UNCED objectives" (Sherman *et al.*, 1998). Large marine ecosystems are regions extending from the nearshore environment, including estuaries and river basins, to the continental shelf or the seaward edge of the coastal current system (Sherman *et al.*, 1998). These regions are generally in excess of 200 000 km^2 and may encompass the whole or part of the Exclusive Economic Zones (EEZ) of several countries. These regions are characterised by unique ecology, rather than politics or economics (Sherman *et al.*, 1998; Heileman *et al.*, 2008). Growing exploitation of fish and other marine resources, coastal pollution, marine mining, marine gas and oil extraction, loss of habitat as well as other factors place large marine ecosystems under significant pressure (Sherman *et al.*, 1998; Heileman *et al.*, 2008).

The large spatial extent of large marine ecosystems allows for subsystems or domains to occur within them. For example, in the Mediterranean Sea large marine ecosystem, the Adriatic Sea forms a subsystem. Subsystems can be defined within large marine ecosystems based on the characteristics of the continental shelves (Sherman *et al.*, 1998). An example of such classification in the United States of America is the Northeast Continental Shelf large marine ecosystem with its four subsystems: Gulf of Maine, George's Bank, Southern New England and the Mid-Atlantic Bight. To date 64 large marine ecosystems has been identified and accounts for nearly 80% of the global fishing yield and most other marine resources (Heileman

et al., 2008). Southern Africa has two large marine ecosystems, i.e. the ACLME and the Benguela Current LME.

Located in the southwest Indian Ocean, the ACLME encompasses the continental shelves and coastal waters of eastern South Africa, Mozambique, Madagascar, the Comoros, the Seychelles, Mauritius and the French overseas department of La Reunion (Heileman *et al.*, 2008). Climatic conditions for the ACLME range from tropical to cold-temperate. The Agulhas Current, a swift flowing western boundary current, is the dominant oceanographic feature within the ACLME and forms part of the anticyclonic gyre of the South Indian Ocean (Beckley, 1998; Lutjeharms, 2006).

2.2 The Agulhas Current

The Agulhas Current is a western boundary current found along the eastern and southern coast of South Africa (Stramma and Lutjeharms, 1997a; Lutjeharms and Ansorge, 2001). Western boundary currents are generated by wind stress patterns that occur over subtropical basins where they close anti-cyclonic circulation (Lutjeharms, 2006). Western boundary currents have source regions that depend on coastal bathymetry and morphology (Lutjeharms, 2006). The Agulhas Current has its origin from three different sources but is mostly fed by the recirculation of the Southwest Indian Ocean sub-gyre. The southern branch of the East Madagascar Current as well as the Mozambique Channel also contribute to the Agulhas Current (Lutjeharms, 2006). The Agulhas Current is considered to be fully formed near or on the border of South Africa and Mozambique. When fully constituted, it follows the continental shelf closely (Grundlingh, 1983; Lutjeharms, 2006). The continental shelf along the east coast of southern Africa, between Maputo and Port Elizabeth, is very narrow and never exceed 30 km offshore and the 200 m isobath. The uncomplicated and steep nature of the shelf stabilizes the Agulhas Current (de Ruijter *et al.*, 1999) thereby reducing the meandering seen in typical boundary currents such as the Gulf Stream (Lutjeharms, 2006). Between Richards Bay and Durban, the continental shelf widens slightly forming the Natal Bight. The Natal Bight is responsible for the infrequent perturbations of the Agulhas Current referred to as Natal Pulses (Lutjeharms and Roberts, 1988). A Natal Pulse moves downstream, growing rapidly in size so that near Port Elizabeth the current core may be up to 200 km seaward of

its normal position (Lutjeharms, 2006). The Natal Pulse causes a number of disruptions to the flow of the Agulhas Current. These include upstream retroflections (van Aken *et al.*, 2013) near Port Elizabeth and the shedding of Agulhas Rings into the south Atlantic Ocean (Lutjeharms, 2006; Beal, 2009; Goschen *et al.*, 2015).

Near Port Elizabeth the continental shelf widens to form the Agulhas Bank where the Agulhas Current shows a dramatic change in its behaviour; particularly on its landward edge. On the Agulhas Bank, the Current meanders more across its average path (Lutjeharms, 2006). In this region, large shear-edge eddies form (Lutjeharms *et al.*, 1989a) long, warm plumes trail along the Agulhas Current (Schumann and Li van Heerden, 1988). Based on its characteristics, the Agulhas Current can be divided into two sections: the northern Agulhas Current and southern Agulhas Current or Agulhas Bank. The northern Agulhas Current flows along the narrow and steep continental shelf with little variation in trajectory, but increasing in size, strength and speed. The border between the northern and southern Agulhas Currents is Port Elizabeth.

The Agulhas Current continues past the Agulhas Bank into the South Atlantic Ocean. Here it undergoes a dramatic change in direction (Bang, 1970), retroflecting back into the South Indian Ocean as the ARC (Lutjeharms and Van Ballegooyen, 1988). The 400 km^2 area where this dramatic change in direction occurs is known as the Agulhas Retroflection.

2.2.1 Northern Agulhas Current

The northern Agulhas Current consists of the section of current that hugs the steep and narrow continental shelf along the east coast of southern Africa with a consistent current trajectory. The high kinetic energy of the East Madagascar current and Mozambique eddy system follows through into the northern Agulhas Current. This kinetic energy may be as high as 500 cm^2 s^{-2} (Lutjeharms, 2006). The kinetic energy of the mean flow persists throughout the northern section and only begins to subside at the southern Agulhas Current. However, the distribution of high eddy kinetic energy continues into and beyond the southern Agulhas Current (Lutjeharms, 2006; Pollard and Read, 2017). According to Lutjeharms (2006) this is an indication of the

exceptionally high speed and energy of the northern Agulhas Current. There is little variability, even seasonal variability, within the northern Agulhas Current (Pearce, 1977b; Lutjeharms, 2006). The mean (± SD) current speed for the northern Agulhas Current is reported to be 1.5 ± 0.5 m s^{-1} by Pearce and Gründlingh (1982). Duncan and Schladow (1981) refer to observed ships drift data in excess of 2.0 m s^{-1} for the northern Agulhas Current. Current speeds as high as 2.6 m s^{-1} have also been reported (Pearce and Gründlingh, 1982; Lutjeharms, 2006). The path that the current follows is very stable. Grundlingh (1983) found that on average the Current meanders less than 15 km to either side. Beal and Bryden (1999) and Bryden *et al.* (2005) indicate that the current can be found within 30 km from the coast for 80% of the time.

Tropical and subtropical surface waters are routinely found within the surface waters of the Agulhas Current (Pearce, 1977b; Beckley, 1998; Lutjeharms, 2006). Tropical surface water originates near the equator and has salinity less than 35.5 and a surface temperature of 24°C or greater (Lutjeharms and Ansorge, 2001; Lutjeharms, 2006). Subtropical surface waters on the other hand have a source further south - between 28 and 38°S, and have a salinity of 35.5 or more (Lutjeharms and Ansorge, 2001; Lutjeharms, 2006). Both tropical and subtropical water bodies are saturated with dissolved oxygen (Lutjeharms, 2006).

Sea surface temperature for the northern Agulhas Current declines by 2°C from north to south throughout the year (Christensen, 1980b). In the north, average temperatures range between 23°C in July and 28°C in February. In the south, just off Port Elizabeth, temperatures range between 21°C in August and 25°C in January (Christensen, 1980b). Salinity at the sea surface for the northern Agulhas Current are on average 35.5, decreasing to 35.3 further along the shelf (Duncan, 1970).

2.2.2 The Natal Bight

The Natal Bight is 50 km wide and 160 km long (Meyer *et al.*, 2002) and is formed where the continental shelf widens between Richards Bay and Durban. This widening of the shelf allows for the formation of a small but persistent upwelling cell near Cape St Lucia (Lutjeharms *et al.*, 1989b; Lutjeharms, 2006). The general

circulation over the Natal Bight, in contrast to other eddies in the northern Agulhas Current, is cyclonic (Lutjeharms, 2006). At the southern end of the Natal Bight, a small lee eddy is often observed just off Durban (Lutjeharms, 2006). The Natal Bight plays an important role in the formation of Natal Pulses which have important impacts on the general circulation downstream (Goschen and Schumann, 1990; Jackson *et al.*, 2012; van Aken *et al.*, 2013; Goschen *et al.*, 2015).

2.2.3 Southern Agulhas Current

The strength of the Agulhas Current peaks around Port Elizabeth and this is where the nature of the Agulhas Current changes dramatically. The narrow shelf starts to widen between Port Alfred and Port Elizabeth, forming the Agulhas Bank. Once past Algoa Bay, it starts to follow the edge of the Agulhas Bank and is no longer stabilised by the steep and narrow continental shelf (Lutjeharms, 2006). The result of this destabilising is an increase in downstream meandering. The current also starts to lose some momentum as observations from ship drift recorded lower surface speeds (Duncan and Schladow, 1981).

Christensen (1980b) reported that the sea surface temperature decreases by about 4°C between Algoa Bay and Cape Agulhas. This drop in temperature can be ascribed to greater heat loss between the ocean and the atmosphere (Lutjeharms, 2006). Maximum sea surface temperature recorded in late summer for the southern Agulhas Current ranged from 23°C, in the southwest, to 26°C near Port Elizabeth in the northeast. In late winter these decrease to 17 and 21°C respectively (Christensen, 1980b). Surface water warmer than 16°C are indicative of Tropical Indian Surface Water whereas, water temperature between 6 and 14°C is South Indian Central Water. The cooler inshore waters found along the coast and upwelling zones are normally South Indian Central Water (Goschen *et al.*, 2015).

2.2.4 The Agulhas Bank

The Agulhas Bank is a triangular-shaped widening of the continental shelf (Hutchings, 1994; Lutjeharms *et al.*, 1996) that extends about 300 km offshore and covers an area of 80 000 km^2 (Lutjeharms *et al.*, 1996). The Agulhas Bank falls within South Africa's Exclusive Economic Zone and is a productive region and a

major nursery and spawning ground for commercial important species such as kingklip (*Genypterus capensis*), Cape anchovy (*Engraulis capensis*), sardine (*Sardinops sagax*), sole (*Austroglossus pectoralis*), squid (*Loligo reynaudii*), hake (*Merluccius capensis*), and yellowtail (*Seriola lalandi*) (Hutchings, 1994; Roberts, 2005; Roberts and van den Berg, 2005; Krug *et al.*, 2014). The Bank is relatively shallow, dropping steeply from the coast to 50 m and then gradually deepening to 200 m. The continental shelf break occurs near the 200 m isobath after which the sea bed drops away to a depth of 1 000 m. The Agulhas Bank is flanked on the eastern side by the Agulhas Current and in the west it is influenced at times by the cold Benguela Current (Chapman and Largier, 1989; Largier *et al.*, 1992).

The Agulhas Bank can be divided into three areas, the eastern, central and western Bank (Lutjeharms, 2006; Jackson *et al.*, 2012). Jackson *et al.* (2012) used the shallow inner bank along the 21°E meridian as the “boundary” between the eastern and western banks. The long and wide eastern Bank is dominated by the warm oligotrophic Agulhas Current (Hutchings, 1994) whereas the western Bank is influenced by the cold nutrient-rich waters of the Benguela Current (Lutjeharms *et al.*, 1996; Lutjeharms, 2006). The bank is also the meeting area for two oceans: the south Indian Ocean and south Atlantic Ocean. Southwest Indian Ocean water has been found on the eastern Agulhas Bank (Swart and Largier, 1987), suggesting that the water is advected onto the Bank. This hydrology, as well as the circulation of the Agulhas Bank, is influenced by the Agulhas Current via a range of processes such as variations in the Current strength, the intrusion of the Agulhas Current via upwelling onto the bank (Lutjeharms *et al.*, 2000a), meanders, filaments and water plumes (Lutjeharms *et al.*, 1989a; Lutjeharms *et al.*, 2003), Natal Pulses (Casal *et al.*, 2009; Goschen *et al.*, 2015) and southerly winds (Goschen and Schumann, 1990). Warm surface water from the Agulhas Current is advected onto the western bank via the eastern bank and cold, central Atlantic water is upwelled from the Benguela Current onto the western bank (Chapman and Largier, 1989; Largier, 1990). Schumann (1999) considered the 10 to 15 km wide coastal region as a separate oceanographic region to that of the eastern, western and central regions (Lutjeharms, 2006) due to the fact that it tends to be dominated by wind driven coastal-upwelling (Schumann *et al.*, 1982; Largier, 1990) and eastward flowing

(alongshore) currents (Roberts and van den Berg, 2005; Roberts, 2010). Another oceanographic area of interest is the cold ridge located offshore between Plettenberg Bay and Mossel Bay. This is a semi-permanent oceanographic feature characterised by the upward doming of the thermocline (Roberts and van den Berg, 2005).

A strong seasonal surface signal in chlorophyll *a* were observed for the Agulhas Bank; peaking around February through to April (Mitchell-Innes *et al.*, 1999; Demarcq *et al.*, 2003). The coastal areas between Port Elizabeth and Cape Agulhas are the most productive (Shannon *et al.*, 1984; Demarcq *et al.*, 2003; Jackson *et al.*, 2012). Shannon *et al.* (1984) and Probyn *et al.* (1995) found that during late summer a subsurface chlorophyll maximum (SCM) formed on the central bank when nitrate became limiting in the upper photic zone. Carter *et al.* (1987) found that that the SCM (at 20 to 55 m depth) was light-limited. On the eastern Agulhas Bank, chlorophyll *a* concentrations were the highest between Port Alfred and Algoa Bay (Barlow *et al.*, 2010). This can be ascribed to the Port Alfred upwelling cell (Lutjeharms *et al.*, 2000a). For the rest of the eastern Agulhas Bank the presence of cold, nutrient-rich water in the region of the cold ridge (Roberts, 2005) can explain the high primary productivity found on the Agulhas Bank.

2.2.5 Natal Pulses

The Natal Pulse originates at the Natal Bight and 4 to 6 of these develop each year (Bryden *et al.*, 2005; Lutjeharms, 2006; Krug *et al.*, 2014). They move south at a rate of 10 and 20 km d^{-1} (van der Vaart and de Ruijter, 2001; Lutjeharms, 2006). Natal Pulses are important drivers in localised upwelling (Bryden *et al.*, 2005) in coastal and shelf regions. Two other important features associated with Natal Pulses are early retroflections (van Aken *et al.*, 2013) and the shedding of Agulhas Rings (van Leeuwen *et al.*, 2000). The Agulhas Rings cause ocean interchange between the Indian and Atlantic Ocean by leaking warm salty water into the Atlantic (Rouault and Penven, 2011).

During a Natal Pulse, the Agulhas Current flows around an inshore cold core cyclonic eddy (Lutjeharms *et al.*, 1989b; Lutjeharms *et al.*, 2003; Goschen *et al.*,

2015). The eddy is trapped between the coast and the inshore edge of the Agulhas Current and is characterised by the upward doming of the isotherms. It is associated with upwelling of cold, nutrient-rich South Indian Central Water (Goschen *et al.*, 2015) along the coast and onto the continental shelf (Lutjeharms and Roberts, 1988; Lutjeharms *et al.*, 1989b; Lutjeharms *et al.*, 2003; Goschen *et al.*, 2015). Goschen *et al.* (2015) showed that upwelling events within Algoa Bay and the shelf as a result of a Natal Pulse can last between one and three weeks and that the cold water can remain around for up to six weeks. Chapman and Largier (1989) suggested that upwelled water within the core of the Natal Pulses could be advected onto the Agulhas Bank. This has subsequently been confirmed by Krug *et al.* (2014).

2.2.6 The Agulhas Retroflection

The southern termination of the Agulhas Current is unique for western boundary systems in that the current direction is more or less reversed. This area is known as the Agulhas Retroflection and is one of the more important oceanic regions of comparable size (Valentine *et al.*, 1993). The area in which the Agulhas Current is turned around is about 400 km in diameter (Lutjeharms, 2006). Measurements and satellite imagery indicated that the retroflection region is dynamic and unstable (Lutjeharms, 1981; Lutjeharms and Van Ballegooyen, 1988; Lutjeharms, 2006). The termination of the Agulhas current is also unique in the sense that it is the only western boundary system that lies on the boundary of two sub-tropical gyres (Lutjeharms, 2006). The close proximity of the two gyres creates unusual conditions for inter-ocean exchanges of water-masses, energy and biota (Lutjeharms, 2006). These have a major impact on global oceanic circulation and biogeography. The nature of the Agulhas Current termination allows for the retention of warm tropical and subtropical surface water in the region for a longer period (Lutjeharms, 2006). This is uncharacteristic of western boundary systems and may have an impact on local and global climates.

The Retroflection plays a key role in the circulation of the Atlantic and Indian Ocean thermocline via water exchange (Gordon, 1985; Lutjeharms and Van Ballegooyen, 1988) that occurs via the shedding of Agulhas Rings (Olson and Evans, 1986;

Lutjeharms and Gordon, 1987). For a more in-depth discussion on the formation and the importance of the Agulhas rings refer to Lutjeharms (2006) and Beal (2009).

Surface water of the Agulhas retroflection has a temperature of between 16°C and 26°C and a salinity exceeding 35.5 (Valentine *et al.*, 1993). The water originates from the tropical zone (Tropical Thermocline Water) of the Indian Ocean. Due to excessive evaporation that occurs in the subtropical zone, the surface water becomes more dense and saline, and sinks to form a subsurface salinity maximum (Gordon *et al.*, 1987; Valentine *et al.*, 1993; Lutjeharms, 2006). This water is known as Subtropical Surface Water and is transported into the Agulhas Retroflection via the Agulhas Current. Below these layers both Atlantic and Indian Central Water is found (Valentine *et al.*, 1993; Lutjeharms, 2006). Central water and other water masses that are of importance to the Retroflection generally occur at depths deeper than the epipelagic and are not discussed here. Further information may be found in Valentine *et al.* (1993).

Nutrient concentrations in the Retroflection are inversely related to temperature (Chapman *et al.*, 1987; Lutjeharms, 2006). The lowest levels of nitrate and phosphate are found on the outer edges of the Retroflection and increases in concentration were found near the Subtropical Convergence (Chapman *et al.*, 1987; Lutjeharms, 2006). Due to inshore upwelling (Eagle and Orren, 1985a), higher concentrations of nutrients are found on the outer edge of the Agulhas Bank (Chapman *et al.*, 1987; Lutjeharms, 2006). Silicon concentrations in the Retroflection are low and patchy with the exception being the waters of the outer edge of the Agulhas Bank (Chapman *et al.*, 1987).

2.2.7 The Agulhas Return Current

Past the Agulhas Retroflection, the Agulhas water flows eastward as the ARC and forms the southern arm of the South Indian anti-cyclonic gyre. Over its length, the Agulhas Current undergoes changes but at the end the ARC still carries remnants of the Agulhas Current waters. Changes are mostly related to loss of heat to the cooler atmosphere and some loss of volume flux via the shedding of Agulhas Rings into the South Atlantic (Lutjeharms, 2006). The ARC is well mixed compared to Agulhas

Current itself, due to the dynamic and turbulent nature of the Retroflection (Lutjeharms, 2006).

The ARC flows parallel to the Subtropical Convergence (Harris and van Foreest, 1978). The Subtropical Convergence is an important oceanographic feature exhibiting a large temperature gradient (Lutjeharms and Ansorge, 2001) and as a result forms a characteristic and unique biological habitat (Lutjeharms, 2006). The trajectory of the ARC is variable and has not been determined with any degree of certainty (Lutjeharms and Ansorge, 2001). The flow is generally zonal (Lutjeharms and Ansorge, 2001) with extensive meridional excursions that may be linked to the bottom topography (Darbyshire, 1972; Lutjeharms and van Ballegooyen, 1984). The ARC extends as far east as 72° (Park *et al.*, 1991; Park *et al.*, 1993; Belkin and Gordon, 1996) and from there it is known as the South Indian Ocean Current (Lutjeharms and Ansorge, 2001). Pollard and Read (2017) showed that the ARC water flow continues unreduced as far as 50°E and that only east of that significant leakage occurs into the Southwest Indian Ocean subtropical gyre. A notable change in the composition of the water column between the Agulhas Retroflection and the ARC is the absence of Tropical Surface Water in the ARC (Lutjeharms and Ansorge, 2001).

2.2.8 Subtropical Convergence Zone

Belkin *et al.* (2009) defined an oceanic front as a “narrow zone of enhanced horizontal gradients of water properties (temperature, salinity, nutrients, etc.) that separates broader areas of different water masses or different vertical structure (stratification).” Fronts play an import role in marine biogeographical regions (Longhurst, 2007; Belkin *et al.*, 2009). The subtropical convergence zone is the transition zone between the Indian Ocean and the Southern Ocean and consists of the Agulhas Return Current, the Subtropical Front (STF) and the Subantarctic Front (SAF). It is a region of complex biogeochemistry, phytoplankton distribution and productivity associated with the transition between subtropical and subantarctic domains (Bathmann *et al.*, 2000; Read *et al.*, 2000). For an in-depth review on the Southern Ocean Fronts between the Greenwich meridian and Tasmania, please see Belkin and Gordon (1996) and references within. The subtropical front is located at a

mean latitude of 41° 40'S (Lutjeharms and Valentine, 1984) and forms a poleward boundary between the warm, salty waters (Read *et al.*, 2000) of the Indian Ocean and the cooler waters of the Southern Ocean. Located adjacent to the Agulhas Return Current is the Agulhas Front, with steep density gradients, temperatures of 15.7°C to 21°C (Lutjeharms and Valentine, 1984), optically clear with low nutrients (Read *et al.*, 2000) and an observed southern limit of 40°S (Lutjeharms and Valentine, 1984). The location of the Agulhas Front close to the STF makes it at times difficult to distinguish the two fronts from one another (Read and Pollard, 1993; Read *et al.*, 2000). The STF is characterised by a mean temperature range of 10.6°C to 17.9°C and a salinity of 34.3 to 35.6 (Lutjeharms, 1985; Lutjeharms *et al.*, 1993). Read *et al.* (2000) showed that nitrate, silicate and chlorophyll *a* was strongly correlated and linked to the front and water mass structure. Chlorophyll *a* concentrations peaked between the STF and SAF with the north and south being low due to nitrate limitation (Read *et al.*, 2000). The proximity of the two fonts to each other determines how intense the upwelling of nutrients will be and the closer the two fronts are to each other the more intense the upwelling and vice versa (Read *et al.*, 2000).

2.3 Seamounts

Seamounts can be characterised by their origin, i.e. volcanic, serpentine mud (Fryer, 1992) or tectonic upliftment (Schidt and Schminke, 2000). Of the three, volcanic seamounts are the most numerous and as a result of their volcanic origin are often clustered in groups (Wessel, 2007; Wessel *et al.*, 2010). Since most seamounts are generated near mid-ocean spreading ridges; plumes or hotspots, and in island arc convergent settings, they are generally located on the oceanic crust, with a limited number located on the continental shelf. Seamounts are generally defined as an independent feature with an elevation above the seabed of 1 000 m or more (Menard, 1964). However, there is no geological reason to exclude smaller features (Wessel, 2007).

Seamounts can further be grouped based on their tectonic origin, i.e. Intraplate seamounts, Mid-ocean ridge seamounts and Island-arc seamounts. It seems that the majority of large seamounts were formed in an intraplate setting (Wessel, 2007). A

distinctive feature of intraplate seamounts is their alignment in linear, sub-parallel chains that correspond to present and past plate motions. The “hotspot hypothesis’, first proposed by Wilson (1963) and elaborated by Morgan (1971) forms the basis of our understanding of how linear-chain forming seamounts develop. The hotspot hypothesis states that seamounts, while remaining more or less stationary above mantle plumes, will increase in height. When the tectonic plate moves, the newly formed seamount is carried away and ceases to be active. The net result is a line of extinct volcanoes. In general, intraplate seamounts tend to have an elevation greater than 1 000 m (Wessel, 2007).

The majority of seamounts are mid-ocean ridge seamounts. They are smaller in size and are believed to be formed near a divergent plate boundary (Batiza, 1982; Lonsdale, 1983; Fornari *et al.*, 1988; Jaroslow *et al.*, 2000; Wessel, 2007). The oceanic crust at divergent plate boundaries tends to be thin and fractured, allowing excess amounts of magma to push through, to form small (< 1000 m in elevation), sub-circular seamounts (Smith and Cann, 1990). Jaroslow *et al.* (2000) showed that most of these new seamounts will be reduced in height when they undergo tectonic deformation by normal faulting.

Island arc seamounts are formed at subduction zones where one oceanic plate is forced underneath the other (Wessel, 2007). As the old seafloor with previous seamounts and a blanket of wet sediments, is forced down into the mantle; pressure and temperature increases, resulting in the formation of an ascending basaltic melt. This magma is more volatile and of a different composition than that found at spreading centres (Wessel, 2007). Island arc seamounts are limited to a narrow strip around subduction zones of oceanic plates. As with hotspot produced seamounts, island arc seamounts tend to be large and can reach the ocean surface to form an island, hence the term island arc seamount.

2.3.1 Seamount impact

Seamounts are important in several disciplines, including biology, ecology, geology, and oceanography. For a detailed survey of the Southwest Indian Ocean Seamounts see Pollard and Read (2017), and Read and Pollard (2017). Ocean circulation can

be influenced by ocean floor bathymetry in several ways. Firstly, large scale features such as ridges and plateaus directly impede ocean flow and can form a barrier that prevents deep water mixing. Small scale features such as seamounts play an important role in the turbulent mixing of the oceans (Kunze and Llewellyn Smith, 2004; Pollard and Read, 2017). Lueck and Mudge (1997) reported that mixing around a shallow seamount may be several orders of magnitude more vigorous than in areas far from seamounts. Seamounts act as an obstacle to oceanic flow that can induce local currents, which in turn can enhance upwelling around the seamount (Wessel, 2007). The nutrient enrichment of the euphotic zone will enhance primary production, supporting a wide variety of life (Rogers *et al.*, 1994).

2.3.2 Seamount Dynamics

2.3.2.1 Steady impinging flows

The interactions between seamounts and ocean currents provides for development of unique habitats (Genin and Boehlert, 1985). Several seamounts were found to deflect local isotherms upwards – a phenomenon that may occur at different locations and depths (Meincke, 1971; Vastano and Warren, 1976; Owens and Hogg, 1980; Gould *et al.*, 1981; Genin and Boehlert, 1985). These deflections are explained by the Taylor column theory (Hogg, 1973; Huppert, 1975; Huppert and Bryan, 1976): Under certain conditions a Taylor column, consisting of deep nutrient-rich water, may remain trapped above the seamount (Hogg, 1973; Huppert, 1975) for a number of days (Boehlert and Genin, 1987). Conditions conducive to this formation include variations in current speed and direction, local density stratification and seamount topography (Genin and Boehlert, 1985; Lavelle and Mohn, 2010).

Seamount-induced upwelling can enhance local biological productivity (Genin and Boehlert, 1985; Dower *et al.*, 1992; Rogers *et al.*, 1994; Comeau *et al.*, 1995; Lavelle and Mohn, 2010). The degree of enhanced productivity is dependent on the residence time of the upwelled waters and how much of it penetrates the euphotic zone (Genin and Boehlert, 1985). Patches of high chlorophyll concentrations develop after a short residence time of upwelled waters, as only the primary producers are influenced. The longer the residence time of the upwelled water, (which can be from

several weeks as reported by Cheney *at al*. (1980) and Richardson (1980) to several months as found by Owens and Hogg (1980)), the greater the influence will be on higher trophic levels. Seamounts can serve as biological hotspots for marine organisms (Lavelle and Mohn, 2010).

2.3.2.2 Oscillatory impinging flows

Tidal, inertial and other oscillatory waves influence seamount circulation. The *inertial frequency* or *f*, is defined as the frequency of "an impulsively displaced particle to return to its initial position on a frictionless plane" (Lavelle and Mohn, 2010). Oscillations travelling towards a seamount can be influenced in two ways. The first is the inertial period, T_f (= 2π/*f*) where *f* = 12 hr/sin(latitude), and the second is the buoyancy period T_N (= 2π/*N*), where *N*, the buoyancy frequency, varies with local ocean stratification (Lavelle and Mohn, 2010). Subinertial oscillations, impinging oscillations with frequencies less than *f*, will be amplified near the seamount (Lavelle and Mohn, 2010). Brink (1995) reported that diurnal tidal currents over Fieberling Guyot seamount were greatly amplified. These amplified oscillations decreased in magnitude away from the seamount and it is said that the oscillations are trapped to the seamount (Lavelle and Mohn, 2010). Seamount morphology will determine the amount of amplification that occurs. Beckmann (1995) showed that rough, broad and steep seamounts have a limited ability to amplify trapped waves. Incident-wave frequencies that are greater than the latitude-dependant frequency but smaller than the buoyancy frequency, are generated and propagated horizontally and vertically away from the seamount (Baines, 2007; Lavelle and Mohn, 2010). These are also known as internal waves. Other currents that can be generated by impinging oscillatory flow are a steady residual current, or rectified current, that is toroidal (see Lavelle and Mohn, 2010 and references within).

2.3.2.3 Vertical circulation and the cold dome

Vertical circulation is driven by the various horizontal currents described previously. The use of long-term current meters on the Fieberling Guyot seamount enabled Brink (1995) to observe a downward circulation of water that spread radially outwards. The extent of such vertical movements is no more than a few hundred

meters (Lavelle and Mohn, 2010). A hydrographic feature linked to seamounts is the presence of a cold dome (Owens and Hogg, 1980; Comeau *et al.*, 1995) and is believed to be connected to the vertical circulation above the seamount (Lavelle, 2006; Lavelle and Mohn, 2010). Owens and Hogg (1980) reported that the extent of the cold water dome is dependent on *f*, the stratification, as well as the size of the seamount.

2.3.2.4 Internal waves and turbulence

Internal waves are generated when a parcel of water, with a wave frequency greater than the buoyancy frequency but less than that of the oscillatory currents, interacts with a seamount (Noble and Mullineaux, 1989). The buoyancy period in the open ocean typically range from a few minutes to several hours. Eriksen (1998) and Holloway and Merrifield (1999) reported that internal waves are propagated both vertically and horizontally away from a seamount in patterns that are dependent on seamount topography and the water-column stratification. As the waves travel within the ocean interior they encounter other waves and this wave-wave interaction results in an increase in frequencies and turbulence (Carrett, 2003). Isolated seamounts and islands produce weak turbulence whereas an ocean ridge will produce a stronger global turbulence (Holloway and Merrifield, 1999). Internal waves are the strongest above the seamounts and thus enhanced turbulence occur above the seamount.

2.3.2.5 Seamounts chlorophyll a

Dower *et al.* (1992) reported an upward movement of the SCM near Cobb Seamount from a depth of around 75 to 40 m. A similar pattern has been recorded for other seamounts, e.g. Corner Rise (Longhurst and Harrison, 1989). Chlorophyll *a* concentrations above and around Cobb Seamount ranged from 0.4 to 1.3 μg l^{-1} (Dower *et al.*, 1992).

Comeau *et al.* (1995) reported that surface chlorophyll *a* for Cobb Seamount was relatively uniform, but that primary production was patchy. The variation or patchiness in primary production was linked to the shallow (> 50 m) thermohaline front that flanked this seamount (Comeau *et al.*, 1995). Near the front, surface waters (< 50 m) showed thermal stratification. This physical change in the water

column was associated with the shallowing and intensifying of the SCM, an increase in diatom biovolume, and an increase in the production to biomass ratio (Comeau *et al.*, 1995). The doming of nutrients above the seamount appeared not to enrich surface waters nor enhance production (Comeau *et al.*, 1995). Rather, growth and production was enhanced through increased stability in the upper water column (Perissinotto *et al.*, 1990; Comeau *et al.*, 1995). Perissinotto *et al.* (1990) showed that increased stability can enhance diatom growth under nutrient-sufficient conditions.

2.4 Upwelling

Upwelling is the process of vertical upward transport from depth towards the surface (Schumann *et al.*, 1982) and it is associated with enhanced primary productivity (Lutjeharms and Stockton, 1987).

Wind induced upwelling is a common oceanographic feature of west mid-latitude coastal areas of continents (Brink, 1983; Mcclain *et al.*, 1984; Lentz, 1992; Schumann, 1999; Castelao *et al.*, 2004). Here the primary cause of offshore Ekman transport and the associated upwelling is equatorward winds.

Wind induced upwelling also occurs in other coastal areas and is well documented along the southern coast of South Africa (Schumann *et al.*, 1982; Schumann *et al.*, 1988; Schumann, 1999; Lutjeharms *et al.*, 2000a; Lutjeharms, 2006). During periods of persistent and strong easterly winds upwelling occurs along the coast, especially at prominent headlands (Schumann *et al.*, 1982; Lutjeharms *et al.*, 2000a). Easterly winds lift the cold, nutrient-rich water from the shelf seabed to above the thermocline (Lutjeharms *et al.*, 2000a). Along the southern coast, upwelling due to westerly winds is more common in summer than winter (Swart and Largier, 1987; Schumann and Martin, 1991). Wind induced upwelling occurs when longshore coastal winds move surface water offshore via Ekman transport. The waters move anti-clockwise in the Southern Hemisphere (Schumann, 1999). Surface waters near the coast are replaced with cooler subsurface water as an adjustment drift (Schumann *et al.*, 1982). The two water masses are usually demarcated by a thermocline or upwelling front. The reverse holds true when the wind blows from the opposite direction,

bringing warm surface water back inshore. Collapsing of the fronts can occur rapidly and the ensuing mixing prevents the system from oscillating between the two states (Schumann, 1999). This increases the retention time of phytoplankton within these systems (Schumann, 1999).

Unrelated to local wind is upwelling that occurs where the continental shelf starts to widen (Pearce, 1977a; Lutjeharms *et al.*, 1989b; Lutjeharms *et al.*, 2000a). Upwelling here tends to occur year-round. Cold nutrient-rich waters onto the shelf and have a marked influence on the physical water characteristics (Lutjeharms, 1991; Lutjeharms *et al.*, 2000a). Two major locations where this occurs along the Agulhas Current are the Natal Bight and widening of the continental shelf to form the Agulhas Bank, also known as the Port Alfred upwelling zone. Carter and D'Aubrey (1988) and Carter and Schleyer (1988) found that at the Natal Bight the biota, nutrients and primary production are also influenced by the persistent upwelling cell. Similar observations for the Port Alfred upwelling zone have also been made by Lutjeharms *et al.* (2000a) – in particular a substantial increase in nitrate and silicate concentrations. The mechanism of upwelling due to the widening of the shelf is described in detail by Gill and Schumann (1979). Both Lutjeharms *et al.* (2000b) and Goschen *et al.* (2015) describe the Port Alfred upwelling cell in detail, the former focusing on the interaction of the Agulhas Current and the Shelf and the latter on the influence of a Natal Pulse on upwelling dynamics. Bryden *et al.* (2005) and Krug *et al.* (2014) reported that upwelling on the Agulhas Bank can also occur due to the presence of a Natal Pulse. Both authors give a detailed description of the processes involved.

Upwelling may also occur at eddies. Intense, shear-edge eddies found along the continental shelf, upwell cold, nutrient-rich water in their cores. Chapman and Largier (1989) suggested that the water lifted by the core will eventually move onto the Agulhas Bank, thus enriching it.

Upwelling can also occur between and near oceanic fronts. Read *et al.* (2000) found that the close proximity of the Subtropical, Agulhas Return and Subantarctic Fronts to each other resulted in increased vertical stability and upwelling.

2.5 The subsurface chlorophyll maximum

The SCM is a consistent feature in the biological profile of the world's oceans. Cullen (2015) defined it as the local chlorophyll *a* maximum maintained by ecological processes that operate on a timescale of a day or longer. The SCM is dependent on upwelling processes, euphotic depth, nutrient gradients and the characteristics of the local phytoplankton community (Franks and Walstad, 1997). The vertical scale can be from approximately one meter to tens of meters, whereas, horizontally it can occur on a sub-mesoscale (ca. 2 km), a mesoscale (20 km - 100 km) (Lévy, 2008) or at large oligotrophic biome scale (>1 000 km;) (Karl, 1999). During phytoplankton blooms, the surface waters are depleted of inorganic nitrogen and the water column stratifies. The SCM then develops at depth (Brown *et al.*, 2015). On a vertical scale, the SCM is formed by biological-chemical-physical interactions and is strongly influenced by stratification and shear gradients (Cullen, 2015). The SCM is shallow, whereas the deep chlorophyll maximum (DCM) is located at greater depths. The depth of both the SCM and DCM is dependent on oceanic stability but they are found between the seasonal pycnocline and the permanent halocline (Brown *et al.*, 2015). In stable oceanic conditions the SCM or DCM occurs near the bottom of the euphotic zone (usually associated with the pycnocline and light levels greater than 0.1 but less than 10%) (Longhurst and Harrison, 1989). Yentsch (1965) was the first to describe the SCM as a global feature of the water column. This was subsequently confirmed by various authors (Venrick *et al.*, 1973; Gieskes *et al.*, 1978; Hayward *et al.*, 1983; Cullen, 2015).

Jamart *et al.* (1979) and Cullen (1982), 2015) proposed mechanisms that contribute to the formation and maintenance of the SCM. These include phytoplankton growth rates near the nutricline; photoacclimation of phytoplankton, the differential sinking rate of phytoplankton at different densities; physiological changes in the carbon:chlorophyll *a* ratios, and differential grazing pressures from zooplankton and fish. In physically dynamic and biologically diverse continental shelf areas, no single mechanism can be used to predict the SCM, but rather a combination of different factors operate at different times (Anderson *et al.*, 1969; Jamart *et al.*, 1979; Fasham *et al.*, 1985; Banse, 1987; Vandevelde *et al.*, 1987).

Longhurst and Harrison (1989) distinguished two types of SCMs. The first is a temporary SCM that forms when, in spring, the upper ocean warms, followed by the subsequent mixing with deep water. The second is a more permanent SCM that occurs where significant density stratification is a permanent feature in the water column. The latter varies regionally with depth. Longhurst and Harrison (1989) provide an in-depth discussion on the formation of the temporary and permanent SCMs.

The use of *in vivo* chlorophyll *a* fluorescence as a measurement of chlorophyll *a* concentration that is an approximation at best (Loftus and Seliger (1975) and Longhurst and Harrison (1989) The reason for this is that the fluorescence signal is a varying and non-linear function of chlorophyll *a.* Furthermore, variations in chlorophyll *a*:fluorescence ratios have been observed between prokaryotes and eukaryotes, between different eukaryote taxa under identical conditions, as well as diurnally. As phytoplankton adapt to changing light conditions, relative fluorescence can change by an order of magnitude within a few minutes (Longhurst and Harrison, 1989). Vincent (1979) reported substantial photoinhibition of fluorescence for diatoms. Together these responses may yield a fluorescence maximum that does not accurately represent of chlorophyll *a* or biomass.

2.6 Nutrient Limitation in the Marine Environment

In the marine environment, nitrogen; phosphorus, silicon (only for diatoms and silicoflagellates) and various other macro- and micronutrients are needed to enhance and maintain phytoplankton growth. Only a few of the elements required for growth are likely to be limiting (Hecky and Kilham, 1988). In the marine environment, only N; P, Si, Fe, Zn, Cu, Co and Mn are found in concentrations equal to or less than that required by phytoplankton (Hecky and Kilham, 1988). All other nutrients occur in non-limiting quantities (Hecky and Kilham, 1988). Thus, nutrient limitation can be considered in the form of nitrogen; phosphorus or silicon depletion with the marine environment being generally nitrogen limited (Smith, 1984). The depletion of nutrients in the epipelagic is the natural consequence of phytoplankton growth and will only persist if phytoplankton growth declines (Minas *et al.*, 1986).

In seawater, nitrate (NO_3^-), nitrite (NO_2^-) and ammonium (NH_4^+), are the sources of inorganic nitrogen. Consequently, the relationship between the concentration of these nutrients, especially nitrate and ammonium, and the rate at which they can be utilised is likely to affect the growth rate of marine phytoplankton. Excess nutrients can be ascribed to low irradiance levels in the mixed layer during winter. Cullen (1991) specifies that this may occur when photosynthetic production does not exceed community respiration. Factors such as light limitation, temperature and the trophic composition of the plankton play an important role in this dynamic (Cullen, 1991).

The growth of marine phytoplankton is often limited by the availability of nitrogen (Ryther and Dunstan, 1971, Lapointe *et al.,* 1992; Pedersen and Borum, 1996, Downing *et al.,* 1999). The concentrations of nitrate relative to phosphate (sumarised as a N to P ratio) increases from near the ocean surface to the ocean depths (Redfield, 1958). This stoichiometric increase is due to the equal rate of release of N and P, but also due to the sinking of decomposing organic matter (Redfield, 1958). Redfield (1958) showed that phytoplankton take up nutrients from the water in a fixed ratio of C:N:P:Si of 106:16:1:15. Jennings *et al.* (1984) proposed ratios of 62:11:1:24 for C:N:P:Si for the Southern Ocean. Redfield (1958) observed that no excessive concentrations of N or P remain when the supply of either N or P is depleted. When nitrate is limiting, nitrogen-fixers become more abundant as they can utilise atmospheric nitrogen. Only when these organisms die and decompose is nitrogen returned as dissolved inorganic ammonium and nitrate to the marine environment, thus increasing nitrogen levels. There is no atmospheric supply of phosphorus and geochemists argue that it is phosphate that governs primary productivity and ocean fertility (Tyrrell, 1999). Redfield (1958) also suggested that it is the availability of phosphorus rather than nitrogen that limits phytoplankton growth.

Tyrrell (1999) reported that large data sets such as GEOSECS and World Ocean Atlas showed that nitrate is usually depleted from oceanic waters before phosphate (N:P < 16:1 (Tyrrell, 1999)). Nutrient depleted or oligotrophic waters usually have trace amounts of phosphate whereas nitrate is generally undetectable. Ryther and Dunstan (1971) showed that the addition of nitrate to oligotrophic waters stimulates phytoplankton production whereas the addition of phosphate does not. It appears

that nitrate is usually the most limiting nutrient in oceanic waters rather than phosphate and, as a result, nitrate concentrations can be considered to regulate and control phytoplankton productivity (Codispoti, 1995).

Lewin (1962) reported that diatoms have an absolute requirement for silicon. The silicon is metabolised to form their frustules. Brzezinski *et al.* (1990) and Brzezinski (1992) reported that when diatoms were deprived of silicon, the progression of cells through the cell cycle ceases. This relationship between silicon and diatoms may control phytoplankton processes in areas where coastal upwelling occurs (Dugdale, 1985) as well as the seas surrounding Antarctica (Sakshaug *et al.*, 1991). In these and other marine regions, soluble reactive dissolved silicon plays an important role in bloom development and its subsequent collapse as well as changes in the floristic composition of the bloom (Conley and Malone, 1992).

Silicon is generally recycled at greater depths than typically found for nitrogen or phosphorus (Dugdale *et al.*, 1995). Living diatom cells are protected against dissolution of the silicon in their frustules by an organic membrane (Lewin, 1962), High dissolution rates of frustules are typically found where the cells are dead (Nelson *et al.*, 1991). It follows that low rates of dissolution will occur in areas of high productivity. The Gulf Stream (Brzezinski and Nelson, 1989) and the surface waters of the Peru Upwelling zone (Dugdale *et al.*, 1995) are examples of regions of high and low dissolution rates, respectively.

In view of Liebig's Law of the minimum (de Baar, 1994), there are two ways to consider nutrient limitation: the stoichiometric approach and the rate-limiting approach. The stoichiometric approach compares environmental nutrient ratios with the composition ratio of the biomass to determine which nutrient will first be depleted. The ratio of Si:N:P in marine water is approximately 16:16:1 (Brzezinski, 1985). If the Si:N ratio is less than one, Si maybe the limiting nutrient (Conley and Malone, 1992). Various authors (Howarth, 1988; Conley and Malone, 1992) used ambient Si:N ratios to determine whether Si or N is limiting. However, different species of diatoms fix Si and N in different ratios (Brzezinski, 1985), giving a considerable variation of cellular Si:N ratios. The stoichiometric approach therefore identifies the nutrient most limiting to the system productivity (Dugdale, 1985). An

alternative to the stoichiometric approach is the rate-limiting (Monod) method. The rate-limiting method clearly indicates which nutrient is limiting for algal growth. This method uses a mathematical model to represent various factors that may limit algal growth by assuming a single controlling nutrient (Dugdale, 1985). To determine which nutrient is limiting, the hyperbolic equation of Monod for nutrient-limited growth of micro-organisms (Button, 1985) is used. The details of this equation and method is beyond the scope of this literature review as it is more commonly used in experiments designed specifically for determining nutrient limitation.

Iron plays an import role in growth of oceanic phytoplankton and iron is often limiting in various marine environments e.g. Southern Ocean (Martin *et al.*, 1990) and northeast Pacific (Martin and Fitzwater, 1988). Large-scale iron fertilisation experiments within the Southern Ocean and other regions showed that phytoplankton biomass and their associated effect on carbon sequestration is enhanced and is known as the 'iron hypothesis' see Blain *et al.* (2007) and references therein.

2.7 Phytoplankton production in the greater Agulhas System

Due to coastal upwelling, high-nutrient, low-chlorophyll water occurs nearshore while offshore waters are generally high-chlorophyll, low-nutrient (Minas *et al.*, 1986). Upwelling is the primary cause of ingress of nutrients in the epipelagic, but the complex interaction of grazing, growth; physiological adaptation as well as horizontal and vertical advection can determine the spatial patterns of nutrients; phytoplankton biomass and ecosystem primary productivity (Jones *et al.*, 1988; Dugdale and Wilkerson, 1989; Cullen, 1991).

The surface waters of the central region of the subtropical Indian Ocean gyre is nutrient poor and have low levels of productivity. Ocean modelling and remote sensing showed that there is a seasonal variation in productivity with a slightly higher productivity in autumn and winter (Lutjeharms, 2006; Barlow *et al.*, 2010). Ryther *et al.* (1966) conducted a series of primary productivity studies within the Indian Ocean and reported a production rate of less than 1.0 g C m^{-2} d^{-1} between 25°N and 40°S. Along the east coast of Southern Africa; productivity values ranged from 0.1 to 3.1 g

C m^{-2} d^{-1}, with the maximum found at the Natal Bight. Further north, at the Delagoa Bight, rates of 0.6 g C m^{-2} d^{-1} were reported by Mitchell-Innes (1967). Published productivity values for the Agulhas Current range from 0.2 to 5.3 g C m^{-2} d^{-1} (Table 2.1).

Carter *et al.* (1987) showed that the eastern and central Agulhas Bank is characterised by a well-developed, SCM that coincides with strong but shallow thermoclines. According to Carter *et al.* (1987) these thermoclines are actively maintained and thus dynamically very stable. However, short term variations do occur with the SCM responding to these fluctuations. The western Agulhas Bank is characterised by deeper thermoclines and a less intense SCM (Carter *et al.*, 1987). Self-shading and the fact that the thermocline is situated below the 1% of surface irradiance level are reasons given by Carter *et al.* (1987) for limited phytoplankton production.

Table 2.1 Primary productivity rates of Agulhas Current waters.

Region	Productivity	
Delagoa Bight	0.6 g C m^{-2} d^{-1}	(Mitchell-Innes, 1967)
	0.2 to 2.2 g C m^{-2} d^{-1}	(Burchall, 1968b, a)
Natal Coast	0.03 to 3.9 µg l^{-1}	(Carter and Schleyer, 1988)
eastern Agulhas Bank	1.2 – 2.8 g C m^{-2} d^{-1}	(Probyn *et al.*, 1994)
Agulhas Bank (coast & mid shelf in summer)	5.3 g C m^{-2} d^{-1}	(Probyn *et al.*, 1994)

2.8 Concentrating phytoplankton

Determining numbers of phytoplankton cells in a water sample is no easy task as there is no single method to do so that is suitable under all conditions and for all

species (Lund *et al.*, 1958). There are three basic methods of concentrating phytoplankton: The first is the settling or sedimentation of preserved phytoplankton from a sample using the Utermöhl method (Utermöhl, 1931). Secondly, a centrifuge can be used to concentrate living or preserved samples as described by Throndsen (1978); and thirdly the concentration of phytoplankton may be measured by means of filtration as proposed by Dodson and Thomas (1978).

In 1931, Utermöhl constructed a series of counting chambers for phytoplankton enumeration. Since then, this method has remained largely unchanged except for a few minor modifications (Utermöhl, 1958; Evans, 1972; Paxinos and Mitchell, 2000). The Utermöhl method has become the standard quantitative method for concentrating and counting phytoplankton (Lund *et al.*, 1958). A chamber is used into which a 5 to 100 ml (Hasle, 1978) sample is poured and left to settle onto a coverslip for later enumeration using an inverted microscope. Most of the phytoplankton cells will settle out over time and therefore this method is useful when phytoplankton abundance is low (Paxinos and Mitchell, 2000). Lund *et al*. (1958) recommended that Lugol's solution be used as a preservative with this method as it stains and increases the weight of the phytoplankton. Buffered formalin has also been successfully used with this method (Reid, 1983; Bollmann *et al.*, 2002), however, in this case, a longer settling time is required (Hasle, 1978).

The worldwide use of the Utermöhl method allow for comparison of phytoplankton composition and biomass in ecosystems around the world (Willén, 1976; Paxinos and Mitchell, 2000). It is also appropriate for studies where the microplankton is size fractionated, with large sampling sets and where there is delayed processing of samples (Reid, 1983). A lower confidence in the data exists for the nanoplankton and picoplankton groups using this method, given the possibilities of cells not settling as well as difficulties with taxonomic differentiation (Reid, 1983; Bollmann *et al.*, 2002). The time taken to settle a sample, which is usually between 24 and 48 hrs (Lund *et al.*, 1958; Willén, 1976; Hasle, 1978; Reid, 1983; Paxinos and Mitchell, 2000), even 72 hrs (Bollmann *et al.*, 2002) is a potential drawback of this method.

Mixed results are obtained when comparing the centrifuge method with the Utermöhl method, but in general, higher cell concentrations were obtained by the former

(Throndsen, 1978). Bollmann *et al.* (2002) also found that membrane filters yielded consistently higher cell concentrations than the Utermöhl method.

2.9 Research conducted in the region

The most comprehensive phytoplankton study in the sACLME was made by Taylor (1966). He identified and composed a list of 414 taxa, indicative of the floristic richness of the system. This study formed part of the Indian Ocean expedition, in which the South African survey frigate, the *Natal,* sailed four cruises between April 1962 and January 1963. Four transects (at Durban; Port St. Johns; Port Elizabeth and Cape Agulhas), were sampled on a seasonal basis with a 65 µm 'N50V' meshnet. Diatoms, representing 238 taxa, were dominant throughout the entire region. Dinoflagellates, representing 159 taxa, were found to be sporadic in occurrence throughout region.

Thorrington-Smith (1969) reported that samples taken along the Natal Coast (Durban) consisted of two main classes of phytoplankton, Bacillariophyceae and Dinophyceae. Two Cyanophyceae species and one Chrysophyceae species were also present. The abundance of dinoflagellates ranged from 0.1 to 2.3% of the total number of cells counted per sample. The ten most common diatoms were seven *Chaetoceros* species, one *Thallassiothrix* species and two *Bacteriastratum* species (Thorrington-Smith, 1969). For a complete species list see Thorrington-Smith (1969).

In the austral summer of 2004, Mohan *et al.* (2011) sampled a transect along the 45° E longitude between the latitudes of 25°S and 56°S. The aim of that study was to understand the distribution patterns of diatoms in relation to sea surface temperature (SST), salinity and nutrient availability. Six diatom species were found: *Fragilariopsis kerguelensis*, *Fragilariopsis separanda*, *Thalassiothrix* sp., *Thalassiosira gracilis, Dactyliosolen* sp. and *Chaetoceros peruvianus*. *Fragilariopsis kerguelensis* was the dominant diatom from 41°S polewards but no diatoms were recorded between 25°S and 40°S. Mohan *et al.* (2011) concluded that the absence of diatoms north of 41°S is due to high SST, salinity and the low nutrient concentrations. The presence of diatoms south of 41°S was associated with lower SST (by 7°C), salinity and higher concentrations of nitrate and silicate.

In conjunction with the pelagic sampling (Mohan *et al.*, 2011), sedimentary core samples were also collected (Mohan *et al.*, 2006). Twenty-four species of diatoms were identified. Seven of these dominated the diatom assemblage: *Fragilariopsis kerguelensis* and *Thalassiosira lentiginosa* were dominant in the south where *F. separanda, Thalassionema nitzschioides, Thalassiothrix* sp., *Eucampia antarctica* and *Azpeitia tabularis* were present in low abundance. The major species identified in the core samples were briefly discussed by Mohan *et al.* (2006), whereas minor species were only listed. The spatial distribution of most of the diatoms in surface sediments appears to have been controlled by the same physicochemical parameters as those described for the sea surface samples.

The number of diatom species found in the two studies is very low compared to the findings of Taylor (1966). Sampling on several cruises between Cape Town, Marion Island and Prince Edward Island yielded detailed descriptions of the diatom community of the Agulhas Retroflection and ARC waters (Froneman *et al.*, 1995; Froneman *et al.*, 1998; Froneman *et al.*, 1999; Froneman and Pakhomov, 2000; Froneman *et al.*, 2004). These studies yielded between 8 and 44 diatom species in assemblages similar to the other studies within the region.

Sampling on hydrographic survey cruises off the Natal Bight and southeast Agulhas Shelf by Barlow *et al.* (2010) yielded mixed diatom-flagellate communities where the euphotic zone was deeper than the mixed layer. More recently, Barlow *et al.* (2014) recorded mixed phytoplankton communities, consisting of flagellates and prokaryotes in both cyclonic and anti-cyclonic eddies within the Mozambique Channel. Flagellates dominated near the DCM, whereas diatom dominance was only reported for regions with nutrient-rich water at or near the DCM and at the coast.

3 The Agulhas Shelf

3.1 Abstract

A survey along the Agulhas Shelf in September and October 2009 showed a strong north-south gradient along the shelf as well as across it. Water temperature decreased from north to south whereas across the Shelf there was an increase in temperature with inshore stations cooler than the offshore ones. Oxygen, nitrate, nitrite; phosphate, silicate and chlorophyll *a* concentrations increased from north to south and decreased across the shelf from the coastline into the Agulhas Current. This resulted in significant differences between the waters of the northern Shelf and those of the southern Shelf. The DCM became shallower in the south, towards the coast and in areas of upwelling. The N:P and N:Si ratios indicated that, for most of the Shelf, waters were nitrogen limited. Nutrients and phytoplankton biomass on the Shelf were controlled by the Agulhas Current via two permanent upwelling regions, the St Lucia and Port Alfred upwelling cells. The phytoplankton community also showed a latitudinal gradient with decreasing diversity from north to south. The most abundant diatom genera for the northern Shelf were *Pseudo-nitzschia* H.Peragallo whereas in the south, *Thalassiosira* Cleve and *Guinardia* H.Peragallo increased in abundance. *Alexandrium* Halim and *Gymnodinium* F.Stein were the most abundant dinoflagellates in the north and south respectively. The environmental drivers associated with the observed species distribution were water temperature and nitrate concentration. These showed a clear latitudinal gradient that remained unaffected by mesoscale variability of the Agulhas Current, thereby allowing the phytoplankton community to persist.

3.2 Introduction

The Agulhas Current is a western boundary current that transports warm Indian Ocean water along the South African coast and dominates the circulation in the southwest Indian Ocean (Lutjeharms, 2006). The Agulhas Current forms near the border between Mozambique and South Africa, with source waters from the Mozambique Channel (Sætre and Da Silva, 1984; de Ruijter *et al.*, 2002), the East Madagascar Current (Lutjeharms *et al.*, 1981), and the South West Indian Ocean

sub-gyre (Stramma and Peterson, 1990; Stramma and Lutjeharms, 1997b). Both the Mozambique Channel and East Madagascar Currents are minor sources with high levels of mesoscale variability. The Agulhas Current narrowly follows the steep continental shelf and was found to be very stable in its location between Durban and Port Elizabeth (Grundlingh, 1983; Lutjeharms *et al.*, 2000a; Lutjeharms, 2006). South of Port Elizabeth, the continental shelf starts to widen, forming the Agulhas Bank. It is here that the Agulhas Current starts to meander (Lutjeharms, 2006). These meanders are accompanied by shear-edge features such as cyclonic eddies and warm plumes (Lutjeharms *et al.*, 2000a).

The subtropical gyre of the southwest Indian Ocean has very limited primary productivity associated with low nutrient concentrations. Lutjeharms (2006), using satellite ocean colour, showed that there is a seasonal signal in primary productivity. The source waters of the Agulhas Current are oligotrophic (Lutjeharms, 2006) and upwelling events along the Agulhas Shelf bring nutrient-rich waters into the system. Two types of upwelling can be found along the Agulhas Shelf. The first occurs due to the effect of bottom stress in the Ekman layer and the vertical movement of colder and denser water masses (Lutjeharms *et al.*, 2000a). This is an inherent part of the dynamics of all western boundary systems (Condie, 1995; Lutjeharms *et al.*, 2000a). The second is the persistent upwelling associated with the Agulhas Current found where the continental shelf widens. The first area with a persistent (year-round) upwelling cell is the northern edge of the Natal Bight (Lutjeharms *et al.*, 1989b; Lutjeharms *et al.*, 2000a; Lutjeharms, 2006). The Natal Bight is a shelf region where the continental shelf widens. This pushes the Agulhas Current slightly offshore, creating lee eddies and the persistent upwelling cell in the north (Lutjeharms, 2006). The second location is along the eastern edge of the Agulhas Bank (Lutjeharms *et al.*, 2000a; Goschen *et al.*, 2012). Schumann (1982) also reported upwelling in this area that occurs during periods of strong and persistent easterly winds. This phenomenon is especially prominent at the capes. He reported substantial volumes of cold water entering Algoa Bay from the north due to large meanders. Roberts (2010) observed an upwelling event associated with a Natal Pulse (water plume) reaching the northern shoreline of Algoa Bay. Cooler waters in the eastern section of Algoa Bay can also be attributed to leakage from the Port Alfred upwelling cell

(Roberts, 2010). More recently, Goschen *et al.* (2015) showed that the upwelling events associated with Natal Pulses lasted for a period of 1 to 3 weeks until the core of the Agulhas Current moved offshore again. These Natal Pulses are a major driver of variability along the eastern edge of the Agulhas Bank (Krug *et al.*, 2014). The largest sector of shelf-edge upwelling occurs near the Natal Bight (Lutjeharms, 2006). These upwelling events along the Agulhas Shelf bring cold nutrient-rich water onto the continental shelf thus enhancing phytoplankton production (Carter and D'Aubrey, 1988; Carter and Schleyer, 1988; Goschen *et al.*, 2015).

Phytoplankton communities are vital to oceanic ecological processes and affect the structure of food webs, nutrient cycles and the transport of organic matter to deep ocean waters. Temperature, salinity and currents are factors that can influence the horizontal distribution of phytoplankton communities, while vertical distribution is primarily determined by irradiance, nutrients and water column stability. In the upper euphotic zone, phytoplankton productivity is generally limited by nutrients (Dugdale and Goering, 1967) while it is limited by light in the lower euphotic zone (Behrenfeld and Falkowski, 1997). The upper euphotic zone productivity may also be affected due to photoinhibition (Kirk, 1994). Phytoplankton is often concentrated in distinct layers: either the DCM or SCM. The DCM is not necessarily related to maximum light nor nutrient concentrations (Cullen, 1982). Mesoscale eddies in tropical and subtropical oligotrophic regions are known to strongly influence both the horizontal and vertical distribution of phytoplankton biomass (Benitez-Nelson *et al.*, 2007; Hansen *et al.*, 2010; Lamont *et al.*, 2014). The depth of the DCM or SCM zone ranges from 15 to 30 m for coastal regions (Jeffrey and Hallegraeff, 1990) and 40 to 130 m in the open ocean (Jeffrey and Hallegraeff, 1990; Hanson *et al.*, 2007a; Barlow *et al.*, 2014).

Nutrient limitation is largely determined by the stoichiometric ratio between the elements silicon (Si, as silicate), nitrogen (N) and phosphorus (P). This is due to the growth requirements of phytoplankton (Redfield, 1958). De-Pauw and Naessens (1991) showed that different nutrient ratios in water samples can be used to indicate the nutrient loading status and predict phytoplankton productivity. The nutrient requirements for phytoplankton species differ and as a result different phytoplankton communities respond differently to the same nutrient conditions. The half-saturation

constant of phytoplankton can also affect how phytoplankton species may respond to nutrient conditions, especially in N limited environments (Eppley *et al.*, 1969). Meyer *et al.* (2002) reported that the main source waters of nutrients for the Natal Bight phytoplankton came from the northern edge and southwards via bottom water. The main source of nutrients for the eastern Agulhas Bank phytoplankton is the Port Alfred upwelling cell (Lutjeharms *et al.*, 2000a).

North of the Agulhas Current, Barlow *et al.* (2014) found that the phytoplankton community was comprised of prokaryotes and small flagellates, with prokaryotes dominant in surface waters. They also reported that dinoflagellates were absent from the Mozambique channel and that diatoms were the dominant phytoplankton group at frontal regions where waters diverge. Barlow *et al.* (2010) also reported that for the south-eastern Shelf of the Agulhas ecosystem, phytoplankton were dominated by either diatoms or diatom-flagellate communities.

Ryther *et al.* (1966) measured primary production rates of <1.0 g C m^{-2} d^{-1} for the open ocean between 25°N and 40°S. Elevated primary productivity (>1.0 g C m^{-2} d^{-1}) was reported along the east African coast and on the northern Agulhas Shelf production ranged from 0.1 to 3.1 g C m^{-2} d^{-1} (Ryther *et al.*, 1966). Primary productivity for the Delagoa Bight was reported to be 0.6 g C m^{-2} d^{-1} (Mitchell-Innes, 1967) while for the Natal Bight productivity was between 0.2 and 2.2. g C m^{-2} d^{-1} (Burchall, 1968b, a). Upwelling on the northern edge of the Natal Bight contributed to higher chlorophyll *a* concentration over the northern Natal Bight (1.0 to 1.5 µg l^{-1}) compared to the southern Natal Bight (<0.5 µg l^{-1}) (Lutjeharms *et al.*, 2000a). Carter and Schleyer (1988) reported that the chlorophyll *a* concentrations range between 0.03 and 3.9 µg l^{-1}. Barlow *et al.* (2008) measured depth-integrated chlorophyll *a* concentrations in the euphotic zone of between 20 and 70 µg l^{-1}. The KwaZulu-Natal coastal waters were found to be dominated by small flagellates with diatoms being more prominent in the cooler waters around the Natal Bight area (Barlow *et al.*, 2008; Barlow *et al.*, 2010).

Phytoplankton may be classified by cell size (e.g. Sieburth, 1979; Poulton *et al.*, 2006): picoplankton (0.7 – 2.0 µm), nanoplankton (2.0 – 20.0 µm) and the larger microplankton (> 20.0 µm). Environmental factors that influence the composition and

dynamics of phytoplankton communities include: light availability, temperature, salinity and nutrients (Poulton *et al.*, 2006; Alves-de-Souza *et al.*, 2008). The time and spatial variation of these environmental factors result in a diverse and dynamic phytoplankton community (Poulton *et al.*, 2006).

This study considered the physico-chemical oceanographic environment as drivers of the phytoplankton communities: their biomass, composition and biogeography. Other studies only investigated portions of the study site considered here, e.g. Natal Bight (Barlow *et al.*, 2008), off Durban (Burchall, 1968b; Carter and Schleyer, 1988) and the south-eastern Shelf of the Agulhas Bank (Barlow *et al.*, 2010). This study is the first to investigate the phytoplankton of the Agulhas Shelf in its entirety and consider the environmental drivers of this community along the Shelf. To do so, the following hypothesis was tested:

The distribution of phytoplankton changes from a

- low-biomass, flagellate-dominant community in the oligotrophic subtropical waters on the northern Shelf to an
- elevated biomass and diatom-dominant community in the cooler mesotrophic waters of the southern Shelf.

3.3 Materials and Methods

3.3.1 Study area

An oceanographic survey was carried out aboard the FRS *Algoa* in September and October 2009. Twenty-one across-shelf transects with two to nine stations each were sampled from the coast, to beyond the 1 000 m isobath (Fig. 3.1). Transects were positioned half a degree apart and stations approximately 10 nautical miles apart. Sampling was conducted within the framework of ACEP II (African Coelacanth Ecosystem Program Phase II) and the ASCLME Project. The study area covered the Agulhas Current and the associated shelf from Ponta do Ouro, Southern Mozambique, to Cape St Francis, South Africa. The two large bays, Algoa Bay and St Francis Bay were also included in the study area.

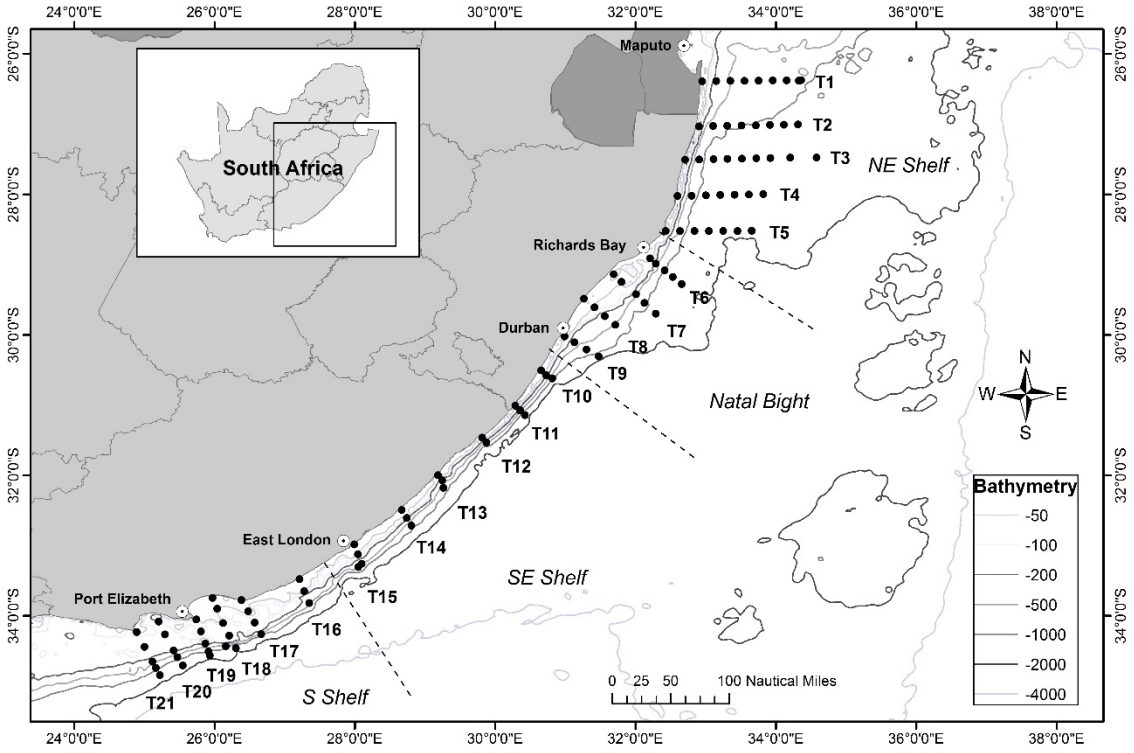

Fig. 3.1 Sampling stations (black dots) of the Agulhas Shelf Cruise. Transects 1 to 5 are on the north-eastern Shelf, transects 6 to 9 represent the Natal Bight, and transects 10 to 15 the south-eastern Shelf – these collectively form the northern Agulhas Shelf. Transects 16 to 21 form the southern Agulhas Shelf. The dashed lines represent the geographical borders between these regions.

3.3.2 Environmental variables

All the environmental data were collected *in situ* from the *FRS Algoa* during Cruise 410 in September and October of 2009. Fluorescence, conductivity, temperature and pressure data were collected using a SeaBird Electronics SBE 911+ CTD and deck unit, together with a SeaBird Electronics 43 dissolved oxygen sensor and a Chelsea Instruments Aquatracka MkIII fluorometer. A 12-way rosette holding twelve 5 l Niskin bottles was used to collect water samples at preset depths for the analysis of nutrients and size-fractionated (>20 µm, 20 – 2 µm and 2 - 0.7 µm) chlorophyll *a*. During each CTD cast the DCM or SCM was determined and water was collected at five depths relative to these: below the DCM/SCM, at the DCM/SCM and at three

depths between the DCM/SCM and the surface (as far as possible) (Fig. 3.2). Samples for nutrient analyses were filtered, frozen (-20°C) and analysed in the laboratory for silicate (SiO_4^{4-}), nitrate (NO_3^-), nitrite (NO_2^-) and phosphate (PO_4^{3-}) concentrations according to Strickland and Parsons (1972) modified for use with a Technicon Auto Analyser II (Mostert 1983). The criteria selected for the mixed layer depth of temperature (MLD_T) or density (MLD_D) were from a near-surface value (10 m depth) where ΔT = 0.2°C or $\Delta\sigma_\theta$ = 0.03 kg m^{-3}, respectively (de Boyer Montégut *et al.*, 2004).

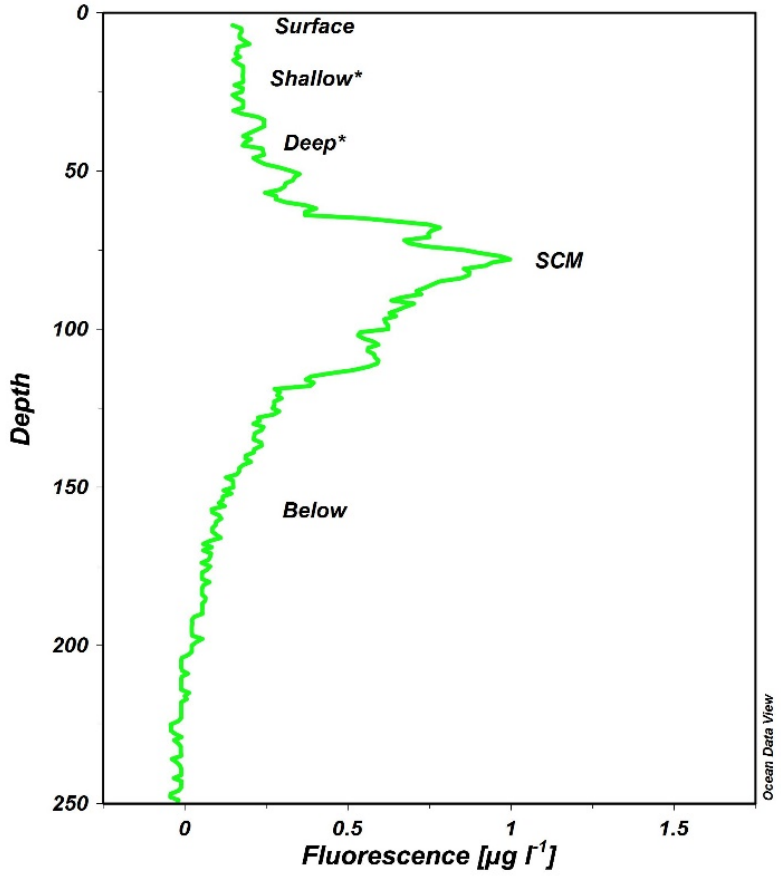

Fig. 3.2 The fluorescence profile of a typical CTD cast indicating the depths sampled. Depths indicated with * were only sampled if the DCM was located at sufficient depth.

3.3.3 Phytoplankton biomass

Size fractionated chlorophyll *a* was measured by filtering 500 ml water samples through a tower of three filters in subdued light. The filters were: 20 µm Millipore

nylon net filters, 2 µm Millipore membrane filters, and 0.7 µm Whatman GFF filters. Filters were frozen (-20°C) for later analysis in the laboratory. Chlorophyll was extracted from samples in the dark for 24 h at -20°C into 90% acetone. Chlorophyll *a* concentration of filtered extracts was determined fluorometrically on a Turner Designs model AU10 (Arar and Collins, 1997).

3.3.4 Phytoplankton cell counts and identification

A litre of water was taken from the surface and the DCM/SCM Niskin bottle and preserved with 2% Lugol's iodine solution (Parsons *et al*., 1989; Karayanni *et al*., 2004). The entire volume was sedimented and cells counted using a Zeiss IM 35 inverted microscope (Utermöhl, 1958) at 630x magnification, with identification to species level where possible. For dominance and species composition a minimum of 300 cells were counted where possible.

In addition, an 80 µm ring net was deployed vertically to below the DCM and drawn up to the surface at 0.5 m s^{-1}. The contents of the cod-end were preserved with 2% Lugol's iodine solution. Permanent slides for light microscopy and stubs for scanning electron microscopy were prepared from these samples in order to identify the majority of the taxa to species level.

3.3.5 Statistical analyses

Main Effects Measures Analysis of Variance was used to determine significant differences among means. When a significant difference among means was found; Pairwise Multiple Comparison Procedures were done to determine differences between means. All analyses were done using R version 3.5.0 (R Core Team, 2018), with packages *vegan* (Oksanen *et al.* 2018), *ggplot2* (Wickham *et al.* 2018) and *mvabund* (Wang *et al.* 2018). Detrended Correspondence Analysis (DCA) was used to determine patterns in the distribution of the species and stations across the study area. Canonical Correspondence Analysis (CCA) was used to relate environmental variables to the stations (and species). Monte Carlo permutation tests (999 unrestricted permutations; $p < 0.05$) were used to assess the significance of the canonical axes showing the relationship between the samples and selected environmental variables. The two most explanatory axes of the CCA and DCA were

plotted as two-dimensional graphs. Environmental variables were plotted as vectors originating from the graph origin. The magnitude of the vector represents the magnitude of the variation in each variable and its direction represents an increase in the value of that particular variable. Abundance and dominance were determined from the cell concentration data, following the criteria proposed by Calijuri *et al.* (2002). Abundant species were those with abundance scores above the mean value of the community, and dominant species were those with values surpassing 50% of the total number of cells. Species diversity and evenness indices were calculated using the *vegan* package in R (Oksanen *et al.*, 2018). Generalized linear models (GLMs) were also used to further explore the relationships between environmental variables and phytoplankton abundance.

3.4 Results

3.4.1 Physical and chemical oceanographic conditions

Based on the characteristics of the continental shelf and the Agulhas Current, the Agulhas Shelf was divided into two major regions: the northern Agulhas Shelf (Transects 1-13) and the southern Agulhas Shelf (Transects 14 – 21). The northern Agulhas Shelf was subdivided into the north-eastern Shelf (Transects 1 – 5), the Natal Bight (Transects 6- 9) and the south-eastern Shelf (Transects 10 -13). The northern Agulhas Shelf was characterised by a fast-flowing Agulhas Current that closely followed the steep and narrow continental shelf. The widening of the continental shelf to form the Agulhas Bank and the associated meandering of the Agulhas Current marked the beginning of the southern Agulhas Shelf. Characteristics are based on those reported by Lutjeharms (2006). Sea surface temperatures (Fig. 3.3) and temperature profiles (Fig. 3.4) for the euphotic zone showed a clear gradient of decreasing temperature from the northern to the southern Agulhas Shelf. Temperatures of the waters of the northern Agulhas Shelf (Transects 1 to 13) ranged from 15.34 to 23.93°C with a mean (± S.D.) of 21.40 ± 1.73°C. The southern Agulhas Shelf (Transects 14 to 22) was significantly cooler ($F = 168.11$; $p < 0.01$; $n = 302$) with temperature ranging from 10.76 to 22.04°C and a mean of 18.12

± 2.72°C. The coefficients of variance for the southern Agulhas Shelf and northern Agulhas Shelf were 15.01 and 8.08%, respectively.

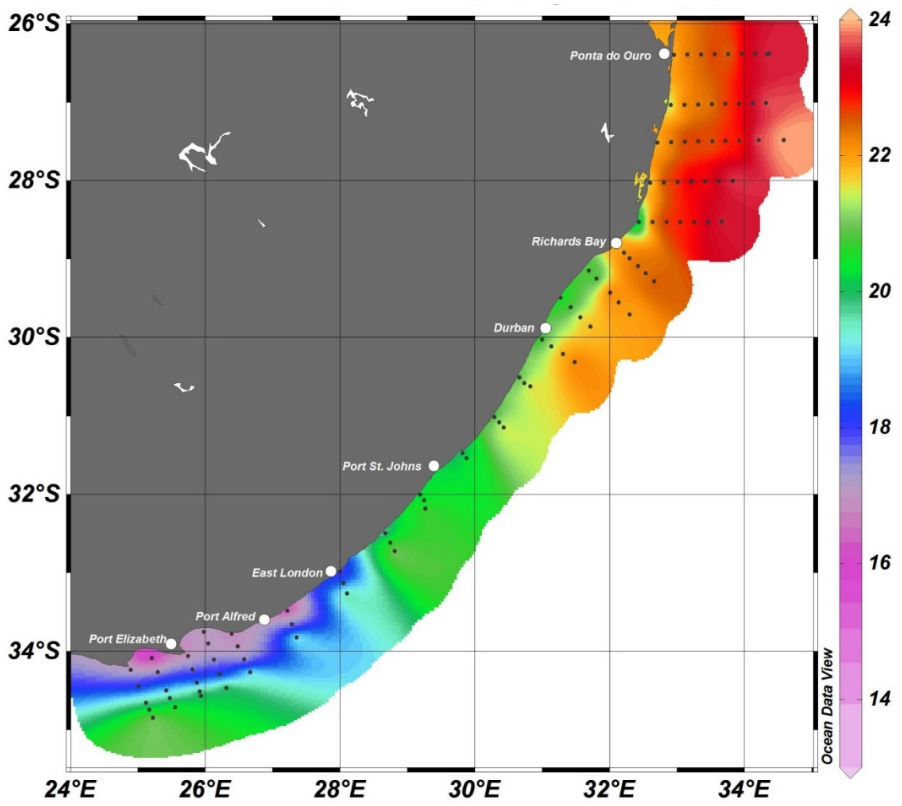

Fig. 3.3 Sea surface temperatures measured along the Agulhas Shelf. The black dots represent the sampling stations.

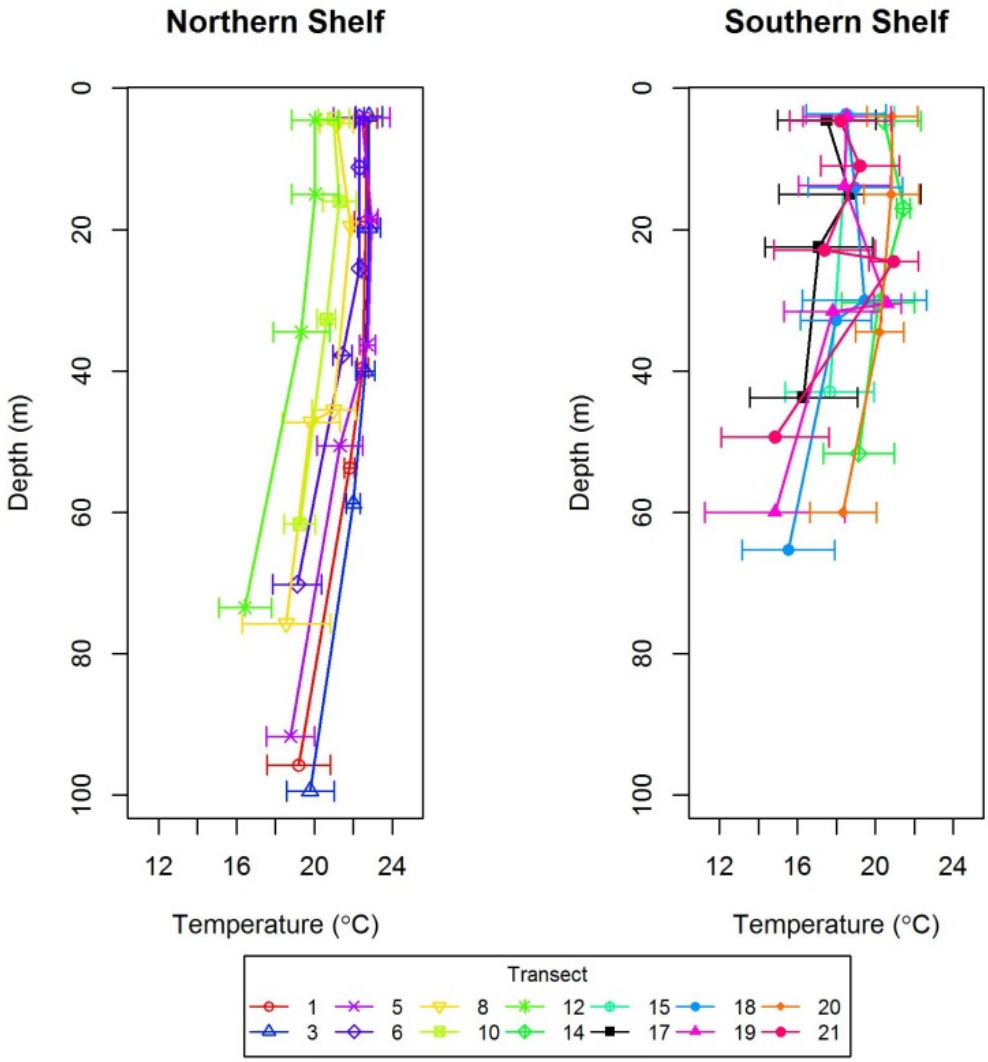

Fig. 3.4 Temperature (mean ± 1 S.D.) profiles measured through the epipelagic zone of the Agulhas Shelf. Transects 1 to 13 form the northern Agulhas Shelf and Transects 14 to 21 the southern Agulhas Shelf.

Salinity was significantly ($F = 12.137$; $p < 0.01$; $n = 302$) lower for the southern Agulhas Shelf compared to the northern Agulhas Shelf. The salinity for the northern Agulhas Shelf epipelagic zone ranged from 35.21 to 35.54 with a mean of 35.39 ± 0.06. The southern Agulhas Shelf epipelagic zone salinity ranged from 34.92 to 35.54 with a mean of 35.36 ± 0.12.

There was a significant decrease in oxygen concentration with depth (Fig. 3.5) below the DCM in both the northern and southern Agulhas Shelf regions ($F = 48.85$; $p < 0.001$; $n = 302$). The more southerly transects showed an elevated oxygen concentration at the DCM (Fig. 3.5). The mean dissolved oxygen concentration was significantly ($F = 32.35$; $p < 0.01$, $n = 302$) higher for the southern Agulhas Shelf epipelagic zone (4.74 ± 0.48 mg l^{-1}) compared to the north (4.49 ± 0.38 mg l^{-1}). The mean dissolved oxygen for the northern shelf DCM (4.53 ± 0.24 mg l^{-1}) was significantly lower ($p < 0.01$; $n = 302$) compared to the southern DCM (4.84 ± 0.44 mg l^{-1}).

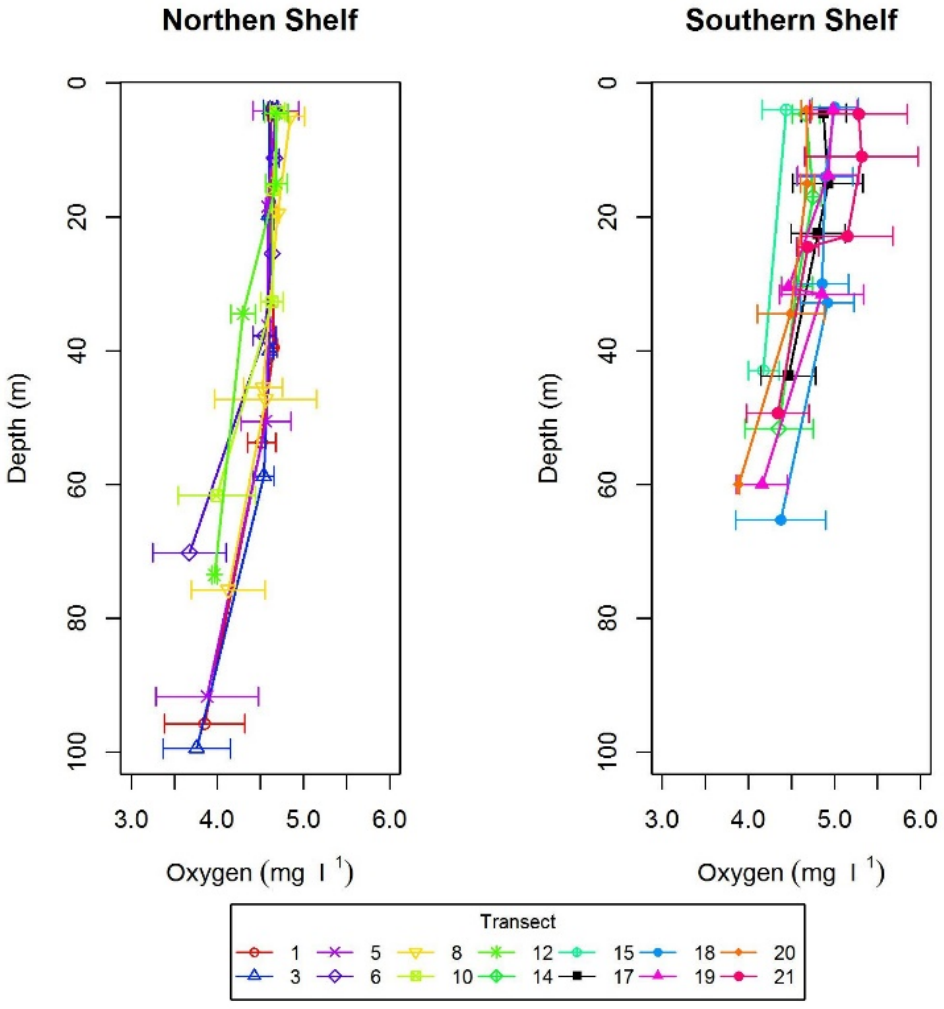

Fig. 3.5 Oxygen (mean mg l^{-1} ± 1 S.D.) concentrations with depth through the epipelagic zone of the Agulhas Shelf. Transects 1 to 13 represent the northern Agulhas Shelf and Transects 14 to 21 the southern Agulhas Shelf.

The nitrite concentrations for Agulhas Shelf waters are shown in Fig. 3.6. The only significant difference ($F = 1.98$; $p < 0.02$; d.f. = 288) in the NO_2^- concentrations was between Transects 15 and 19 with NO_2^- concentrations being higher at Transect 15. Transects 1, 3, 5, 19, 20 and 21 had high NO_2^- concentrations at the DCM (Fig. 3.6).

The nitrate concentrations showed a similar increase with depth at all Transects (Fig. 3.7). The only significant difference in nitrate concentrations was between Transects 3 and 18 ($F = 19.61$; $p < 0.01$; d.f. = 72) and Transects 3 and 21 ($F = 8.51$; $p < 0.01$; d.f. = 72). Nitrate concentrations of the waters of the southern shelf (4.56 ± 5.22 µM) were significantly higher ($F = 24.49$; $p < 0.001$; d.f. = 302) compared to the northern shelf (2.11 ± 3.39 µM). Nitrate concentrations increased southwards along the coast.

Phosphate also showed the same gradient, increasing concentrations southwards along the coast (Fig. 3.8). Transects 3, 5 and 9 of the northern Shelf were found to have significantly lower phosphate concentrations ($F = 9.66$; $p < 0.05$; d.f = 186) compared to the southern transects (such as 16, 18, 19 and 21). Mean concentrations at depth of Transect 3 (0.27 ± 0.23 µM) were significantly ($F = 17.63$; $p < 0.001$; d.f =109) lower compared to Transect 16 (0.81 ± 0.24 µM), 18 (0.73 ± 0.38 µM), 19 (0.75 ± 0.42 µM) and 21 (0.67 ± 0.40 µM). Transect 5 (0.43 ± 0.35 µM) had significantly ($F = 5.45$; $p < 0.001$; d.f =99) lower concentrations of phosphate when compared to transect 18 (0.73 ± 0.38 µM) and 19 (0.75 ± 0.42 µM). Transect 9 (0.47± 0.33 µM) had significantly lower concentrations compared to those measured at Transect 21 (0.67 ± 0.40 µM).

No significant differences ($F = 1.49$; $p > 0.05$; d.f. = 288) were recorded in silicate concentrations between any of the transects of the study sites (Fig. 3.9). At all transects, silicate concentrations remained constant between the surface and DCM after which they increased with depth. All the nutrients showed a significant positive correlation with depth (Table 3.1).

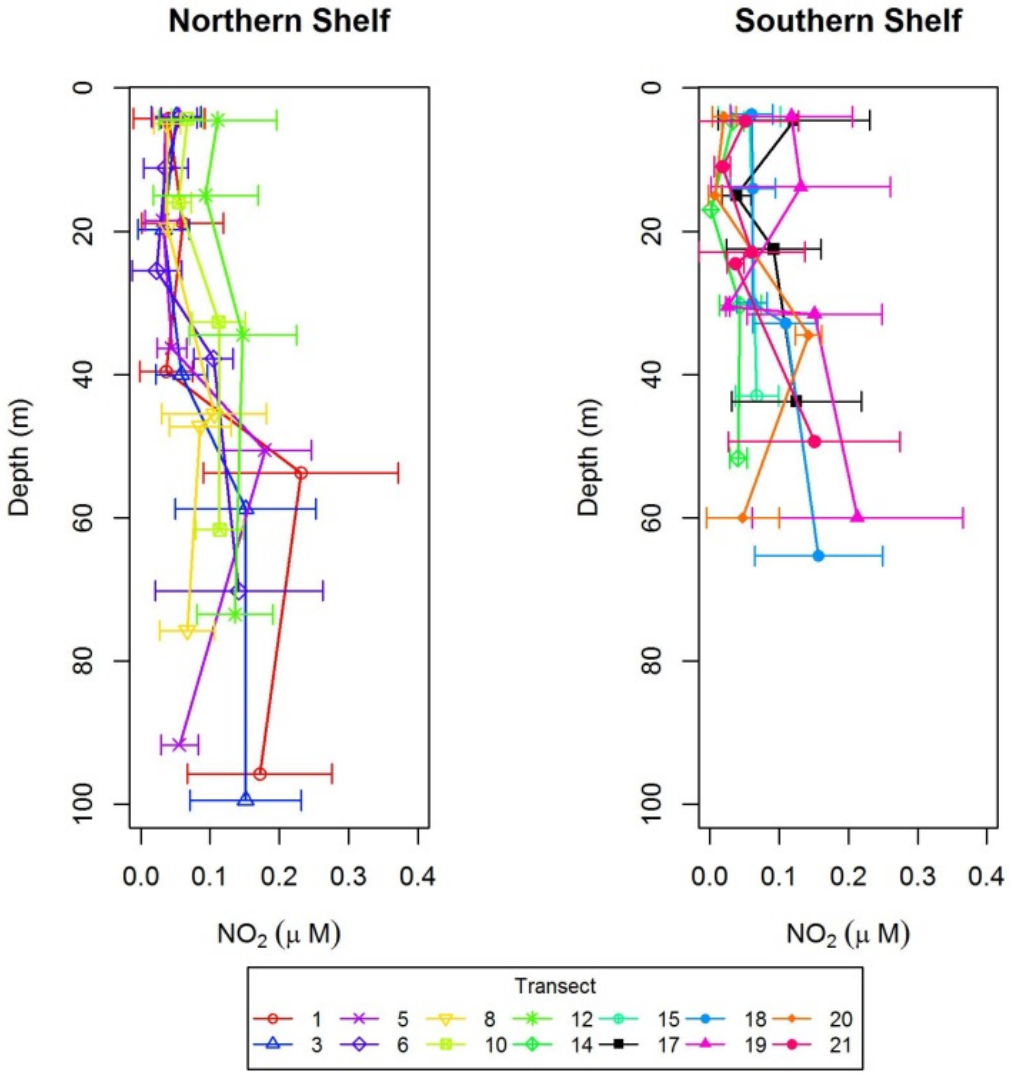

Fig. 3.6 Nitrite (mean µM ± 1 S.D.) concentrations in the epipelagic waters of the Agulhas Shelf. Transects 1 to 13 represent the northern Agulhas Shelf and Transects 14 to 21 the southern Agulhas Shelf.

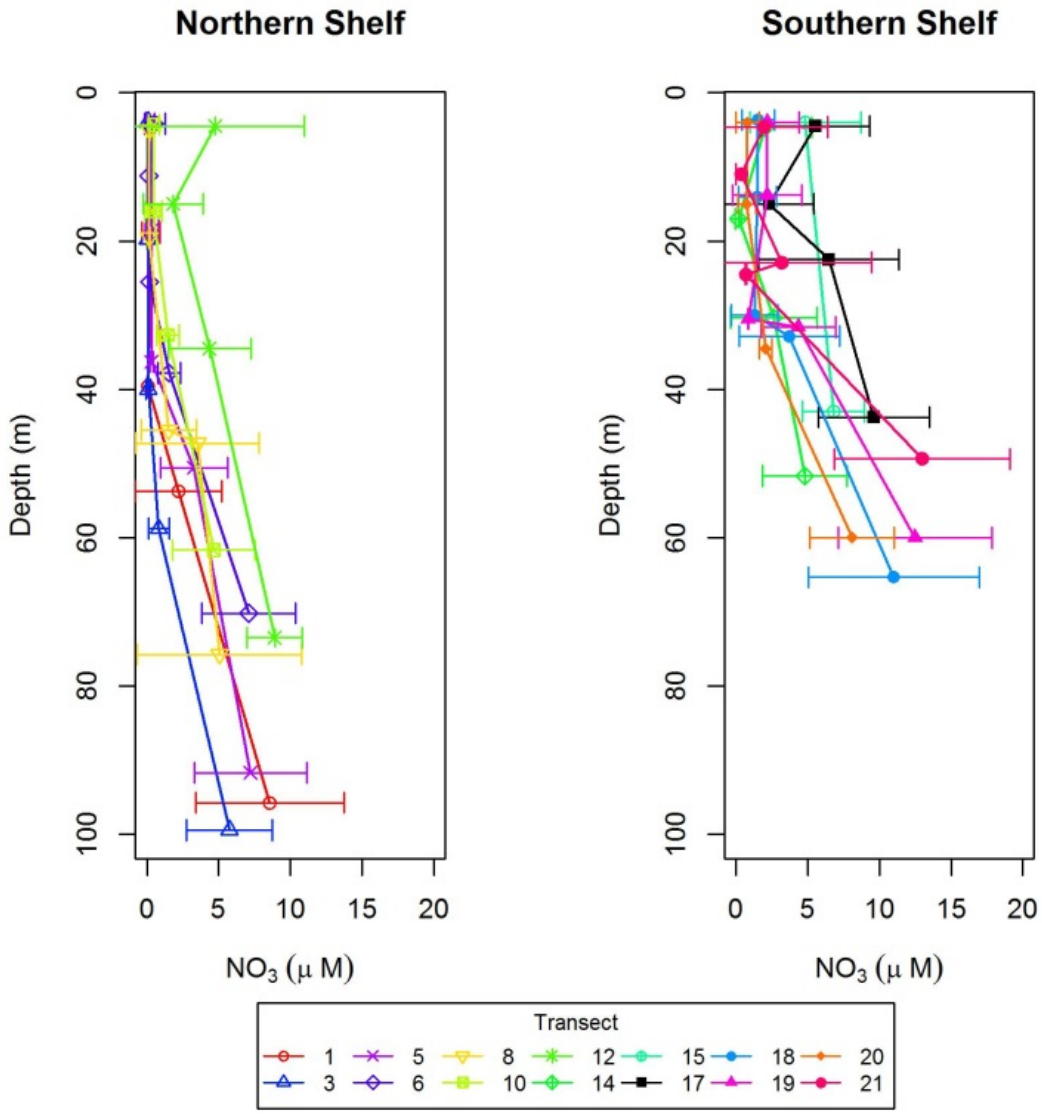

Fig. 3.7 Nitrate (mean μM ± 1 S.D.) concentrations in the epipelagic zone of the Agulhas Shelf. Transects 1 to 13 represent the northern Agulhas Shelf and Transect s14 to 21 the southern Agulhas Shelf.

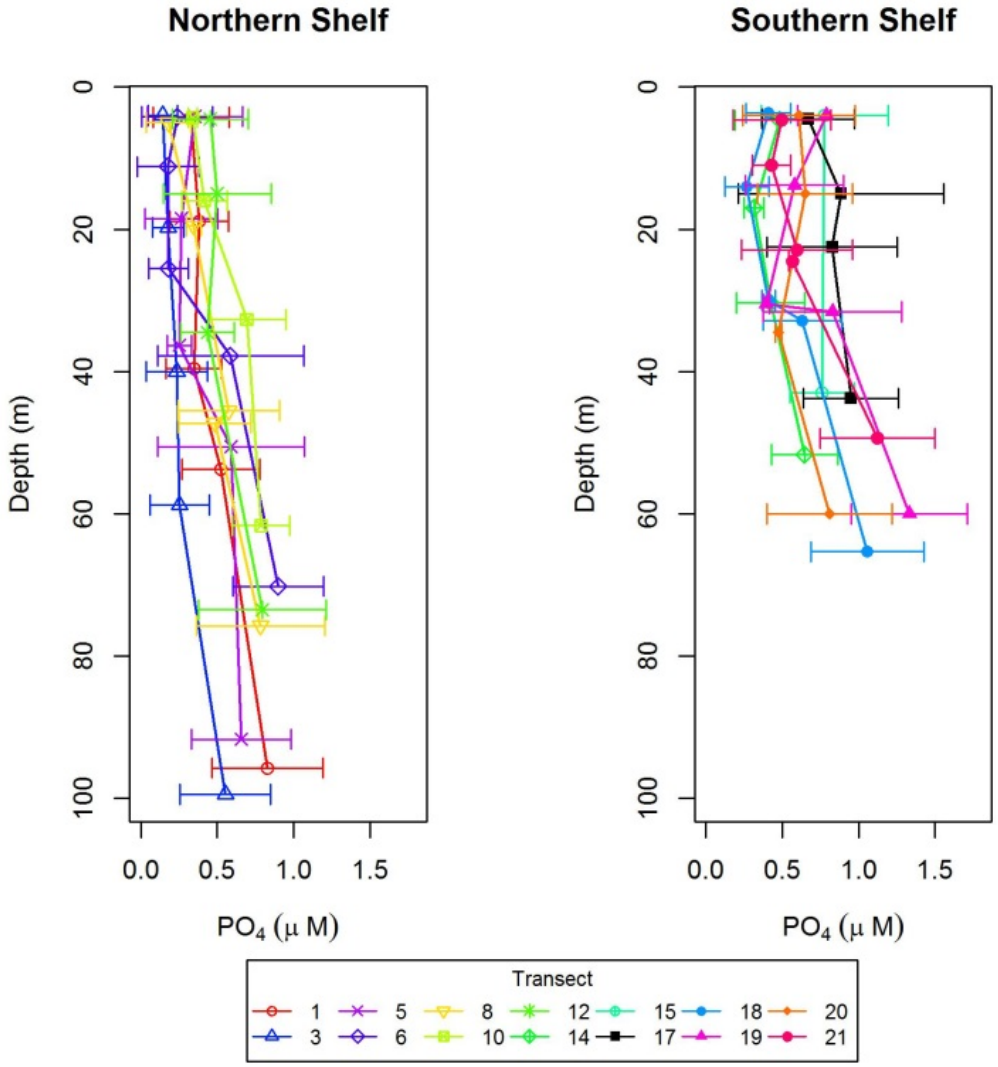

Fig. 3.8 Phosphate (mean µM ± 1 S.D.) concentrations in the epipelagic zone of the Agulhas Shelf. Transects 1 to 13 represent the northern Agulhas Shelf and Transects 14 to 21 the southern Agulhas Shelf.

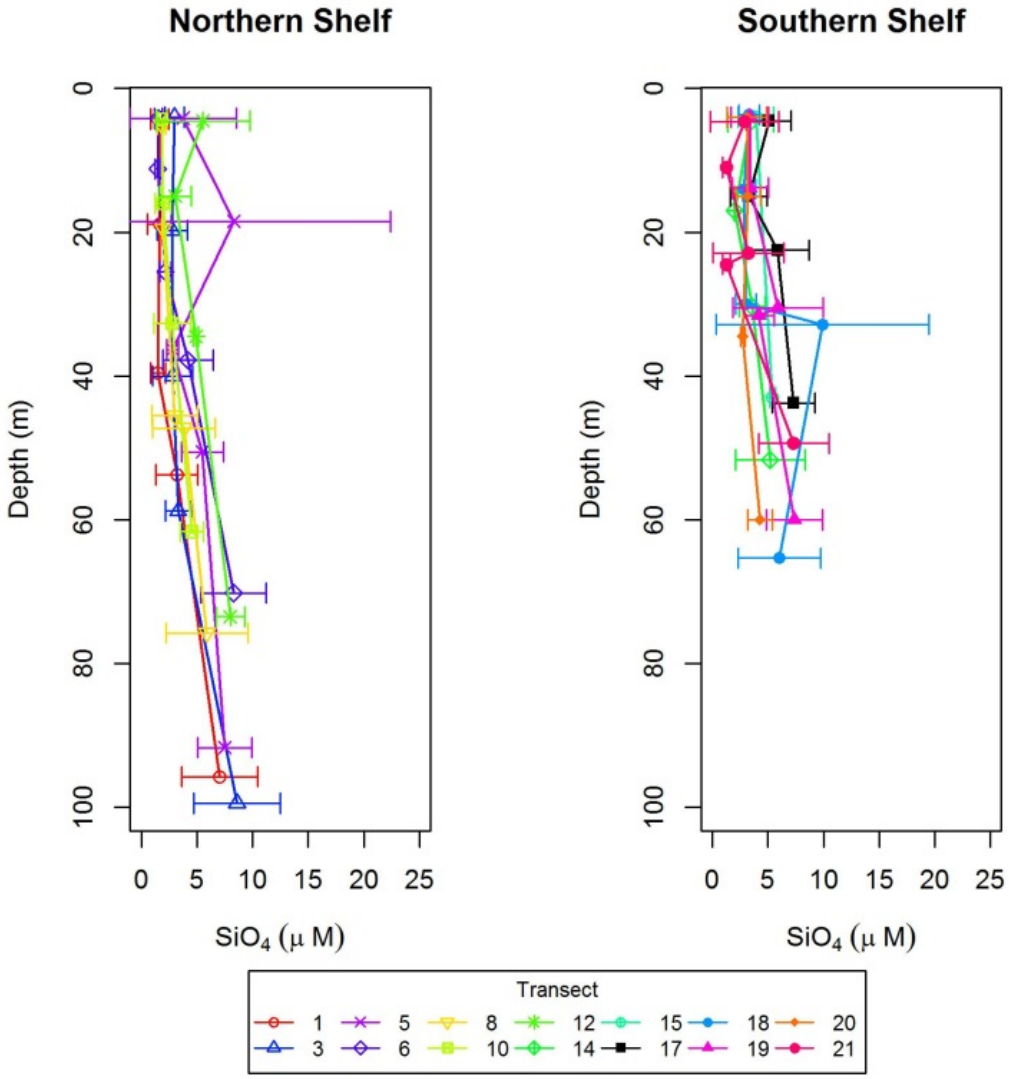

Fig. 3.9 Silicate (mean µM ± 1 S.D.) concentrations in the epipelagic zone of the Agulhas Shelf. Transects 1 to 13 represent the northern Agulhas Shelf and Transects 14 to 21 the southern Agulhas Shelf.

Deviation of regression lines from the Redfield ratio (Fig. 3.10) indicate nitrogen limitation for all waters of the Agulhas Shelf, with the exception of Transect 21 (Cape St Francis) where the N:P ratio was 16:1. The lowest N:P ratios were recorded at Transects 5 (3.6:1) and 6 (3.9:1) (Fig. 3.10).

Transects 1, 9, 11, 13, 15, 16, 20 and 21 silicon was marginally limited (Fig. 3.11). The highest N:Si ratios were found at Transects 16 (2.1:1), 20 (2.0:1) and 21 (1.9:1).

Table 3.1 Pearson correlation analysis with pairwise deletion of the environmental variables measured in the waters of the Agulhas Shelf. Significant correlations are coded as follows: *** p < 0.001, ** p < 0.01, * p << 0.05. Positive correlations are blue and negative correlations are red.

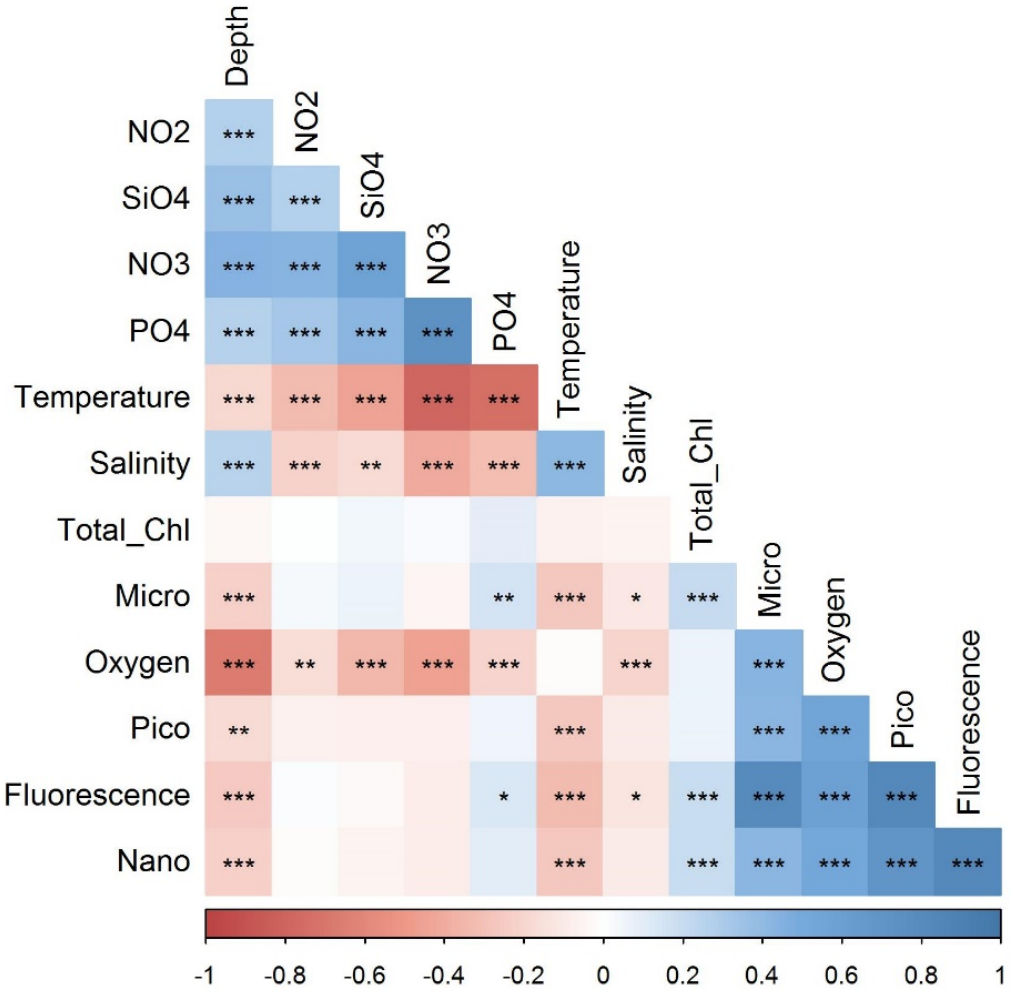

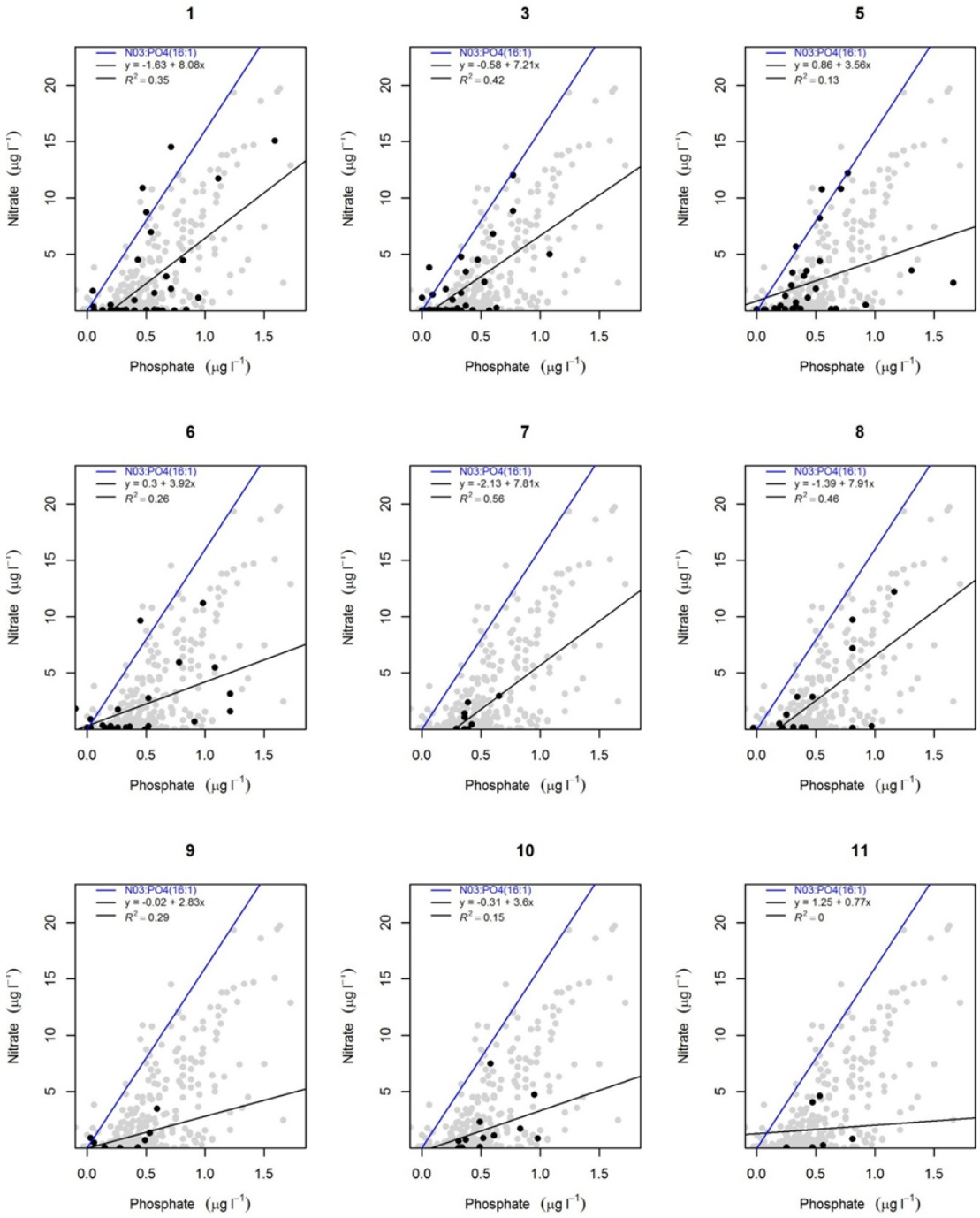

Fig. 3.10 Concentrations of nitrate versus phosphate for all samples collected from surface waters to those at 200 m depth at Transects 1 to 11. The black line is the regression line for the data and the blue line represents the Redfield Ratio (N:P = 16:1). Grey dots are all stations whereas the black dots represent the samples for the specific transect.

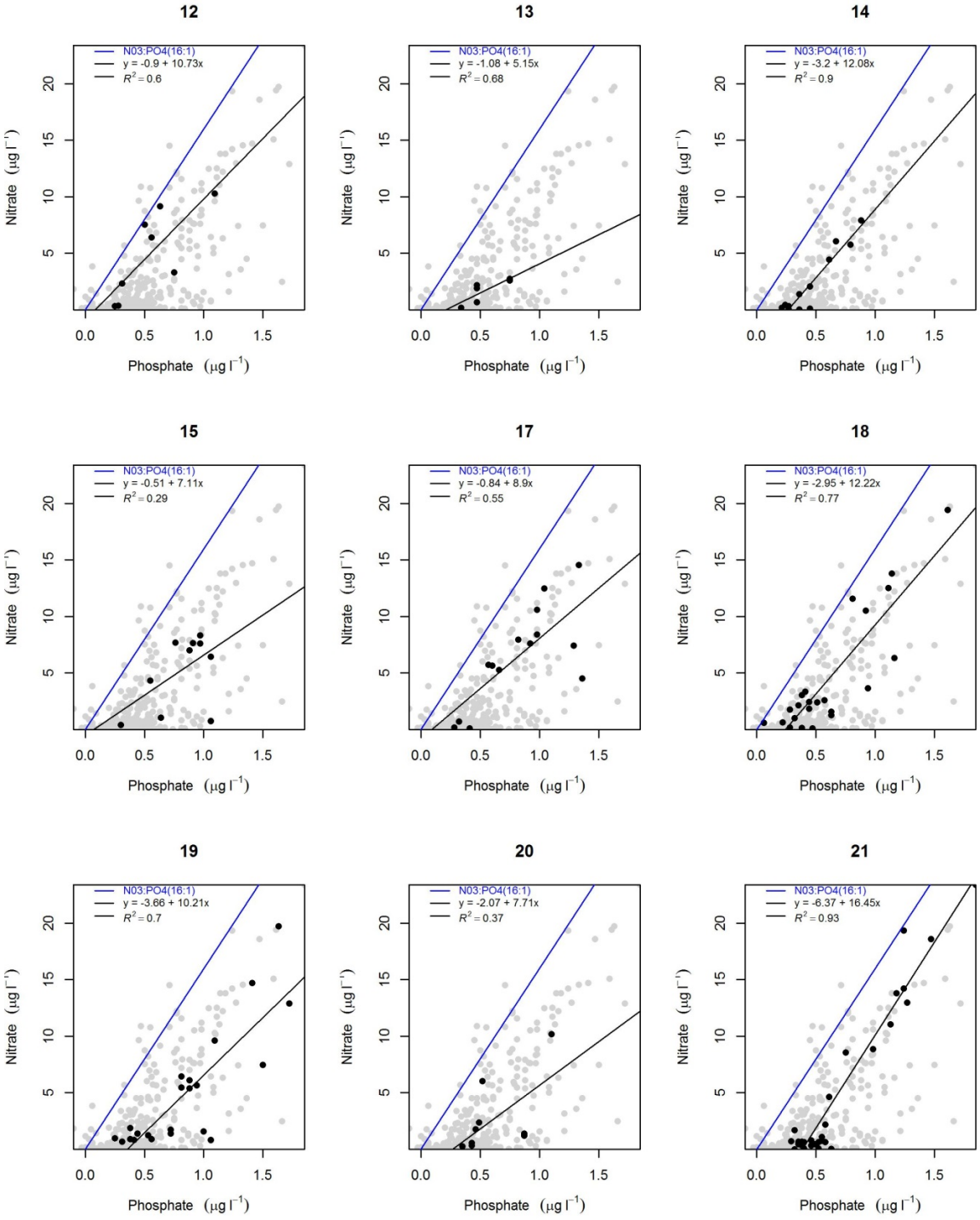

Fig. 3.10 Concentrations of nitrate versus phosphate for all samples collected from surface waters to those at 200 m depth at Transects 12 to 21. The black line is the regression line for the data and the blue line represents the Redfield Ratio (N:P = 16:1). Grey dots are all stations whereas the black dots represent the samples for the specific transect.

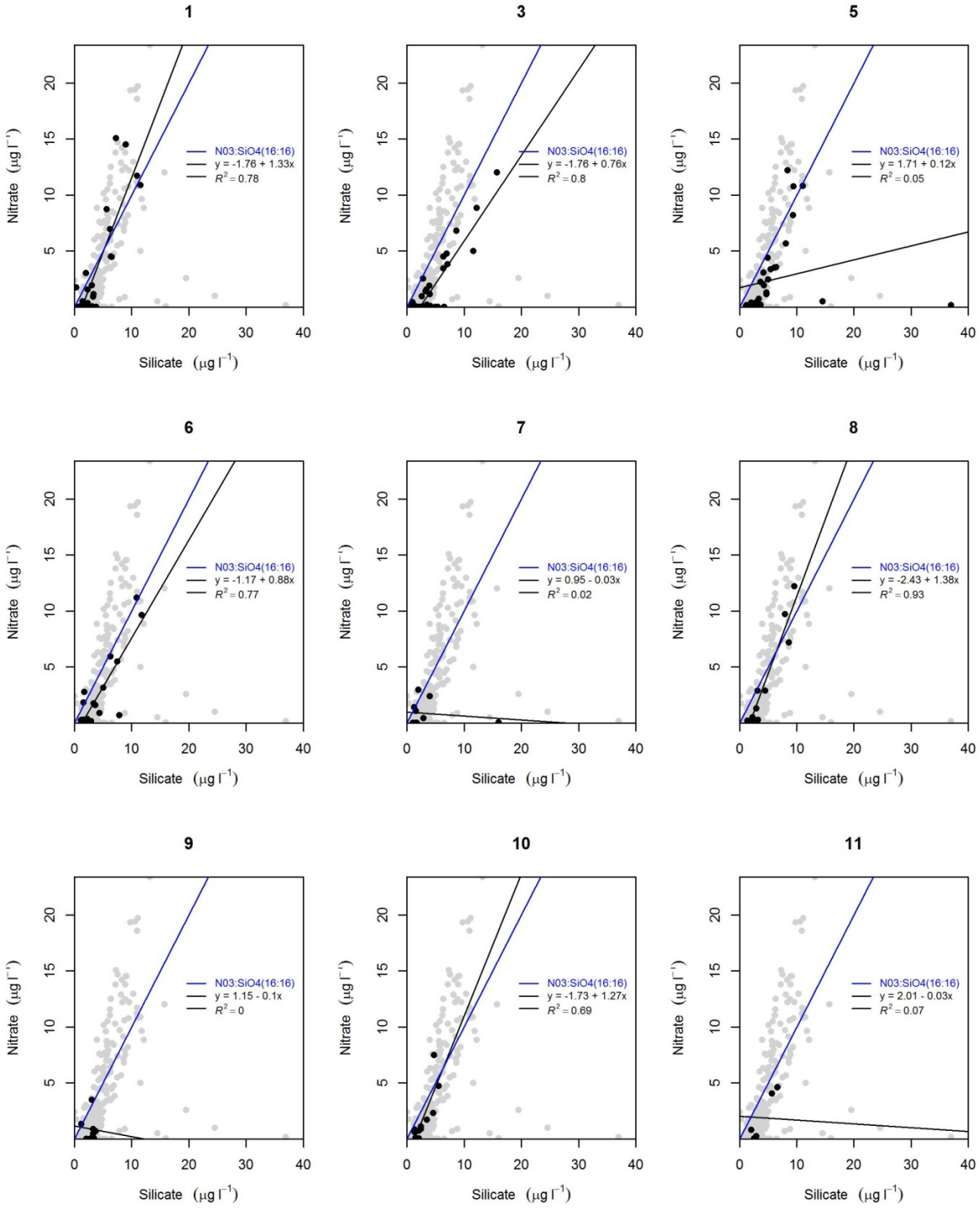

Fig. 3.11 Concentrations of nitrate versus silicate for all samples collected from surface waters to those at 200 m depth at Transects 1 to 11. The black line is the regression line for the data and the blue line represents the Redfield Ratio (N:P = 1:1). Grey dots are all stations whereas the black dots represent the samples for the specific transect.

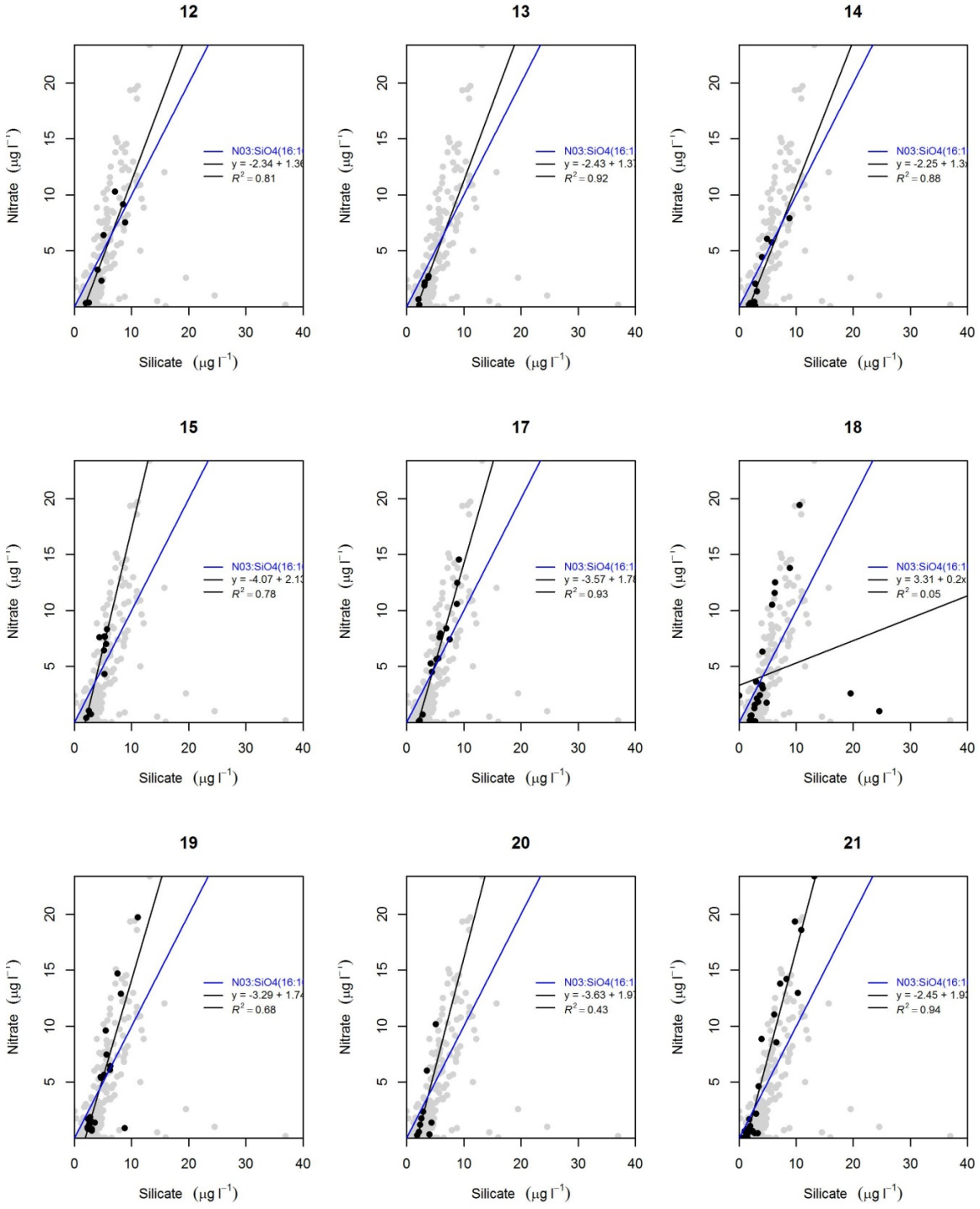

Fig. 3.11 Concentrations of nitrate versus silicate for all samples collected from surface waters to those at 200 m depth at Transects 12 to 21. The black line is the regression line for the data and the blue line represents the Redfield Ratio (N:P = 16:16 (Redfield Ratio). Grey dots are all stations whereas the black dots represent the samples for the specific transect.

All four nutrients showed significant negative correlations (Table 3.1) with temperature (Fig. 3.12) as well as with salinity (Fig. 3.13). At temperatures of <20°C the euphotic zone is characterised by nutrient-rich waters (>10 µM). A salinity over 35.1 and temperatures greater than 13°C separate the euphotic zone of the southern-most transects (20 and 21) from the rest, especially noticeable below the DCM.

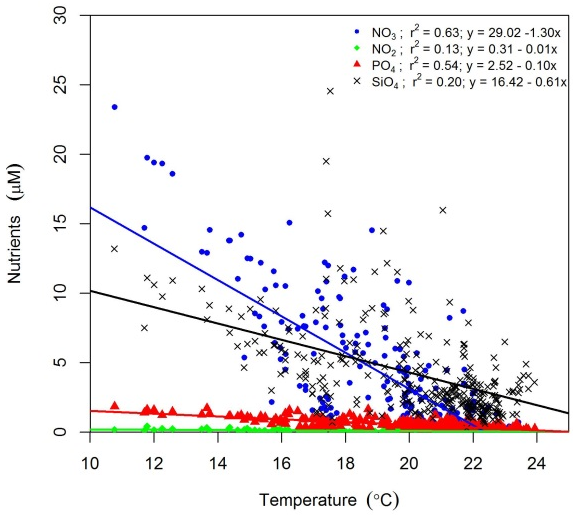

Fig. 3.12 Concentrations of nutrients (NO_2^-, NO_3^-; PO_4^{3-} and SiO_4^{4-}) versus temperature for all the euphotic zone stations (n=302).

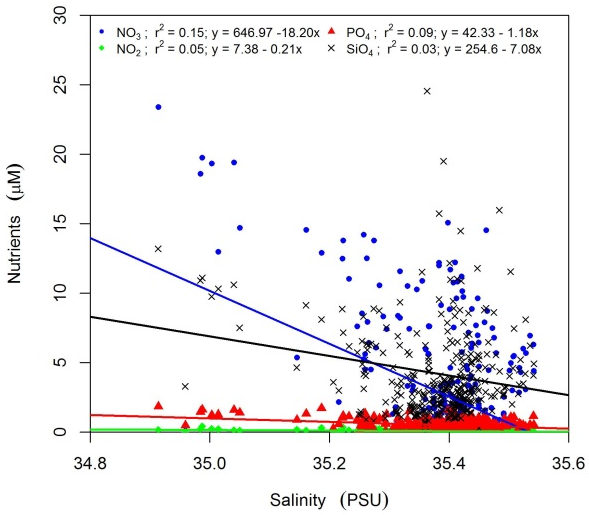

Fig. 3.13 Concentrations of nutrients (NO_2^-, NO_3^-; PO_4^{3-} and SiO_4^{4-}) versus salinity for all the euphotic zone stations (n=302).

3.4.2 Spatial variability of phytoplankton

Chlorophyll *a* concentrations were higher near the coast (Fig. 3.14), especially in areas where upwelling is known to occur. The depth of the chlorophyll *a* maximum varied considerably - ranging between 10 m and 101 m but was associated with both the pycnocline and nutricline (Fig. 3.15 and Fig. 3.16). Selected graphs of *in situ* chlorophyll *a* concentration with depth are included to illustrate the difference in the phytoplankton distribution of known upwelling zones with that measured on the coastal shelf (Fig. 3.15 and Fig. 3.16). The *in situ* chlorophyll *a* concentrations

measured at Transect 1 shows a typical pattern of phytoplankton distribution in oligotrophic waters - the DCM occurred between 50 and 101 m depth (Fig. 3.15a). At the DCM, microphytoplankton contributed 67% of the total chlorophyll *a*, whereas nano- and picophytoplankton contributed 18 and 14%, respectively. At the time of the study, the surface waters of this transect were dominated by microphytoplankton, contributing 55% to the total chlorophyll *a*.

Transect 5 is located on the northern edge of the Natal Bight and the offshore stations showed the same pattern as that observed at Transect 1 (Fig. 3.15b). The DCM was located at a depth of approximately 50 m. Located on the edge of the Natal Bight, the inshore station of Transect 5 showed a significantly higher ($F = 2.11$; $p < 0.001$; d.f = 232) chlorophyll *a* concentration compared to other stations, with the inshore station located near Cape St. Francis being the only exception. At this transect, nanophytoplankton concentrations increased from 0.10 ± 0.06 µg l^{-1} near the surface to 1.05 ± 1.47 µg l^{-1} at the DCM. Microphytoplankton showed the opposite trend (Fig. 3.18) with a decrease from near the surface (1.19 ± 2.82 µg l^{-1}) to the deeper waters (0.70 ± 0.66 µg l^{-1}). South of Durban, Transect 9 formed the southern boundary of the Natal Bight (Fig. 3.14). The DCM for the two nearshore stations was located at a depth of 20 to 30 m whereas the stations located further offshore had a DCM at depths of 50 to 60 m (Fig. 3.15c). The chlorophyll maximum at Transect 13 occurred between the surface and 25 m depth with a rapid decline in chlorophyll *a* concentrations below that (Fig. 3.16a). East of Port Elizabeth (Transect 17) the chlorophyll maximum was also located between the surface and a depth of 25 m but this pattern extended from the inshore station towards the inshore edge of the Agulhas Current core. Chlorophyll *a* concentrations of the surface waters near the Agulhas Current core were lower than those measured above the shelf (Fig. 3.14 and Fig. 3.16c). A patch of chlorophyll *a* with a concentration of > 2 µg l^{-1} was located above the south-eastern edge of the Agulhas Bank (Fig. 3.16c). The depth of the DCM at Transect 21 ranged between 10 and 42 m. Total chlorophyll *a* concentrations for the waters of Transect 21 ranged between 0.19 and 8.65 µg l^{-1}. Micro-, nano- and picophytoplankton contributed 40%, 29% and 31% of the total chlorophyll *a*.

Picophytoplankton contributed the least (Fig. 3.20) to the total biomass of phytoplankton and showed no significant ($F = 2.6$, $p > 0.05$; d.f. = 288) difference between transects apart from Transect 21. Vertical distribution of picophytoplankton showed no significant difference ($F = 0.12$; $p > 0.05$, d.f. = 297) between the surface, shallow and DCM waters. However, the deep (0.17 ± 0.17 µg l^{-1}) and below DCM (0.17 ± 028 µg l^{-1}) concentrations were significantly lower ($F = 0.12$; $p > 0.05$, d.f. = 297) than those measured at the DCM (0.45 ± 0.55 µg l^{-1}). Mean picophytoplankton concentrations ranged from 0.08 ± 0.07 to 0.41 ± 0.36 µg l^{-1} measured at Transect 1 to 20 to 0.83 ± 1.13 µg l^{-1} for Transect 21. The picophytoplankton of Transect 21 above DCM contributed more to total phytoplankton biomass than micro- and nanophytoplankton did (Fig. 3.20).

Chlorophyll *a* concentrations for microphytoplankton ranged from 0.30 ± 0.38 (Transect 3) to 1.10 ± 0.86 µg l^{-1} (Transect 21). Transect 21 had significantly ($F = 2.90$; $p < 0.05$, d.f = 288) higher microphytoplankton concentrations compared to Transects 1, 3, 5 and 8. Transect 19 had significantly ($F = 2.90$; $p < 0.05$, d.f = 288) higher microphytoplankton concentrations compared to Transect 3. Nanophytoplankton showed no significant difference ($F = 2.82$; $p < 0.05$, d.f = 288) with depth. The DCM on the other hand had a significantly higher nanophytoplankton component than the shallow waters as well as those below the DCM ($F = 2.82$; $p < 0.05$, d.f = 288).

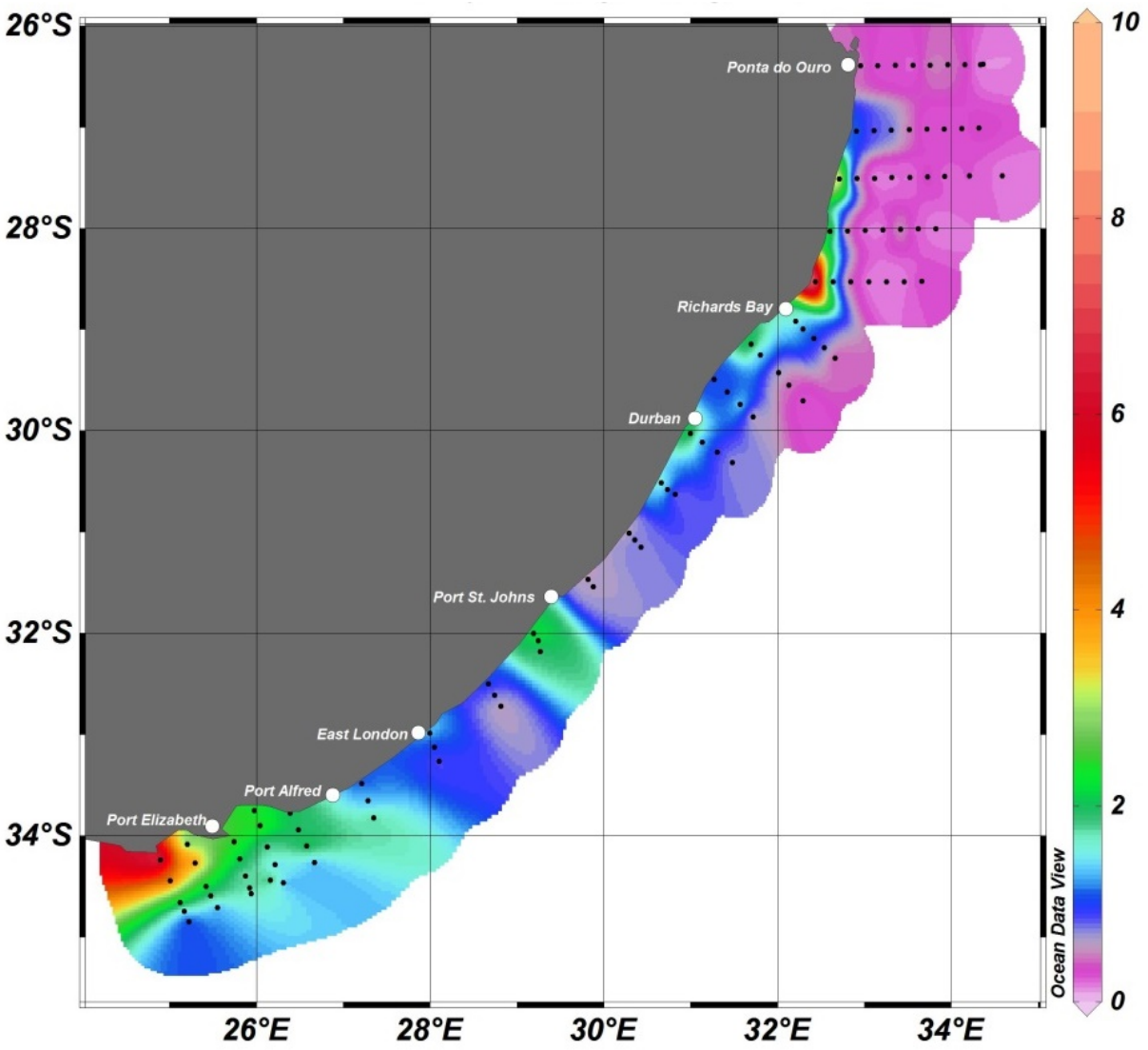

Fig. 3.14 Chlorophyll *a* concentrations (µg l^{-1}) measured along the Agulhas Shelf. The black dots represent the sampling stations.

Transect 1

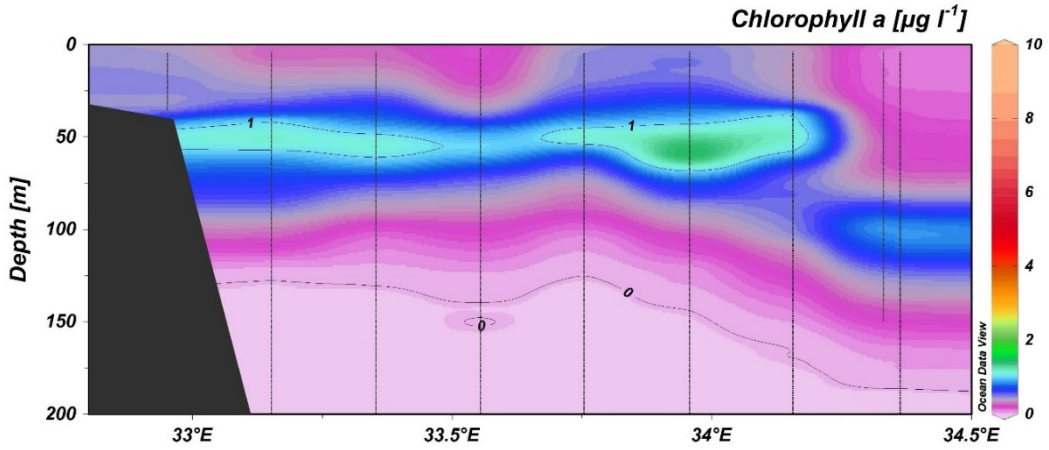

Transect 5

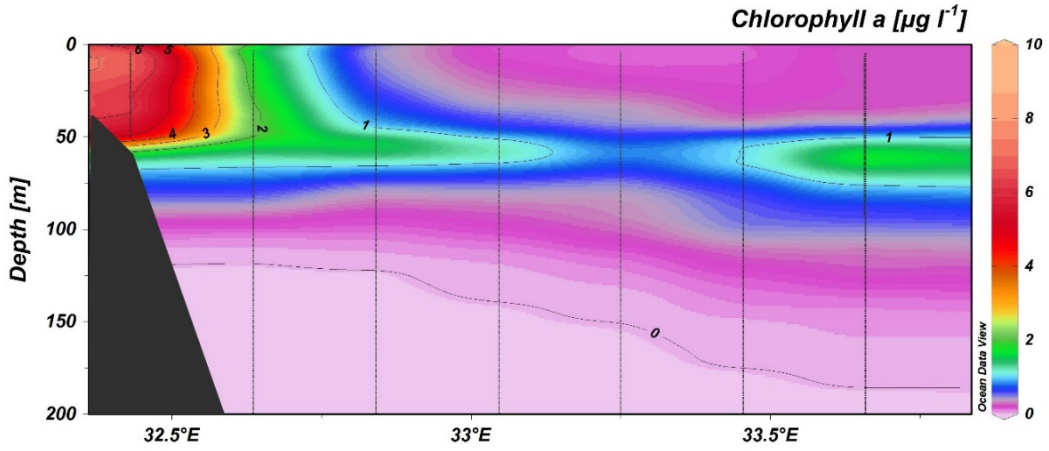

Transect 9

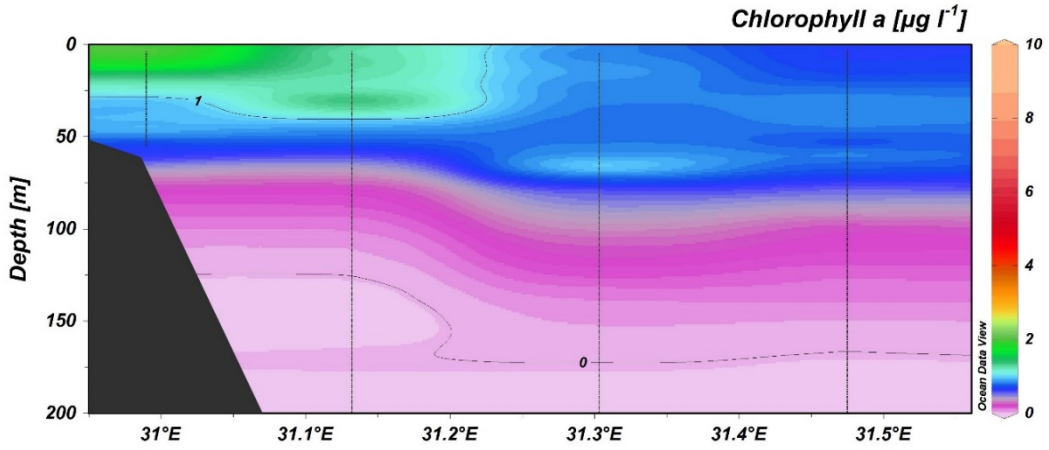

Fig. 3.15 Latitudinal depth transects of chlorophyll *a* (µg l^{-1}) concentration for waters of Transects 1, 5 and 9 along the Agulhas Shelf.

Transect 13

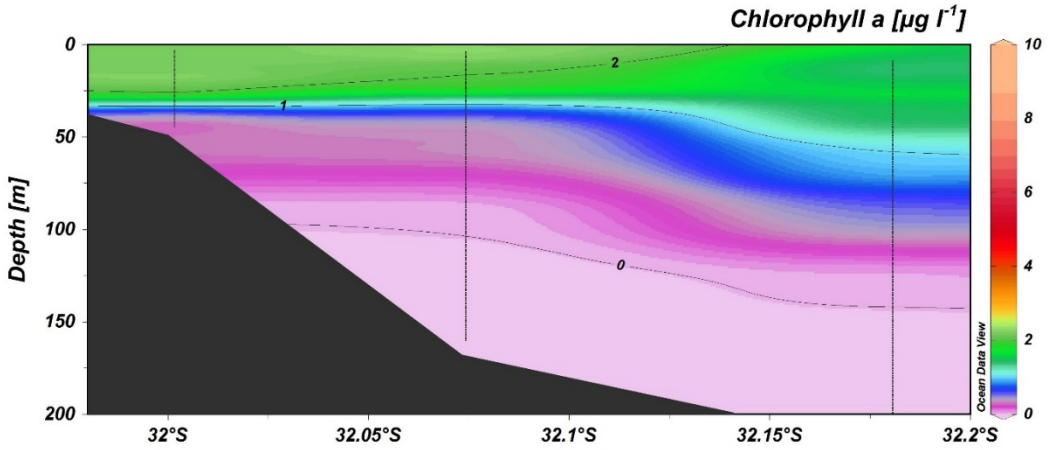

Transect 17

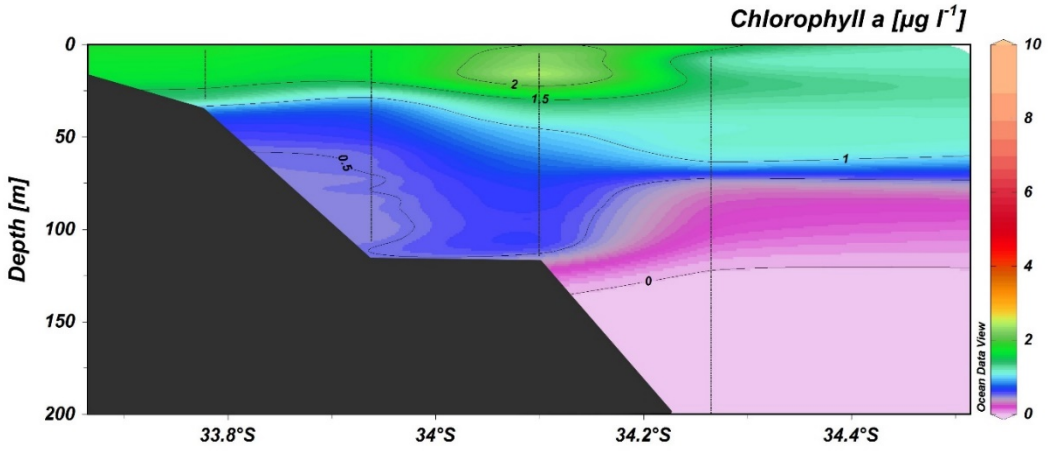

Transect 21

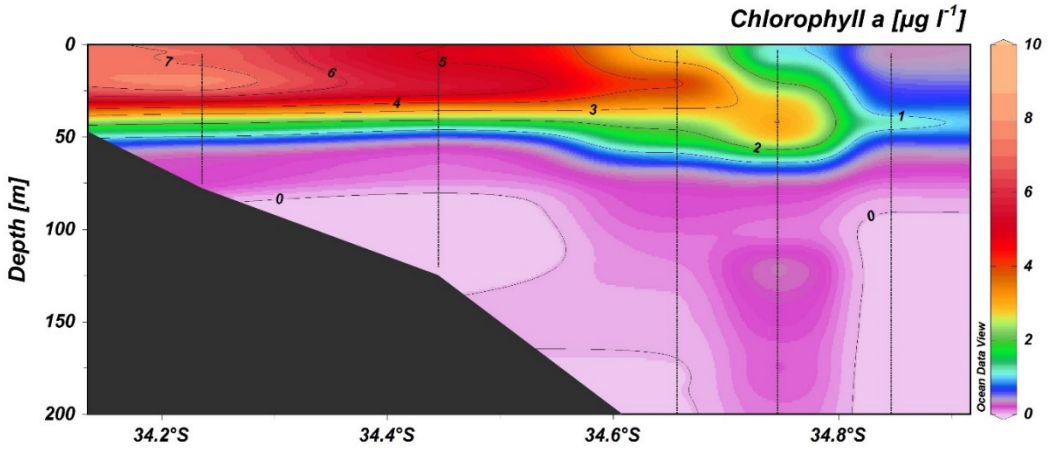

Fig. 3.16 Longitudinal depth transects of chlorophyll *a* (µg l^{-1}) concentrations for waters of Transects 13, 17 and 21 along the Agulhas Shelf.

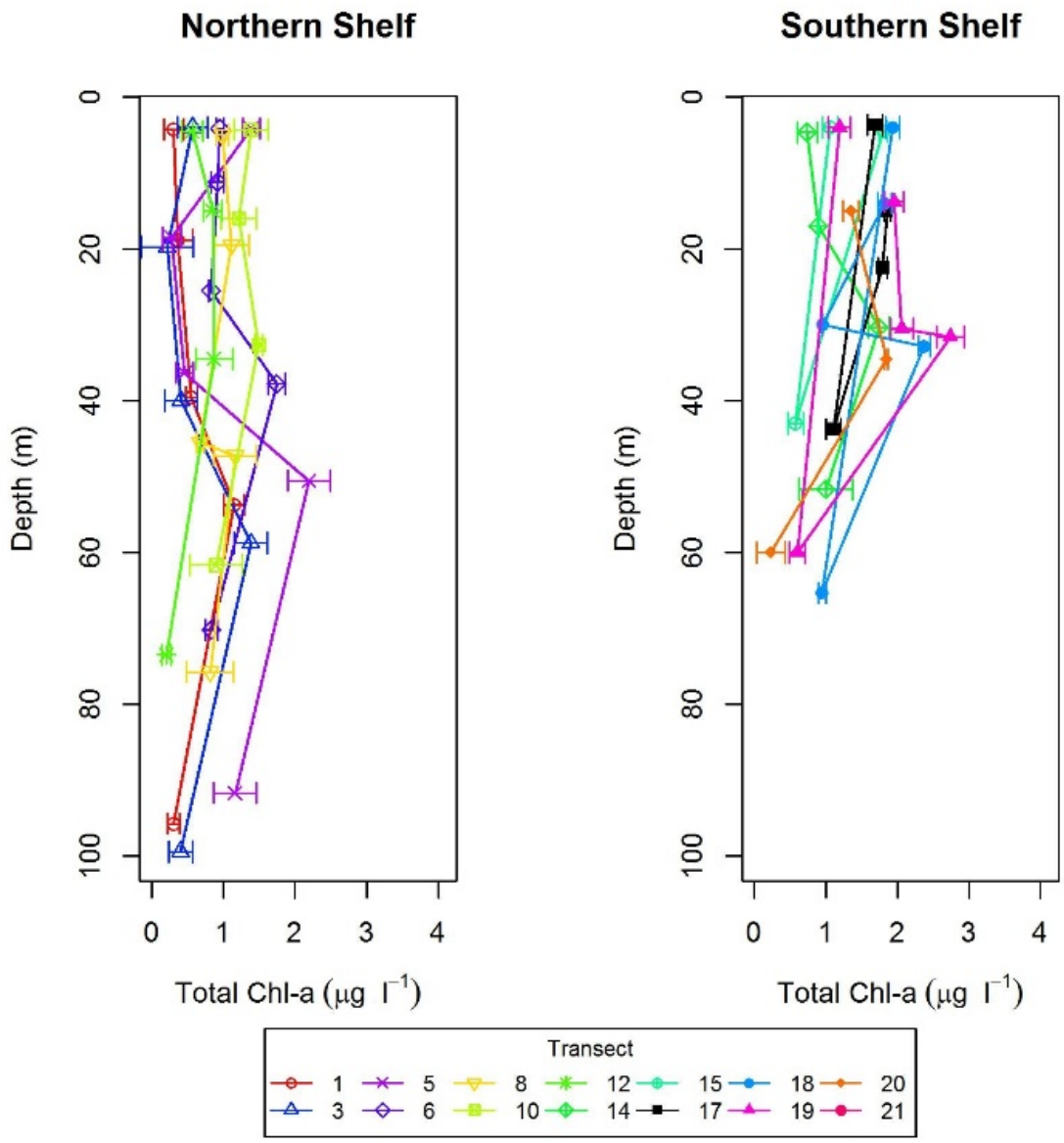

Fig. 3.17 Chlorophyll *a* (mean µg l^{-1} ± 1 S.D.) concentrations in the epipelagic zone of the Agulhas Shelf. Transects 1 to 13 represent the northern Agulhas Shelf and Transects 14 to 21 the southern Agulhas Shelf.

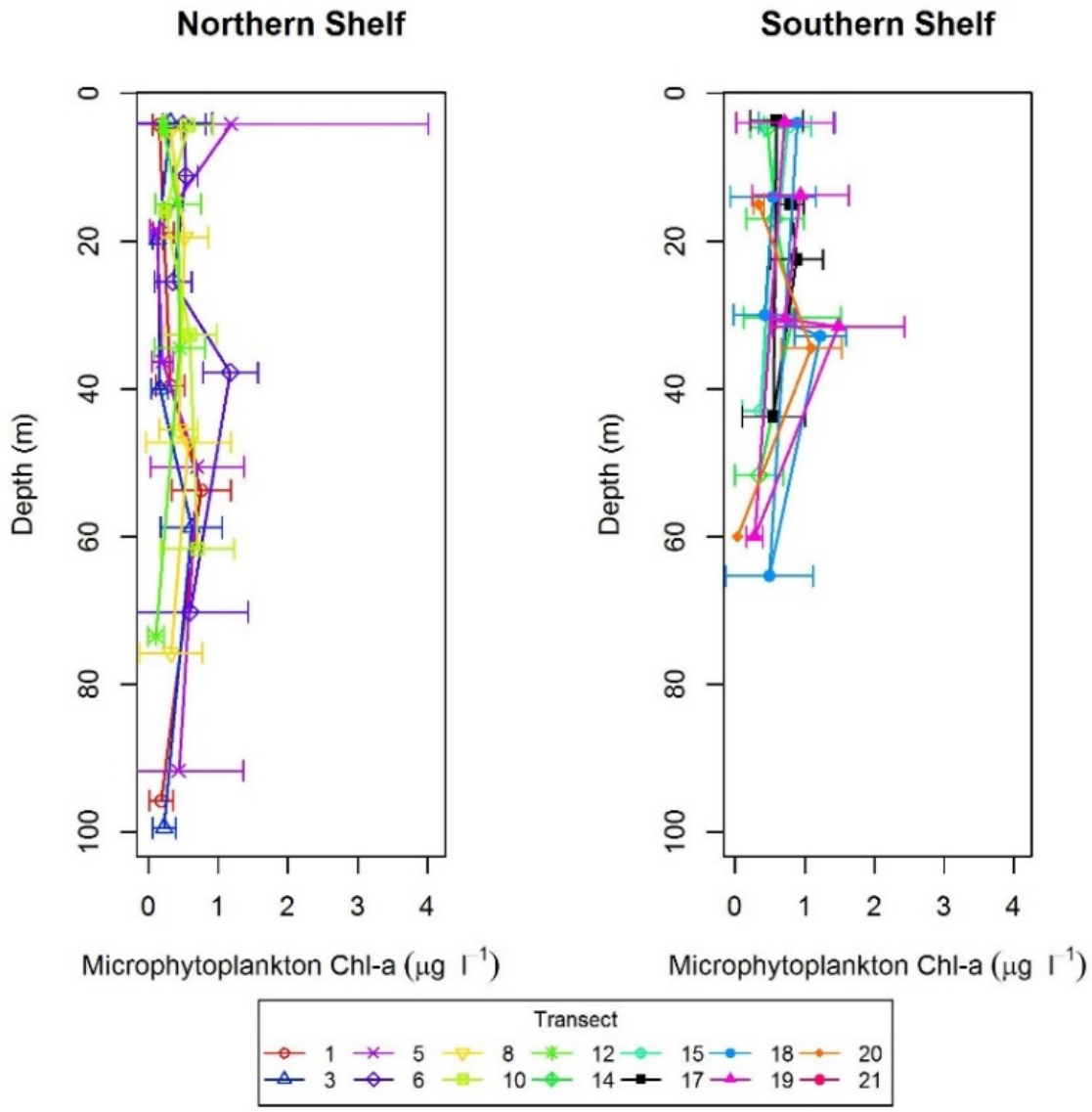

Fig. 3.18 Microphytoplankton chlorophyll *a* (mean µg l^{-1} ± 1 S.D.) concentrations in the epipelagic zone of the Agulhas Shelf. Transects 1 to 13 represent the northern Agulhas Shelf and Transects 14 to 21 the southern Agulhas Shelf.

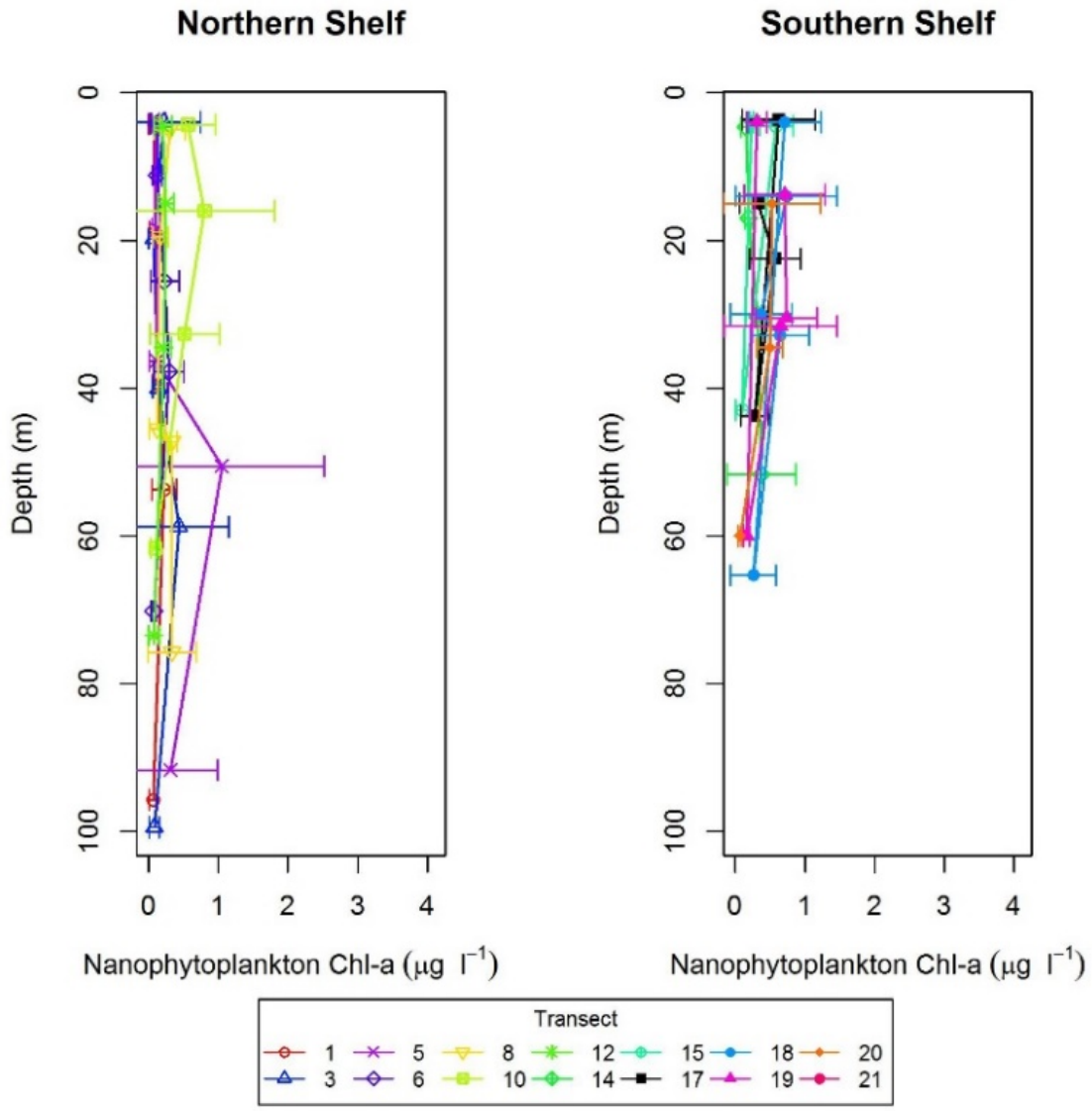

Fig. 3.19 Nanophytoplankton chlorophyll *a* (mean µg l^{-1} ± 1 S.D.) concentrations in the epipelagic zone of the Agulhas Shelf. Transects 1 to 13 represent the northern Agulhas Shelf and Transects 14 to 21 the southern Agulhas Shelf.

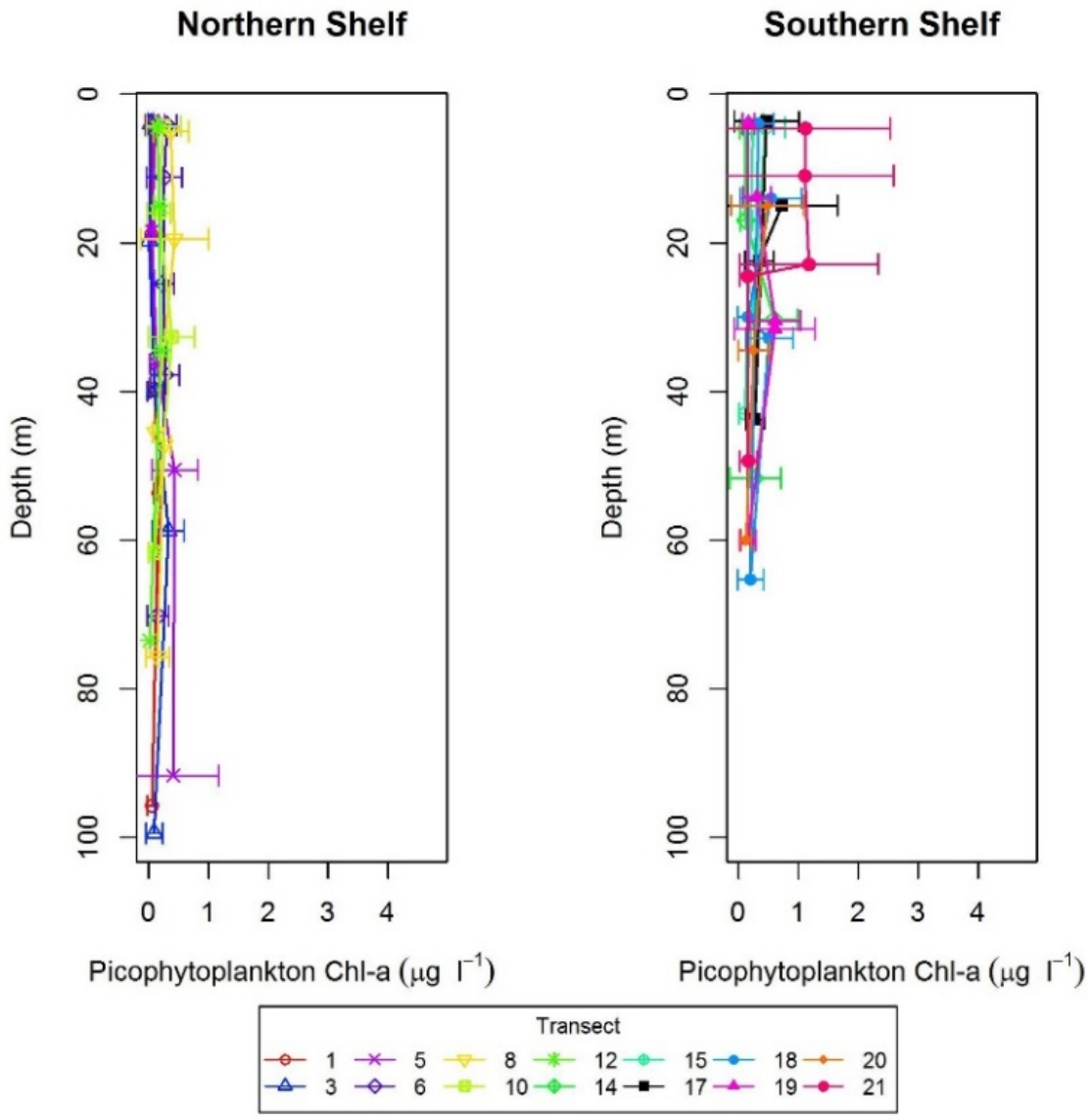

Fig. 3.20 Picophytoplankton chlorophyll *a* (mean µg l^{-1} ± 1 S.D.) concentrations in the epipelagic zone of the Agulhas Shelf. Transects 1 to 13 represent the northern Agulhas Shelf and Transects 14 to 21 the southern Agulhas Shelf.

3.4.3 Phytoplankton composition

A total of 118 phytoplankton taxa were recorded during the survey: 71 diatoms, 37 dinoflagellates, six silicoflagellates, two chlorophyte flagellates, one prymnesiophyte and one coccolithophore. The dominant genera (> 1 000 counts), in order of

dominance were: *Pseudo-nitzschia* spp. (diatom), *Thalassiosira* Cleve sp. (diatom), *Alexandrium* spp. (dinoflagellate), *Gymnodinium* spp. (dinoflagellate) and *Guinardia* spp. (diatom). These five genera contributed a total of 68% of all the cell counts. At the time of the survey *Pseudo-nitzschia* spp. was found to be four times more abundant than *Guinardia* spp.

The composition of the functional groups and the total number of phytoplankton species for 12 transects along the Agulhas Shelf is given in Fig. 3.21. Species diversity was greater in the northern Agulhas Shelf compared to the south. Evenness ranged from 0.48 to 0.92 with a mean of 0.69, thereby indicating a relative even distribution of species across the study site. The transect with the highest diversity was Transect 3 with 48 taxa recorded at the DCM and 50 taxa at the surface. Transect 5 had the second highest diversity with 41 and 36 taxa at the surface and DCM, respectively. Transect 7 was the only transect where a coccolithophore was found. The prymnesiophyte, *Chrysochromulina hirta* Manton was only found in the surface waters of Transect 21. Only six sites showed a dominance (>50% of counts) by one species (Table 3.2). Transect 1 was numerically dominated by dinoflagelates. Functional group dominance also changed from dinoflagellates to diatoms for Transects 3 to 21. There was a significant decline ($p < 0.001$; d.f = 24) in abundance of *Pseudo-nitzschia* spp. along the coast from north (Transect 3) to south (Transect 21). The cooler waters of the south showed an increase in abundance of *Thalassiosira* sp. and *Guinardia* spp. A similar change was also observed for dinoflagellates, with *Alexandrium spp.* being more abundant in the north and *Gymnodinium* spp. in the south.

Multivariate analysis grouped the 118 taxa into the following groups (Fig. 3.22): northern shelf (Transects 1- 13) and southern shelf (Transects 14 to 21). While the groups shared many of the same species, especially the more abundant ones such as *Pseudo-nitzschia* spp. and *Alexandrium* spp., rare taxa such as *Neidium septentrionale* Cleve-Euler and species in the genera *Stephanopyxis* (Ehrenberg) Ehrenberg and *Navicula* Bory were outliers of the southern shelf community. For the northern community, two species of *Oxytoxum* Stein, *Asterolampra sarcophagus* (Wallich) Greville and *Ceratium contortum* (Gourret) Cleve were outliers. The northern Shelf group consisted of smaller but overlapping communities Fig. 3.22.

A few taxa were only found in specific regions, for example the genus *Surirella* Turpin was only present in the waters of the south-eastern Agulhas Shelf, whereas the genera *Lithodesmium* Ehrenberg and *Scrippsiella* Balech ex A.R.Loeblich III were only present in the waters of the southern Agulhas Shelf.

Table 3.2 Transects where the phytoplankton was dominated by one genera (>50% of total).

Station and depth	Transect	% of counts	Dominant species	Species richness	Diversity score	Evenness score
9444_DCM	1	54.74	*Pseudo-nitzschia* spp.	29	1.89	0.56
9460_DCM	7	52.80	*Alexandrium* spp.	13	1.43	0/56
9484_Surface	15	51.10	*Thalassiosira* sp.	31	1.82	0.60
9491_DCM	17	55.19	*Guinardia* spp.	22	1.79	0.58
9500_DCM	19	50.32	*Thalassiosira* sp.	27	2.02	0.61
9508_DCM	21	58.31	*Thalassiosira* sp.	17	1.45	0.51

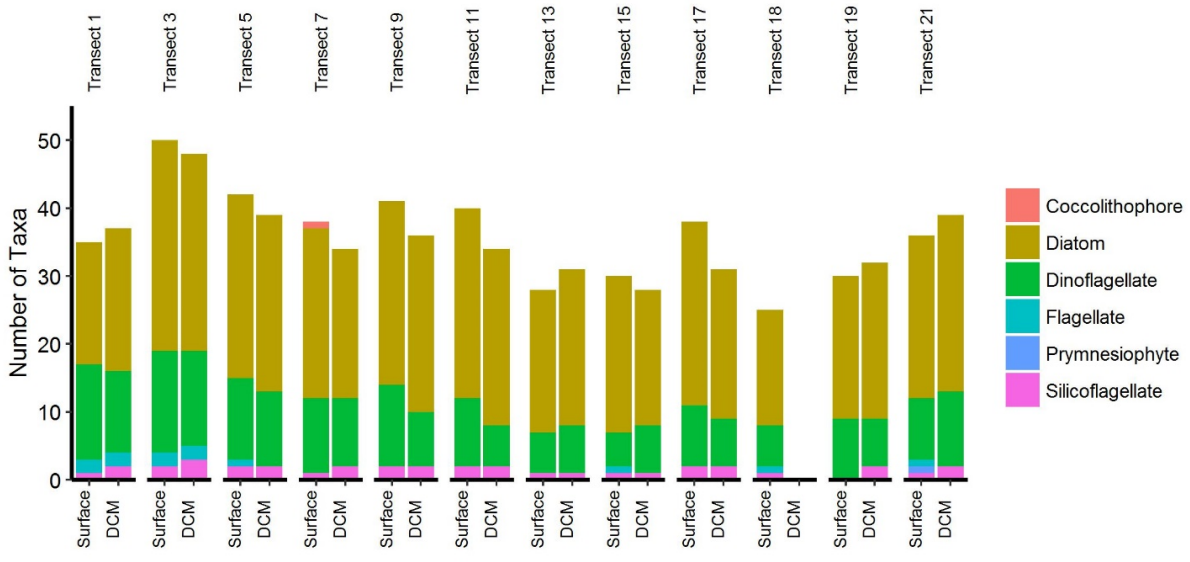

Fig. 3.21 Composition of the phytoplankton from the surface and deep chlorophyll maximum (DCM) of the 12 transects along the Agulhas Shelf.

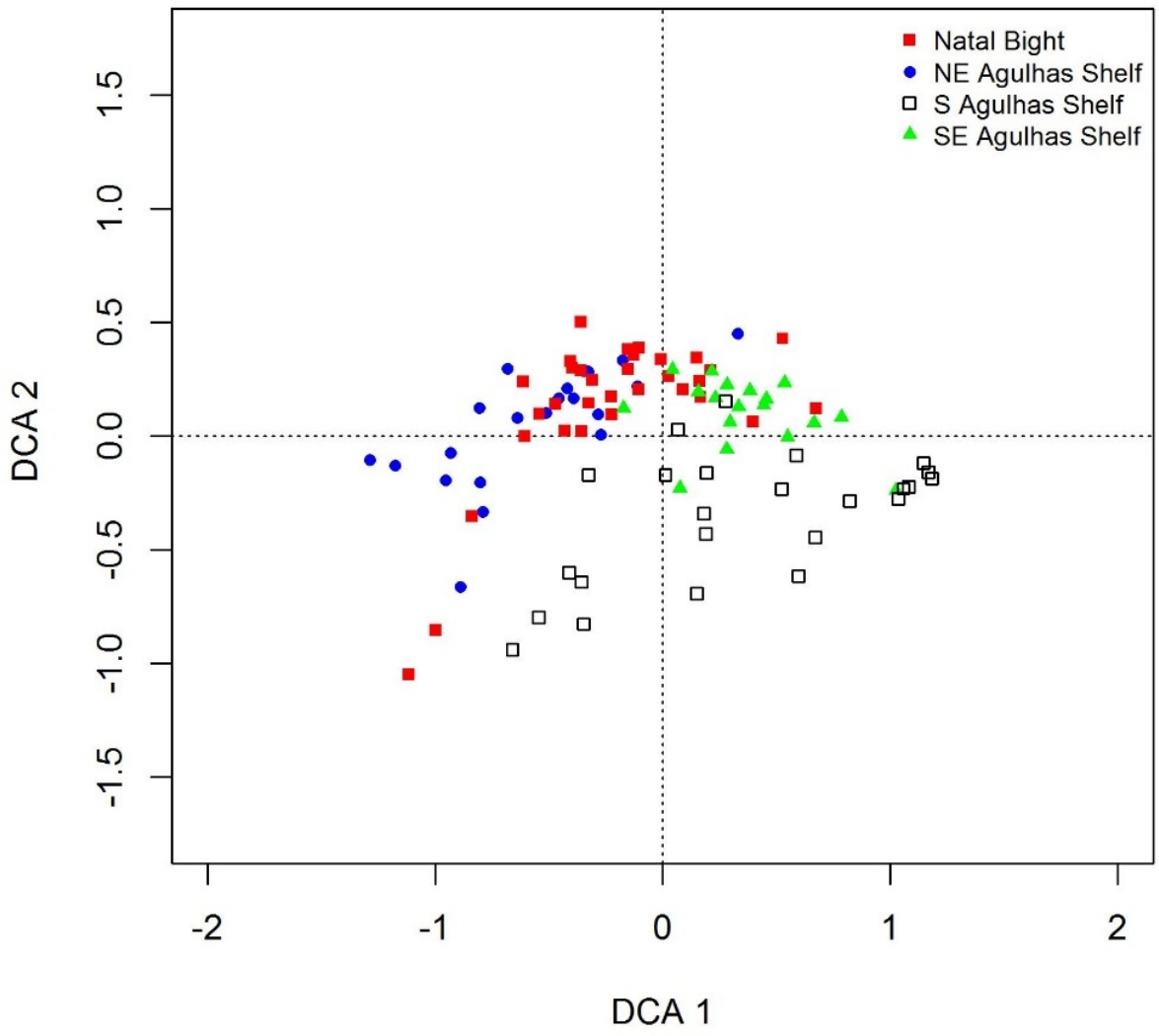

Fig. 3.22 Detrended Correspondence Analysis of phytoplankton samples from the 12 transects along the Agulhas Shelf. Solid symbols represent the northern Agulhas Shelf and empty squares the southern Agulhas Shelf.

Fig. 3.23 represents the abundance of the most abundant species for the Agulhas Shelf. Three of the 12 species were dinoflagellates and nine were diatoms. The dominance of *Pseudo-nitzschia* spp. and *Thalassiosira* sp. is evident.

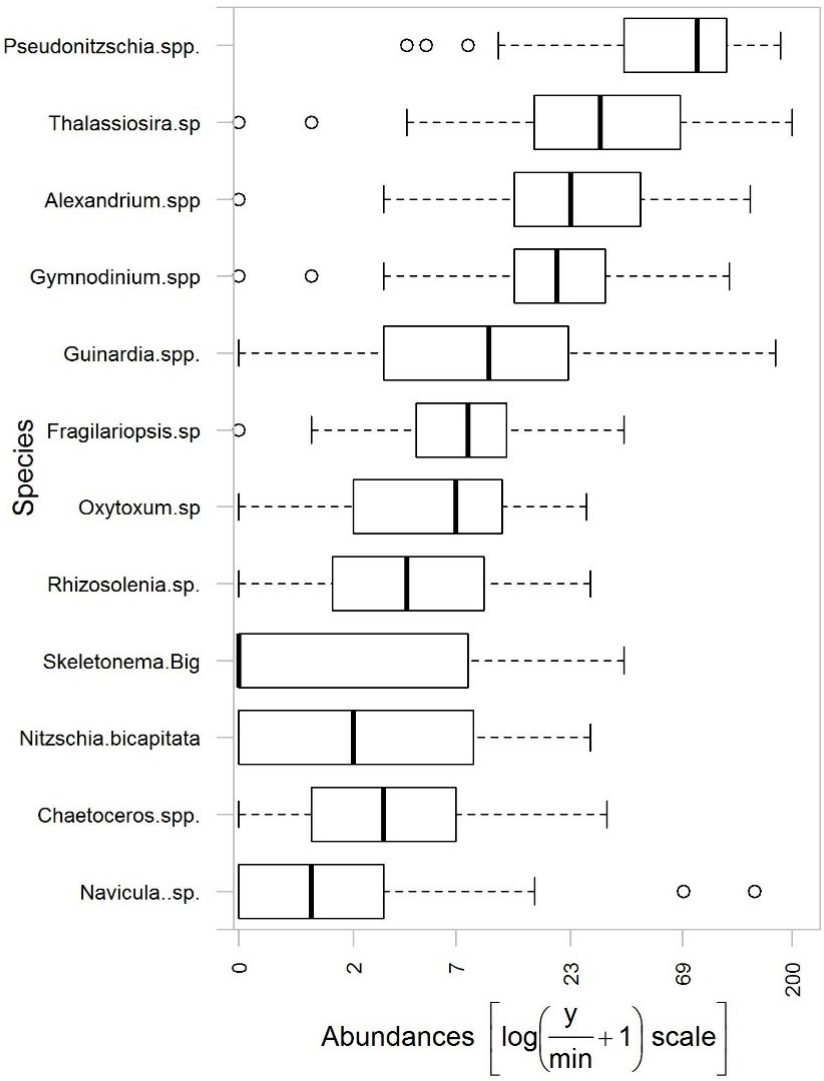

Fig. 3.23 The abundance of the most abundant species/genera of for the Agulhas Shelf. ○ represents outliers, bars represent the minimum and maximum, and the solid line is the median.

3.4.4 Environmental drivers of phytoplankton variability

The environmental drivers for the Agulhas Shelf are shown in Fig. 3.24 and Table 3.3. The eigenvalues for CCA 1 and CCA 2 were 0.172 and 0.078, explaining 73% of the total variance of the distribution. The first canonical axis accounted for 50% of this. The strongest correlations were between the first canonical axis and temperature (r = -0.91), oxygen (r = 0.77); phosphate (r = 0.40) and nitrate (r = 0.0.36). The second canonical axis accounted for 23% of the cumulative variation and was negatively correlated to oxygen (r = -0.53) and nitrite (r = -0.14) and

positively correlated to salinity (r = 0.56), nitrate (r = 0.55) and phosphate (r = 0.32). The north-eastern Shelf was characterised by warmer than average seawater, higher than average salinity and deeper bathymetry. These transects also had deeper than average DCMs. The southern Agulhas Shelf had higher than average oxygen; phosphate and nitrate concentrations as well as cooler than average seawater temperatures. Higher than average salinity was observed for the stations along the very narrow continental shelf between Durban and East London (Transects 9 to 15).

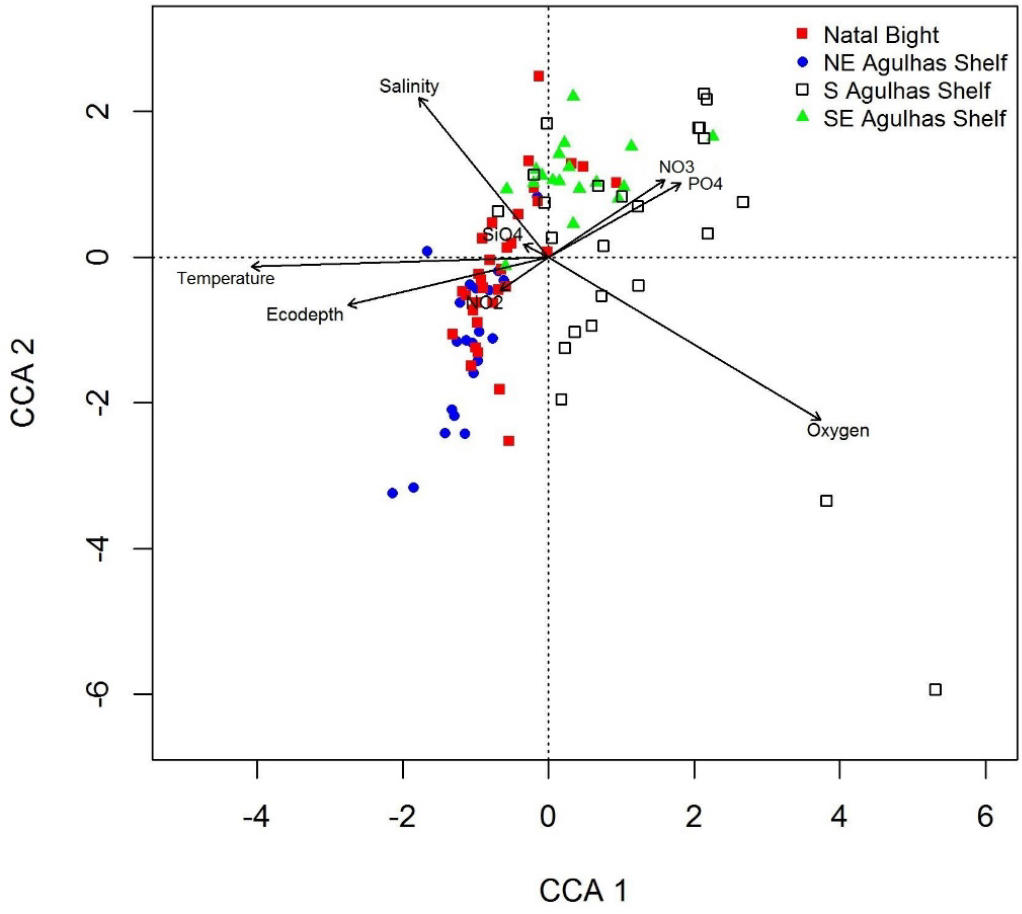

Fig. 3.24 Canonical Correspondence Analyses samples as constrained by environmental variables. The environmental drivers are indicated by the vectors. Solid symbols represent the northern Agulhas Shelf and open symbols the southern Agulhas Shelf.

A generalized linear model also confirmed that phytoplankton communities differed between the four regions of the Agulhas Shelf. The environmental drivers for this difference in community structure are provided in Table 3.3. From Table 3.3 it is clear that temperature, salinity and nitrite are the important environmental drivers for the different phytoplankton communities of the regions of the Agulhas Shelf.

Table 3.3. The GLM model of environmental drivers of phytoplankton community differences of the Agulhas Shelf.

Environmental Variable	d.f.	Dev.	p
Intercept	94		
Region	91	1264.8	0.001***
Temperature	90	472.3	0.001***
Salinity	89	265.5	0.001***
Dissolved Oxygen	88	183.3	0.001***
Nitrate	87	178.9	0.001***
Nitrite	86	189.6	0.001***
Silicate	85	125.0	0.031 *
Phosphate	84	125.6	0.045 *

Sigificance Codes: *** p = 0.001, ** p = 0.01, * p = 0.05

3.5 Discussion

3.5.1 Physical and chemical oceanography

The geographical spread of the transects along the Agulhas Shelf sampled during the survey in 2009 showed significant differences in temperature, salinity and dissolved oxygen within the waters of the euphotic zone. The range in epipelagic temperature (10.76 to 23.93°C), salinity (34.91 to 35.54) and dissolved oxygen (3.17 to 6.24 mg l^{-1}) observed in the Agulhas Current along the continental shelf is consistent with previously reported literature (Christensen, 1980a; Lutjeharms *et al.*, 2000b; Lutjeharms, 2006; D'Addezio and Subrahmanyam, 2016). Cooler upwelling regions along the coast were also observed. These upwelling regions are consistent with those reported in the literature (Schumann *et al.*, 1982; Lutjeharms *et al.*, 2000a; Lutjeharms, 2006; Goschen *et al.*, 2012; Krug *et al.*, 2014; Goschen *et al.*, 2015). Surface water to the north of the Natal Bight (Transects 6 - 9) was 1 to 2°C cooler compared to surface water of the stations located off the Natal Bight (Fig. 3.3). Upwelling regions were observed near East London; Port Alfred as well as the eastern shores of St. Francis Bay (Fig. 3.3). Fig. 3.3 clearly shows two temperature gradients, one across the Agulhas Shelf and the second in a north-south direction along the Shelf. Surface salinity plots indicate distinct water masses along the shelf. The surface salinity measurements in the vicinity of Port Alfred and southwards had a relatively low mean salinity of 35.3, lower than that of the adjacent surface waters of the Agulhas Current. Lutjeharms *et al.* (2000a) made a similar observation for the Port Alfred region. On the northern Shelf, the opposite pattern was observed - inshore stations had a mean salinity of 35.4, higher than that of the adjacent surface waters of the Agulhas Current.

The distribution of nutrients plays an important role in controlling the composition of phytoplankton communities. Nitrogen and phosphorus are the main inorganic nutrients needed for growth in marine ecosystems, although silicate could limit the growth of diatoms (Yool and Tyrrell, 2003; Crombet *et al.*, 2011). Iida and Odate (2014) reported that diatoms do not grow in concentrations below 0.001 µg l^{-1} silicate. The Agulhas Shelf exhibited strong cross-shelf nutrient gradients with concentrations consistently higher at the inshore stations compared to the stations

near the Agulhas Current core. Nitrate showed a strong north-south gradient along the shelf (Fig. 3.7). This was expected, as the Agulhas Current is nitrate-poor and most likely consists of subtropical surface waters (Lutjeharms *et al.*, 1996). Elevated surface nutrients found at certain locations along the Shelf were associated with river mouths, bays and prominent capes, anthropogenic inputs and upwelling events along the coast. The surface nutrient concentrations just north of Richards Bay and south of East London were the highest for the Agulhas Shelf. This is particularly pronounced for phosphate, where concentrations greater than 0.75 µM were measured. Nutrient concentrations also increased with depth on the Agulhas Shelf to levels similar to that found below the thermocline. Nutrients are mostly biologically depleted in the euphotic waters and the thermal stratification of the water column forms a barrier to nutrient replenishment from deeper waters, restricting their availability to the euphotic zone (Lutjeharms *et al.*, 1996). The concentrations of nitrate, nitrite; phosphate and silicate at depth ranged from 0.28 to 23.39 µmol l^{-1}, 0 to 0.42 µmol l^{-1}, 0.06 to 1.85 µM and 0.01 to 15.71 µM, respectively. These values are in range with those that are reported for South Indian Central Water (Meyer, 1992), Natal Bight (Meyer *et al.*, 2002), Agulhas Shelf (Lutjeharms, 2006) and eastern Agulhas Bank waters (Lutjeharms *et al.*, 1996; Lutjeharms, 2006).

Nitrate and phosphate concentrations for the northern Natal Bight are within the range reported by Meyer *et al.* (2002), but are towards the lower end of the range. Surface silicate concentrations recorded in the northern Natal Bight during this study were more variable and extended both the maximum and minimum concentrations reported by Meyer *et al.* (2002). Meyer *et al.* (2002) showed that nutrient concentrations decreased southwards over the Natal Bight. This study, however, an increase in nitrate concentrations in surface waters was recorded southwards over the Natal Bight. Transects 6, 7 and 9 reached maximum concentrations of 1.82, 1.40 and 1.35 µmol l^{-1}, respectively. Silicate concentrations also increased southwards over the Natal Bight with maximum concentrations ranging between 1.82 and 3.41 µM for Transect 6 and 9 respectively. Phosphate concentrations decreased southwards over the Natal Bight with maximum concentrations ranging between 0.31 and 0.59 µM for Transect 8 and 9. The low nitrate concentrations along the Natal Bight suggest that at the time of sampling the phytoplankton of these waters were

nitrate limited. The deviation below the Redfield Ratio lines in Fig. 3.10 (3-9) and Fig. 3.11 (3-9) for N:P (16:1) and N:Si (1:1) supports this result. The N:Si slopes of 2-3:1 (Fig. 3.11) implies greater biotic depletion of nitrate relative to silicate. The deviation away from the N:Si Redfield Ratio of 1:1 suggests that the nitrate uptake was by phytoplankton that do not utilise silicate. Read *et al.* (2000) made a similar observation for the frontal zone between the Southwest Indian Subtropical gyre and the Southern Ocean.

From East London (Transect 14) southwards, there is a marked increase in nitrate concentrations. Although this area has a high nutrient concentration, the chlorophyll *a* response did not reflect this (Fig. 3.14), suggesting that at the time of the sampling upwelling had occurred but the phytoplankton had not yet responded. Surface nutrients were lower for Algoa Bay compared to St Francis Bay.

The distribution and composition of phytoplankton communities were influenced by temperature and the distribution of nutrients. Using half saturation constants (K_s), it is possible to determine whether the nutrient concentrations measured on the Agulhas Shelf are sufficient to support phytoplankton growth. This constant shows the ability of phytoplankton to utilise low nutrient concentrations and this is of ecological significance. For nitrate Eppley *et al.* (1969) reported a *Ks* value of ≤ 0.2 µM for natural oligotrophic marine communities and ≥ 1.0 µM for eutrophic conditions. Pondaven *et al.* (1998) in their model used a *Ks* value for nitrate and silicate of 0.3 - 0.8 µM and 0.83 µM, respectively. However, these values are for diatoms in the Southern Ocean. The nitrate in the epipelagic ranged from 0.01 to 23.39 µM. The median of 0.89 µM for nitrate is close to the reported Ks values, suggesting that about half the stations sampled for the Agulhas Shelf were nitrate limited for diatoms. Most of these nitrogen-limited samples were collected from the surface waters of the south-eastern Agulhas Shelf and Natal Bight. Considering the lower end of the *Ks* scale, it appears that large parts of the Agulhas Shelf have sufficient nitrate to support oligotrophic marine communities. Silicate concentrations of Agulhas Shelf waters are sufficient to support diatom communities – this were generally higher (~ 2 µM) than the *Ks* of 0.83 µM. Nishikawa *et al.* (2010) reported *Ks* values of 0.68 to 6.67 µM for phosphate uptake for various phytoplankton taxa. This range of values will classify the Agulhas Shelf, with a maximum concentration of 1.85 µM, as

phosphate limited. However, the deviations from the N:P Redfield Ratio of 16:1 (Fig. 3.10) does not support this. Certain functional groups show a preference toward specific nutrient ratios. Howarth (1988) reported that blue-green algae prefer low N:P ratios and diatoms prefer high Si:P (Sommer, 1994). Dinoflagellates prefer both low N:P and Si:P ratios (Margalef, 1978). The positive correlations (Table 3.1) between nitrate and phosphate as well as phosphate and chlorophyll *a* concentrations suggested that phytoplankton biomass was controlled by the availability of these nutrients. Temperature was inversely correlated with chlorophyll *a*, nitrate and phosphate (Table 3.1). Rykaczewski and Dunne (2010) and Van de Poll *et al.* (2013) make reference to the importance of temperature in determining nutrient availability for phytoplankton by influencing vertical exchange with deeper nutrient-rich water. An increase in temperature will lead to an increase in stratification (Rykaczewski and Dunne, 2010; Thomas *et al.*, 2012) of the epipelagic waters. This, in turn, will reduce the availability of nutrients in the surface waters for phytoplankton and may favour some functional groups more than others. An increase in stratification and less ingress of nitrogen (in the form of nitrate) will be disadvantageous towards diatoms as they prefer well mixed, upwelled waters to keep them suspended within the euphotic zone and supply them with nitrogen. Dinoflagellates on the other hand are more motile and are able to move between nutrient-rich waters at depth and the euphotic zone, making them more competitive within stratified waters. Observed abundance data for the Agulhas Shelf support both scenarios of preference by functional groups.

3.5.2 Spatial variability of phytoplankton

Barlow *et al.* (2008) found that phytoplankton biomass appeared to be greater in the Natal Bight than the Delagoa Bight. In this study, only the southern section of the Delagoa Bight was sampled, however, from Fig. 3.14 it is clear that the surface chlorophyll *a* was lower for the Delagoa Bight area (mean 0.45 ± 0.69; range 0.05 to 3.66 µg l^{-1}; n = 26) compared to the Natal Bight area (mean 1.09 ± 1.47; range 0.1 to 8.23 µg l^{-1}; n = 31). Surface chlorophyll *a* concentration for the eastern section of the Agulhas Bank, including Algoa Bay and St Francis Bay (mean 2.15 ± 1.79; range 0.08 to 8.47 µg l^{-1}; n = 26), was higher compared to both Delagoa and Natal Bight.

The overall trophic status of the Natal Bight may be classified as mesotrophic. However, towards the north and in the core of the Agulhas Current, surface waters appear to be oligotrophic. This is expected, as the source of the Agulhas Current is from oligotrophic waters (Lutjeharms, 2006). The overall trophic status of the Natal Bight and the St Lucia upwelling cell may be classified as mesotrophic. This is most likely due to eddy-driven upwelling processes. Diatoms, especially *Pseudo-nitzschia* spp. contributed most to surface chlorophyll *a* as was observed by Barlow *et al.* (2008). The steep continental shelf region south of Durban to the east of Port Alfred may be classified as oligotrophic. The eastern section of the Agulhas Bank and Cape St. Francis were mesotrophic with elevated biomass measured around Cape St. Francis. The diatoms *Thalassiosira* sp. and *Guinardia* spp. were the more abundant genera in the southern waters.

3.5.3 Phytoplankton composition

The phytoplankton community showed a north-south gradient of decreasing diversity along the shelf. Diatoms and dinoflagellates were the dominant phytoplankton functional groups. Due to their enhanced nutrient uptake rates, the oligotrophic waters of the Indian Ocean are characterised by small size classes of phytoplankton groups such as chlorophyte flagellates (Twomey *et al.*, 2007). Barlow *et al.* (2008) found that both the Delagoa and Natal Bight phytoplankton communities were generally dominated by the small flagellates with patches where diatoms were dominant. However, small flagellates were only numerically dominant in the surface waters of Transect 1. Barlow *et al.* (2008) also reported that small flagellates were generally dominant in waters where total chlorophyll *a* was less than 1 µg l^{-1} and diatoms were most prominent at higher concentrations. In the Arabian Sea, nanophytoplankton were abundant in waters with chlorophyll *a* concentrations were between 0.3 and 0.7 µg l^{-1} (Bouman *et al.*, 2005). In the temperate waters of the northeast Atlantic, chlorophyll *a* concentrations ranged between 0.4 and 1 µg l^{-1} (Barlow *et al.*, 2004).

The dominant diatom and dinoflagellate genera for the northern shelf were *Pseudo-nitzschia* spp. and *Alexandrium* spp. that accounted for a large percentage of the cell counts. A large proportion of the taxa were widespread throughout Shelf waters.

Although the environmental and biological data separates the Shelf stations into northern and southern communities, the species composition was sufficiently similar to be considered a single community. It is only the rare species that separated the phytoplankton community into northern and southern communities.

3.5.4 Environmental drivers of phytoplankton variability

The environmental drivers most closely associated for the observed species distribution of Agulhas Shelf waters were temperature and nitrate concentration. Similar results were found by Barlow *et al.* (2008) in that temporal changes in diatom and dinoflagellate communities could be related to temperature and nutrients. Various studies have demonstrated that temperature is an important environmental parameter that influences biological processes in the ocean and that phytoplankton community structures vary in a regular and predictable pattern with temperature (Bouman *et al.*, 2003; Bouman *et al.*, 2005; Platt *et al.*, 2005; Barlow *et al.*, 2008). In general, it has been observed that at lower temperatures the phytoplankton is dominated by microphytoplankton (such as diatoms), nanophytoplankton is more abundant at intermediate temperatures, and picophytoplankton is the most abundant size class at high temperatures (Bouman *et al.*, 2003; Bouman *et al.*, 2005). The results of this study suggest that temperature is an important environmental parameter that has an influence on phytoplankton community structure along the Agulhas Shelf. The constrained ordination analysis showed a negative correlation between nitrate and silicate concentrations indicating that either one or the other nutrient was limiting at any point in time. The ordination showed that nitrite and silicate had no significant influence on the distribution and composition of the phytoplankton communities.

3.6 Conclusions

The Agulhas Current controls the distribution and movement of nutrients along the Agulhas Shelf over the largest part of the Shelf. It does this predominantly by forcing upwelling at various locations, such as the Natal Bight and the eastern Agulhas Bank. It is these upwelling events that are the main source of nutrients for the Shelf and from these upwelling sites nutrients are moved southwestward with a

concomitant increase in primary productivity along the Shelf. Nitrate was the most limiting nutrient during the survey of the Shelf area with silicate being limiting towards the southern part of the Shelf. It is doubtful that this would have had a negative impact on diatom production because of the constant allochthonous introduction of inorganic nutrients from the Port Alfred upwelling cell as well as from wind induced upwelling events at prominent capes. Secondly, diatoms are more abundant in regions of upwelling than dinoflagellates and other functional groups utilizing the availability of upwelled nitrate for growth. Outflow from rivers such as the Thukela, can also be a source of nutrients to the Natal Bight especially during the wet season (Scharler *et al.*, 2016). This increase in nutrients in the Thukela mouth region was most notable in sedimentary samples.

The null hypothesis proposed was that there is no change in the phytoplankton community along the Shelf. This could not be completely rejected. The oligotrophic water in the north was not dominated by chlorophyte flagellates. Diatoms were in general the dominant functional group over the Agulhas Shelf, with a few exceptions along the coast. This study contributes significantly to our knowledge of phytoplankton distribution and ecology along the Agulhas Shelf. This survey, however; provided only a snapshot and so could not resolve f processes that have time scales of more than a day.

4 The Agulhas Bank

4.1 Abstract

The distribution of phytoplankton across the Agulhas Bank is mainly linked to various upwelling events along the eastern and western Agulhas Bank. The environmental drivers most responsible for the observed species distribution on the Agulhas Bank were temperature and phosphate. On the eastern Agulhas Bank; phytoplankton distribution and surface chlorophyll *a* is bound to the inshore edge of the Agulhas Current. Chlorophyll *a* and nutrients in the Agulhas Current are typical of oligotrophic, subtropical surface waters that are relatively unproductive when compared to the meandering inshore waters. *Thalassiosira weissflogii* (Grunow) G.Fryxell & Hasle*; Pseudo-nitzschia* H.Peragallo spp. and *Guinardia* H.Peragallo spp. were the more abundant in the eastern Bank coastal waters and contributed the most to surface chlorophyll *a* for the Agulhas Bank. Both the eastern and western Agulhas Bank were mesotrophic in nature with localised patches of increased biomass around prominent capes. The phytoplankton community showed an east-west gradient of decreasing diversity across the Bank. Diatoms were the dominant (>50% of total number of species) phytoplankton taxonomic group with the other functional groups making a significantly smaller contribution to the phytoplankton community.

4.2 Introduction

Fully constituted on the South African-Mozambican border, the Agulhas Current is a warm western boundary current that narrowly follows the continental shelf of the east coast of South Africa. Near the latitude of Port Elizabeth, the continental shelf starts to widen forming the Agulhas Bank. The Agulhas Bank is a triangular-shaped widening of the continental shelf (Hutchings, 1994; Lutjeharms *et al.*, 1996) that extends approximately 300 km offshore and covers an area of 80 000 km^2 (Lutjeharms *et al.*, 1996). The Agulhas Bank falls within South Africa's Exclusive Economic Zone (EEZ) and is a productive region and an important spawning ground for commercial species such as kingklip (*Genypterus capensis*), anchovy (*Engraulis capensis*), sardine (*Sardinops sagax*), sole (*Austroglossus pectoralis*), squid (*Loligo*

reynaudii), hake (*Merluccius capensis*), and yellowtail (*Seriola lalandi*) (Hutchings, 1994; Roberts, 2005; Roberts and van den Berg, 2005).

The Agulhas Bank can be divided into three areas, the eastern, central and western Bank (Lutjeharms, 2006; Jackson *et al.*, 2012). Jackson *et al.* (2012) used the shallow inner bank along the 21°E meridian as the boundary between the eastern bank and western banks. The long and wide eastern Bank is dominated by the warm oligotrophic Agulhas Current (Hutchings, 1994) whereas the western Bank is influenced by the cold nutrient-rich waters of the Benguela Current (Lutjeharms *et al.*, 1996; Lutjeharms, 2006). The Agulhas Bank is the meeting area for two oceans, the Indian Ocean and Atlantic Ocean. Swart and Largier (1987) found water from the southwest Indian Ocean on the eastern Agulhas Bank, suggesting that the water is advected onto the Bank. This cross-shelf transport, the hydrology, as well as the circulation of the Agulhas Bank is influenced by the Agulhas Current via a range of processes such as variations in the Agulhas Current strength, the intrusion of the Agulhas Current via upwelling on to the bank (Lutjeharms *et al.*, 2000a), meanders, filaments, water plumes (Lutjeharms *et al.*, 1989a; Lutjeharms *et al.*, 2003), Natal Pulses (Casal *et al.*, 2009) and southerly winds (Goschen and Schumann, 1990). The narrow and steep western bank is influenced by both the Agulhas Current and the Benguela Current. With the former, warm surface water is advected onto the western bank via the eastern bank and with the latter, cold central Atlantic water is upwelled onto the western bank (Chapman and Largier, 1989; Largier, 1990). Schumann (1999) considered the 10 to 15 km wide coastal region as a separate oceanographic region to that of the eastern, western and central regions (Lutjeharms, 2006). This coastal region tends to be dominated by wind driven coastal-upwelling (Schumann *et al.*, 1982; Largier, 1990) and eastward flowing (alongshore) currents (Roberts and van den Berg, 2005; Roberts, 2010). Another oceanographic area of interest is the cold ridge, located offshore between Plettenberg Bay and Mossel Bay. The cold ridge a semi-permanent oceanographic feature where there is an upward doming of the thermocline (Roberts and van den Berg, 2005).

This study focussed on the physico-chemical oceanographic environment as drivers of phytoplankton biomass, composition and biogeography. Various studies have

focussed on specific sections of the Bank, e.g. Algoa Bay (Goschen *et al.*, 2015), the eastern Agulhas Bank (Probyn *et al.*, 1995; Roberts, 2005) and western Agulhas Bank (Largier *et al.*, 1992; McMurray *et al.*, 1993; Mitchell-Innes *et al.*, 1999). This study is the first to investigate the Agulhas Bank as a whole and determine the environmental drivers of the phytoplankton community and biomass across the Bank. To determine whether the Agulhas Bank has an influence on the biological productivity we developed the following hypothesis:

Phytoplankton on the Agulhas Bank changes from

- an elevated biomass, diatom-dinoflagellate dominated community in the mesotrophic waters of the eastern Agulhas Bank to
- a low biomass, diatom dominant community in the waters of the western Agulhas Bank.

4.3 Study Area

An oceanographic survey was done onboard the FRS *Algoa* in August and September 2010. Fifteen across-shelf transects with two to sixteen oceanographic stations each were sampled from the coast to beyond the 1 000 m isobath (Fig. 4.1). Transects were positioned half a degree apart and stations approximately 10 nautical miles apart. Environmental data were collected *in situ* from the *FRS Algoa* during Cruise 411. Sampling was conducted within the framework of ACEP II (African Coelacanth Ecosystem Program Phase II) and the ASCLME (Agulhas and Somali Current Large Marine Ecosystems) Project. The study area covered the Agulhas Bank from Port Alfred to Cape Hangklip, South Africa. The two large bays, Algoa Bay and St Francis Bay, were also included within the study area, even though they were also sampled as part of the Agulhas Shelf cruise.

The methodology and statistical analysis used in this study was identical to that presented in sections 3.3.2, 3.3.3, 3.3.4 and 3.3.5.

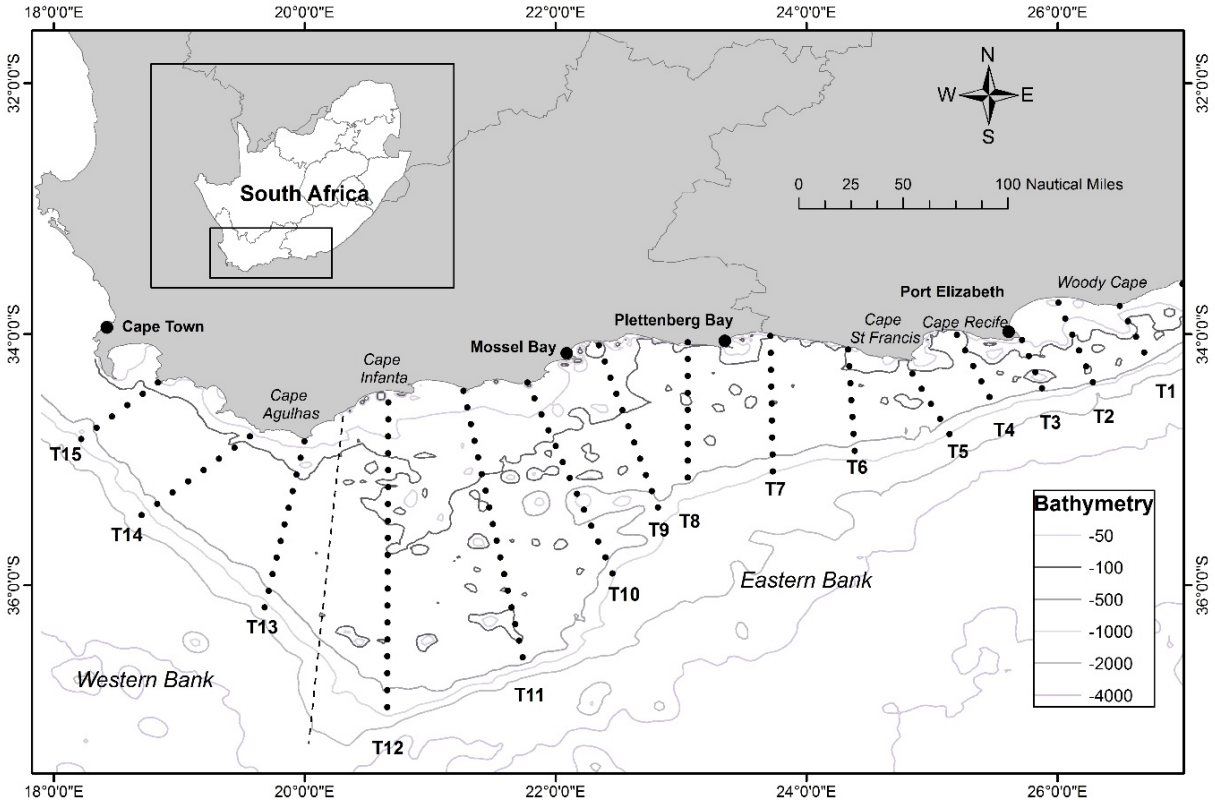

Fig. 4.1 The Agulhas Bank study area showing the position of the sampling stations (black circles) in 15 transects. Transects 1 to 12 form the eastern Bank and transects 13 to 15 the western Bank. The dashed line represents the geographical border between the two biogeographic regions. (Note: Other studies separate Transects 9 to 12 as the central Bank.)

4.4 Results

4.4.1 Physical and chemical oceanographic conditions

The division of the Agulhas Bank into the eastern and western Agulhas Bank are based on similar divisions reported in literature (Largier *et al.*, 1992; Lutjeharms, 2006; Roberts, 2010; Jackson *et al.*, 2012). Sea surface temperatures (Fig. 4.2) showed significant ($F = 27.72$; $p < 0.01$; d.f. = 437) spatial variability within the euphotic zone of the Agulhas Bank, with the eastern bank (Transects 1 to 12) being warmer than the western bank (Transects 13 to 15). Surface waters on the bank itself were cooler than those near the edge of the bank. Areas of coastal upwelling were observed near the prominent capes. Depth integrated temperatures for the

eastern Agulhas Bank ranged from 12.24 to 22.01°C with a mean temperature of 16.76 ± 2.03°C (Fig. 4.3). On the western bank temperatures ranged from 13.24 to 17.57°C with a mean of 15.73 ± 0.91°C (Fig. 4.3).

The salinity of the waters of the eastern Agulhas Bank (35.04 to 35.47, mean 35.35 ± 0.07) was significantly ($F= 6$; $p < 0.01$; d.f. = 437) lower than those of the western Agulhas Bank (35.12 and 35.47, mean 35.37 ± 0.08). Both the profiles for the eastern ($p < 0.01$; d.f. = 211) and western ($p < 0.01$; d.f. = 76) Agulhas Bank showed a significantly lower salinity below the chlorophyll *a* maximum (Fig. 4.4). A sea surface plot of salinity (Appendix: Agulhas Bank; Fig. 9.1) shows a latitudinal gradient over the Agulhas Bank, increasing towards the offshore stations.

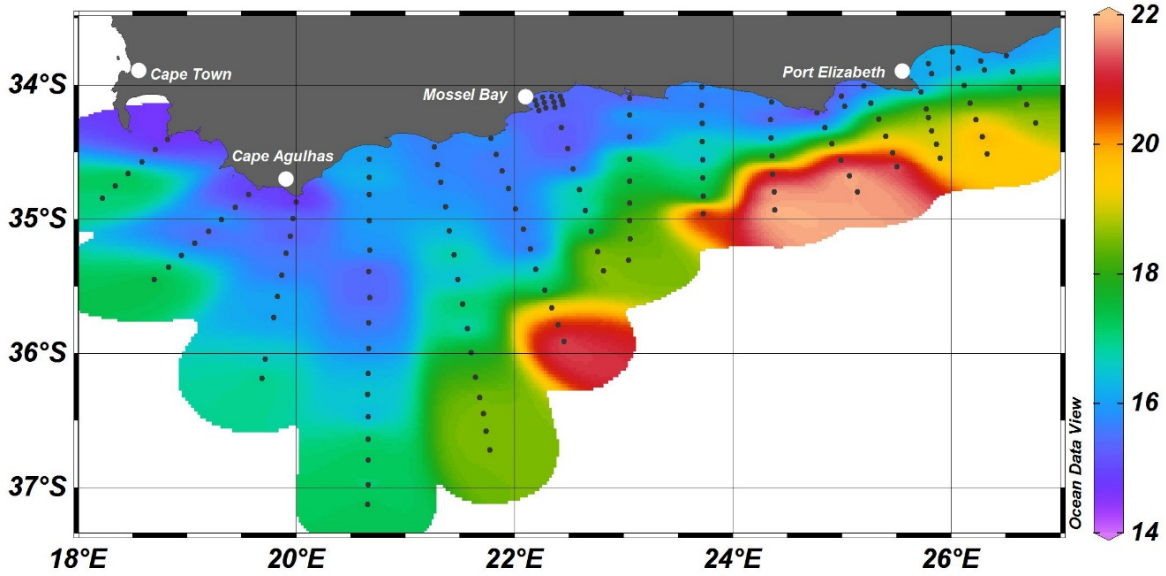

Fig. 4.2 Sea surface temperature (SST) of the waters of the Agulhas Bank. The black dots represent the sampling stations.

The dissolved oxygen profiles (Fig. 4.5) for the eastern and western Agulhas Bank showed significantly ($F= 69.85$; $p < 0.01$; d.f. = 289) lower dissolved oxygen concentrations in waters below the DCM. The mean oxygen concentration for the DCM was 5.36 ± 0.37 mg l^{-1} and below the DCM was 4.84 ± 0.59 mg l^{-1}. The mean dissolved oxygen for the eastern and western Agulhas Bank epipelagic zone was 5.13 ± 0.54 mg l^{-1} and 5.23 ± 0.46 mg l^{-1}, respectively (Fig. 4.5).

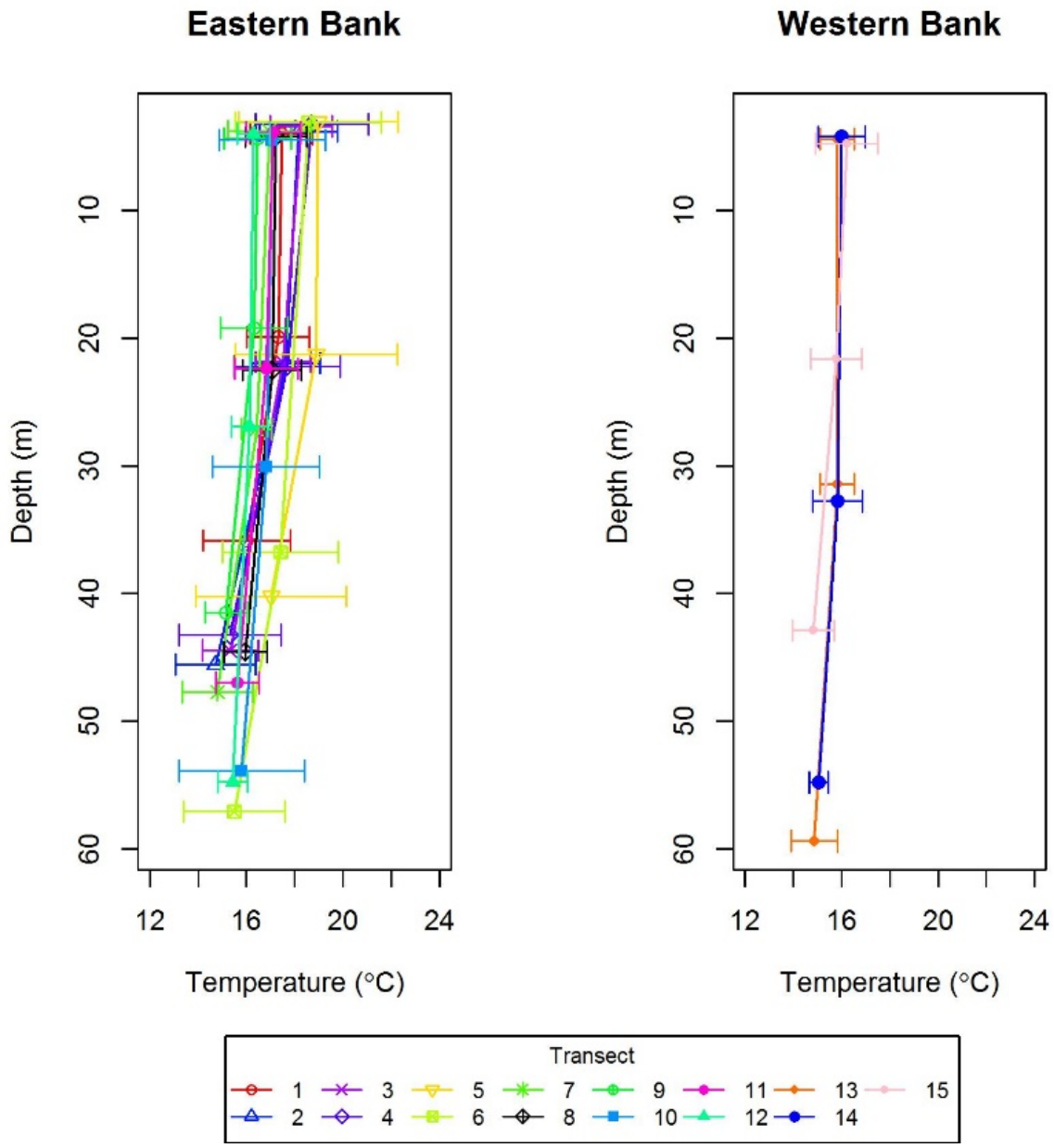

Fig. 4.3 Temperature profiles of the epipelagic zone of the Agulhas Bank. Transects 1 to 12 form the eastern Bank and Transects 13 to 15 form the western Bank.

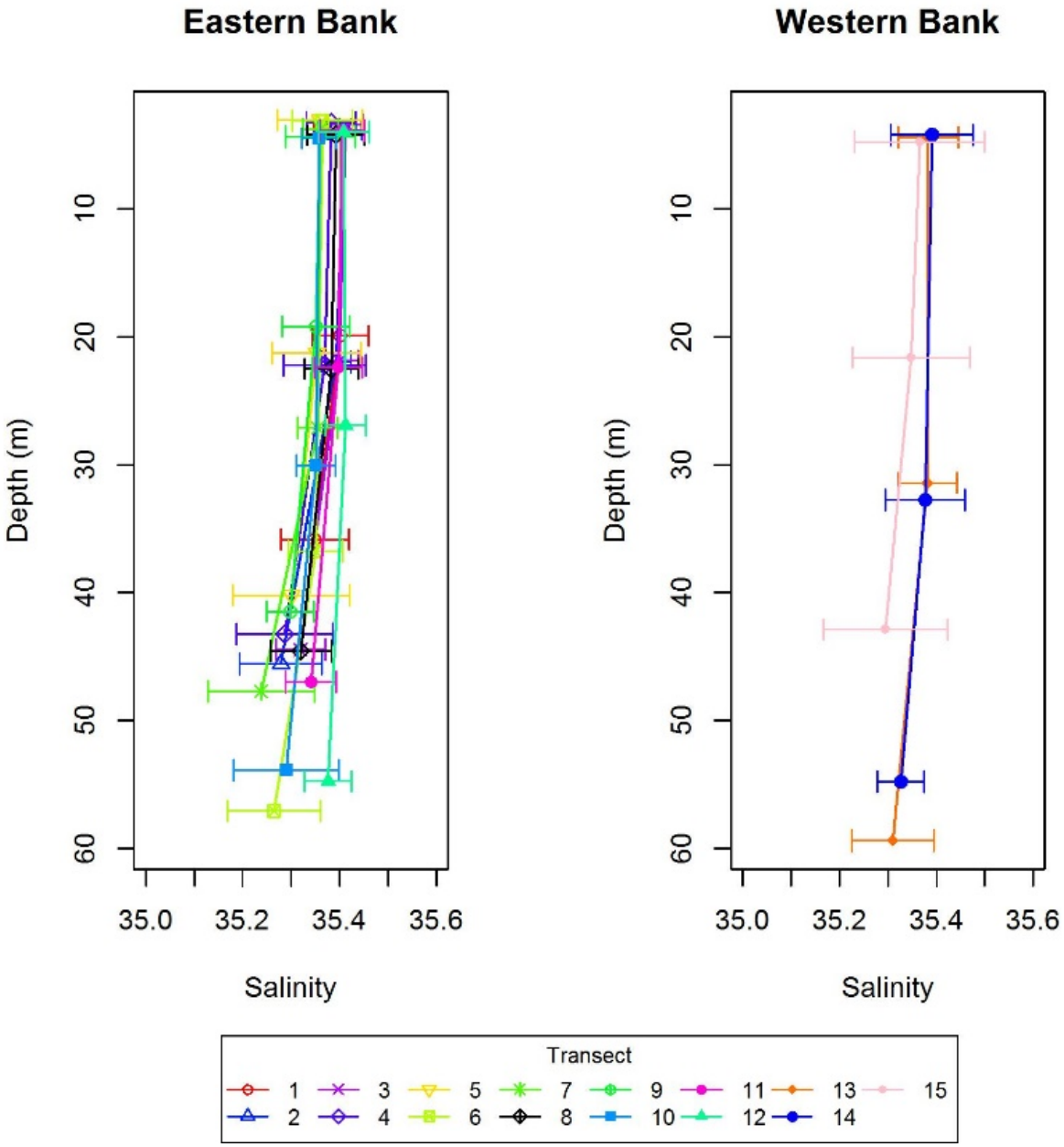

Fig. 4.4 Salinity profiles of the epipelagic zone of the Agulhas Bank. Transects 1 to 12 form the eastern Bank and Transects 13 to 15 form the western Bank.

The nitrite concentrations of the waters of the Agulhas Bank are shown in Fig. 4.6. No significant difference ($F = 0.04$; $p > 0.05$; d.f. = 394) in concentrations were found between the eastern and western Agulhas Bank as well as between the various transects ($F = 1.08$; $p > 0.05$; d.f. = 394). Nitrite concentrations significantly

increased (F = 6.52; p < 0.01; d.f. = 394) with depth (Fig. 4.6). Surface, DCM and below the DCM nitrite concentrations were 0.10 ± 0.08, 0.12 ± 0.07 and 0.15 ± 0.08 µM, respectively.

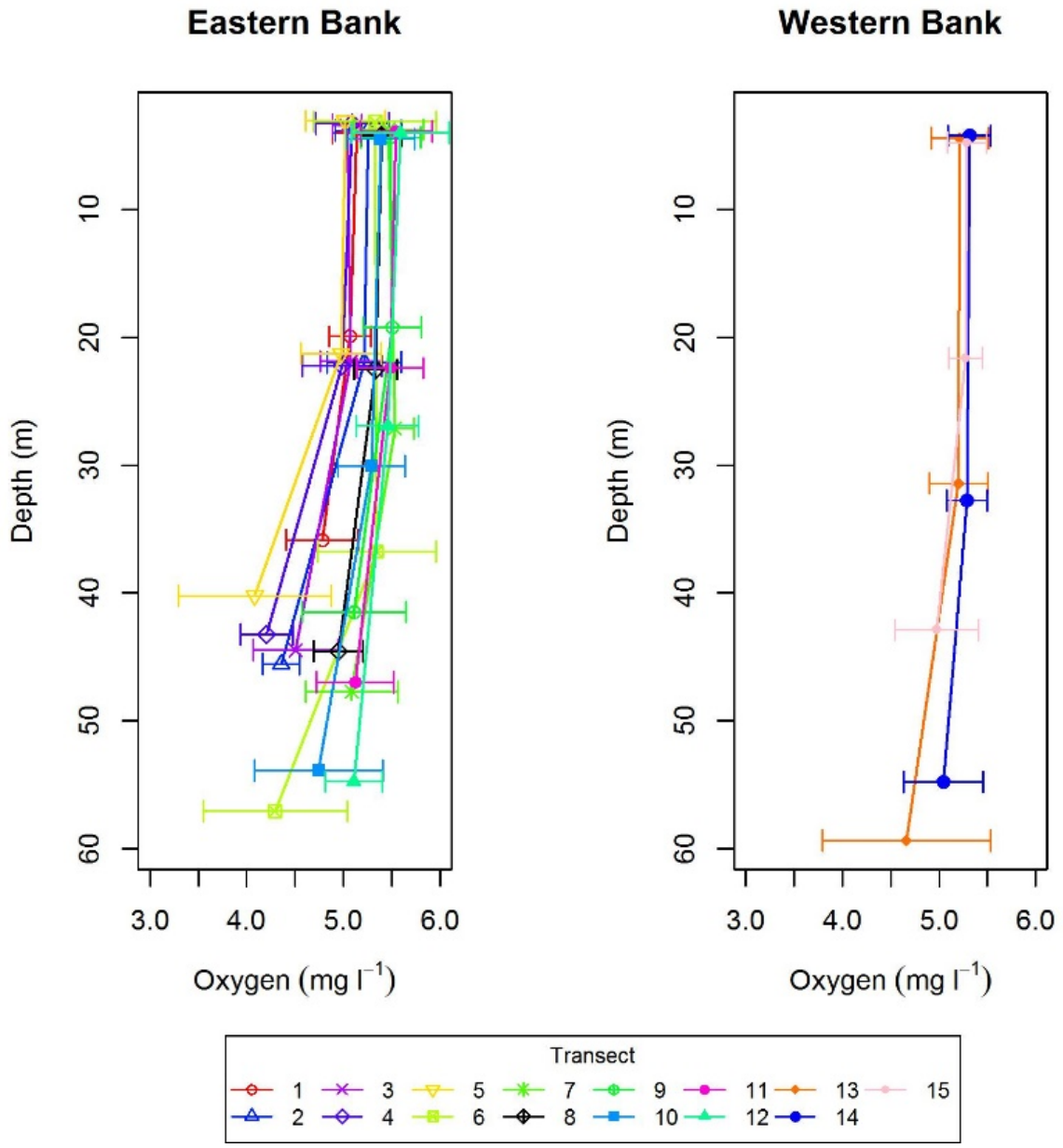

Fig. 4.5 Dissolved oxygen profiles of the epipelagic zone of the Agulhas Bank. Transects 1 to 12 form the eastern Bank and Transects 13 to 15 form the western Bank.

The nitrate concentrations for the Agulhas Bank are shown in Fig. 4.7. Concentrations were fairly uniform with a few exceptions: Transects 1 and 3 showed a significant difference ($F = 12.00$; $p < 0.05$; d.f. = 145) to Transects 11, 12 and 14. The eastern Agulhas Bank (2.81 ± 3.23 µM) had significantly ($F = 11.11$; $p < 0.01$; d.f. = 394) higher nitrate concentrations compared to the western Agulhas Bank (1.79 ± 2.04 µM). Mean surface and DCM concentrations of nitrate across the Agulhas Bank was 1.25 ± 1.62 µM and 1.47 ± 1.60 µM. This was significantly ($F = 63.53$; $p < 0.01$, d.f = 390) lower than concentrations below the DCM (4.92 ± 3.65 µM).

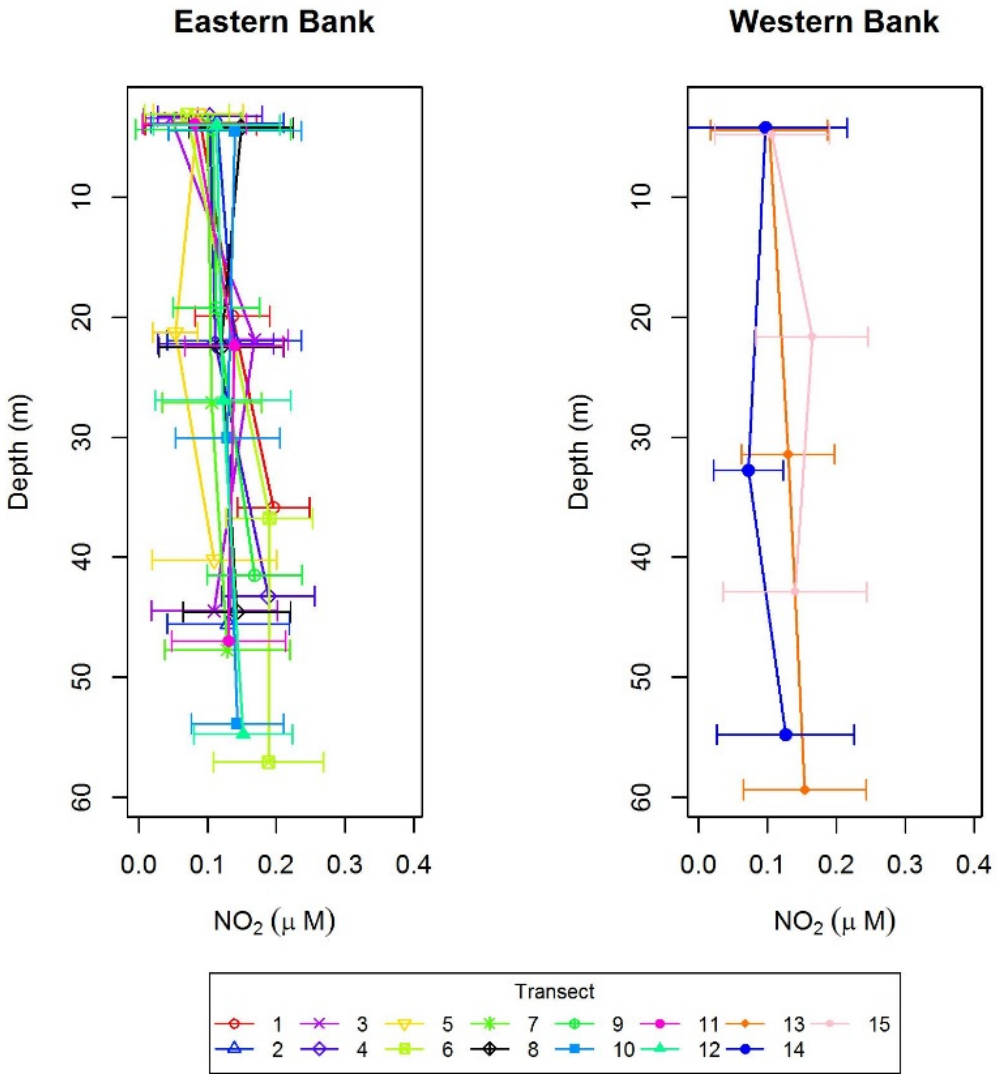

Fig. 4.6 Nitrite concentrations in the epipelagic zone of the Agulhas Bank. Transects 1 to 12 form the eastern Bank and Transects 13 to 15 form the western Bank.

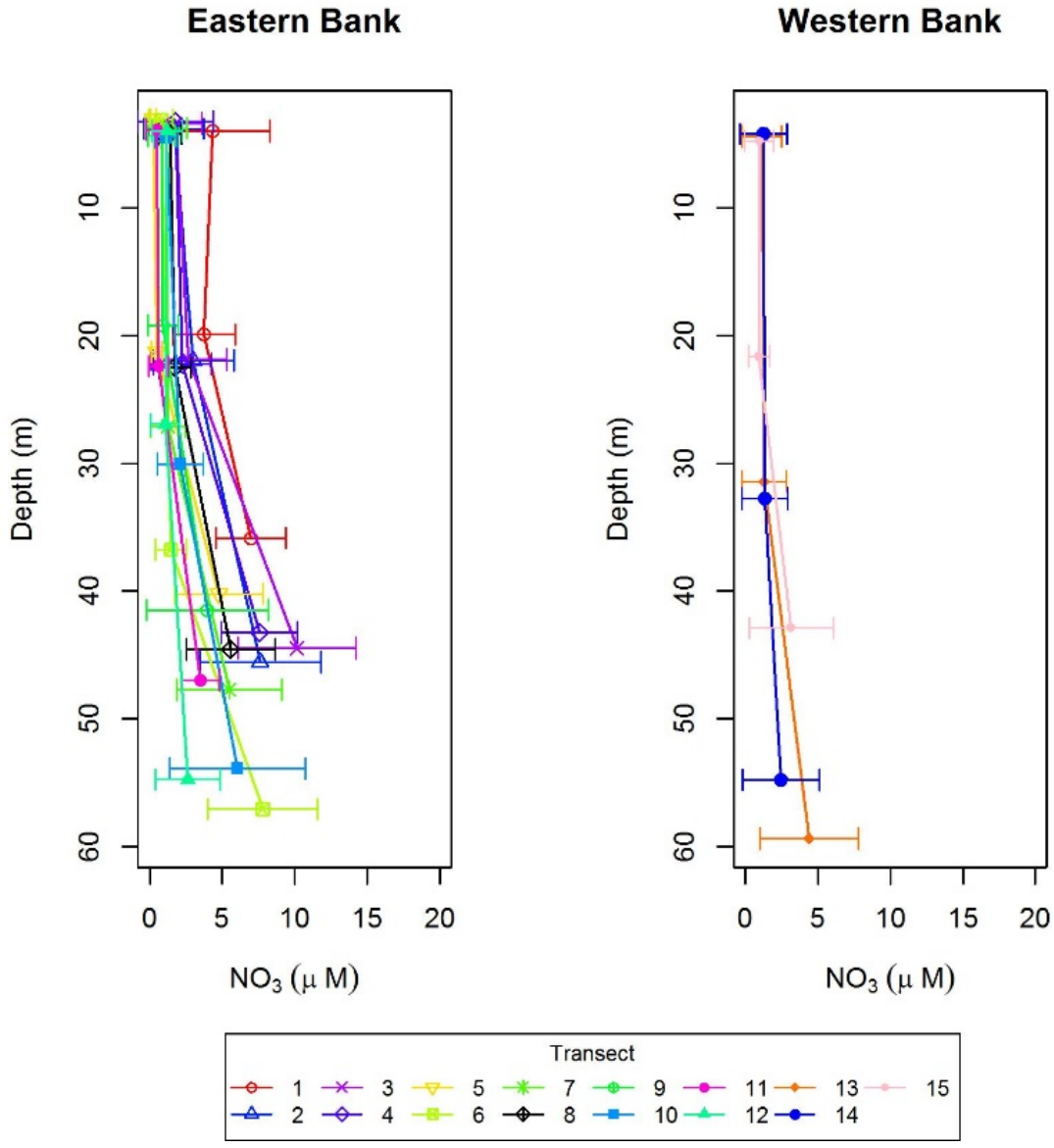

Fig. 4.7 Nitrate concentrations in the epipelagic zone of the Agulhas Bank. Transects 1 to 12 form the eastern Bank and Transect 13 to 15 form the western Bank.

The phosphate concentrations of water on the Agulhas Bank are shown in Fig. 4.8. Phosphate concentrations for the eastern Agulhas Bank epipelagic zone ranged from 0 to 2.41 µM with a mean of 0.52 ± 0.29 µM and for the western bank from 0 to 1.94 µM with a mean of 0.48 ± 0.31 µM. Transect 14 had significantly ($F = 1.69$; $p <$

0.05; d.f. = 394) higher phosphate concentrations than Transects 4 to 14 with the exception of Transect 13. Phosphate concentrations remained relatively constant in the upper epipelagic zone of the Agulhas Bank but below the DCM , concentrations were significantly higher (F = 34.92; p < 0.01; d.f. = 390). Mean surface, DCM and below DCM concentrations for the Agulhas Bank were 0.39 ± 0.22, 0.43 ± 0.24 and 0.72 ± 0.48 µM, respectively.

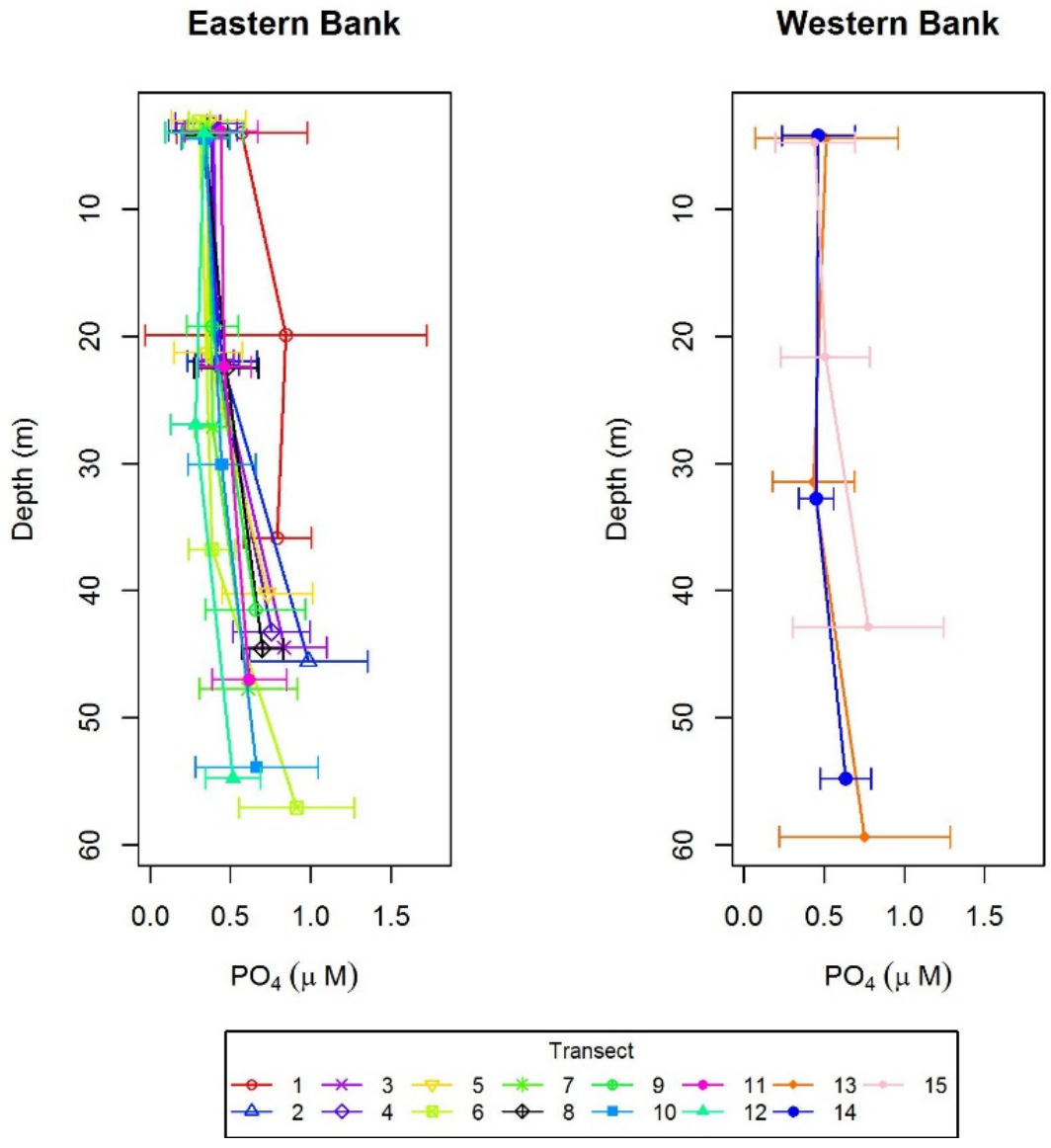

Fig. 4.8 Phosphate concentrations in the epipelagic zone of the Agulhas Bank. Transects 1 to 7 form the eastern Bank and Transect 13 to 15 form the western Bank.

Silicate concentrations in the epipelagic zone of the Agulhas Shelf are shown in Fig. 4.9. Silicate concentrations ranged from 0.04 to 61.61 µM with a mean of 5.09 ± 3.47 µM and 5.72 ± 7.30 µM for the eastern and western Agulhas Bank, respectively. Transect 13 had significantly higher ($F = 2.25$; $p < 0.05$; d.f. = 379) concentrations of silicate compared to transects 3, 7, 10, 11 and 12. Mean silicate concentrations at the surface (4.10 ± 3.77 µM) and the DCM (4.70 ± 4.53 µM) showed no significant change with depth. However, silicate concentrations below the DCM were significantly higher ($F = 10.89$; $p < 0.01$; d.f. = 390; mean of 7.10 ± 5.44 µM).

The deviation of regression lines from the Redfield ratio in Fig. 4.10 and Fig. 4.11 indicates nutrient limitation for various transects along the Agulhas Bank. Transect 3, situated off Cape Recife, was the only transect that was not nitrate limited with a N:P ratio of 16.1:1. Transect 2, 4 and 6 had N:P ratios of 8.24:1, 12.26:1 and 9.87:1, respectively. The lowest N:P ratios were measured at transect 11 (2.45:1) and 14 (2.87:1). Transects 2 and 3 were silicate limited (Fig. 4.11).

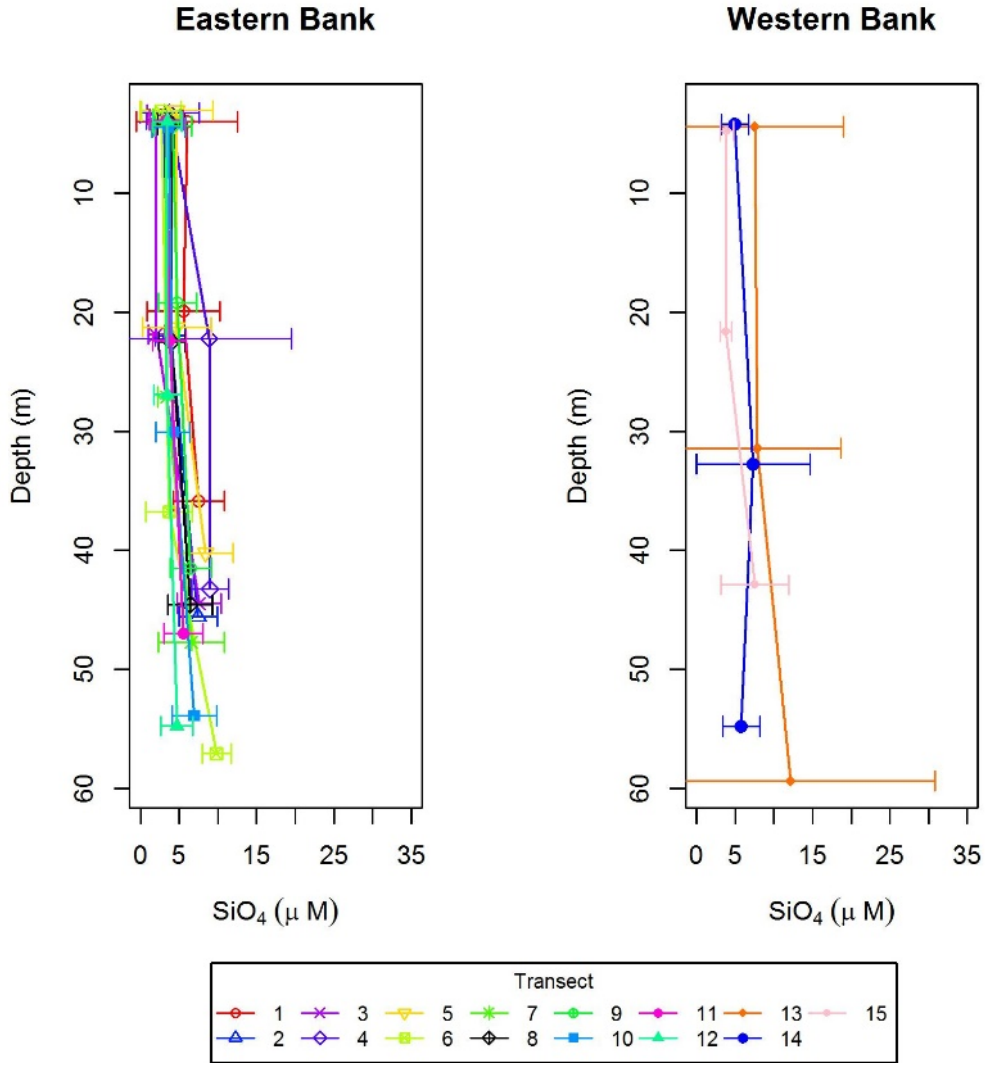

Fig. 4.9 Silicate concentrations in the epipelagic zone of the Agulhas Bank. Transects 1 to 7 form the eastern Bank and Transects 13 to 15 form the western Bank.

The four nutrients had a significant inverse correlation with temperature (Table 4.1). Furthermore, all the nutrients, except nitrite, showed a significant correlation with salinity (Table 4.1). Plotting the nutrients against temperature (Fig. 4.12) and salinity (Fig. 4.13), there was a negative linear relationship with both and can be divided into two categories. The first category was where water temperature was 18°C and the salinity was below 35.5. The second category was where water temperature was above 18°C and salinity was below 35.5.

Table 4.1 Pearson correlation analysis with pairwise deletion of the environmental variables measured in the waters of the Agulhas Bank. Significant correlations are coded as follows: *** p < 0.001, ** p < 0.01, * p << 0.05. Positive correlations are blue and negative ones are red.

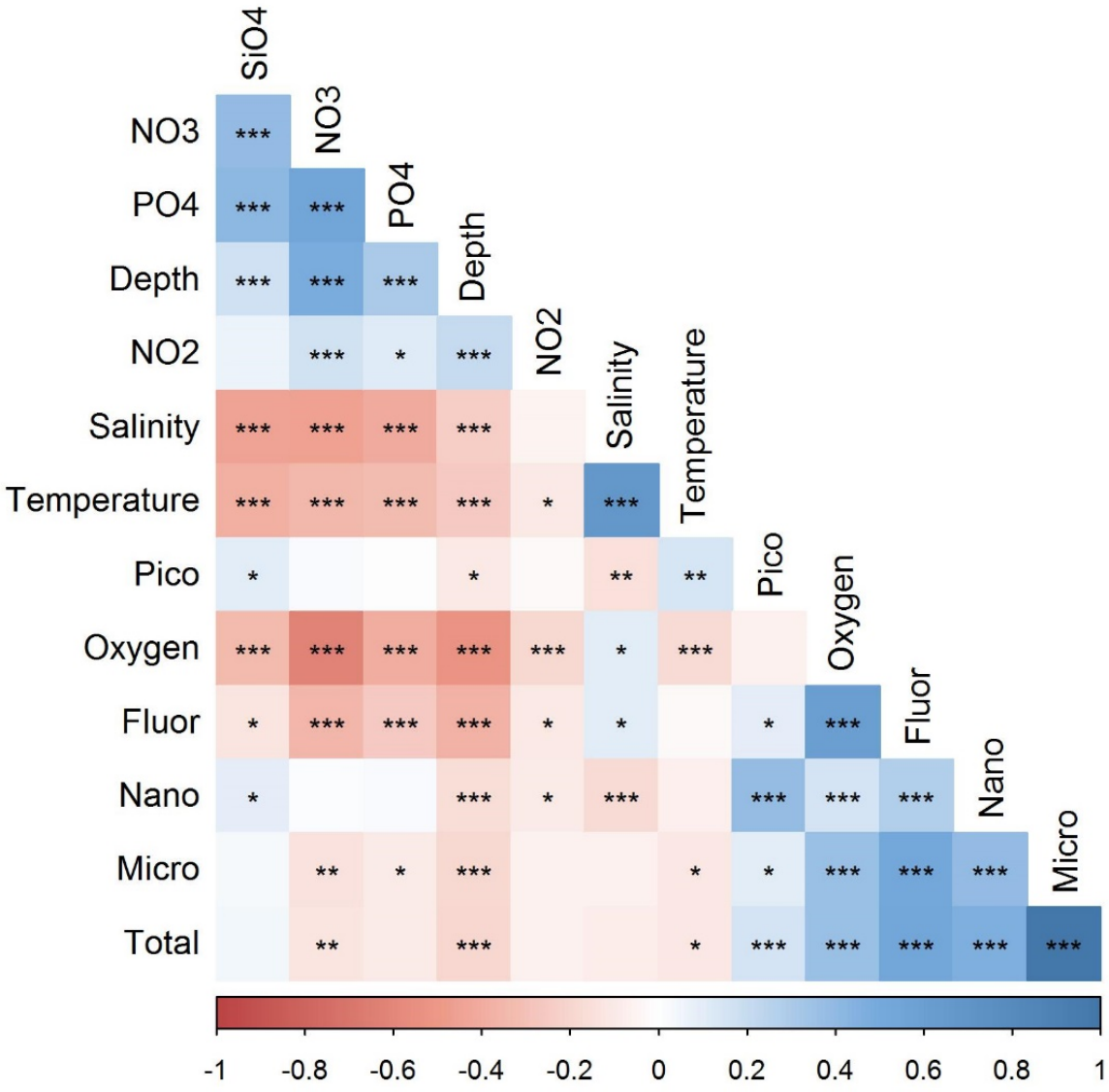

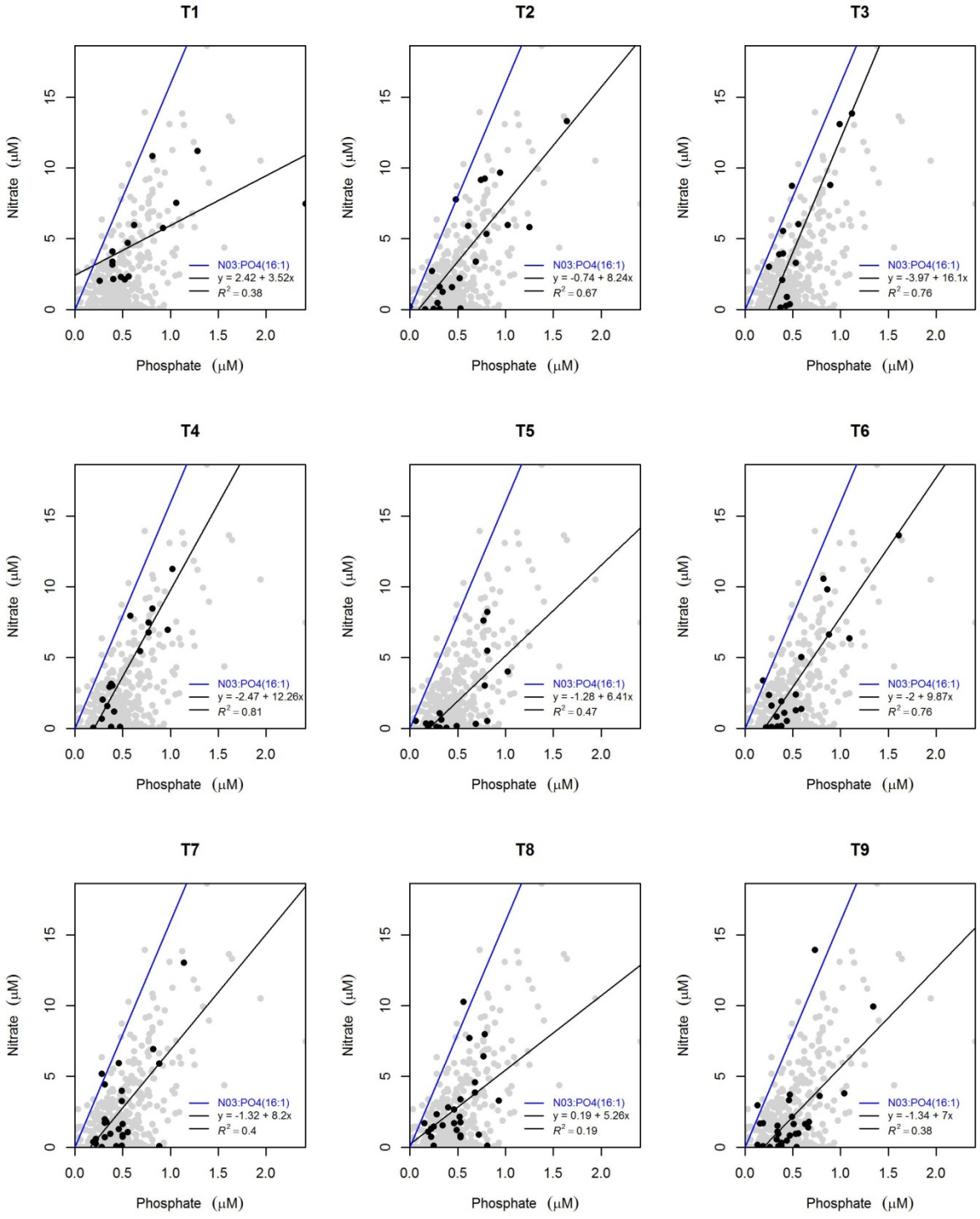

Fig. 4.10 Concentrations of nitrate versus phosphate in the epipelagic zone of the Agulhas Bank. The black line is the regression line for the data and the blue line represents the Redfield Ratio (N:P = 16:1). Grey dots are all stations whereas the black dots represent the samples for the specific transect.

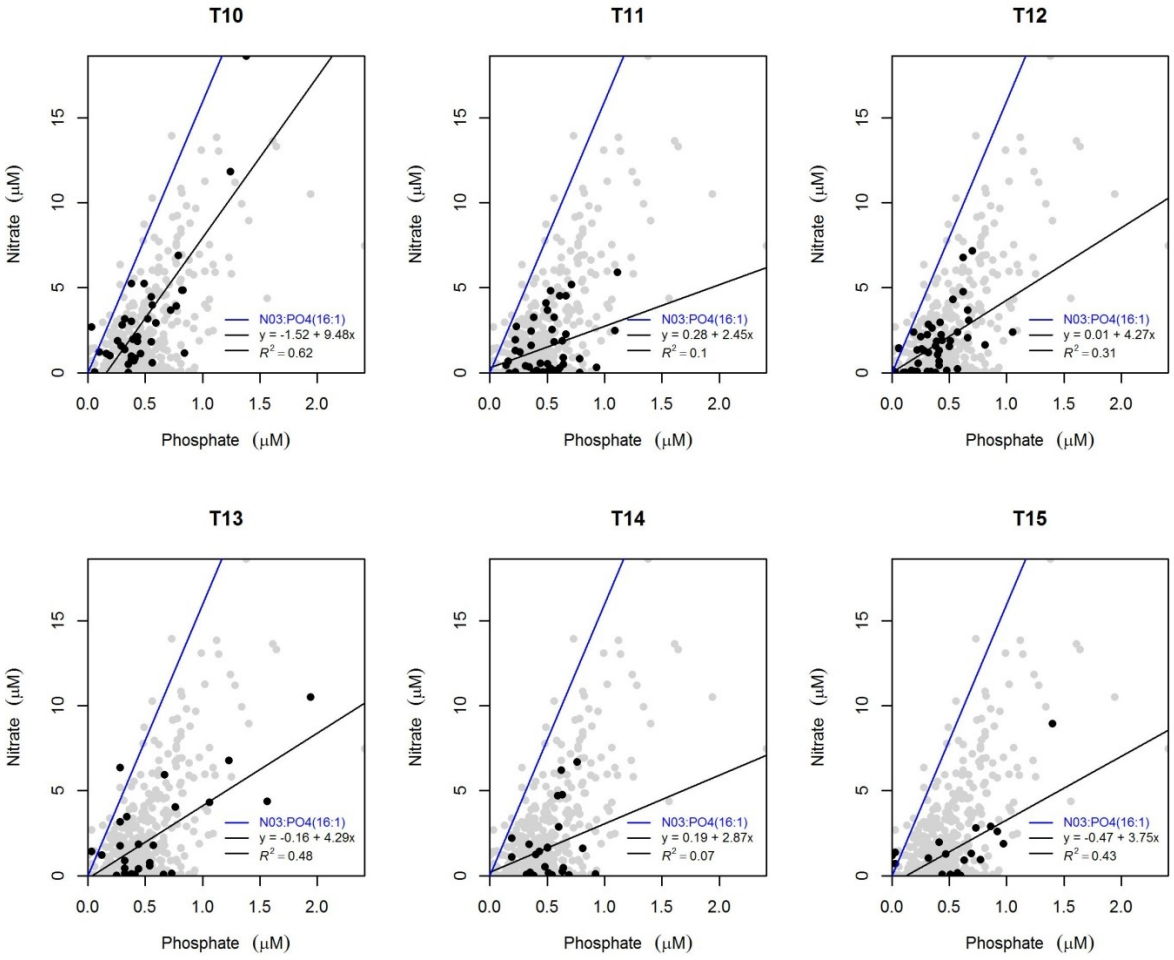

Fig. 4.10 Concentrations of nitrate versus phosphate in the epipelagic zone of the Agulhas Bank. The black line is the regression line for the data and the blue line represents the Redfield Ratio (N:P = 16:1). Grey dots are all stations whereas the black dots represent the samples for the specific transect.

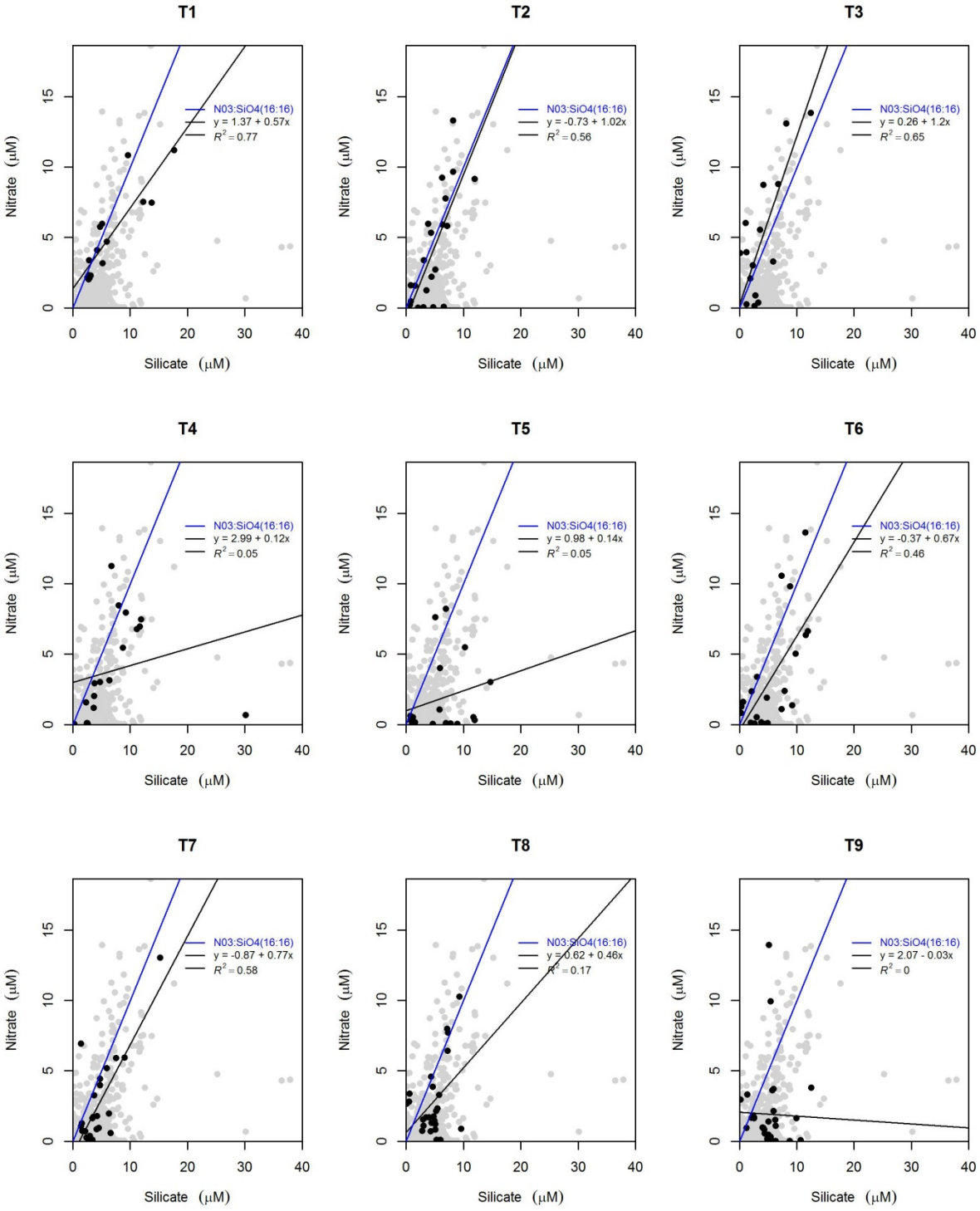

Fig. 4.11 Concentrations of nitrate versus silicate in the epipelagic zone of the Agulhas Bank. The black line is the regression line for the data and the blue line represents the Redfield Ratio (N:Si = 1:1). Grey dots are all stations whereas the black dots represent the samples for the specific transect.

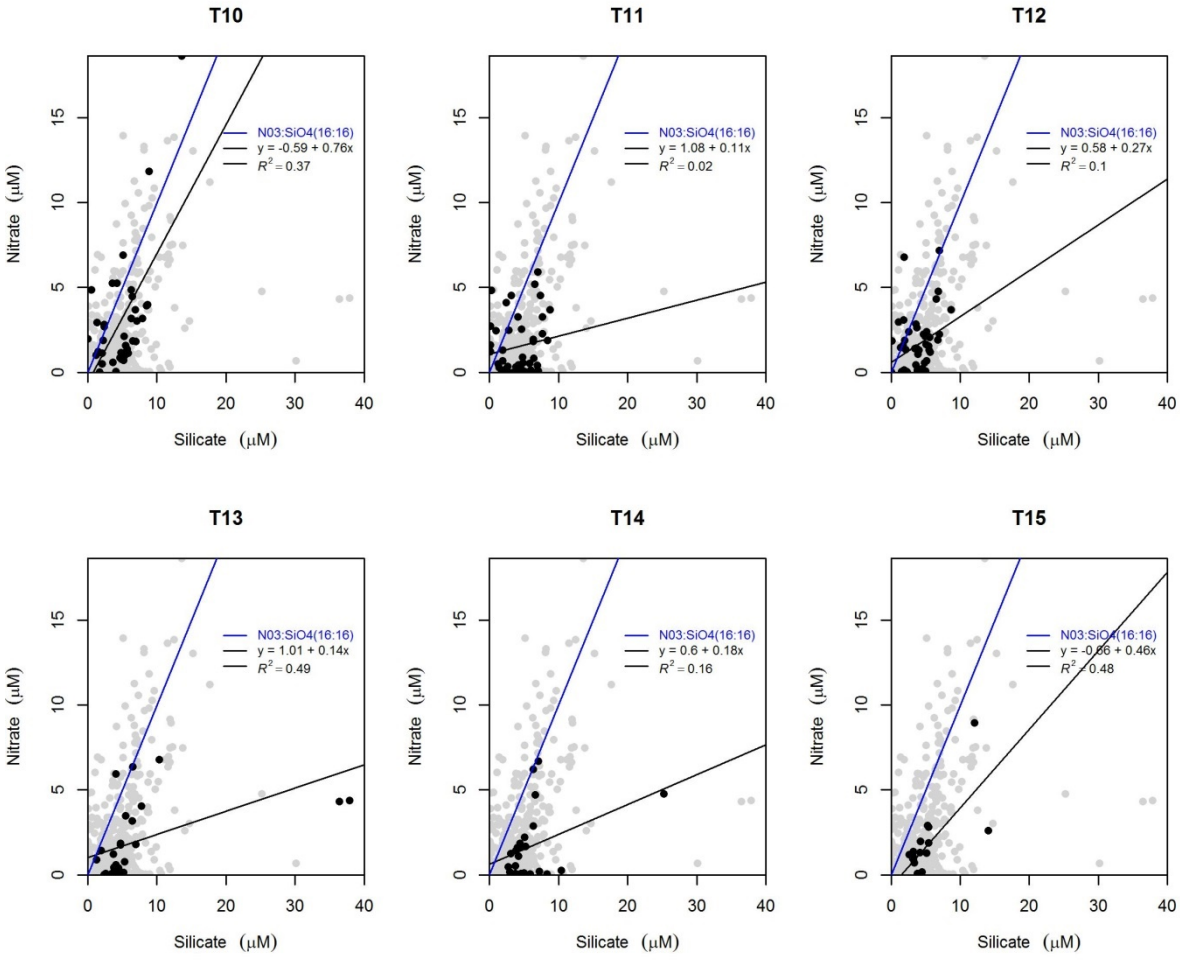

Fig. 4.11 Concentrations of nitrate versus silicate in the epipelagic zone of the Agulhas Bank. The black line is the regression line for the data and the blue line represents the Redfield Ratio (N:Si = 1:1). Grey dots are all stations whereas the black dots represent the samples for the specific transect.

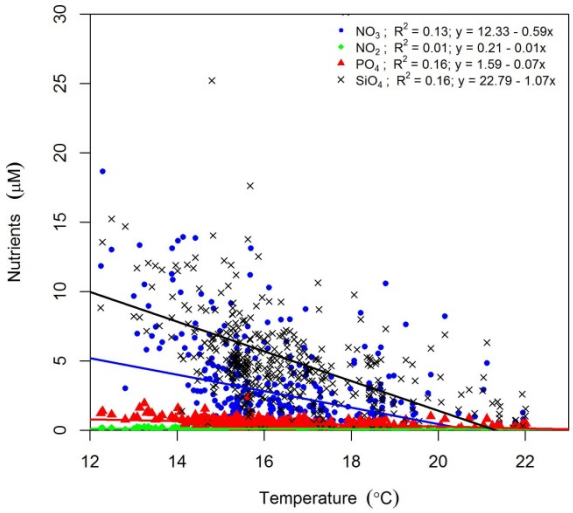

Fig. 4.12 Concentrations of nutrients (NO_2^-, NO_3^-; PO_4^{3-} and SiO_4^{4-}) versus temperature for all the euphotic zone stations of the Agulhas Bank (n=392).

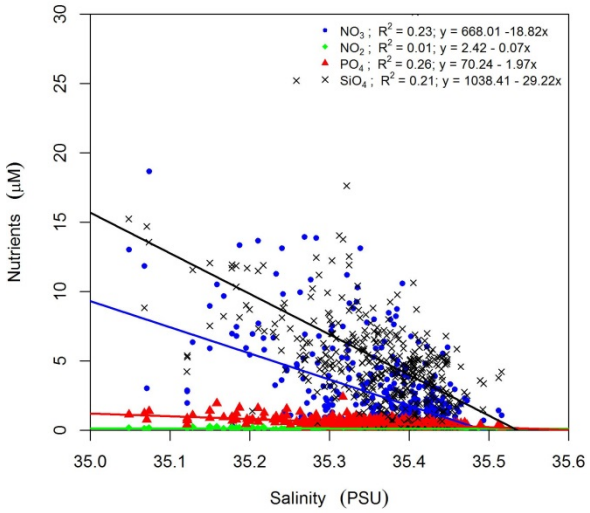

Fig. 4.13 Concentrations of nutrients (NO_2^-, NO_3^-; PO_4^{3-} and SiO_4^{4-}) versus salinity for all the euphotic zone stations of the Agulhas Bank (n=392).

4.4.2 Spatial variability of phytoplankton

The depth of the chlorophyll *a* maximum was highly variable on the Agulhas Bank, ranging from 3 to 80 m with a mean depth of 21.25 ± 13.52 m (Fig. 4.15, Fig. 4.16, Fig. 4.17). Most of the stations (112 of 147 stations or 76%) had an SCM that was associated with both the nutricline; pycnocline and the mixed layer depth. The chlorophyll *a* concentration measured at the SCM ranged from 0.42 to 18.03 µg l^{-1} with a mean concentration of 4.50 ± 3.26 µg l^{-1}. Chlorophyll *a* concentrations were generally higher near the coast, in the central bank region, as well as in areas of known upwelling. Lower concentrations of chlorophyll *a* were measured in the Agulhas Current proper and at the western edge of the Agulhas Bank (Fig. 4.15, Fig. 4.16, Fig. 4.17). Areas of upwelling were observed near and around prominent capes and headlands. Selected graphs of chlorophyll *a* concentration at depth (Fig. 4.15, Fig. 4.16, Fig. 4.17) illustrate the difference in chlorophyll *a* profiles for coastal and offshore areas.

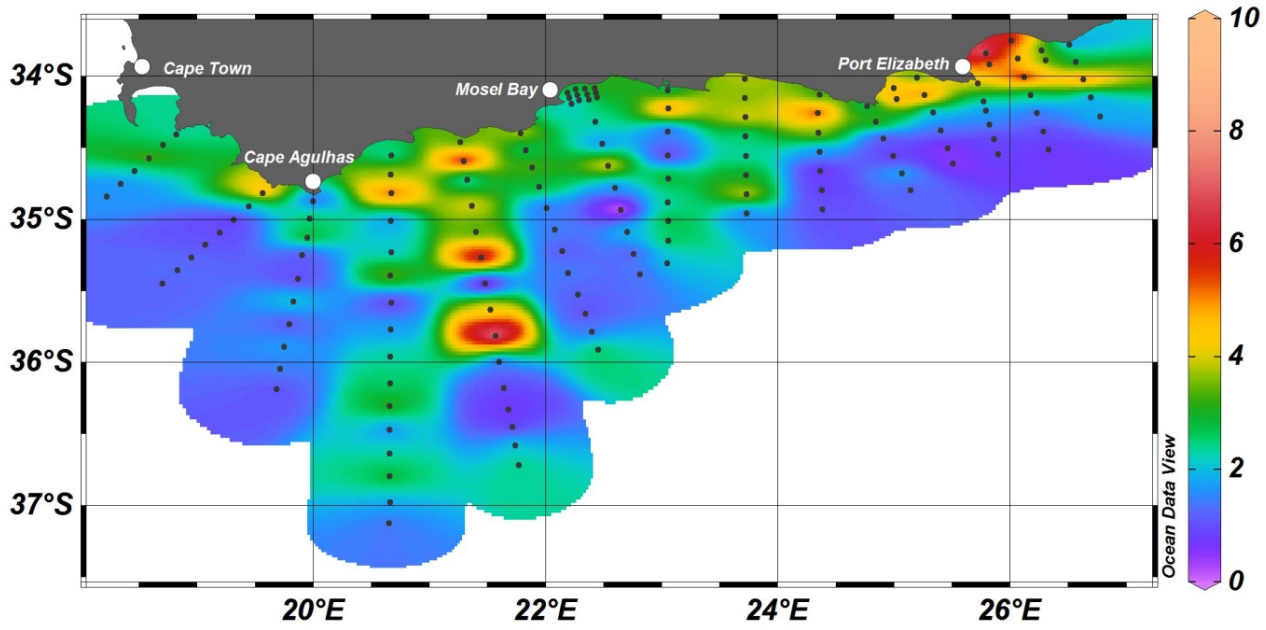

Fig. 4.14 Sea surface plot of chlorophyll *a* (µg l^{-1}) of the Agulhas Bank.

The *in situ* chlorophyll *a* data for Transect 1 showed a region of high chlorophyll *a* on the edge of the Agulhas Bank (Fig. 4.15a). Here the SCM was located near the surface and ranged between 7 and 33 m with a mean depth of 18.2 ± 12.8 m. At the SCM, microphytoplankton contributed 89.73% to the total chlorophyll *a*, whereas nano- and picophytoplankton contributed 7.87 and 2.40%, respectively. At the time of the study, the surface waters of Transect 1 were dominated by microphytoplankton contributing 88.80% to the total chlorophyll *a*.

At transect 3, the *in situ* chlorophyll *a* showed a region of high concentration in the coastal zone around Cape Recife dissipating southwards towards the Agulhas Current (Fig. 4.15b). The SCM was located near the surface (7 m) and extended to a maximum depth of 30 m with a mean depth of 12.67 ± 10.32 m. The mean chlorophyll *a* concentration for the SCM was 3.43 ± 2.72 µg l^{-1}. Within the SCM, microphytoplankton contributed 95.12% to the total chlorophyll *a*, whereas nano- and picophytoplankton contributed 4.22 and 0.63%, respectively. At the time of the study the surface waters of Transect 3 were dominated by microphytoplankton contributing 84.52% to the total chlorophyll *a*.

Transect 1

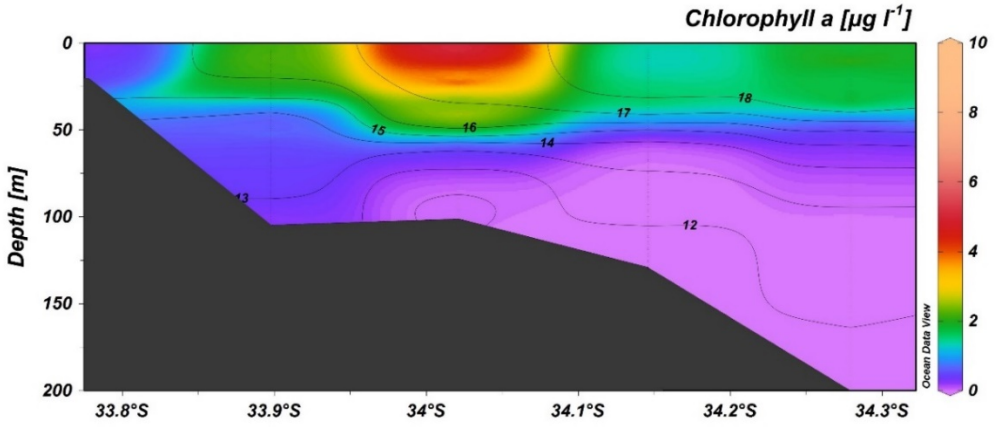

Transect 3

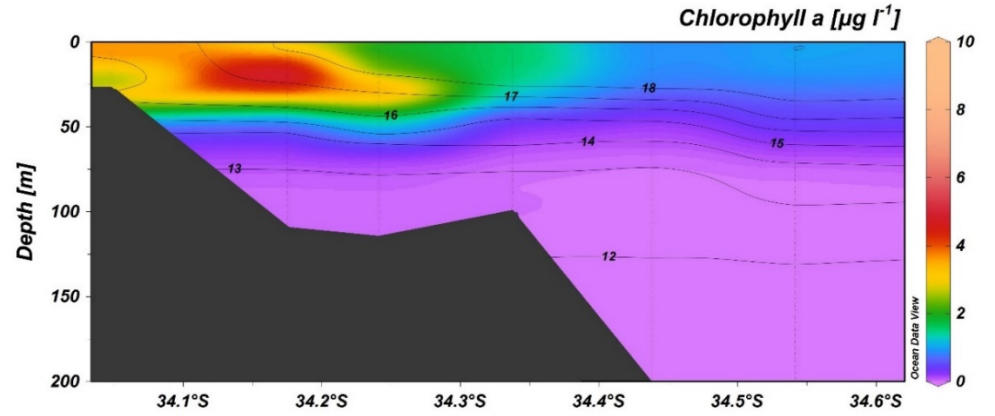

Transect 5

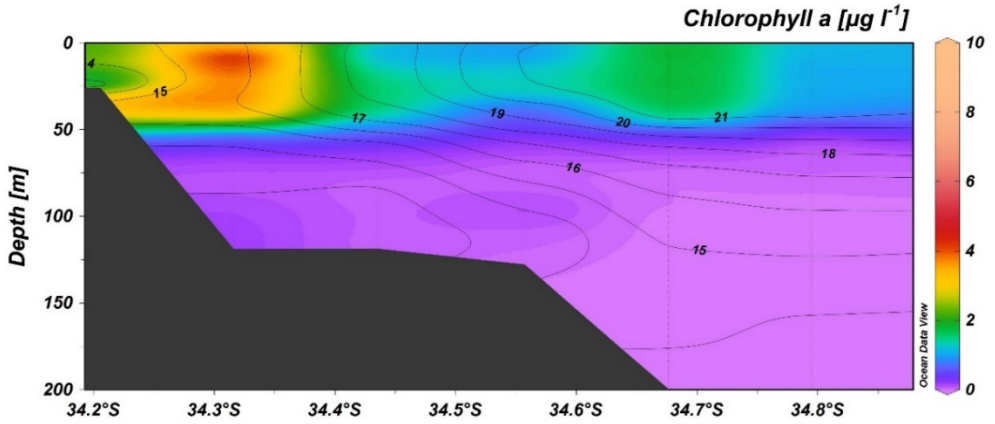

Fig. 4.15 Latitudinal depth transects of chlorophyll *a* (µg l^{-1}) concentrations for Transects 1(a), 3(b) and 5(c) along the Agulhas Bank. Isotherms are in °C.

Transect 7

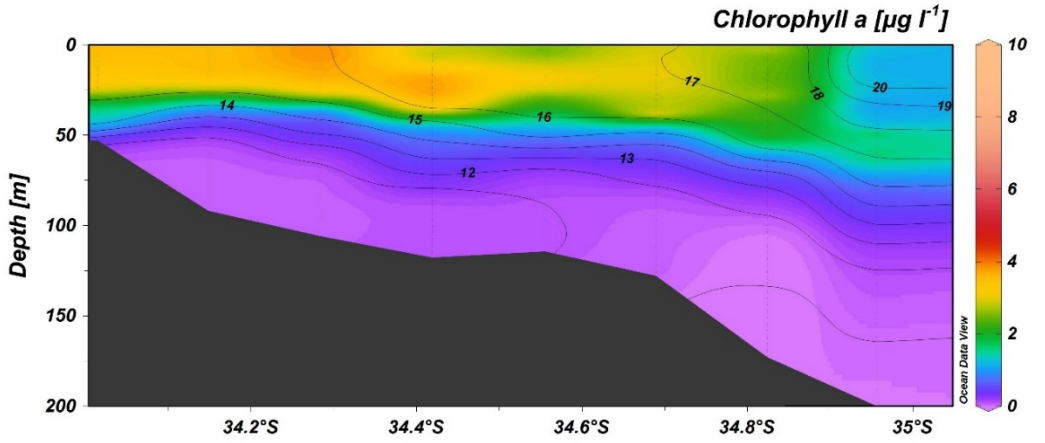

Transect 9

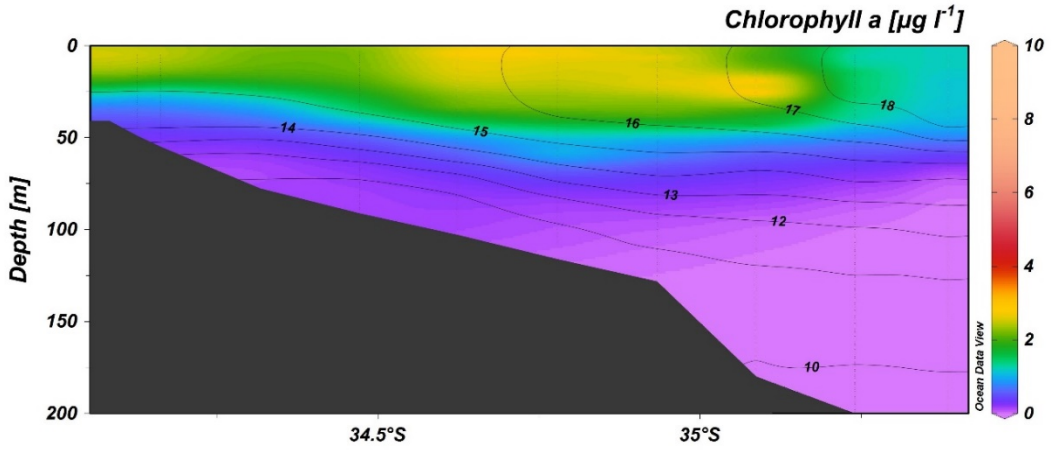

Transect 11

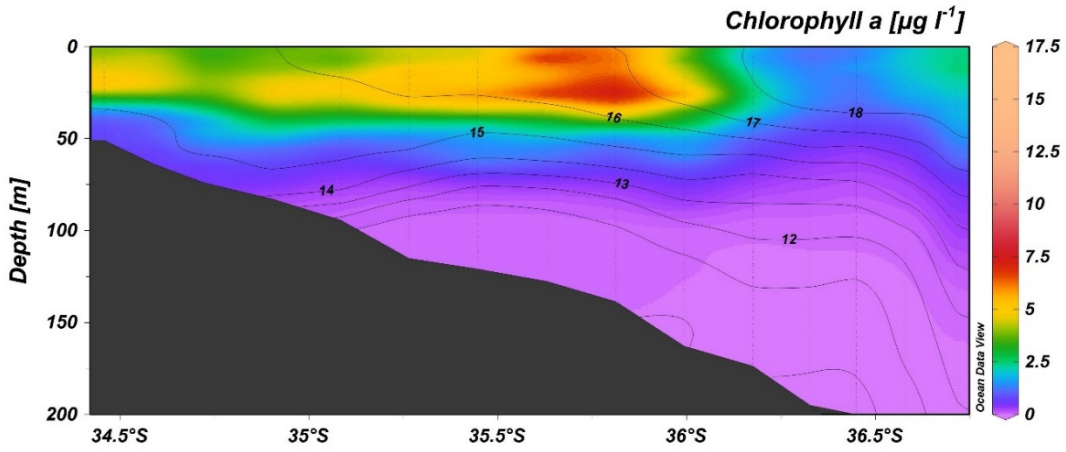

Fig. 4.16 Latitudinal depth transects of chlorophyll a (µg l^{-1}) concentrations for Transects 7(a), 9(b) and 11(c) along the Agulhas Bank. Isotherms are in °C.

Transect 13

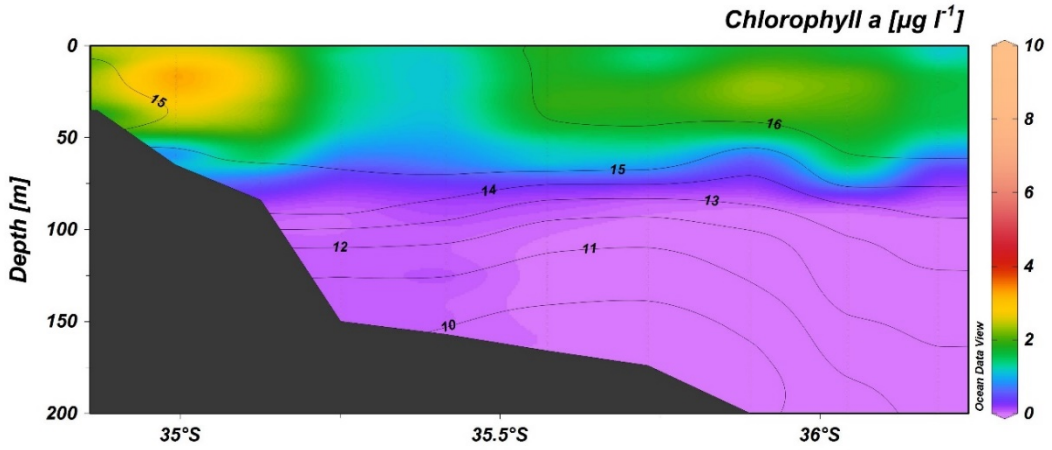

Transect 15

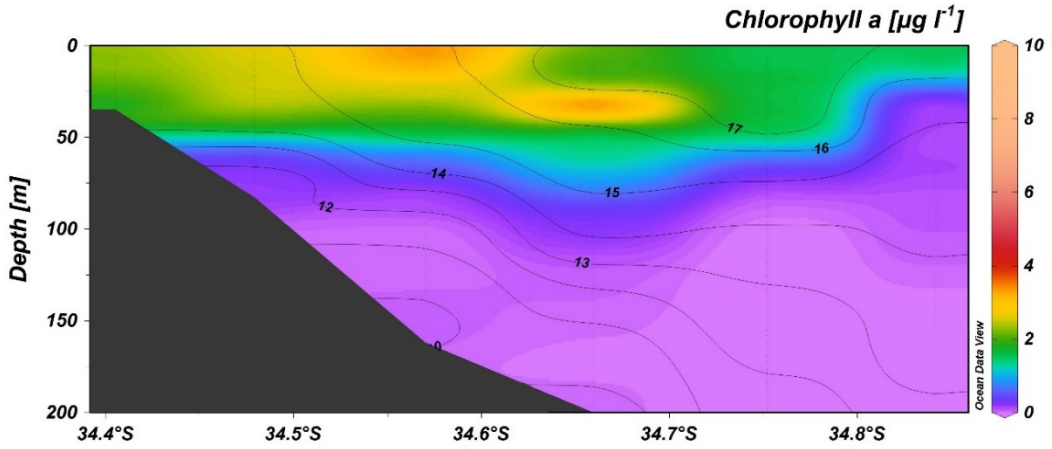

Fig. 4.17 Latitudinal depth transects of chlorophyll *a* (µg l^{-1}) concentrations for Transects 13(a) and 15(b) along the Agulhas Bank. Isotherms are in °C.

Transect 5 (Fig. 4.15c) was located off Cape St Francis and had a similar *in situ* chlorophyll *a* profile to that measured at Transect 3 (off Cape Recife). The depth of the SCM ranged between 4 and 37 m with a mean depth of 20.50 ± 13.95 m. The chlorophyll *a* concentration of SCM waters ranged between 1.19 and 6.28 µg l^{-1} with a mean of 2.54 ±1.89 µg l^{-1}. Micro-, nano- and picophytoplankton contributed 87.98, 6.75 and 5.27%, respectively to the total chlorophyll *a* within the SCM.

A SCM was the most dominant feature of Transect 7. It is clear from the sea surface temperature (Fig. 4.2) and the formation of a DCM (Fig. 4.16a) that the last station of Transect 7 was located within the Agulhas Current proper. The DCM was located at

a depth of 49 m whereas the SCM of the other stations of Transect 7 was located between 3 and 38 m with a mean depth of 17.57 ± 13.95 m. Chlorophyll *a* concentrations of the SCM waters ranged between 3.64 and 7.84 µg l^{-1} with a mean of 4.54 ± 1.48 µg l^{-1}. The DCM had a maximum concentration of 4.04 µg l^{-1}. Microphytoplankton was the dominant component of total chlorophyll *a*, contributing 84.61% whereas nano- and picophytoplankton contributed 10.85 and 4.54%, respectively.

Chlorophyll *a* (Fig. 4.14 & Fig. 4.16b) on Transect 9, located off Mossel Bay was significantly ($F = 1.82$; $p < 0.01$; d.f = 379) lower than those measured at Transect 7. At Transect 9, the mean chlorophyll *a* concentration was slightly more elevated at 4.10 ± 1.93 µg l^{-1}. The SCM was located between 3 and 40 m with a mean depth of 15.80 ± 12.90 m. Micro-, nano- and picophytoplankton contributed 83.61, 11.30 and 5.08%, respectively to total chlorophyll *a*.

Transect 11 was highly productive at the time of sampling with high surface (Fig. 4.14) and deeper (Fig. 4.16c) chlorophyll *a* concentrations ranging from 1.62 to 18.03 µg l^{-1} with a mean 7.93 ± 5.24 µg l^{-1}. The SCM was located between 4 and 48 m with a mean depth of 18.4 ± 12.05 m. A vertical station plot of potential density anomaly or sigma-theta (Appendix: Agulhas Bank; Fig. 9.2) showed that the mixed layer depth was correlated with the SCM. Micro-, nano- and picophytoplankton contributed 90.71, 6.44 and 2.85%, respectively to total chlorophyll *a* at Transect 11.

The SCM for Transect 13 (Fig. 4.17a) ranged between 9 and 32 m with a mean depth of 22.30 ± 7.68 m. This was deeper than at Transect 11 and it showed the least amount of variation between stations. There was a significant ($F = 4.52$; $p < 0.001$; d.f. = 70) drop in chlorophyll between Transect 11 (7.93 ± 5.24 µg l^{-1}) and Transect 13 (2.36 ± 1.06 µg l^{-1}). Chlorophyll *a* for Transect 13 ranged between 0.96 and 4.81 µg l^{-1}. Micro-, nano- and picophytoplankton contributed 91.13, 6.08 and 2.79%, respectively to total chlorophyll *a*. Two areas of higher productivity were evident in this transect: one close to the coast and at a sharp rise in the bottom topography; and second was further offshore and closer to the western edge of the Agulhas Bank.

The depths and chlorophyll *a* concentration of the SCM at Transect 15 (Fig. 4.17b) ranged between 9 and 30 m and 1.64 and 4.58 µg l^{-1}, respectively. The mean depth of the SCM was located at 22.3 ± 7.68 m and with a mean chlorophyll *a* concentration of 2.84 ± 1.11 µg l^{-1}. Micro-, nano- and picophytoplankton contributed 92.89, 5.13 and 1.98%, respectively to total chlorophyll *a*. A vertical station plot of potential density anomaly or sigma-theta (Appendix: Agulhas Bank; Fig. 9.3) showed that the mixed layer depth ranged between 10 and 52 m.

4.4.3 Phytoplankton composition.

A total of 89 phytoplankton taxa were recorded during the survey: 54 diatoms, 28 dinoflagellates, five silicoflagelates, one flagellate, one prymnesiophyte and no coccolithophores. The dominant genera (>1 000 counts), in order of dominance were: *Thalassiosira weissflogii* (diatom), *Gonyaulax* Diesing spp. (dinoflagellate); *Pseudo-nitzschia* spp. (diatom), *Alexandrium* Halim spp. (dinoflagellate), and *Guinardia* spp. (diatom). These five genera combined contributed 63.13% of the total cell counts.

Species diversity in general was greater on the eastern Agulhas Bank than on the western Agulhas Bank. The values ranged from 0.78 (Transect 15) to 2.84 (Transect 5) across the study site, indicating low diversity in the phytoplankton community. Evenness ranged from 0.40 to 0.87 with a mean of 0.65, thereby indicating a relatively even distribution of species. The composition of the phytoplankton and the phytoplankton species richness of samples taken from 8 transects along the Agulhas Bank is shown in Fig. 4.18. Transect 5 had the highest diversity with 39 taxa at the SCM and 36 taxa at the surface. Transect 1 had the second highest diversity with 32 taxa at the SCM and 38 at the surface. The prymnesiophyte*, Chrysochromulina hirta* Manton was only recorded in the surface waters of Transect 5. Eleven samples showed dominance (>50% of counts) of only one species (Table 4.1). Six of these were dominated by the diatom, *Thalassiosira weissflogii*. The rest were dominated by the dinoflagellate, *Gonyaulax* sp.*,* with one exception (where *Protoceratium triestina* was the dominant species). There is a significant ($p < 0.05$; d.f. = 50) decrease in *Alexandrium* spp. abundance across the Agulhas Bank. *Gonyaulax* spp. were more abundant towards the central region of the Agulhas Bank. The diatom *T.*

weissflogii was the only species that was recorded at every station on the Agulhas Bank.

Table 4.2 Sites where the phytoplankton was dominated by only one species.

Station and profile	Transect	% of counts	Dominant species	Species richness	Diversity score	Evenness score
10223_DCM	1	55.19	*Guinardia* sp.	22	1.79	0.58
10238_DCM	3	50.32	*T. weissflogii*	27	2.02	0.61
10255_DCM	5	58.31	*T. weissflogii*	17	1.45	0.51
10284_DCM	9	76.51	*T. weissflogii*	15	1.07	0.39
10284_Surface	9	64.35	*T. weissflogii*	11	1.28	0.53
10315_Surface	11	51.15	*Gonyaulax* sp.	17	1.67	0.58
10316_DCM	11	56.62	*T. weissflogii*	14	1.32	0.50
10316_Surface	11	61.95	*Gonyaulax* sp.	16	1.60	0.57
10346_DCM	13	62.75	*Gonyaulax* sp.	19	1.55	0.53
10364_Surface	15	75.47	*Protoceratium triestina*	4	0.78	0.56
10367_DCM	15	56.76	*Gonyaulax* sp.	26	1.77	0.54

An ordination of the phytoplankton composition grouped the 89 taxa into the following communities (Fig. 4.19): eastern Agulhas Bank (Transects 1 - 11) and western Bank (transects 12 - 15) communities. The eastern bank community was then split into two smaller communities, i.e. inshore of the Agulhas Current and the Agulhas Current proper. However, these distinctions are not that clear as both communities shared many of the same species, especially the more abundant species such as *T. weissflogii*; *Pseudo-nitzschia* spp., *Gonyaulax* spp. and *Alexandrium* spp.

Fig. 4.20 represents the 12 most abundant species found on the Agulhas Bank.

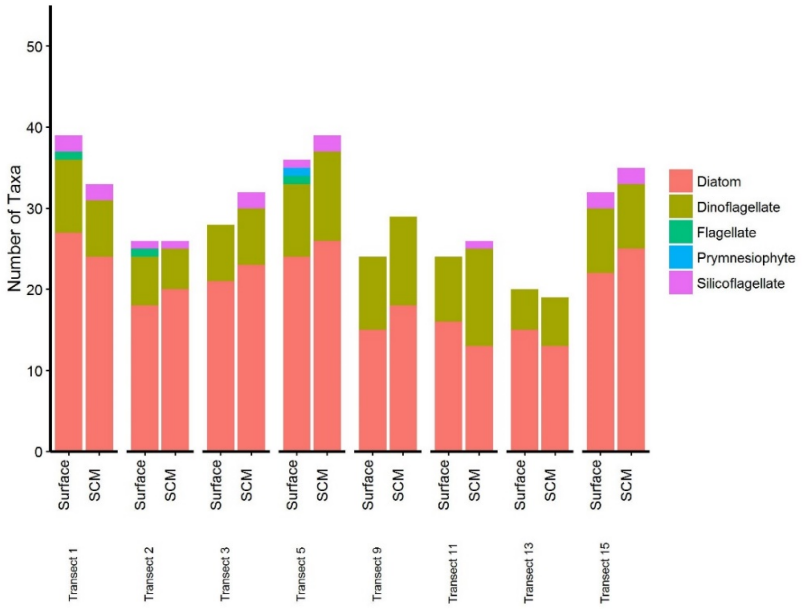

Fig. 4.18 Composition of phytoplankton from the surface and SCM of the 8 transects along the Agulhas Bank.

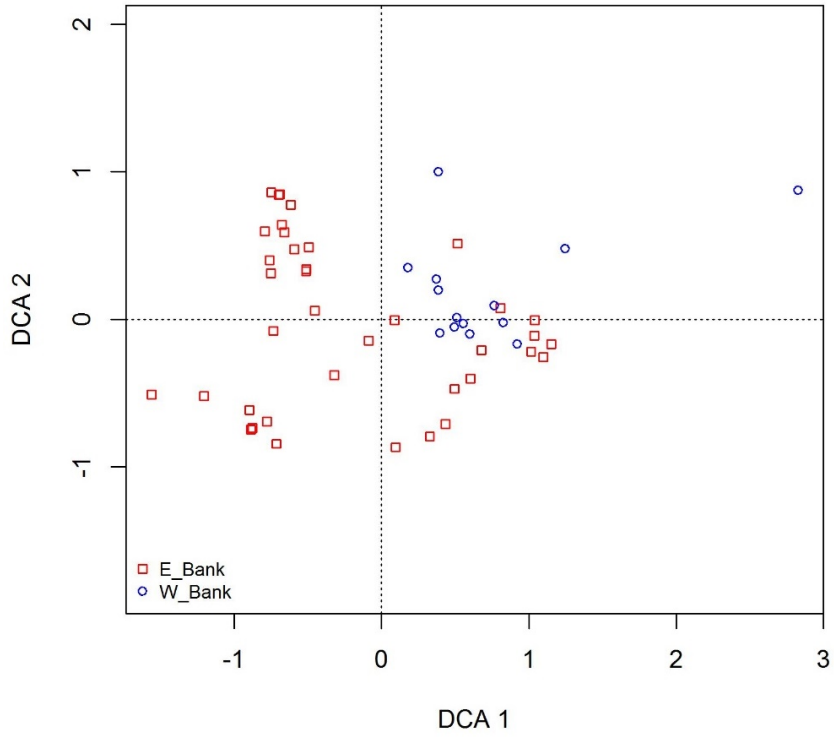

Fig. 4.19 Detrended Correspondence Analysis of the phytoplankton samples of the Agulhas Bank.

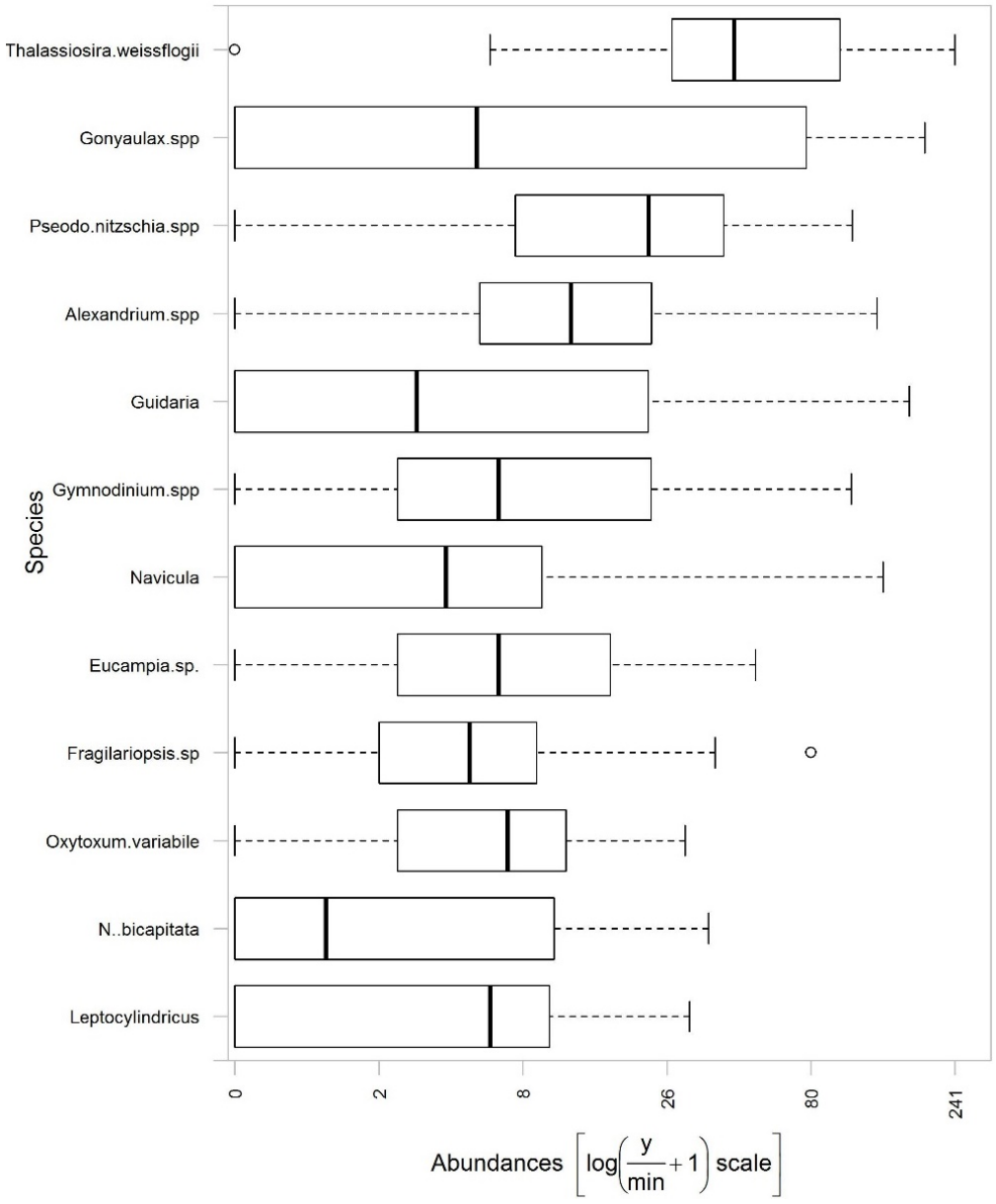

Fig. 4.20 The 12 most abundant species found in the phytoplankton of the Agulhas Bank. ○ represents outliers, bars represent the minimum and maximum, and the solid line is the median.

4.4.4 Environmental drivers of phytoplankton variability

The environmental drivers of the phytoplankton on the Agulhas Bank are shown in Fig. 4.21. The first canonical axis accounted for 43% of the species-environment relationship. The strongest correlations were between the first canonical axis and nitrite (r = 0.99), temperature (r = -0.73) and phosphate (r = -0.70). The second canonical axis accounted for 25% of the cumulative variation and was negatively correlated to nitrate (r = -0.99) and positive to salinity (r = 0.88). Temperature (p = 0.01; d.f. = 47) and phosphate (p = 0.04; d.f. = 47) were the only significant environmental drivers for the Agulhas Bank.

A generalized linear model also confirmed that phytoplankton communities varied between the eastern and western Agulhas Bank. The drivers for this change in community structure are provided in Table 4.3. From Table 4.3 it is clear that region, temperature, nitrate and nitrite are important environmental drivers that shape phytoplankton communities between the eastern and western Agulhas Bank.

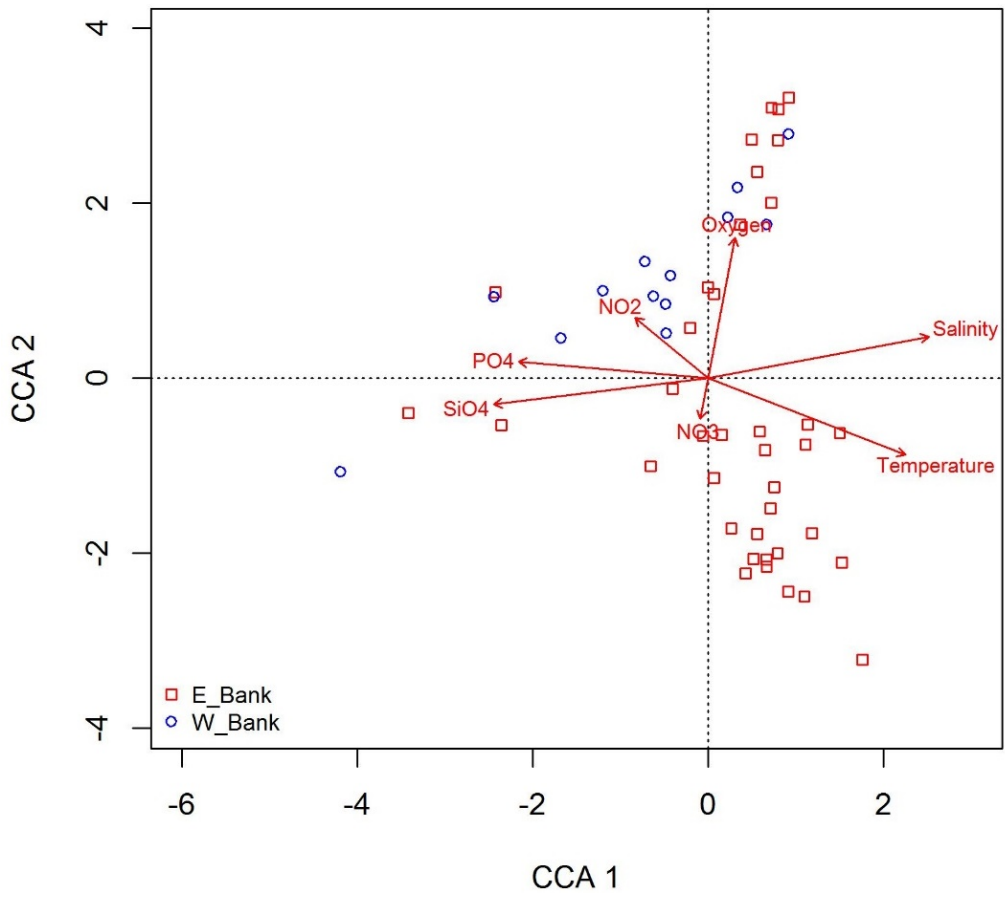

Fig. 4.21 Canonical Correspondence Analyses of the stations constrained by environmental variables.

Table 4.3. ANOVA results from a Generalised Linear Model of the Agulhas Bank.

Environmental Variable	d.f.	Dev.	p
Intercept	51		
Region	50	240.08	0.001***
Temperature	49	195.79	0.001***
Salinity	48	113.47	0.109
Dissolved Oxygen	47	113.78	0.023*
Nitrate	46	199.19	0.001***
Nitrite	45	135.56	0.001***
Silicate	44	147.56	0.034*
Phosphate	43	89.81	0.109

Sigificance Codes: *** p = 0.001, ** p = 0.01, * p = 0.05

4.5 Discussion

4.5.1 Physical and chemical oceanography

The transects across the Agulhas Bank showed significant differences in water temperature, salinity and dissolved oxygen within the euphotic zone. A strong horizontal gradient in surface temperature showed the inshore boundary of the Agulhas Current to be near the 200 m isobath. Vertical section plots of chlorophyll *a* – temperature plots for the eastern Agulhas Bank (Fig. 4.15 to Fig. 4.17) highlighted the influence of the Agulhas Current in trapping chlorophyll *a* between the coast and the inshore boundary of the Agulhas Bank at the 18°C isotherm. The chlorophyll *a* - temperature gradient of the boundary was most pronounced from Cape Recife up to Transect 11 where the coldest inshore water (<15°C) was found. In the vicinity of Transects 11 and 12, the Agulhas Current retroflects in a south-easterly direction

(Lutjeharms and Van Ballegooyen, 1988) and the immediate influence of the Agulhas Current diminishes.

The water of the Agulhas Current proper had temperatures over 20°C, whereas most of the Bank was covered with water colder than 18°C. The range in epipelagic temperature (12.24 to 21.99°C), salinity (34.04 to 35.52) and dissolved oxygen (2.65 to 6.62) of the Agulhas Bank is consistent with previously reported literature (Carter *et al.*, 1987; Chapman and Largier, 1989; Probyn *et al.*, 1994; Lutjeharms *et al.*, 1996; Roberts, 2005; Lutjeharms, 2006; Jackson *et al.*, 2012; Goschen *et al.*, 2015; D'Addezio and Subrahmanyam, 2016).

During the study a Natal Pulse was present and caused the intrusion of warm Agulhas Current water onto the Agulhas Bank (Jackson *et al.*, 2012). Krug *et al.* (2014) observed that when the leading edge of a Natal Pulse intrudes onto the shelf, warm water temperature anomalies occur both at the surface and near the seabed. Natal Pulses play a major role in setting up the isotherms on the Agulhas Bank and in intensifying the seasonal thermocline (Chapman and Largier, 1989). Winter storms and wave action may result in isothermal mixing of the water column and the breakdown of the seasonal thermocline (Eagle and Orren, 1985b). The cold core of a Natal Pulse tends to be nutrient-rich due to upwelling that is associated with the strong cyclonic circulation found within the core (Bryden *et al.*, 2005; Krug *et al.*, 2014; Goschen *et al.*, 2015). The cold water consists of South Indian Central Water that can dome up over the shelf and break the surface along the inshore boundary of the Agulhas Current (Lutjeharms *et al.*, 2000a; Goschen *et al.*, 2015).

Other upwelling regions were also observed around prominent capes such as Cape St Francis and Cape Agulhas. These areas of upwelling are consistent with those reported in the literature (Lutjeharms *et al.*, 2000a; Lutjeharms, 2006; Jackson *et al.*, 2012; Goschen *et al.*, 2015). Sea surface temperature (Fig. 4.2) shows that the cold ridge was absent during the September 2010 cruise. However Jackson *et al.* (2012) reported that the source water for the cold ridge was located at depth, between Transect 7 and 9.

Transect 1, near Port Alfred, is a known area of upwelling (Lutjeharms *et al.*, 2000a). A sea surface temperature plot (Fig. 4.2) of the Agulhas Bank does not indicate

active upwelling at the time of sampling and Jackson *et al.* (2012) made a similar observation. However, a sea surface chlorophyll *a* plot (Fig. 4.14) showed that a upwelling event possibly occurred earlier, transporting nutrient-rich waters westwards towards the adjacent Algoa Bay (Goschen *et al.*, 2012). The upwelling cell located off Port Alfred is believed to be the major source of nutrients for the eastern Agulhas Bank (Lutjeharms *et al.*, 1996). These upwelling processes are also important components of the heat and salinity budgets for the Agulhas Bank (Lutjeharms *et al.*, 2000a).

Epipelagic water on the Agulhas Bank is well oxygenated (Fig. 4.5), especially on the eastern and inner central bank (minimum ≥3 ml l^{-1}). This is likely due to the active shelf-edge upwelling along the inner boundary of the Agulhas Current (Chapman and Largier, 1989; Lutjeharms *et al.*, 2000a; Roberts, 2005). Dissolved oxygen concentrations reported in here are in range with that found in previous studies (Roberts, 2005; Lutjeharms, 2006). Roberts (2005) reported that for dissolved oxygen, the western and inner central Agulhas Bank were similar and share characteristics with the eastern Agulhas Bank and the West Coast. The eastern Agulhas Bank and outer central Bank were similar as they contain Subtropical Surface Water. During our cruise there was, however, a reversal in dissolved oxygen concentrations of the inner and outer central bank. Eagle and Orren (1985b) and Chapman and Largier (1989) showed similar seasonal variation of dissolved oxygen over the Agulhas Bank when the thermocline is well developed. Our data set also showed that dissolved oxygen on the inner central Bank was the highest compared to the rest of the Agulhas Bank, at ≥6 ml l^{-1}. Only Algoa Bay had such high levels of dissolved oxygen.

Nutrient distribution plays an important role in the distribution and composition of phytoplankton communities. In marine ecosystems, nitrogen and phosphorus are the main inorganic nutrients needed for growth, although silicate could limit the growth of diatoms (Yool and Tyrrell, 2003; Crombet *et al.*, 2011). The surface distribution of nutrients (Appendix: Agulhas Bank; Fig. 9.4) shows strong regional differences in concentrations over the Agulhas Bank. The phosphate and silicate concentrations were less variable on the western Bank than the eastern Bank. Both were characterised by pronounced cross-shelf gradients. Lutjeharms *et al.* (1996) reported

similar results but found the western Bank to be more nutrient rich with a stronger cross-shelf gradient than the eastern Bank. The station off Cape Agulhas had extremely high surface silicate and phosphate concentrations, substantially increasing the variability of these nutrients on the western Bank. On the eastern Bank, silicate and phosphate concentrations were found to be higher around the prominent capes and bays, as well as in the vicinity of the upwelling zone near Port Alfred. Lutjeharms *et al.* (2000a) suggested that upwelling at the far eastern Agulhas Bank contributed a high nutrient load to the rest of the Bank. The presence of upwelled water is even more evident in the nutrient-temperature relational graphs (Fig. 4.12). Surface silicate and phosphate were higher in the vicinity of the cold ridge region but lower than at the coast. The silicate and phosphate concentrations of the eastern Bank suggest that Subtropical Surface Water is the predominant source of surface water across the Agulhas Bank, whereas South Atlantic Water is the main source for the western Bank. Phosphate and silicate concentrations were well within the characteristic nutrient ranges for South Atlantic Water (Largier *et al.*, 1992) and for Subtropical Surface Water (Henry, 1975; Goschen and Schumann, 1988).

The sea surface distribution of nitrate shows regions of higher concentrations. These are prominent along the various headlands, capes and bays as well as the southern end of the cold ridge. Surface nitrate concentrations above most of the cold ridge region were low (<1 µM). However, towards the southern end and just west of the cold ridge, patches of higher nitrate concentration (2-3 µM) were observed, suggesting that upwelling was present, but very weak. Smaller regions of higher nitrate concentration were also found along the eastern edge of the Agulhas Bank (Lutjeharms *et al.*, 2000a). This is believed to be due to the advection of nutrient-rich waters on to the bank due to of the Agulhas Current (Lutjeharms, 2006). These regions had lower nutrient concentrations compared to the areas along the coast. The transects between Port Alfred and Cape St Francis showed pronounced cross-shelf gradients for nitrate as expected considering the Agulhas Current contributes nutrient-depleted water to the surface (Lutjeharms *et al.*, 1996). Silicate and phosphate concentrations found in this study are within range of those reported in

the literature (Probyn *et al.*, 1994; Probyn *et al.*, 1995; Lutjeharms *et al.*, 1996; Lutjeharms *et al.*, 2000a; Lutjeharms, 2006).

The differences in nutrient distributions on the Agulhas Bank can be associated with different processes, bottom topography and offshore influences. For example, the eastern Agulhas Bank is broad and flat, deepening from west to east, whereas the western Bank is narrow, steep and deepens in an across-shelf direction. This has an influence on the depth of the thermocline. The increase in depth of the thermocline for the eastern Bank is alongshore, but cross-shelf for the western Bank (Largier and Swart, 1987). With the direct relationship between the thermocline and nutricline depth (Probyn *et al.*, 1994), the same cross-shelf variation was expected for the western Agulhas Bank. Bottom topography can therefore partially explain the variation in the cross-shelf nutrient variations for the Agulhas Bank. Wind-driven coastal upwelling around capes could also be a mechanism accounting for the cross-shelf nutrient gradients observed during this study.

The waters around Cape Recife (Transect 3, Fig. 4.10) and Cape St Francis (Transect 21, Table 4.1) appear to be the only region along the coast where excess nitrate was found. The Agulhas Shelf was found to be more silicate limited than the Agulhas Bank. The dissolution of large concentrations of diatom frustules (Nelson *et al.*, 1991) from previous upwelling events could lead to the increase in silicate over the Agulhas Bank.

4.5.2 Spatial variability of phytoplankton

The upper water column of the Agulhas Bank was characterised by a mean chlorophyll *a* concentration of 4.50 ± 3.26 µg l^{-1} with the highest (>10 µg l^{-1}) concentrations found in Algoa Bay, the upwelling-dominated coastal areas of the eastern Agulhas Bank and the cold ridge. On the eastern Agulhas Bank; phytoplankton distribution and surface chlorophyll *a* was bounded by the inshore edge of the Agulhas Current. Chlorophyll *a* and nutrients within the Agulhas Current proper was relatively low and unproductive compared to the meandering inshore waters.

During cruises in 1970 and 1980, the upper water column of the Agulhas Bank showed similar characteristics to those reported here. A mean chlorophyll *a* concentration of 1.48 µg l^{-1} was found here, with the highest concentrations (>3 µg l^{-1}) measured in the western sector of the upwelling-dominated coastal area (Probyn *et al.*, 1994). Mitchell-Innes *et al.* (1999) reported that during late winter (August-September), chlorophyll *a* concentrations on the western Agulhas Bank ranged between 0.4 and 5.7 µg l^{-1} with a mean of 1.9 µg l^{-1}. The eastern Agulhas Bank on the other hand was characterised by local patches of moderate (>2 µg l^{-1}) chlorophyll *a* concentration that were associated with the upwelling that occurs west of Cape St Francis or with the cold ridge. These moderate patches of chlorophyll *a* may also extend towards the south-east shelf of the Agulhas Bank (Probyn *et al.*, 1994). In our study, the surface (Fig. 4.14) and vertical distribution plots (Fig. 4.15) clearly showed a similar pattern of chlorophyll *a* distribution along the eastern shelf of the Agulhas Bank. This upwelling-productive zone along the coast, bounded by the 18°C isotherm, varied from <5 to 50 km across the shelf. Outside this productive zone, mean chlorophyll levels were low (<2 µg l^{-1}). Mitchell-Innes *et al.* (1999) reported that these vertical and cross shelf distribution patterns of chlorophyll *a* are seasonal due to changes in hydrographic structure and nutrient availability. They also reported that newly upwelled water had very low concentrations (<0.5 µg l^{-1}) of chlorophyll *a* and only attained peak concentrations (5-25 µg l^{-1}) later in mature upwelled water.

The SCM extended from near the surface to a depth of 20 to 30 m for the eastern Agulhas Bank, and 9 to 30 m for the western Bank. These were shallow for late winter conditions (16.6 to 101 m), but more in line with spring and summer conditions for the western Agulhas Bank (Mitchell-Innes *et al.*, 1999).

Thalassiosira weissflogii, Pseudo-nitzschia spp. and *Guinardia* spp. contributed most to surface chlorophyll *a* concentrations. A similar observation was made by Mitchell-Innes *et al.* (1999). Both the eastern and western Agulhas Bank were mesotrophic in nature with localised patches of increased biomass around prominent capes and headlands. The diatoms, *T. weissflogii*. and *Guinardia* spp., were the most abundant taxa in the eastern Bank coastal waters.

Phytoplankton communities in the oligotrophic subtropical ocean tend to be dominated by picophytoplankton in terms of primary productivity, chlorophyll *a* and cell concentration (Platt *et al.*, 1983; Zubkov *et al.*, 1998; Poulton *et al.*, 2006). Regions of high chlorophyll *a* concentration that are associated with areas of coastal upwelling and other upwelling processes, can lead to significant changes in the size structure of the community (Poulton *et al.*, 2006). This can also lead to the increase in the abundance of diatoms and dinoflagellates (Barlow *et al.*, 2002; Barlow *et al.*, 2004). For the Agulhas Bank, both these statements hold true: Microphytoplankton dominated the phytoplankton community with diatoms and dinoflagellates being the most abundant taxa within the upwelling regions. This however, was not only limited to the upwelling regions of the Agulhas Bank but to the Bank as a whole.

4.5.3 Phytoplankton composition

The phytoplankton community showed an east-west gradient with decreasing diversity from east to west. Diatoms were the dominant (>50% of total number of species) phytoplankton functional group with the other functional groups making up a significantly ($p < 0.05$; d.f. = 50) smaller contribution to the phytoplankton community. Species diversity for the Agulhas Bank was lower compared to that of the Agulhas Shelf.

The dominant diatom for both the eastern and western Agulhas Bank was *Thalassiosira weissflogii* and accounted for a large percentage of the number of cells. On the eastern Agulhas bank, *Alexandrium* spp. were found to be the most abundant dinoflagellate and *Gonyaulax* spp. on the western Agulhas Bank. The environmental and biological data separated the Bank stations into eastern and western communities. The eastern community can be subdivided into two additional smaller communities, i.e. inshore and offshore. The offshore community was located within the Agulhas Current proper and contained species such as the cosmopolitan *Ceratium fusus* (Ehrenberg) Dujardin, that prefer warm oligotrophic waters. The inshore community contained species that prefer less saline, cooler and nutrient-rich waters. These species tend to be larger in size (>20 µm) and they contributed most to total chlorophyll *a*. However, the species composition was sufficiently similar for

the phytoplankton of these two regions to still be considered a single community. It was only rare species that differed on the eastern and western Bank.

4.5.4 Environmental drivers of phytoplankton variability

The environmental drivers most responsible for the observed species distribution in waters of the Agulhas Bank were temperature and phosphate. Temperature and nutrients are known to determine the physiological state of the cells and therefore regulate uptake and deposition rates (Brzezinski, 1985; Blank *et al.*, 1986). Various studies have demonstrated that temperature is an important environmental variable that influences biological processes in the ocean and that the phytoplankton community structure varies in a regular and predictable pattern with temperature (Bouman *et al.*, 2003; Bouman *et al.*, 2005; Platt *et al.*, 2005; Barlow *et al.*, 2008).

Hulburt and Rodman (1963) showed that most phytoplankton, especially diatoms, preferred lower salinities (<34). Although most phytoplankton species prefer lower salinity, they also frequent higher salinities. For example, *Oxytoxum* Stein spp. was found throughout the salinity range (Hulburt and Rodman, 1963). Coccolithophores are characteristic of the tropical and open ocean and prefer salinity greater than 34.5. Several of the species recorded in this study were found to grow better at lower salinity, but within a certain tolerance range (Nordli, 1953; García *et al.*, 2012). At lower salinities, the rate of silicification increases for diatoms (Tuchman *et al.*, 1984; Vrieling *et al.*, 1999). This is thought to help protect cells against osmotic stress (Olsen and Paasche, 1986; Vrieling *et al.*, 1999).

The ecological drivers of phytoplankton distribution across the Agulhas Bank are mainly linked to various upwelling events along the eastern and western Agulhas Bank. Upwelled waters on the Agulhas Shelf (Chapter 2) as well as the Agulhas Bank consisted mainly of cold nutrient-rich South Indian Central Water. The significant correlation between temperature and salinity (Table 4.1) may indicate the origin of the water masses within the Agulhas Bank: e.g. cooler water on the eastern bank tends to be fresher and must therefore be of South Indian Central Water origin. Both temperature and salinity had significant negative correlations with nutrients. The Agulhas Current proper is characterised by higher temperature and salinity as

well as low levels of nutrients – as is characteristic of Subtropical Surface Water. Both the Agulhas Shelf and Agulhas Bank chlorophyll *a* biomass associated with Subtropical Surface Water was generally low. Thus, upwelling and the associated mixing of the water masses drive phytoplankton variability across the Agulhas Shelf and the Agulhas Bank, especially the eastern Bank.

4.6 Conclusions

Nitrate was the most limiting nutrient during the survey of the Agulhas Bank. It is doubtful that this would have had a negative impact on phytoplankton growth because of the constant allochthonous introduction of inorganic nutrients from various upwelling across the Agulhas Bank, e.g. Natal Pulses and wind induced upwelling events along the prominent capes (Schumann, 1999; Goschen *et al.*, 2015). It is evident that these upwelling events can bring sufficient nutrients onto the Agulhas Bank to sustain phytoplankton growth across the Bank. The advection of cold, nutrient-rich South Indian Central Water onto the eastern bank by the Agulhas Current and associated Natal Pulses can keep the Shelf edge of the eastern Bank in a state of nitrate excess. Further west, surface nutrients are supplied through upwelling associated with the cold ridge, maintaining productivity and the community structure across the Agulhas Bank. It is these upwelling events and the associated water masses that drive phytoplankton variability across the Agulhas Bank, especially the eastern Bank. Diatoms prefer regions of upwelling - more so than dinoflagellates and other functional groups. They have an ability to utilise “new nitrate” for growth and may also use the upliftment of isotherms to keep them suspended within the euphotic zone.

The null hypothesis that there is no change in the phytoplankton community across the Agulhas Bank could not be completely rejected. It is the abundance in the cosmopolitan species across the Bank that changes as there is no single dominant species. Diatoms were, in general, the dominant functional group over the Bank. This study contributed significantly to our knowledge of phytoplankton distribution and ecology along the Agulhas Bank. This survey, however; provided only a snap shot and could not resolve a number of processes that have time scales of more than a day.

5 The Agulhas Retroflection

5.1 Abstract

A survey of the Agulhas Retroflection in the South Indian Ocean in March 2011 showed a strong gradient across the Agulhas Current proper and into the surrounding waters. All nutrients, with nitrite being the exception, showed clear concentration gradients, both vertically and horizontally across the Retroflection area. The gradient is the steepest near the edge of the Agulhas Current and within the SCM. Nutrients were also elevated in the surrounding waters below the SCM. The Retroflection waters appear to be nitrogen limited for phytoplankton (a deviation from the Redfield ratio). CCA and Generalised Linear Models indicated that temperature, salinity and phosphate were the primary drivers of phytoplankton assemblages for the Agulhas Retroflection area. Species diversity of waters of the Agulhas Current decreased along its path with low diversity recorded in the Agulhas Current water. The 80 observed taxa separated into two communities, Agulhas Current and non-Agulhas Current communities. The Agulhas Current community was found where the temperature was above 17°C and the salinity above 35.45. The non-Agulhas Current community preferred cooler temperatures (<17°C) and a lower salinity (< 35.45). It is clear that frontal systems may form barriers between phytoplankton communities.

5.2 Introduction

Phytoplankton are important components of all aquatic ecosystems. In marine systems they have important functions in primary production, biochemical cycles and regulating the global carbon budgets in the world's oceans. Phytoplankton communities are dynamic and may vary between areas as well as within the same water body. This variation is due to the complex hydrological features that are associated with them.

The study site is an area just east of the normal Agulhas Retroflection region, south of Africa (16°E to 22°E according to Dencausse *et al.* (2010); Fig. 5.1) and often experience early Agulhas Retroflection (van Aken *et al.*, 2013). The Agulhas Current

turns on itself and returns eastwards as the ARC at about 39°S (Dencausse *et al.*, 2010), The Agulhas Retroflection plays a pivotal role in heat exchange between the Indian and Atlantic Oceans (Gordon, 1985) in the form of Agulhas Rings (Lutjeharms and Van Ballegooyen, 1988). The area is highly dynamic and unstable and as a consequence the area should be characterised by intermittent and short-lived phytoplankton communities. It is, in particular, of interest to determine which of the environmental drivers shape these communities.

The objective of this snapshot observation was to study the phytoplankton community structure in the Agulhas Retroflection area of the ACLME by characterizing species composition and chlorophyll *a* in relation to the prevailing physico-chemical variables. The information obtained from the study would be useful in contributing to our knowledge of the phytoplankton communities that occur within the sACLME. To determine whether the Agulhas Current has an influence on the biological productivity we developed the following hypothesis:

The phytoplankton community of the Agulhas Retroflection changes from a low biomass and dinoflagellate dominated community in the oligotrophic waters of the Agulhas Current to an elevated biomass, diatom dominated community in the Agulhas Retroflection.

5.3 Study Area

An oceanographic survey was carried out aboard the *FRS Africana* in March 2011. Three transects with a total of nineteen oceanographic stations were sampled southeast of Cape Agulhas and past the 1000 m isobath. Transect one was orientated from north to south, transect two southwest to southeast and transect three was from east to west with stations approximately 10 nautical miles apart. Sampling was conducted within the framework of ACEP II (African Coelacanth Ecosystem Program Phase II) and ASCLME (Agulhas and Somali Current Large Marine Ecosystems Project). The study area covered the Agulhas Retroflection from 36°S to 39°S and 21°E to 24°E. The methodology and statistical analysis used in this study was identical to that presented in sections 3.3.2, 3.3.3, 3.3.4 and 3.3.5. The

study area covered the Agulhas Retroflection from 36°S to 39°S and 21°E to 24°E (Fig. 5.1).

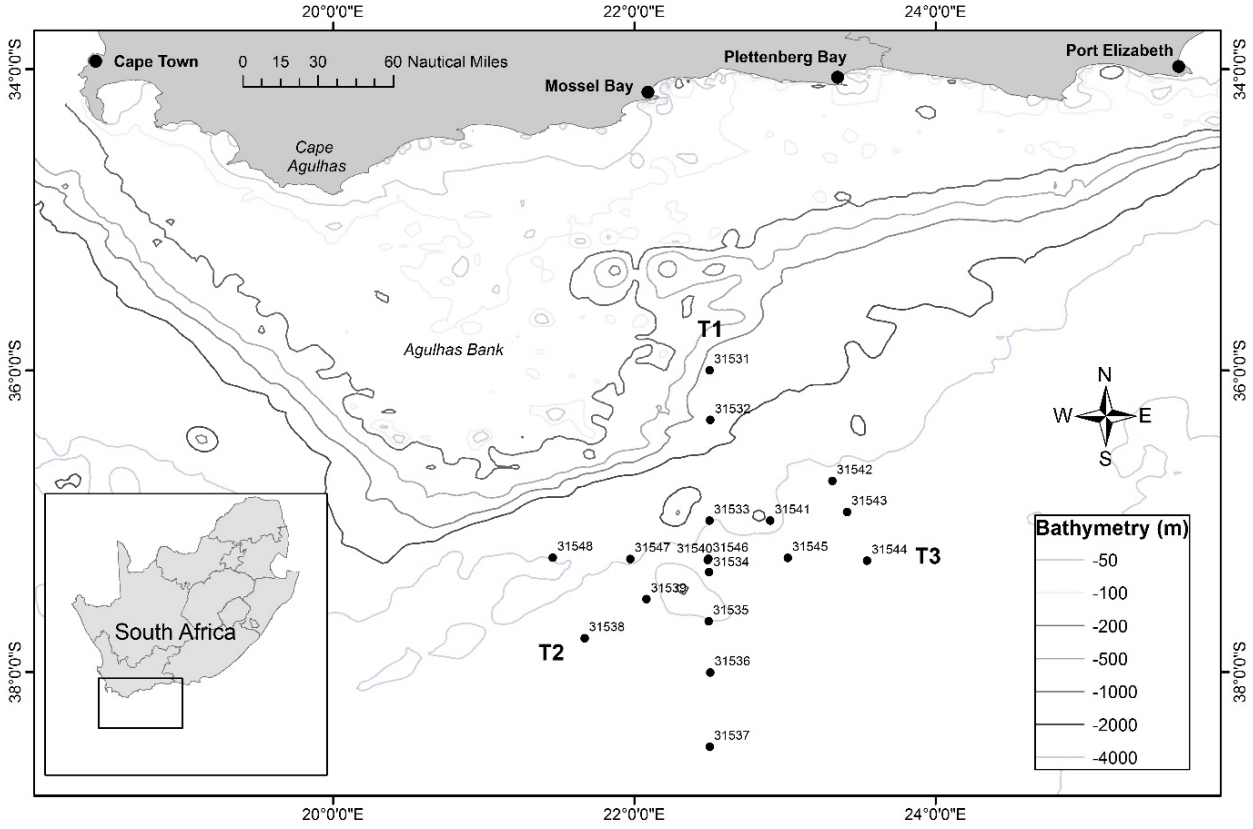

Fig. 5.1 The Agulhas Retroflection study site showing the position of the sampling stations (black circles).

5.4 Results

5.4.1 Physical and chemical oceanographic conditions

The sea surface temperature of the study area at the time of sampling is shown in Fig. 5.2. The northern section of the study area was cooler compared to the southern section with a plume of warm water dissecting the study area. Sea surface temperature ranged from 21.90 to 26.16°C with a mean of 23.60 ± 1.52°C. Fig. 5.3 shows the temperature profiles for the selected transects at depth. The epipelagic temperatures for the Agulhas Retroflection Area ranged from 12.25 to 26.16°C with a mean of 20.20 ± 3.90°C. The aggregated data for the north-south transect had a

mean temperature of 20.37 ± 3.65°C, with a maximum of 25.68°C. The east-west transect was slightly cooler and showed more variance with a mean temperature of 19.55 ± 4.65°C. The eastern-most station (Fig. 5.1: 31545) of Transect 1 was located within the Agulhas Current and had the highest recorded temperature of 26.16°C. Transect 2 (SW to SE) had a mean temperature of 20.40 ± 3.92°C. There was no significant difference ($F = 0.20$; $p > 0.05$; d.f. = 51) between the three transects. However, temperature did show a significant ($F = 40.02$; $p < 0.05$; d.f. = 51) gradient with depth.

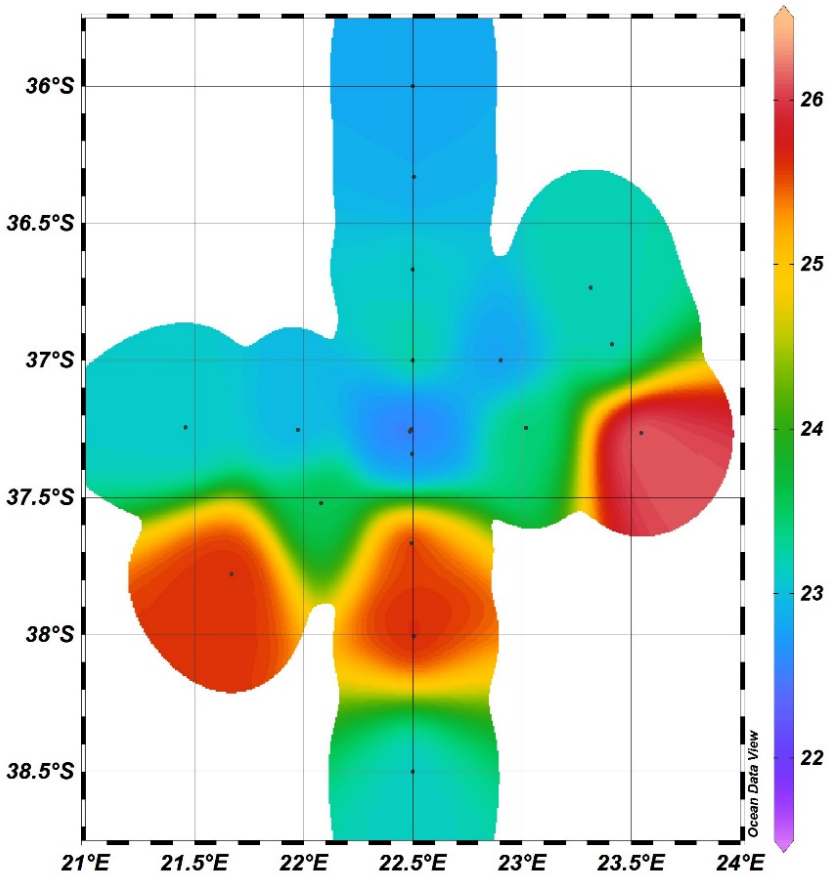

Fig. 5.2 Sea surface temperature measured in the Agulhas Retroflection. The black dots represent the sampling stations.

(a) North - South

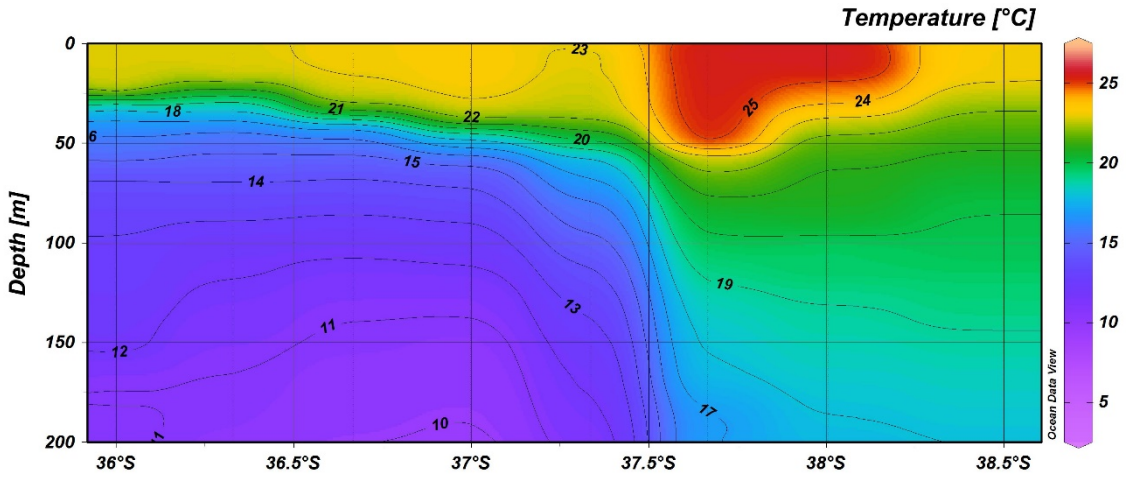

(b) East - West

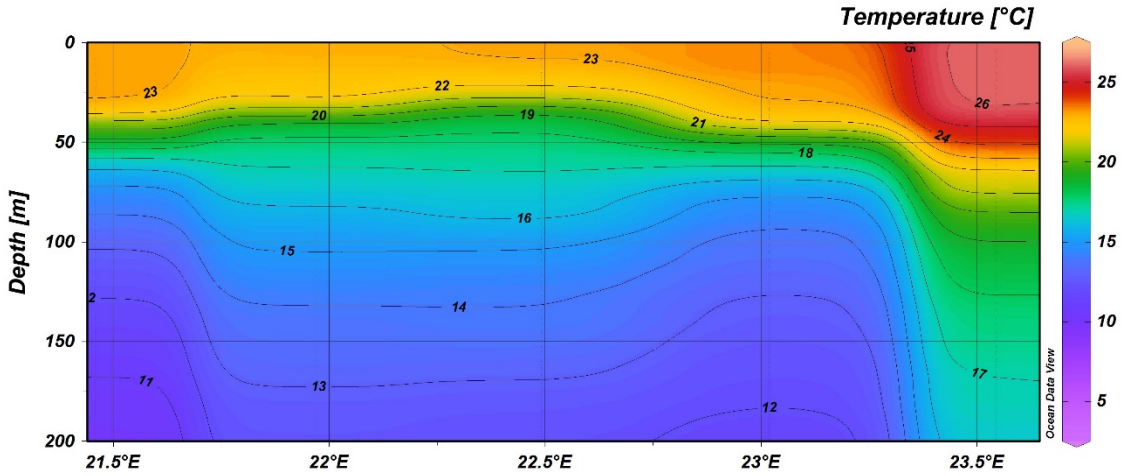

Fig. 5.3 Temperature (°C) profiles through the epipelagic zone of the Agulhas Retroflection Area. The orientation of Transect 1 (a) is north to south and for Transect 3 (b) is east to west.

Discreet salinity samples for the Agulhas Retroflection ranged from 35.11 to 35.63 with mean of 35.39 ± 0.11. There was no significant difference ($F = 0$; $p > 0.05$; d.f. = 51) between the salinity of the Transects nor at the different depths. A latitudinal plot (Fig. 5.4a) of salinity shows a gradient across the Agulhas Retroflection, with the northern section being slightly fresher than the southern section. Vertical profiles of

temperature (Fig. 5.3) and salinity (Fig. 5.4) show a clear delineation between the Agulhas Current and the surrounding body of water.

(a) North - South

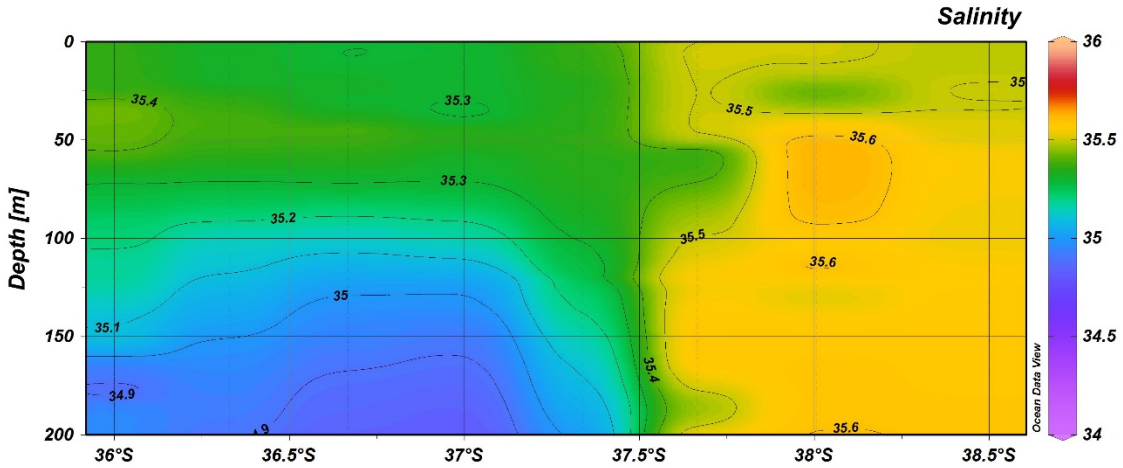

(b) East - West

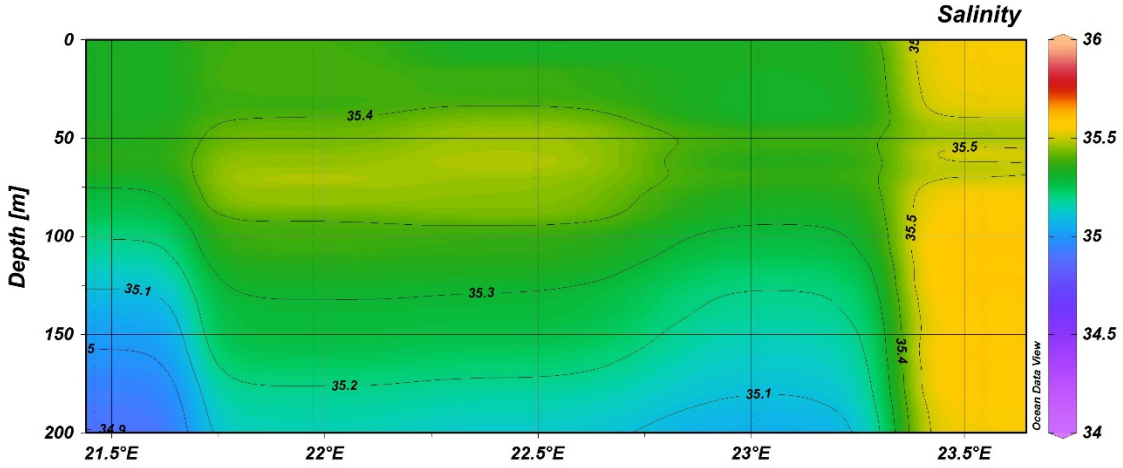

Fig. 5.4 Salinity profiles through the epipelagic zone of the Agulhas Retroflection Area. The orientation of Transect 1 (a) is north to south and for Transect 3 (b) is east to west.

Oxygen concentrations across the Agulhas Retroflection area ranged from 3.37 to 4.81 mg l^{-1} with a mean of 4.32 ± 0.39 mg l^{-1}. There was no observed difference ($F = 1.84$; $p > 0.05$; d.f. = 51) in oxygen concentrations between the Transects. Oxygen concentration at (4.19 mg l^{-1}) and below (3.98 mg l^{-1}) the SCMs were significantly lower ($F = 11.20$; $p < 0.05$; d.f. = 51) compared to the surface (4.59

mg l^{-1}). In Fig. 5.5a, a patch of low oxygen (< 3.75 mg l^{-1}) concentration suggests that this body of water may have come from Tropical Thermocline waters, whereas elevated levels of oxygen can be an indication that Subtropical Surface Water is present. Temperature-salinity plots (Appendix: Agulhas Retroflection; Fig. 9.5) of the water masses support this and show that South Indian Central Water is located deeper within the euphotic zone.

(a) North - South

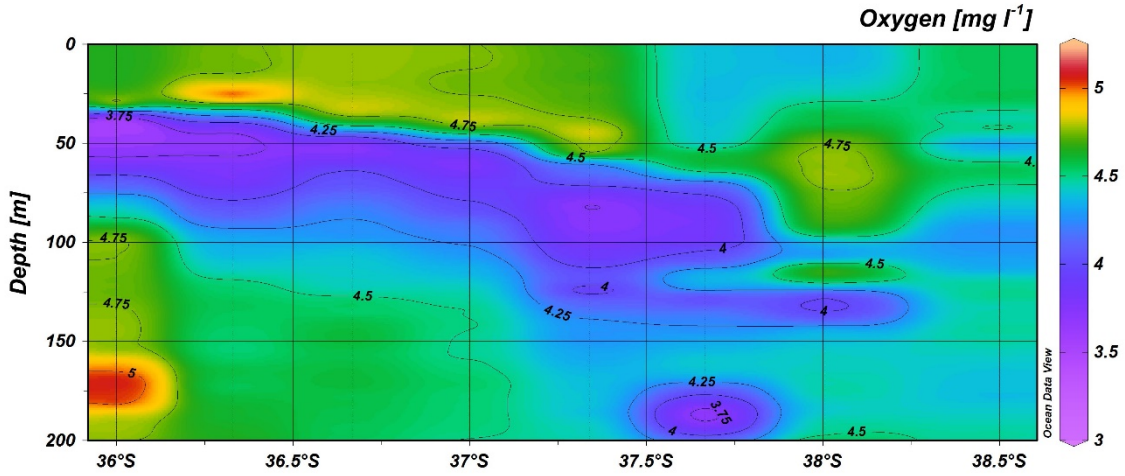

(b) East - West

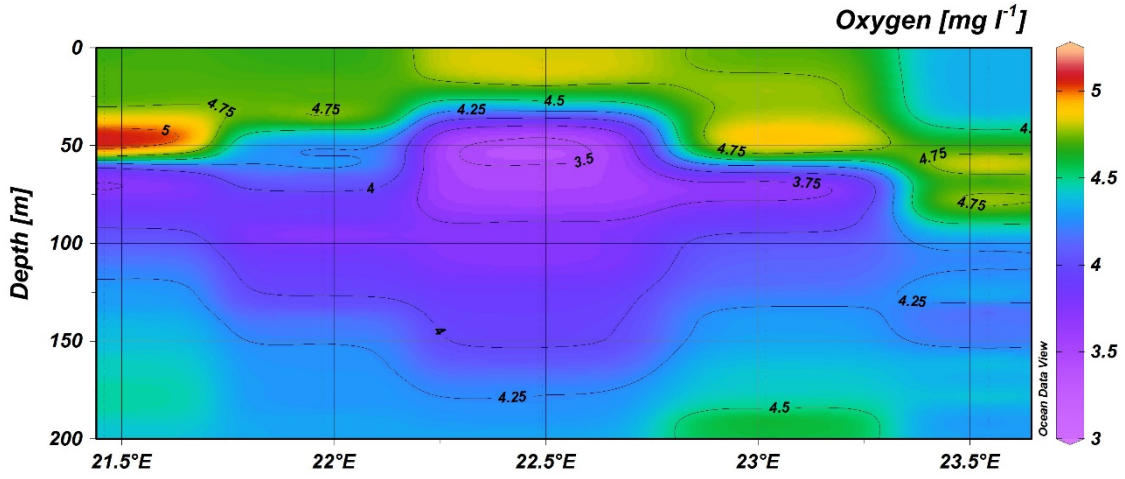

Fig. 5.5 Oxygen (mg l^{-1}) profiles through the epipelagic zone of the Agulhas Retroflection Area. The orientation of Transect 1 (a) is north to south and for Transect 3 (b) is east to west.

The nitrate concentrations for the Agulhas Retroflection epipelagic area are shown in Fig. 5.6. Nitrate concentrations ranged from 0 to 12.51 μM with a mean of 2.39 ± 3.49 μM. Surface waters across the Retroflection had nitrate concentrations between 0 and 0.56 μM with a mean of 0.15 ± 0.18 μM. Nitrate concentrations within the SCM were slightly elevated, with values ranging from 0 to 7.04 μM and a mean of 2.31 ± 2.28 μM. Below the SCM, nitrate concentrations of the water were significantly higher ($F = 12.15$; $p < 0.01$; d.f. = 49), ranging from 1.1 to 12.51 μM, with a mean of 6.24 ± 4.34 μM. Fig. 5.6a shows a north-south gradient across the Retroflection with the northern section having elevated nitrate concentrations and the Agulhas Current being oligotrophic. The east-west transect (Fig. 5.6b) also shows elevated levels of nitrate outside of the Agulhas Current. Nitrite concentrations were very low across the Retroflection ranging from 0 to 0.24 μM with a mean of 0.03 ± 0.06 μM. Nitrite appears to be associated with Tropical Thermocline Water and lower oxygen concentrations (Fig. 5.5 and Fig. 5.7).

Phosphate concentrations for the Agulhas Retroflection Area ranged from 0 to 0.95 μM with a mean of 0.25 ± 0.27 μM. The profile (Fig. 5.8a) of phosphate shows a decreasing gradient in concentration from north to south. The east to west transect (Fig. 5.8b) showed a short, but clear gradient of increasing phosphate between the Agulhas Current and surrounding water. Both transects displayed an increasing phosphate concentration at depth for the area outside of the Agulhas Current. By contrast, within the Agulhas Current, no such gradient was observed. Mean surface nitrate concentration was 0.02 ± 0.03 μM and was significantly lower ($F = 37.95$; $p < 0.01$; d.f. = 49) than that at the SCM (0.30 ± 0.15 μM) and below the SCM (0.59 ± 0.21 μM).

Silicate concentrations for the Agulhas Retroflection Area are shown in Fig. 5.9. Concentrations ranged from 0 to 7.97 μM with a mean of 2.49 ± 2.42 μM. Both transects (Fig. 5.9a and b) showed an increase in silicate concentration with depth with surface concentrations being very low (< 1 μM). The north-south transect showed a gradient in silicate concentrations, with the north having higher concentrations compared to the south. The change in gradient is most significant around 37.5 °S which is near the edge of the Agulhas Current. Silicate concentrations within the Agulhas Current remained constant and similar to the

surface concentrations. For the east-west transect (Fig. 5.9b) a significant change in concentration was observed with depth with slightly elevated levels of silicate within the Agulhas Current but only below the SCM. The mean surface concentration was 0.52 ± 0.48 µM and this was significantly lower ($F = 28.86$; $p < 0.01$; d.f. = 49) than that at the SCM (2.52 ± 1.31 µM) or below the SCM (5.64 ± 2.19 µM).

(a) North - South

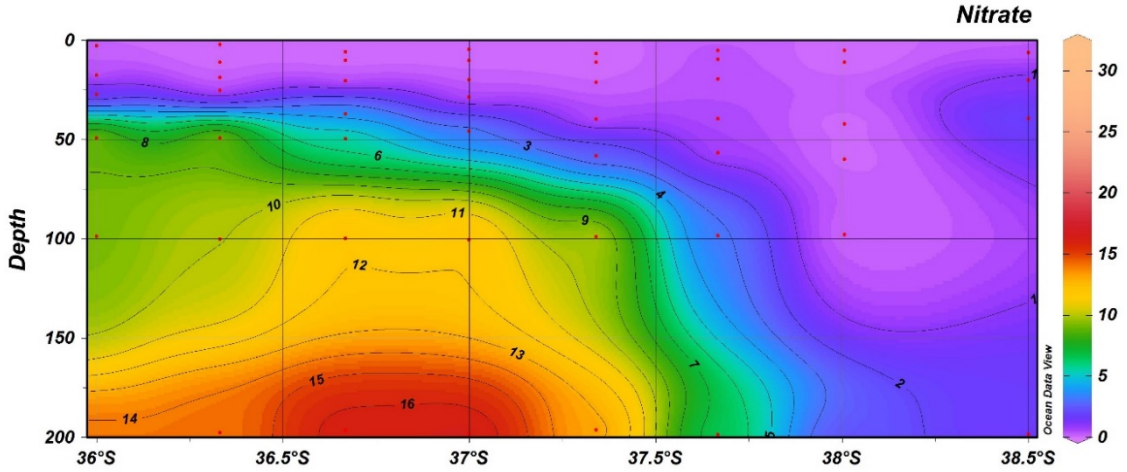

(b) East - West

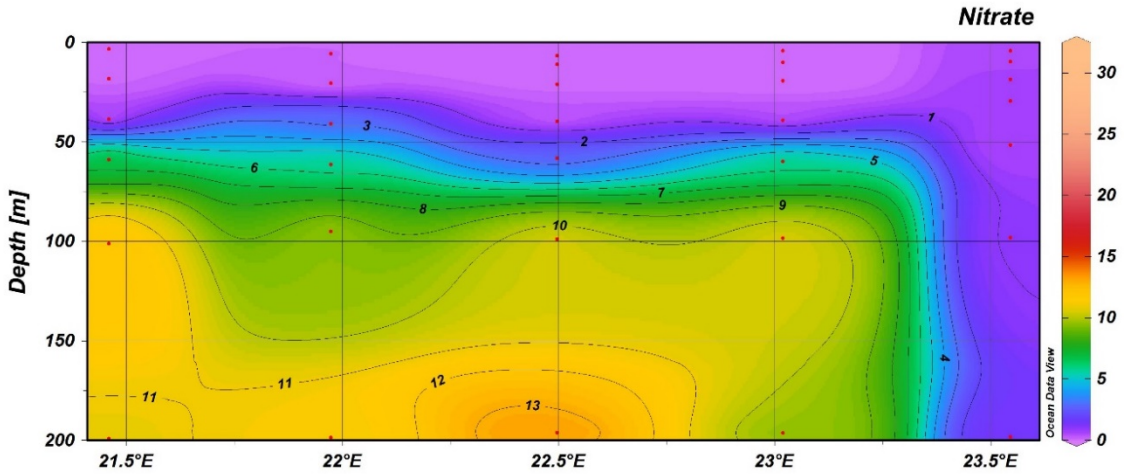

Fig. 5.6 Nitrate (µM) profiles through the epipelagic zone of the Agulhas Retroflection Area. The orientation of Transect 1 (a) is north to south and for Transect 3 (b) is east to west. Red dots are the location of the samples.

(a) North - South

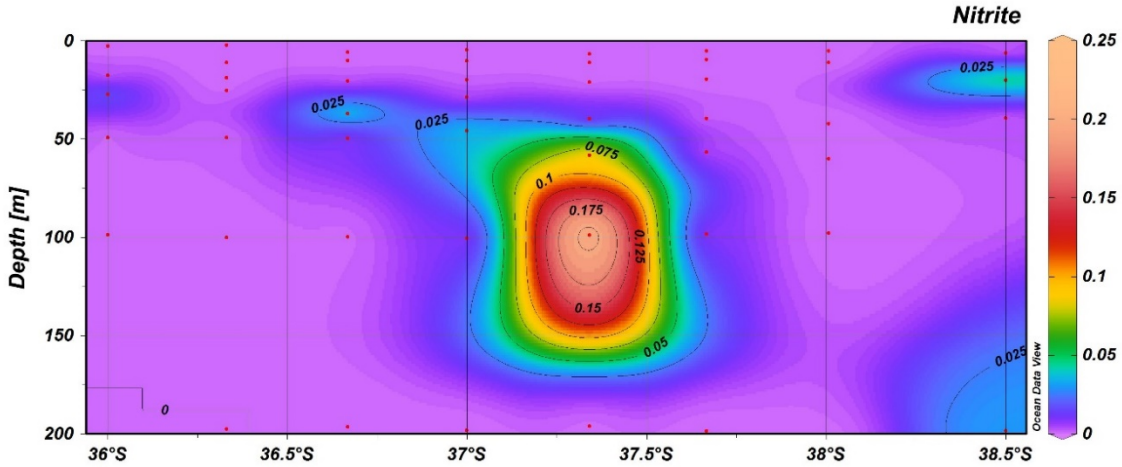

(b) East - West

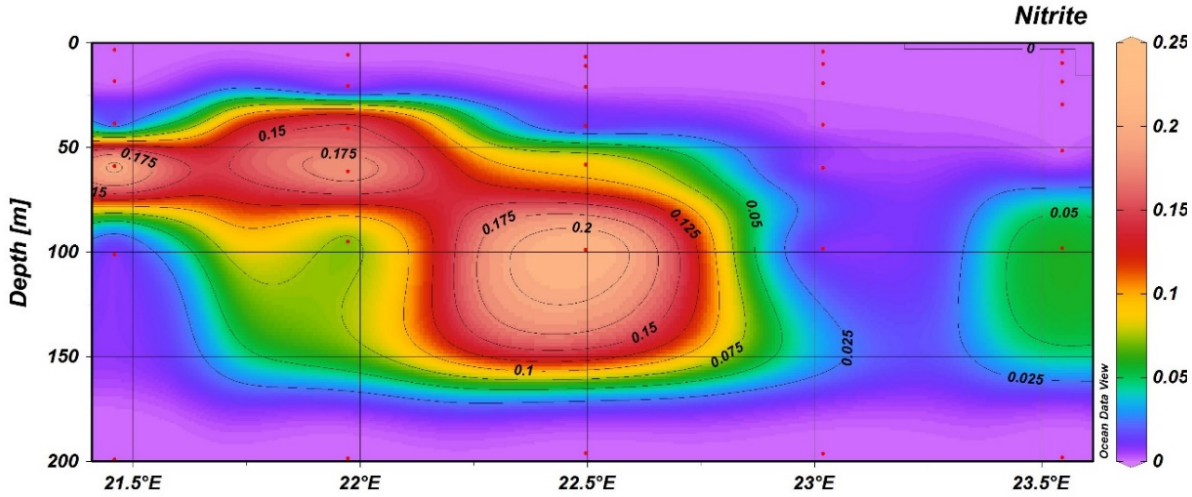

Fig. 5.7 Nitrite (µM) profiles through the epipelagic zone of the Agulhas Retroflection Area. The orientation of Transect 1 (a) is north to south and for Transect 3 (b) is east to west. Red dots are the location of the samples.

All nutrients, with nitrite being the exception, showed clear concentration gradients, both horizontally and vertically, across the Retroflection area. The gradient is the steepest near the edge of the Agulhas Current and within the SCM. The concentrations were elevated in the surrounding waters (outside of the Agulhas Current but below the SCM).

The deviation of the regression lines from the Redfield ratio in Fig. 5.10 and Fig. 5.11 indicates nitrogen limitation for the Agulhas Retroflection Area. All three transects appear to be nitrate limited, but this is especially true for Transect 2. Transect 1, 2 and 3 had a N:P ratios of 12.17:1, 3.64:1 and 15.24:1, respectively. Transects 1 and 3 had N:Si ratios of 1.48:1 and 1.64:1, respectively.

(a) North - South

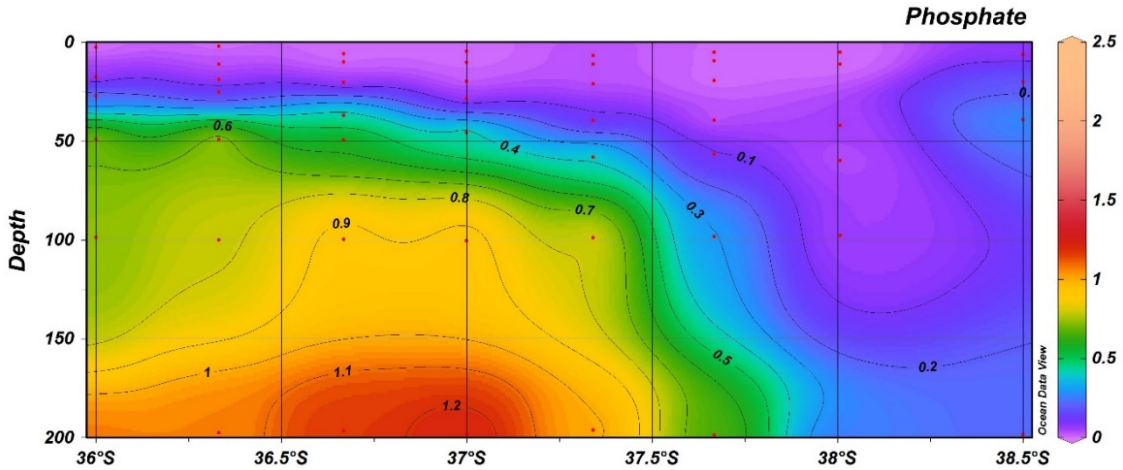

(b) East - West

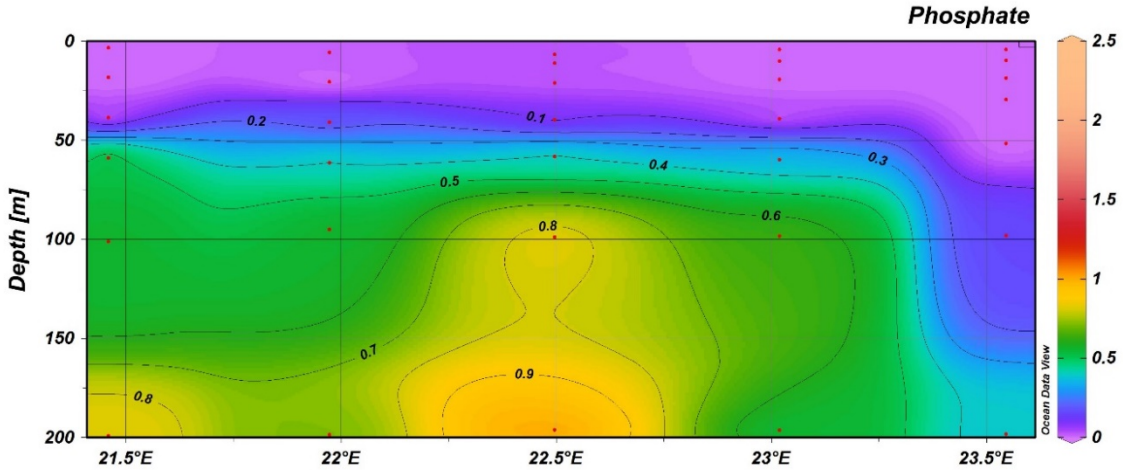

Fig. 5.8 Depth profiles of phosphate (µM) through the epipelagic zone of the Agulhas Retroflection Area. The orientation of Transect 1 (a) is north to south and Transect 3 (b) is east to west.

The four nutrients had significant negative correlations with temperature and oxygen (Table 5.1). Plotting the nutrients against temperature (Fig. 5.12) and salinity (Fig. 5.13), the nutrients showed an inverse linear relationship with both and can be divided into two categories. The first category is when the temperature is 17°C and the salinity is 35.45; then there are higher nutrient concentrations in the deep waters below the chlorophyll *a* maximum. The second category occurs when the temperature is above 17°C and salinity is above 35.45; then nutrient concentrations are low in the upper euphotic zone.

(a) North - South

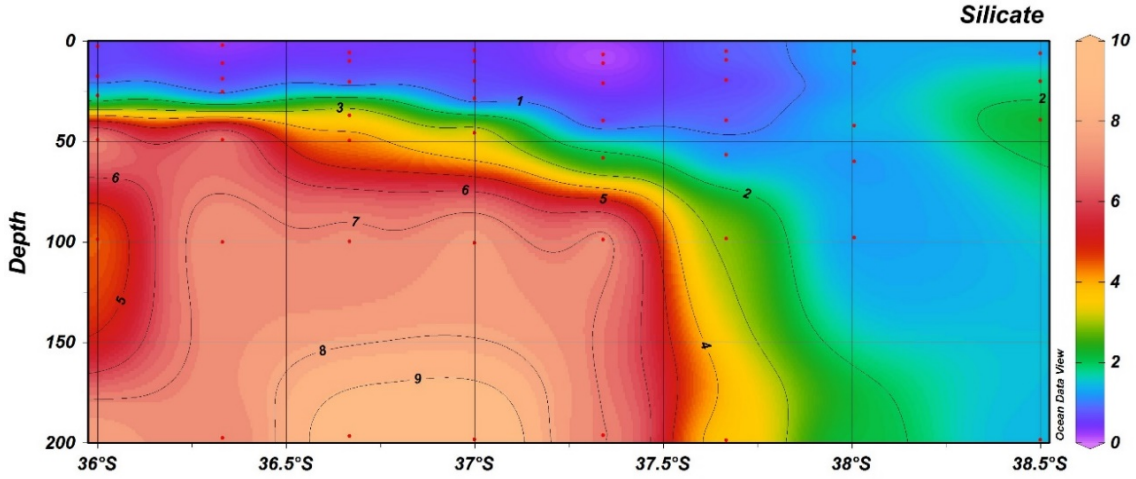

(b) East - West

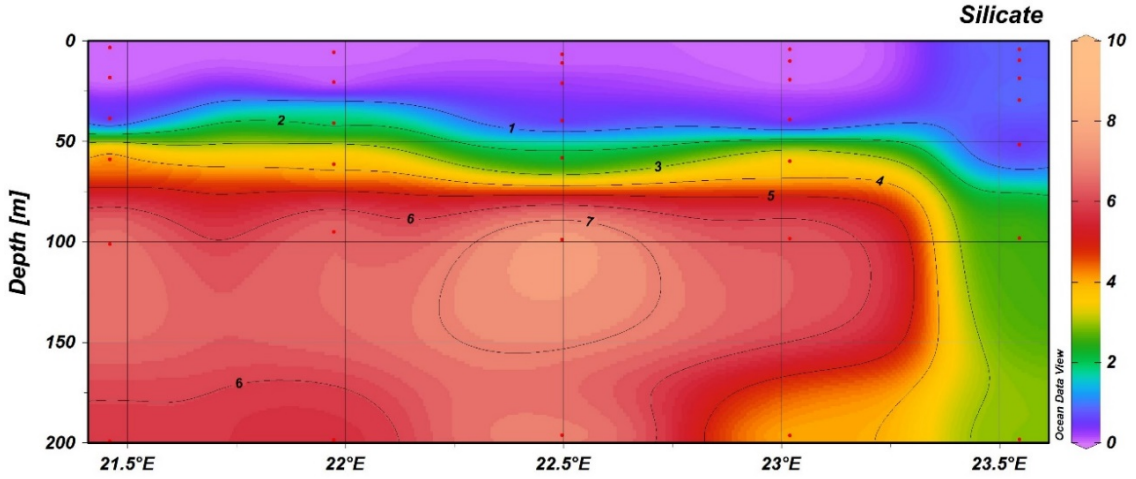

Fig. 5.9 Depth profiles of silicate (µM) through the epipelagic zone of the Agulhas Retroflection Area. The orientation of Transect 1 (a) is north to south and Transect 3 (b) is east to west.

Table 5.1 Pearson correlation analysis with pairwise deletion of the environmental variables of the Agulhas Retroflection. Significant correlations are indicated as follows: *** p < 0.001, ** p < 0.01, * p < <0.05.

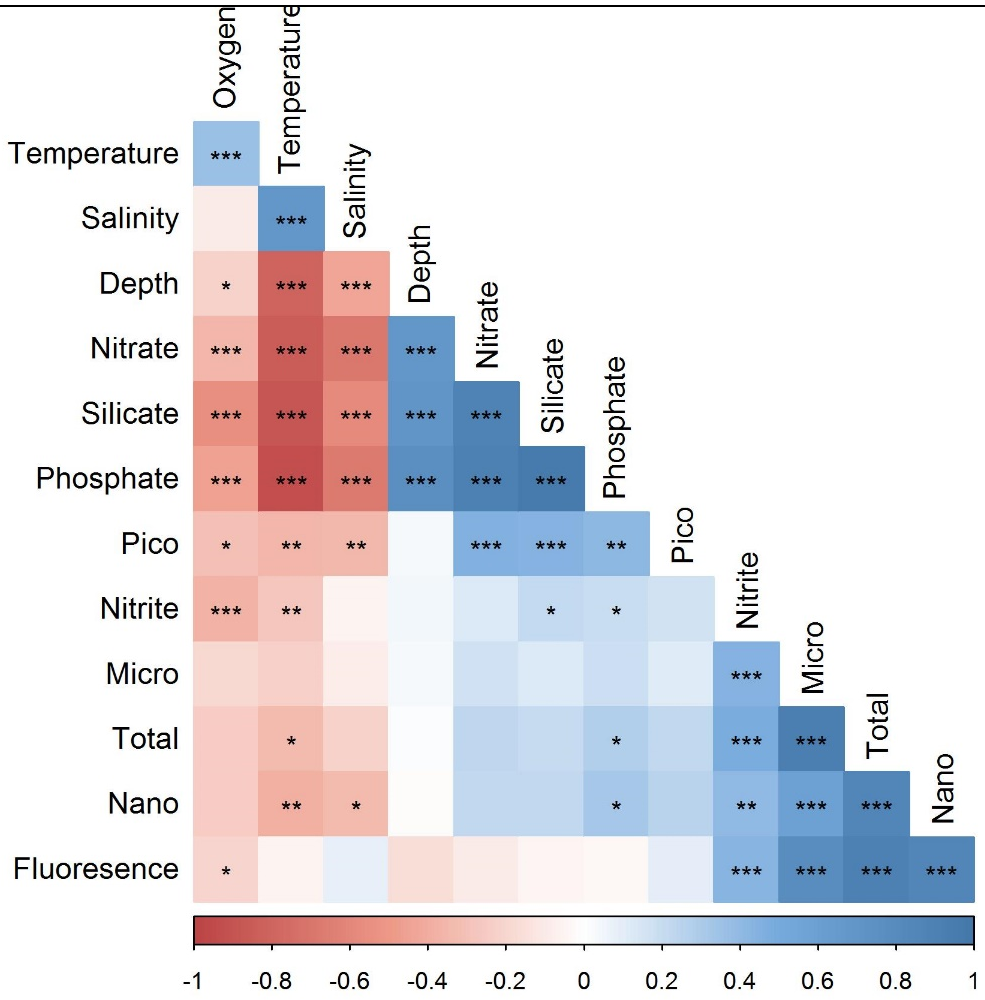

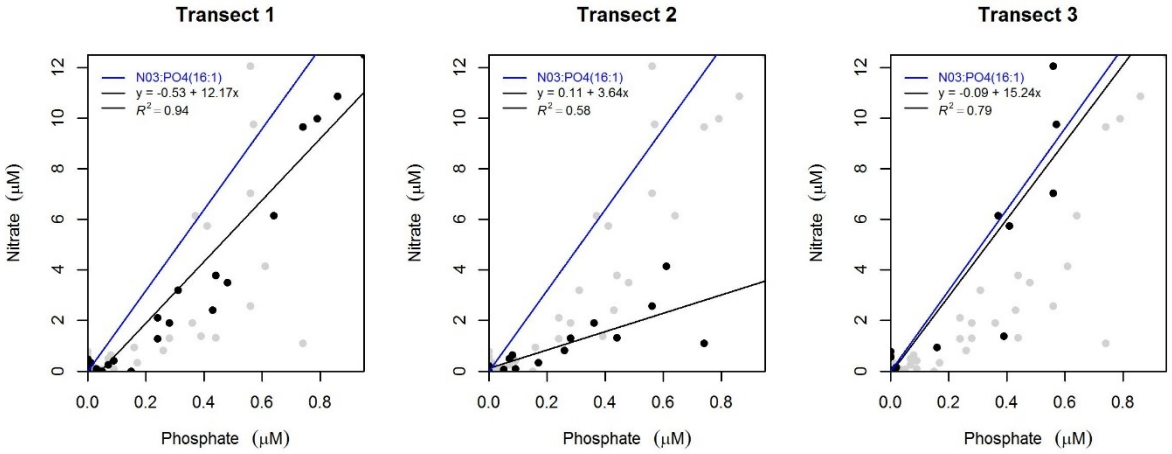

Fig. 5.10 Concentrations of nitrate versus phosphate in the epipelagic zone of the Agulhas Retroflection. The black line is the regression line for the data and the blue line represents the Redfield Ratio (N:P = 16:1). Grey dots are all stations whereas the black dots represent the samples for the specific transect.

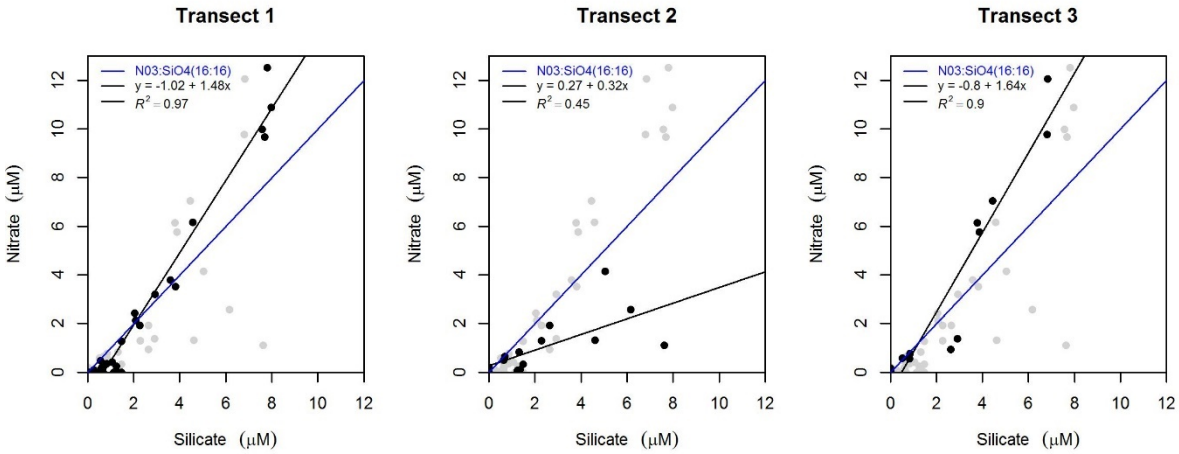

Fig. 5.11 Concentrations of nitrate versus silicate in the epipelagic zone of the Agulhas Retroflection. The black line is the regression line for the data and the blue line represents the Redfield Ratio (N:P = 16:1). Grey dots are all stations whereas the black dots represent the samples for the specific transect.

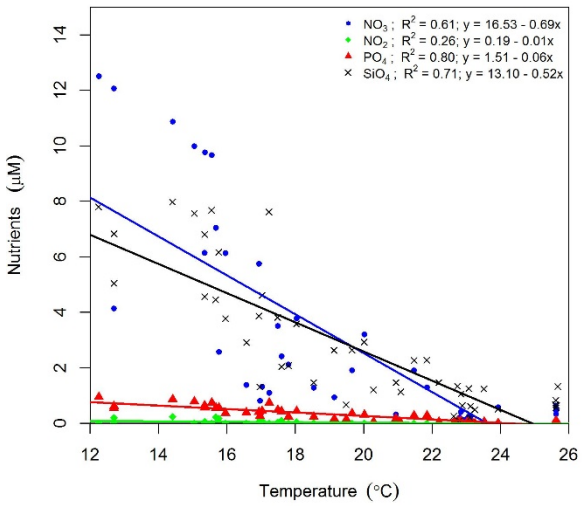

Fig. 5.12 Concentrations of nutrients (NO_2^-, NO_3^-; PO_4^{3-} and SiO_4^{4-}) versus temperature for all the euphotic zone stations of the Agulhas Retroflection area (n=54).

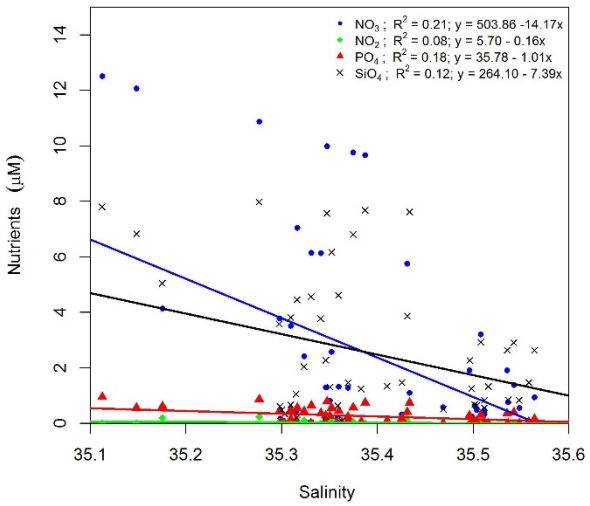

Fig. 5.13 Concentrations of nutrients (NO_2^-, NO_3^-; PO_4^{3-} and SiO_4^{4-}) versus salinity for all the euphotic zone stations of the Agulhas Retroflection area (n=54).

5.4.2 Spatial variability of phytoplankton

The depth of the chlorophyll *a* maximum for the Agulhas Retroflection area ranged between 25.07 and 98.02 m with a mean of 52.14 ± 21.89 m. The majority of the stations (14 out 16) showed the presence of a SCM. The other two had a DCM - both of these were in the Agulhas Current. The chlorophyll *a* concentration at the depth of the chlorophyll *a* maximum ranged from 0.24 to 4.11 µg l^{-1} with a mean of 1.66 ± 0.94 µg l^{-1}. Chlorophyll *a* concentrations at the DCM were less than 1 µg l^{-1}. Fig. 5.14 shows the distribution of chlorophyll *a* as well as temperature measured in epipelagic waters. The condensing of the isotherms at 37.5°S and 23.4°E forms the boundary between the surrounding water and the Agulhas Current.

The *in situ* chlorophyll *a* data for Transect 1 showed a region of high chlorophyll *a* outside of the Agulhas Current (Fig. 5.14a). The chlorophyll maximum was located at a depth of between 25 and 93 m with a mean of 48.29 ± 23.32 m. Micro-, nano- and

picophytoplankton contributed 27 ± 11%, 70 ± 10% and 3 ± 3% to the total chlorophyll *a* for the SCM, respectively. At the time of the study the surface waters of Transect 1 were dominated by nanophytoplankton contributing 63 ± 0.14% to the total chlorophyll *a*.

(a) North - South

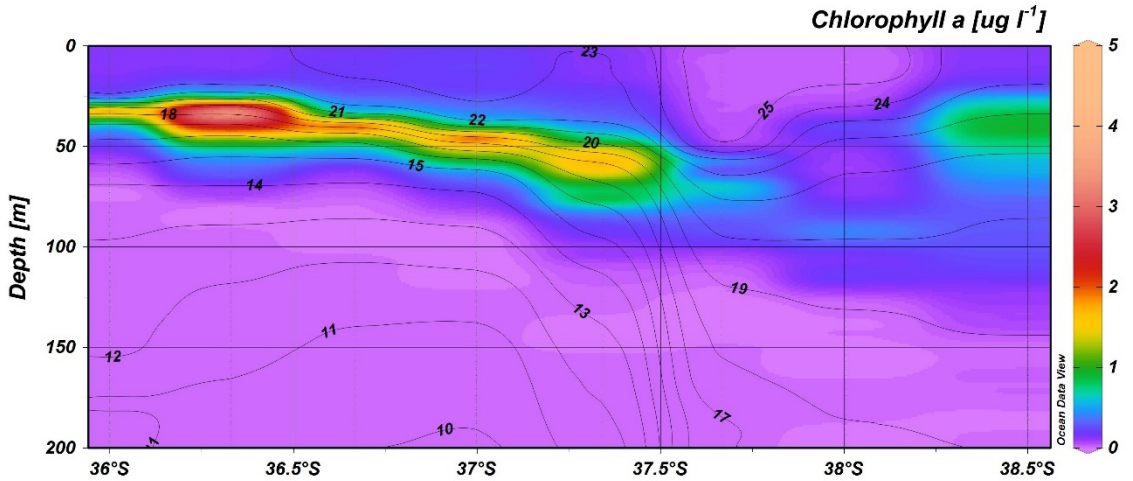

(b) East - West

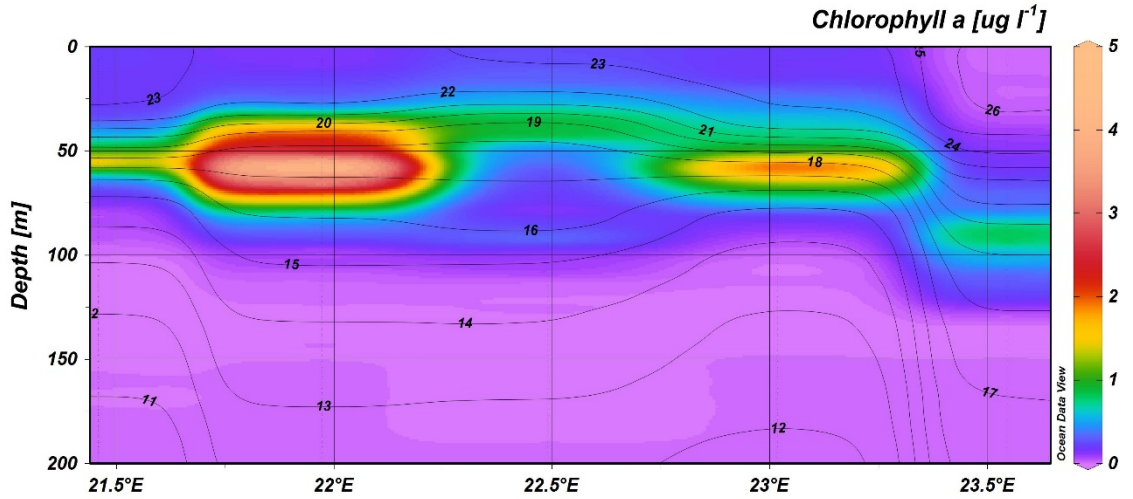

Fig. 5.14 Chlorophyll *a* (µg l^{-1}) profiles with an overlay of isotherms through the epipelagic zone of the Agulhas Retroflection Area. The orientation of Transect 1 (a) is north to south and for Transect 3 (b) is east to west.

For Transect 3 the depth of the SCM ranged between 58.81 and 98.02 m with a mean of 69.42 ± 19.09 m. Nanophytoplankton contributed 61 ± 24% to the total chlorophyll *a*, whereas micro- and picophytoplankton contributed 37 ± 25% and 2 ± 1%, respectively.

5.4.3 Phytoplankton composition

A total of 80 phytoplankton taxa were recorded during the survey: 44 diatom, 30 dinoflagellate, four silicoflagelate, one chlorophyte flagellate, one prymnesiophyte and no coccolithophore taxa. Only two taxa (>1 000 counts) were found to be dominant during the survey: *Gonyaulax* Diesing spp., a dinoflagellate, and the centric diatom, *Thalassiosira weissflogii* (Grunow) G.Fryxell & Hasle. These two taxa made up 44.52% of the total counts and were co-dominant within the epipelagic. The next three most abundant taxa (P*rotoceratium* R.S.Bergh sp., *Pseudo-nitzschia* H.Peragallo sp. and *Alexandrium* Halim spp.) collectively contributed 17.18% of the total counts.

Species diversity was the lowest (1.07) at the SCM for the northern-most station of Transect 1. The highest diversity (2.80) was found at the surface of the eastern-most station of Transect 3. Evenness ranged from 0.35 to 0.83 with a mean of 0.71, thereby indicating a relative uneven distribution of species.

Two sites showed dominance (> 50% of counts) of one species and they are listed in Table 5.2. Both *T. weissflogii* and a chlorophyte flagellate were the only species that were observed at every station for the Agulhas Retroflection Area and their abundance remained relatively constant throughout the study area.

Multivariate analysis grouped the 80 taxa into the following communities (Fig. 5.15): Agulhas Current and non-Agulhas Current communities. The Agulhas Current community differed slightly from the non-Agulhas Current community, but the distinctions are not that clear, as they shared many of the same species, especially the more abundant ones such as *T. weissflogii*; *Pseudo-nitzschia* spp., *Gonyaulax* Diesing spp. and *Alexandrium* spp.

Table 5.2 Sites in the Agulhas Retroflection Area where one phytoplankton species was dominant.

Station and profile	Transect	% of counts	Dominant species	Species richness	Diversity score	Evenness score
31531_DCM	Transect 1	77.22	*T. weissflogii*	21	1.07	0.35
31532_Surf	Transect 1	64.52	Chlorophyte flagellate	23	2.38	0.76

Fig. 5.16, represents the 12 most abundant species for the Agulhas Retroflection Area. Six of these were dinoflagellates and six were diatoms, thus an even distribution between the two functional groups. The dominance of *Gonyaulax* spp. and *T. weissflogii* is evident.

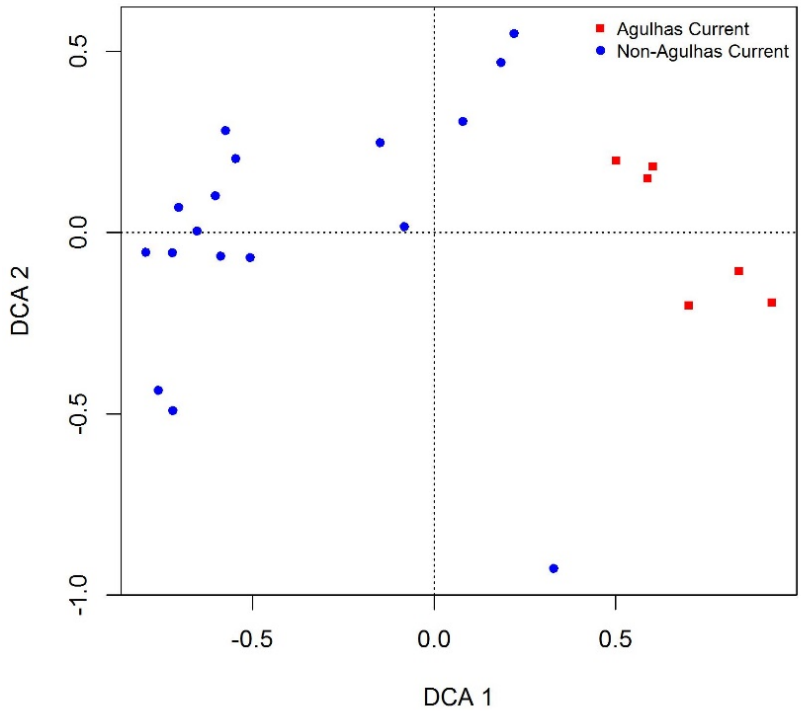

Fig. 5.15 Detrended Correspondence Analysis of the phytoplankton samples of the Agulhas Retroflection Area.

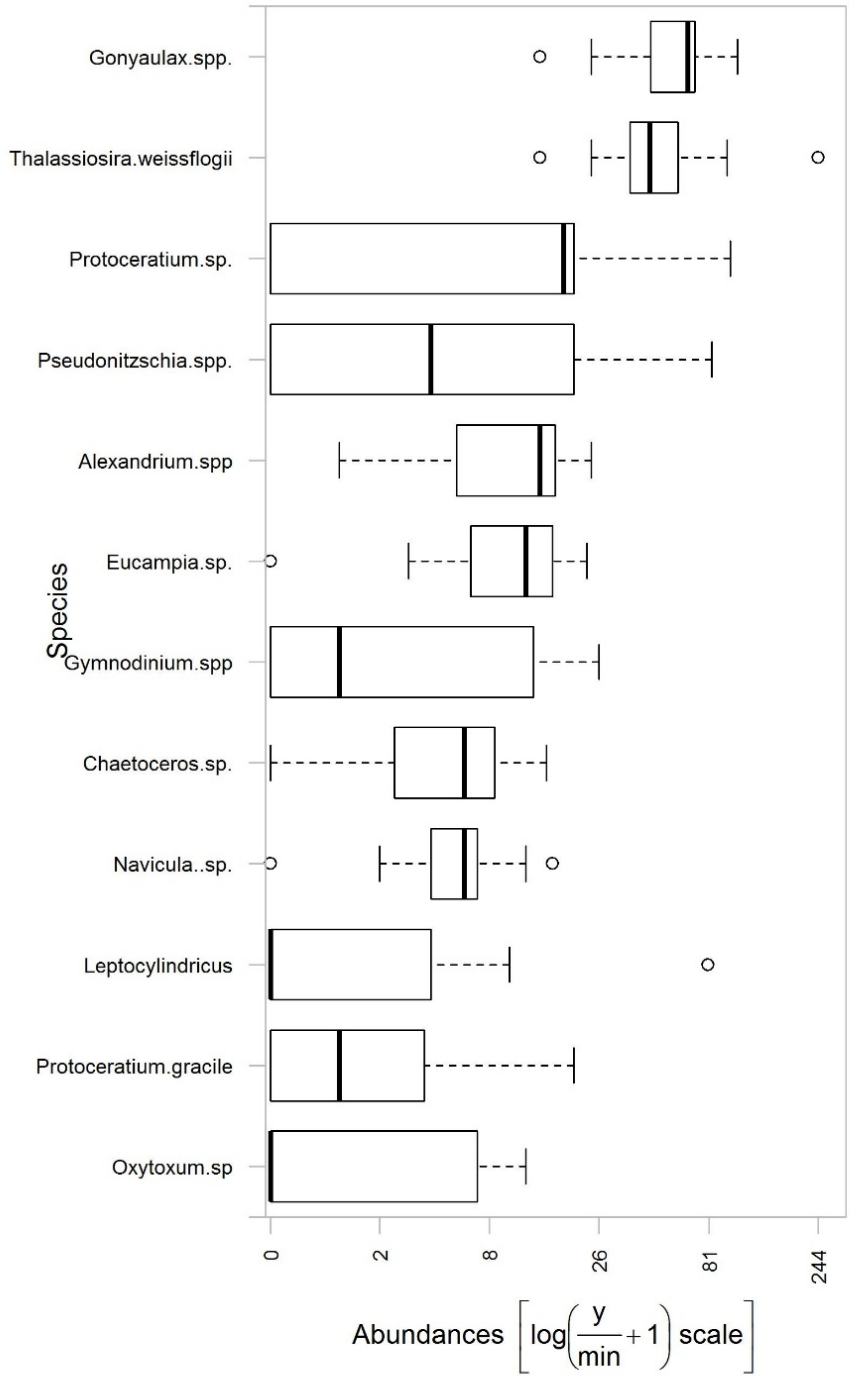

Fig. 5.16 The 12 most abundant species for the Agulhas Retroflection Area. ○ represents outliers, bars represent the minimum and maximum, and the solid line is the median.

5.4.4 Environmental drivers of phytoplankton variability

Statistical relationships between environmental variables and phytoplankton communities were explored using CCA (Fig. 5.17). The eigenvalue of Axis 1 was 0.155 and Axis 2 was 0.103, explaining 52.52% of the total variance of species distribution. The species–environment correlations for the first two axes were 0.492 and 0.376, indicating a strong relationship. The Monte Carlo test confirmed the significance of the relationship model ($p < 0.01$). The first canonical axis was positively correlated to salinity ($r = 0.94$) but was negatively correlated with nitrate ($r = -0.84$). On the other hand, the second canonical axis had a positive relationship with silicate ($r = 0.87$) but was negatively correlated with oxygen ($r = -0.98$). Temperature was positively correlated with salinity (r = 0.23) and oxygen (r = 0.63), and temperature showed a negative correlation with phosphate (r = -0.89), silicate (r = -0.80), nitrate (r = -0.81), nitrite (r = -0.65) and, as a result, the N:P ratio (r = −0.308). Consistent with the results of the Pearson correlation analysis (Table 5.1), the CCA results (Fig. 5.17) revealed that the phytoplankton community showed positive correlations with phosphate (r = 0.72), silicate (r = 0.63), nitrate (r = 0.59) and nitrite (r=0.51) for the Agulhas Retroflection area. The three non-Agulhas Current Stations (Fig. 5.17, blue stations) towards the bottom of the ordination, are the surface stations close to the edge of the Agulhas Bank. These separated from the rest of the non-Agulhas Current stations as an area of low nutrient concentration near the surface. The Agulhas Current and non-Agulhas Current stations are separated by a difference in salinity (Fig. 5.4).

A generalised linear model, modelling the three primary drivers; temperature, salinity and phosphate obtained from the CCA ordination (Fig. 5.17) showed that there are different phytoplankton communities within the Agulhas Retroflection Area based on these three variables. Salinity and phosphate, as individual environmental drivers do not separate the phytoplankton communities, but in relation with each another, and together with temperature, they do. Salinity and phosphate were the most significant environmental drivers of the phytoplankton community within the Agulhas Retroflection area (LRT = 175.3; $p < 0.01$).

Table 5.3 ANOVA results for the GLM model of the Agulhas Retroflection Area.

Environmental driver	d.f.	Dev	Pr(>Dev)
Temperature	21	172.5	0.027*
Salinity	20	153.4	0.058
PO_4^{3-}	19	110.6	0.282
Temperature:Salinity	18	133.1	0.072
Temperature:PO_4^{3-}	17	142.7	0.068
Salinity:PO_4^{3-}	16	175.3	0.010**
Temperature:Salinity:PO_4^{3-}	15	131.9	0.009**

Sigificance codes: '**' 0.01 '*' 0.05

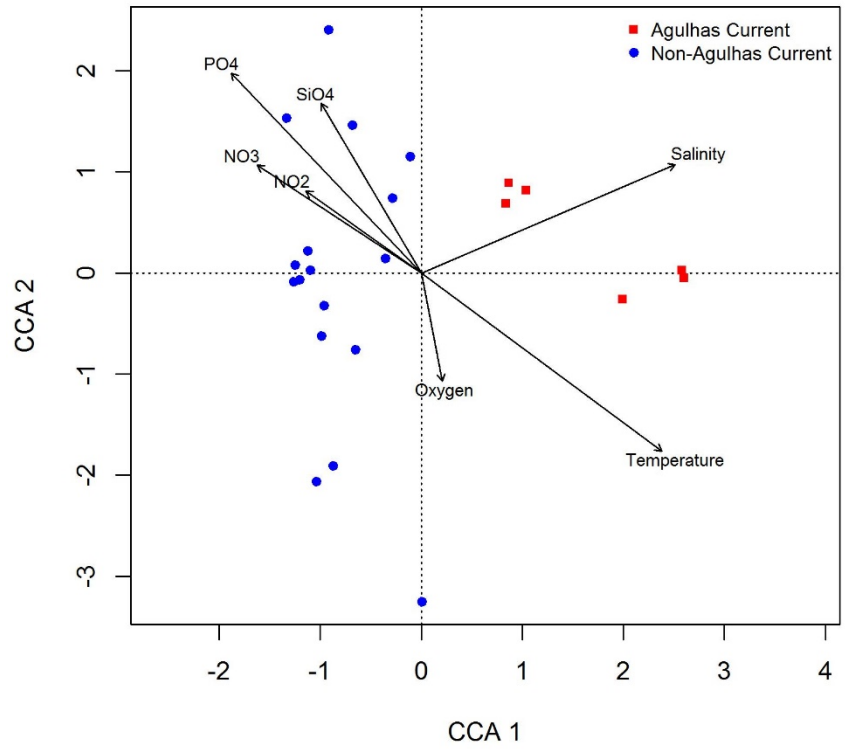

Fig. 5.17 Canonical Correspondence Analysis of the environmental variables measured at the sites sampled in the Agulhas Retroflection Area. Environmental variables used are temperature, salinity, dissolved oxygen (oxygen), nitrite (NO2), nitrate (NO3); phosphate (PO4) and silicate (SiO4).

5.5 Discussion

5.5.1 Physical and chemical oceanography

During the survey it was believed that a Natal Pulse or eddy was sampled and therefore this specific region was selected as the Agulhas Retroflection. However, sea surface temperatures (Fig. 5.2) showed that this was not the case and sampling was, in fact, conducted near the southern end of the Agulhas Current (Goschen; pers. comm.). The location of the sampling area, however, is known for its early Retroflection of the Agulhas Current (van Aken *et al.*, 2013), but this was also not detected during the cruise (Goschen; pers. comm.).

The geographical spread of the various stations across the Agulhas Retroflection area showed significant changes in temperature, salinity and dissolved oxygen within the euphotic zone. A surface plot of temperature (Fig. 5.2) as well as vertical plots of temperature (Fig. 5.3), salinity (Fig. 5.4) and oxygen (Fig. 5.5) showed a clear boundary between the Agulhas Current and non-Agulhas Current stations in this region. The Agulhas Current waters were characterised by higher ocean surface temperature (>24 °C) and salinity greater than 35.5. Epipelagic water for the non-Agulhas Current stations was cooler compared to that of the Agulhas Current. The range in epipelagic temperature (12.25 to 26.16°C), salinity (35.11 to 35.63) and dissolved oxygen concentrations (3.37 to 4.81) observed for the Agulhas Retroflection area is consistent with previously reported literature (Gordon, 1985; Chapman *et al.*, 1987; Gordon *et al.*, 1987; Lutjeharms and Van Ballegooyen, 1988; Lutjeharms *et al.*, 1992; Lutjeharms and Ansorge, 2001; Lutjeharms, 2006; van Aken *et al.*, 2013). Temperature, salinity and oxygen concentrations of waters of the Agulhas Current stations of the Retroflection were similar to the Agulhas Shelf and Bank stations.

The distribution and composition of phytoplankton communities were influenced by the distribution of nutrients. In marine ecosystems, nitrogen and phosphorus are the main inorganic nutrients needed for growth, although silicate could limit the growth of diatoms (Yool and Tyrrell, 2003; Crombet *et al.*, 2011). Silicate is needed for the formation of their frustules and therefore diatoms are especially influenced by silicate

concentrations. The silicate concentration of waters in the Agulhas Retroflection Area (0-7.97 µM) were well above the minimum threshold (≤ 0.001 µM) needed for diatoms to grow (Iida and Odate, 2014). The positive correlations (Table 5.1) between nitrate or phosphate and chlorophyll *a* suggested that open-ocean phytoplankton biomass was controlled by the availability of these nutrients. Temperature was inversely correlated with chlorophyll *a*, nitrate and phosphate. Van de Poll *et al.* (2013) suggested that temperature is important in determining nutrient availability for phytoplankton by influencing vertical exchange with deeper nutrient-rich water.

The vertical distribution of nutrients (Fig. 5.6 to Fig. 5.9) shows strong regional differences in concentrations within the epipelagic regions of the Agulhas Retroflection Area. With phosphate and silicate concentrations showing close similarity in their distribution. Both transects in the Agulhas Retroflection Area were characterised by strong latitudinal and longitudinal nutrient (NO_3^-; PO_4^{3-} and SiO_4^{4-}) concentration gradients across the Agulhas Current.

In oligotrophic temperate to subtropical waters, nutrient availability is generally considered to be the main factor affecting growth rates of phytoplankton (Dugdale and Goering, 1967) and community species composition (DiTullio *et al.*, 1993). Nitrogen and phosphate are generally considered to be the two major nutrients that affect phytoplankton growth (Hecky and Kilham, 1988). In marine environments, where the average ratio for N:P is less than the Redfield ratio of 16:1, nitrogen is generally considered to be limiting (Redfield, 1958; Weber and Deutsch, 2012). Where the N:P ratio is over 16:1, phosphorus is considered to be limiting. The N:P ratio of Agulhas Retroflection waters of Fig. 5.10) is closely matched to that of ocean waters on average (Weber and Deutsch, 2012).

Chapman *et al.* (1987) found that silicate levels for the Agulhas Retroflection Area were low and patchy, except near the Agulhas Bank. Silicate concentrations measured in our study were similar to those Chapman *et al.* (1987).

5.5.2 Spatial variability of phytoplankton

Various authors identified frontal systems as areas of high productivity and they are a feature within the Agulhas Current (Chapman *et al.*, 1987). Surface chlorophyll *a* concentrations tended to increase southwards towards the SCZ. Lutjeharms (2006) reported that there was little difference in surface chlorophyll concentrations between the various water masses, but that a band of high concentration appears near the boundaries between them. The chlorophyll *a* profiles measured here (Fig. 5.14) illustrate this band of high phytoplankton biomass at the Agulhas Current boundary. It is believed that water column stability and cross-boundary transport of nutrients is responsible for this (Chapman *et al.*, 1987). The absence of intrusion of South Indian Central Water into the SCM could be an indication that upwelling caused by shear was negligible. Over much of the study area, the SCM was less than 25 m in width and was situated at a depth of approximately 50 m. Above the SCM, chlorophyll *a* concentrations were low. It appears that the SCM was associated with both the thermocline and the nutricline. A similar observation was made by Chapman *et al.* (1987) for the Agulhas Retroflection and by Anderson (1969) for the oceanic waters off the Oregon coast.

The surface waters of the Agulhas Retroflection Area appear to be characteristic of nutrient-poor subtropical waters, although the Agulhas Retroflection phytoplankton community was mostly dominated by nanophytoplankton in our study and not picophytoplankton. In oligotrophic subtropical waters, picoplankton are generally the dominant component in terms of primary productivity, chlorophyll *a* and cell concentrations (Zubkov *et al.*, 1998).

5.5.3 Phytoplankton composition

The phytoplankton community was found to be different between the Agulhas Current and non-Agulhas Current, as well as between the surface and the SCM. There was a minor change in dominance from dinoflagellates to diatoms. The other taxa made a substantially smaller contribution to the phytoplankton, but this could be an artefact of the preservation method used (Sonnekus *et al*., 2017).

A small proportion of the taxa found in the waters of the Agulhas Retroflection Area were cosmopolitan and recorded at all the stations. Despite this, the presence of a few dominant species was sufficient to group the 80 taxa into the two phytoplankton communities that corresponded with the Agulhas Current and non-Agulhas Current waters. Boden *et al.* (1988) also reported two different diatom communities for the Agulhas Retroflection region, the Agulhas Retroflection Group and the Agulhas Current Group. However, these two communities were based on a much larger geographical area than our study. The most abundant species in the Agulhas Retroflection Group were *Pseudoeunotia doliolus* (= *Fragilariopsis doliolus*), *Chaetoceros peruvianus*, *Rhizosolenia stolterfothi*, *Cylindrotheca closterium* (= *Nitzschia closterium*), *Nitzschia* chains, *Thalassiosira* spp. and *Thalassiothrix* spp. (Froneman *et al.*, 1999).

The dominant species of the waters of the Agulhas Retroflection area in this study were *Thalassiosira weissflogii* (diatom) and a species of *Gonyaulax* (dinoflagellate). A total of 44 diatom and 30 dinoflagellates species were recorded. Boden *et al.* (1988) reported 35 diatom species from the Agulhas Retroflection Area. They, however, only reported on diatoms and ignored the other taxa. Froneman and Pakhomov (2000) reported that the total number of diatom species was highly variable and ranged between 8 and 44 species. The diatom community recorded during this study was similar to those observed in previous studies carried out in the same region (Boden *et al.*, 1988; Froneman *et al.*, 1995; Froneman *et al.*, 1999; Froneman and Pakhomov, 2000). Although diatom species appear to be similar for the Agulhas Retroflection Area, there was considerable variability in the dominants. This variability may be due to the complex hydrological processes found within the region (Froneman and Pakhomov, 2000). The most abundant dinoflagellate genera for the Agulhas Retroflection area were *Gonyaulax* sp.; P*rotoceratium* sp., *Alexandrium* sp., *Gymnodinium* sp., and *Protoceratium gracile* – these were cosmopolitan in their distribution. Two species of dinoflagellates that did not occur in the Agulhas Current community were *Oxytoxum constrictum* (F.Stein) Bütschli and a *Gyrodinium* sp. Four species of silicoflagellates were recorded in the area: a *Mesocena* Ehrenberg sp., *Dictyocha fibula* Ehrenberg*, Dictyocha octonaria* Ehrenberg and *Dictyocha speculum* Ehrenberg. The latter two were not recorded in

the Agulhas Current community. The prymnesiophyte, *Chrysochromulina hirta* Manton was only recorded at three SCM stations. Rhodes and Burke (1996) found that *C. hirta* prefers lower temperatures and died at temperatures exceeding 25°C suggesting that temperature is a key factor in its distribution. It is possible to use the four species not recorded for the Agulhas Current Community as indicator species (Smayda, 1958) to distinguish the various water masses. An absence of these four species can be an indication that water mass modification occurred, resulting in their absence (Froneman and Pakhomov, 2000).

Irigoien *et al.* (2004) found that on a global scale, marine phytoplankton diversity is a unimodal function of their biomass. Biodiversity patterns are generally consistent between oceanographic regions. During blooms, diversity is low whereas maximum diversity has been found at intermediate levels of phytoplankton biomass. The low species richness observed for the Agulhas Current region likely reflects the oligotrophic nature of these subtropical waters. However, species richness can also be low due to the lack of direct allochthonous input of nutrients into the Agulhas Current. Any nutrient input is quickly utilized by a few bloom-forming taxa, especially diatoms. The vertical stratification of the Agulhas Current will allow the heavier diatoms to settle out, thereby reducing both chlorophyll *a* concentration and species abundance. The Agulhas Current also appears to be a separate water mass and this “isolation” will limit any cross-boundary transfer between it and the surrounding waters.

5.5.4 Environmental drivers of phytoplankton variability

The results of the CCA showed that temperature, salinity and phosphate were the primary drivers of phytoplankton assemblages for the Agulhas Retroflection area. Temperature is a common factor influencing phytoplankton growth and distribution (Canale and Vogel, 1974; Rhee and Gotham, 1981; Schabhüttl *et al.*, 2013). The strong positive correlation between temperature and silicate is linked to the presence of diatoms as the most dominant functional group. Salinity in conjunction with temperature can be used as an indication of where large water masses originated and hence it is import in the distribution of phytoplankton within the Agulhas Retroflection. Powell *et al.* (1989) found that salinity was a poor predictor for

mesoscale patterns in chlorophyll *a* and that it rather reflects mixing or transportation processes than phytoplankton dynamics.

The non-Agulhas Current community can be separated by the Agulhas Current community based on a threshold of temperature and salinity: The Agulhas Current phytoplankton occur when the temperature is above 17°C and the salinity is above 35.45.

5.6 Conclusions

The results of this study suggest that changes in phytoplankton species composition within the Agulhas Retroflection area reflect changes in the physico-chemical variables associated with different water masses. It is clear that frontal systems may form barriers between phytoplankton communities. The observed variation in the phytoplankton community was prominent only between the surface and the SCM.

The study area, although located near the Retroflection, serves as a proxy for the Retroflection itself. This region was relatively more stable compared to the Agulhas Shelf and Agulhas Bank, removed from the direct influences of the coast and the processes associated with the continental shelf. It would be of interest though to investigate the phytoplankton dynamics in a region of high variability such as the Retroflection proper. Not only would the Retroflection be of interest, but the area west of it as well. This will shed light on how far the Agulhas Current influences the phytoplankton dynamics towards the west, and whether there is a transition zone between the sACLME and the Benguela Current BCLME.

6 Agulhas Return Current - Phytoplankton and nutrient dynamics of six South Indian Ocean seamounts

6.1 Abstract

A survey of six seamounts and two transects through the subtropical convergence zone (SCZ) in the South Indian Ocean in November and December 2009 showed a strong latitudinal gradient from the subtropics to the Subantarctic Front (SAF). Concentrations of oxygen, nitrate, nitrite, soluble reactive phosphorus as well as phytoplankton biomass (measured as chlorophyll *a*) increased while salinity and temperature decreased with an increase in latitude. These differences resulted in significant differences in the phytoplankton communities between seamounts. The chlorophyll *a* maximum became shallower at higher latitudes, changing from a depth of ~85 m in the subtropics to ~35 m over the seamounts and in the SCZ. The mixed layer depth also increased from ~50 m in the subtropics to ~100 m at higher latitude stations. The N:P and N:Si ratio indicated that nitrate was limiting at all the seamounts except one, at which silicate was the limiting nutrient. The phytoplankton community also showed a latitudinal gradient with decreasing diversity and a change in dominance from dinoflagellates in the tropics to diatoms towards the SCZ. The dominant diatom genus of the survey (>50% of the cell counts) was *Pseudo-nitzschia*. Nutrients exhibited an inverse linear relationship with temperature and salinity. The oligotrophic subtropical areas differed from the mesotrophic seamounts in temperature (17.5°C) while waters over seamounts north and south of the Agulhas Return Current (ARC) differed in salinity (34.7). The phytoplankton (148 taxa) responded to this difference, resulting in three communities: the subtropical seamount phytoplankton (Atlantis, Walters and their off-mount samples); phytoplankton of the waters north of the ARC (Melville, Sapmer, MoW) and phytoplankton south of the ARC (Coral, SCZ1) characterised by a bloom of *Phaeocystis antarctica* Karsten. The environmental drivers most strongly linked to these observed differences were nitrate and temperature. These displayed a clear latitudinal gradient unaffected by mesoscale variability of the ARC eddy field thereby allowing the three phytoplankton communities to persist. Phytoplankton biomass was

enhanced in the shallow (<200 m) seamount waters, although the speed of the currents suggests an allochthonous origin.

6.2 Introduction

At the Agulhas Retroflection the Agulhas Current turns east and continues as the ARC, the fourth and last of the four biogeographical areas investigated in this study. Six seamounts, four off-mount stations and two SCZ transects are used to describe the ARC region, with a focus on the eastern termination region of the ARC.

Seamounts are defined as “geographically isolated topographic features on the seafloor taller than 1 000 m…” (Staudigel and Clague, 2010). Approximately 172 000 submarine seamounts, hills and knolls have been identified around the world’s oceans based on this definition (Yesson *et al.*, 2011). Seamounts are important as they appear to support relatively large planktonic, benthic and higher consumer biomass when compared to the surrounding ocean, especially in the oligotrophic waters of the subtropics (Clark *et al.*, 2010). Less than 1% of seamounts have been studied and although they are not as isolated or constitute centres of endemism as initially thought, they remain hotspots of biological activity in the deep sea (Clark *et al.*, 2012; Priede and Froese, 2013; Djurhuus *et al.*, 2017; Read and Pollard, 2017).

The least studied seamounts in the world’s oceans are the deep seamounts located in the high latitudes of the Southern Ocean (Clark *et al.*, 2010). The Southwest Indian Ocean, incorporating the ASCLME, is one of the least explored ocean regions of the world (Lutjeharms and Bornman, 2010). The western sector of the Southern Indian Ocean is one of the most energetic and globally important hydrographic regions of the world’s oceans (Read *et al.*, 2000; Beal *et al.*, 2011). The Agulhas Current flows along the east coast of South Africa as a fast boundary current until south of the continent where it retroflects (Agulhas Retroflection), with most of its water flowing eastward along the Subtropical Convergence as the ARC. The rest of the water is injected into the South Atlantic through the shedding of Agulhas Rings (Lutjeharms, 1985; Lutjeharms and Ansorge, 2001; Boebel *et al.*, 2003; Lutjeharms, 2006; Paldor and Lutjeharms, 2009; Lutjeharms and Bornman, 2010; Beal *et al.*,

2011). The trajectory of the ARC is influenced by bottom topography, e.g. the Southwest Indian Ocean Ridge, which can result in extensive meridional excursions and formation of eddies (Lutjeharms and Ansorge, 2001). The ARC, the STF (also known as the SCZ) and the SAF form transitions between warm and saline subtropical waters and cold and less saline subantarctic waters, creating an area of complex biogeochemistry, phytoplankton productivity and biogeography (Laubscher *et al.*, 1993; Bathmann *et al.*, 1997; Read *et al.*, 2000; Fiala *et al.*, 2003).

Seamounts project from the seafloor into the water column, where they form obstacles to ocean flow that can generate internal waves (Kaneko *et al.*, 1986; Toole *et al.*, 1997; Kunze and Llewellyn Smith, 2004), give rise to ocean eddies (Royer, 1978; Cheney *et al.*, 1980), cause asymmetric current acceleration and recirculation (Mysak and Magaard, 1983; White and Walker, 1985; White *et al.*, 2007; Lavelle and Mohn, 2010), allow development of Taylor columns (Eide, 1979; Owens and Hogg, 1980; Genin and Boehlert, 1985; Dower *et al.*, 1992; Rogers, 2004; Arístegui *et al.*, 2009; Clark *et al.*, 2010) and increase vertical mixing (White *et al.*, 2007). Genin and Boehlert (1985), Boehlert and Genin (1987), Genin and Dower (2007) and Dower *et al.* (1992) recorded elevated levels of primary production over the summit of seamounts. However, they and numerous other studies, have recorded no evidence of a persistent seamount effect on phytoplankton biomass (Comeau *et al.*, 1995; Odate and Furuya, 1998; Mourino *et al.*, 2001; Genin, 2004; White *et al.*, 2007; Arístegui *et al.*, 2009; Mohn *et al.*, 2009; Drazen *et al.*, 2011; Young *et al.*, 2011; Misic *et al.*, 2012).

The cruise on board the R/V *Dr Fridtjof Nansen* targeted six seamounts spread across 15° of latitude and longitude. This study focussed on the physico-chemical oceanographic environment as drivers of phytoplankton biomass, composition and biogeography. To determine whether the selected seamounts of the South Indian Ocean are centres of enhanced biological productivity, we developed the following hypotheses:

- The phytoplankton changes from a low biomass, flagellate dominated community in the oligotrophic subtropical waters to an elevated biomass and diatom dominant community in the mesotrophic ARC and SCZ.

- The phytoplankton community above the summit of a seamount has a higher concentration of microphytoplankton (diatoms) than elsewhere. This community is concentrated in an SCM. The surrounding oligotrophic water, where pico- and nanoplankton are dominant, has a DCM layer.

6.3 Study area

Seamounts in the Southern Indian Ocean are concentrated on the mid-ocean ridges; particularly the Southwest Indian Ocean Ridge and along plateaus such as the Madagascar and Mascarene Plateaux. The Madagascar Ridge extends southwards from the island of Madagascar for about 1 100 km. The shallowest section (15 m), Walter's Shoal, is located roughly 400 nautical miles south of Madagascar and 600 nautical miles east of South Africa (Fig. 6.1). The seamounts on the 2 000 km long Southwest Indian Ocean Ridge are highly diverse as the northeast-striking ridge crosses several major oceanographic boundaries marked by the closely spaced STF, the ARC and the SAF (Read et al., 2000; Lutjeharms, 2007; Garcia et al., 2013). As the Southwest Indian Ocean Ridge crosses this oceanographic boundary, the southernmost seamounts are in sub-Antarctic waters and the northernmost in subtropical waters, with those in between lying within the western part of the subtropical gyre characterized by eddies and highly variable oceanography (Read *et al.*, 2000; Sultan *et al.*, 2007; Garcia *et al.*, 2013; Pollard and Read, 2017; Read and Pollard, 2017). The latitudinal range also follows a productivity gradient from mesotrophic in the south to oligotrophic in the north (Read *et al.*, 2000). The five seamounts sampled along the Southwest Indian Ridge were Atlantis Bank, Samper Bank, Middle of What, Coral and Melville Bank (Fig. 6.1, Table 6.1). A nameless seamount north of Walters Shoal on the Madagascar Plateau was included (Fig. 6.1, Table 6.1) and will be referred to as Walters.

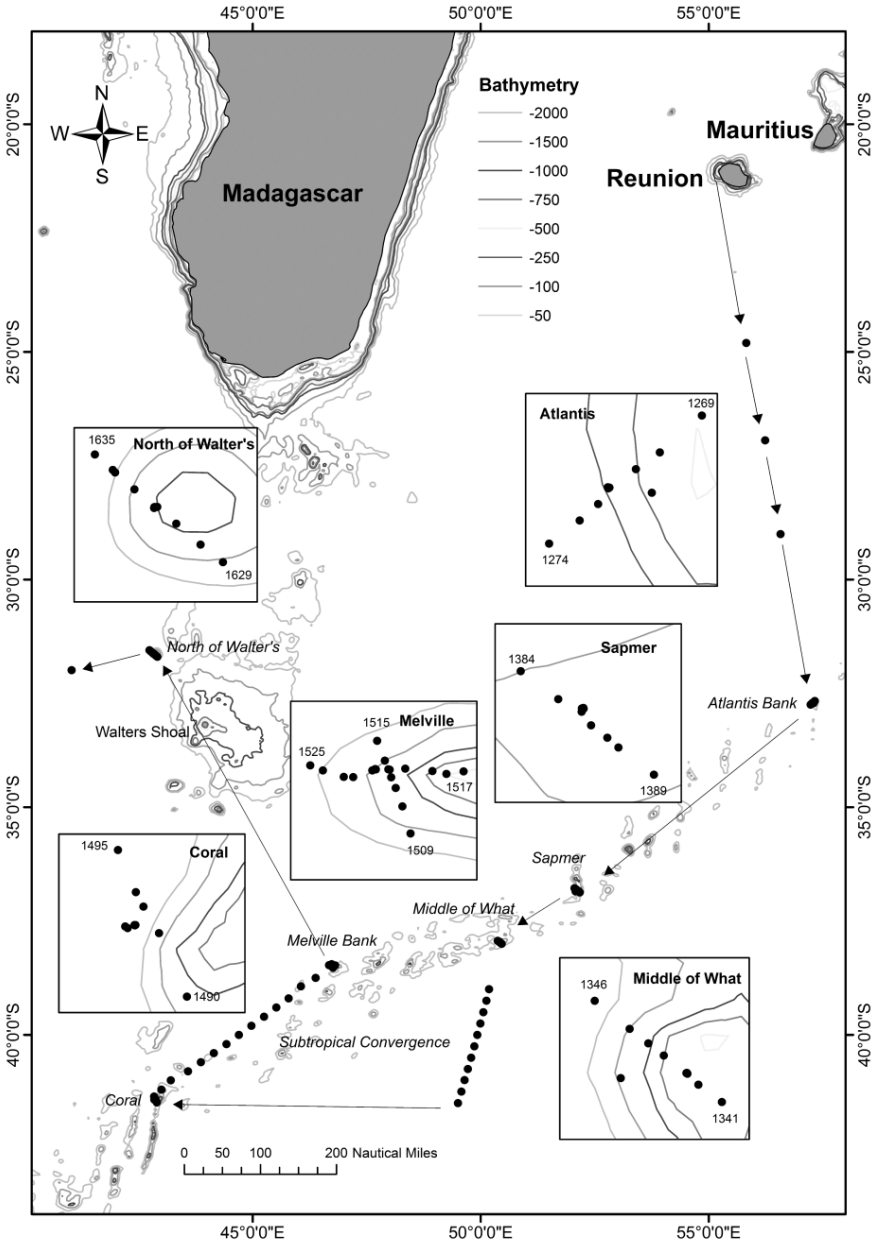

Fig. 6.1 The Agulhas Return Current study site indicating the cruise track and position of the environmental stations (black circles). Individual seamounts are enlarged to show transect positions and station numbers.

All the environmental data were collected *in situ* from the R/V *Dr Fridtjof Nansen* during Cruise 410 in November and December of 2009. Transects were chosen for their topographic features and were located over the peak of each seamount. In addition to the transect, an hourly measurement of physical conditions between the surface and the summit of the seamounts continued for 24 hours. A few stations

were also sampled between the seamount stations (off-mount) and two transects were also sampled across the SCZ (Fig. 6.1). The methodology and statistical analysis used in this study was identical to that presented in sections 3.3.2, 3.3.3 and 3.3.4.

Table 6.1 The stations sampled, depth of the summit, coordinates and the sampling date on which each of six seamounts was sampled (SCZ transects and off-mount stations shown in Fig. 6.1).

Seamount	Stations	Summit (m)	Latitude (S)	Longitude (E)	Date
Atlantis	1217 - 1274	842	32° 42.87’	057° 17.84’	2009/11/17
Sapmer	1275 - 1346	332	36° 50.87’	052° 04.88’	2009/11/21
Middle of What (MoW)	1347 - 1389	1100	37° 57.56’	050° 24.79’	2009/11/25
Coral	1401 - 1495	205	41° 25.44’	042° 50.82’	2009/12/01
Melville	1509 - 1600	108	38° 31.56’	046° 45.74’	2009/12/06
Walters	1601 - 1635	1255	31° 34.33’	042° 45.78’	2009/12/12

6.4 Results

6.4.1 Physical and chemical oceanographic conditions

Temperature profiles of the euphotic zone showed a clear gradient of decreasing temperature with an increase in latitude and depth. The only exception to this was Sapmer Seamount that had significantly lower ($p < 0.05$; $n = 165$) water temperatures than Melville and MoW to the south (Fig. 6.2). Coral Seamount had significantly lower temperatures ($p < 0.05$; $n = 304$) and salinity ($p < 0.05$; $n = 304$) than any of the other seamounts (Fig. 6.2 and Fig. 6.3).

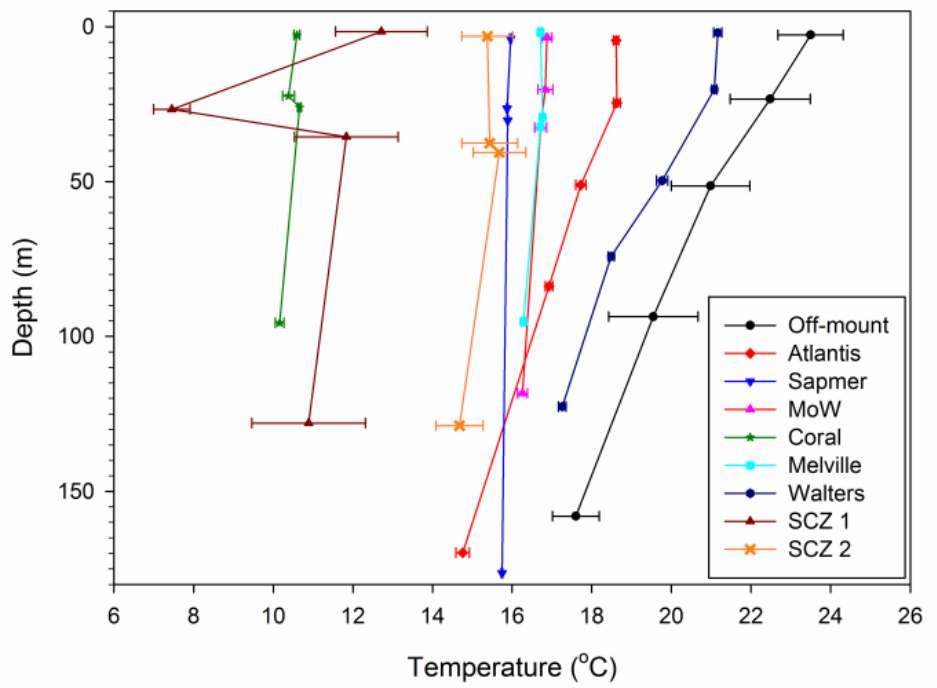

Fig. 6.2 Temperature profiles through the epipelagic zone of six seamounts, the off-mount stations and the two subtropical convergence transects.

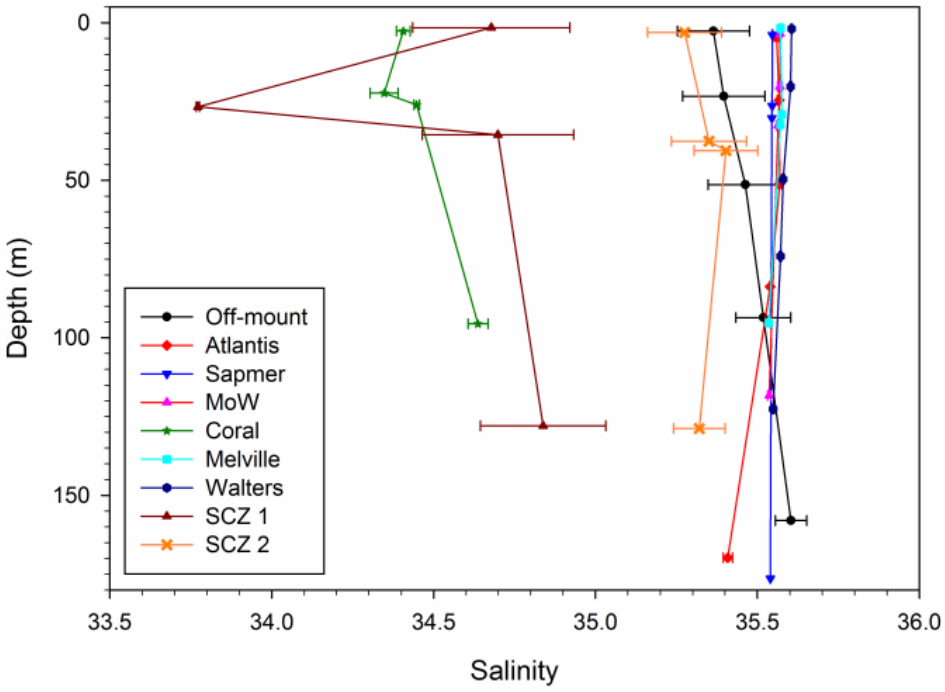

Fig. 6.3 Salinity profiles through the epipelagic zone of six seamounts, the off-mount stations and two subtropical convergence transects.

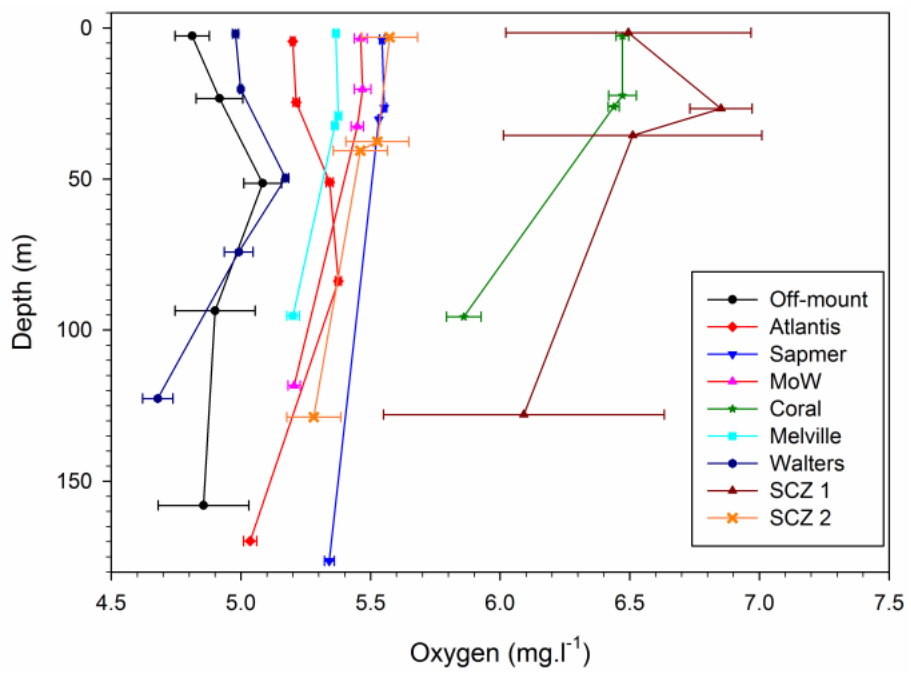

Fig. 6.4 Oxygen profiles through the epipelagic zone of six seamounts, the off-mount stations and two subtropical convergence transects.

The dissolved oxygen profiles also showed a gradient of increasing oxygen with increase in latitude (Fig. 6.4). The oxygen concentration increased at the DCM (Fig. 6.9). This zone of elevated oxygen is deeper in the subtropics (Off-mount, Walters and Atlantis) compared to the SCZ (Coral and SCZ1) (Fig. 6.4). Sapmer had no significant difference ($F = 7.2$; $p > 0.05$; $n = 38$) in any of the physical variables with depth.

The only significant difference ($F = 14.27$; $p < 0.05$; $n = 113$) in NO_2^- concentrations were between Atlantis and Coral seamounts. Off-mount and Walters had elevated NO_2^- concentrations at the DCM (Fig. 6.5; Fig. 6.9a). All the profiles showed a decrease in nitrite from the surface to mid depths, before the values increased again in deeper waters (Fig. 6.6). The nitrate profiles showed a similar pattern and gradient as the physical variables, with Coral and SCZ1 differing from the rest of the sites (Fig. 6.5). Coral had a significantly higher ($F = 41.69$; $p < 0.05$; $n = 304$) nitrate concentration compared to the other seamounts.

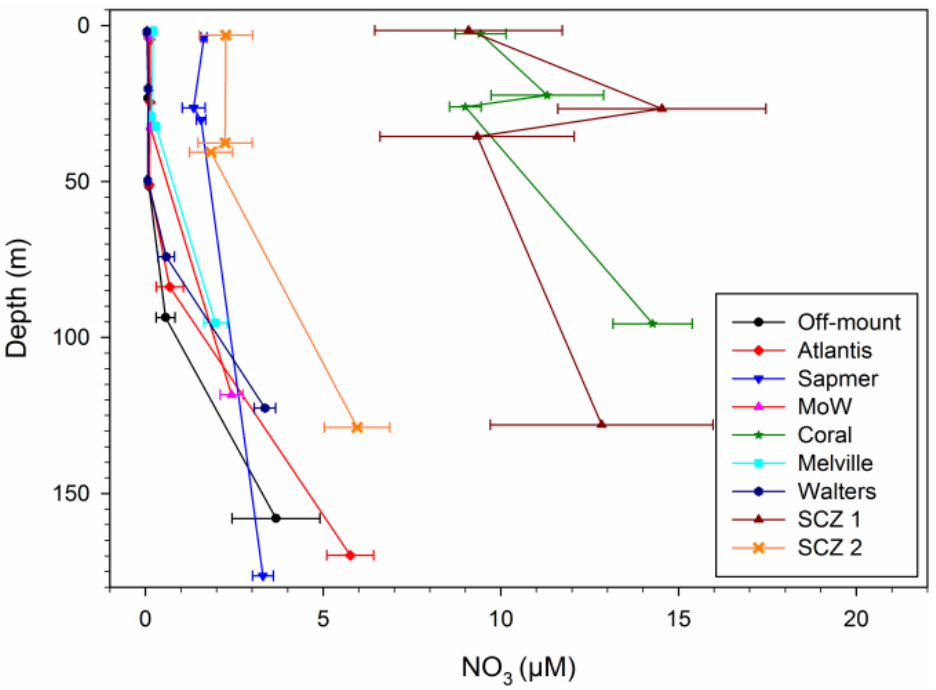

Fig. 6.5 Nitrate concentrations in the epipelagic zone of the six seamounts, the off-mount stations and two subtropical convergence transects.

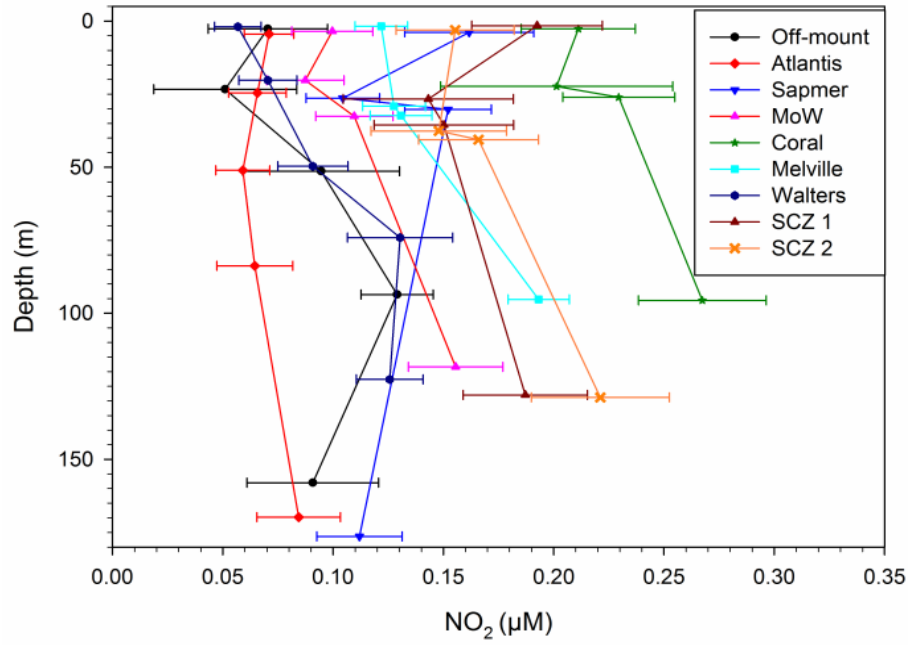

Fig. 6.6 Nitrite concentrations in the epipelagic zone of six seamounts, the off-mount stations and two subtropical convergence transects.

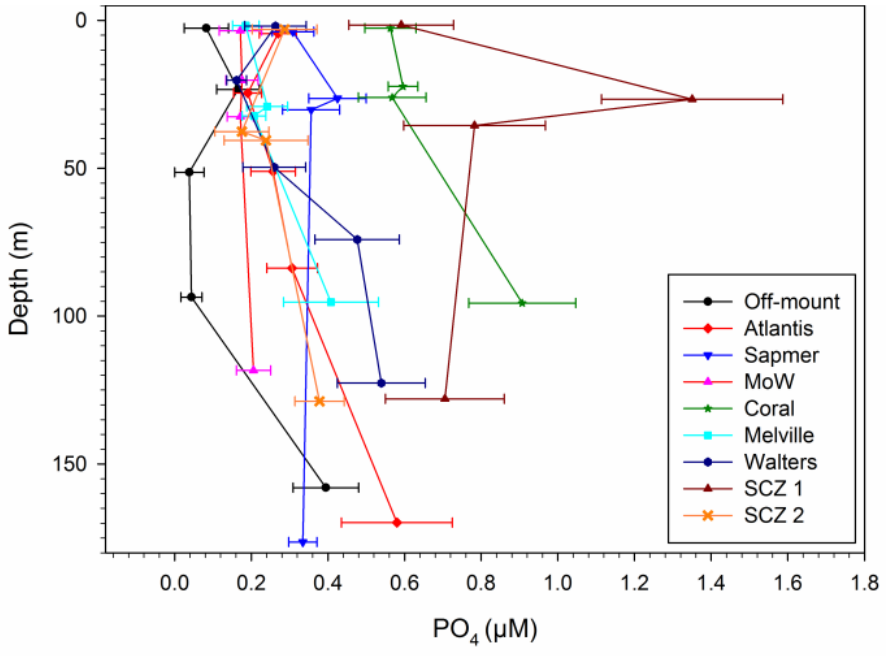

Fig. 6.7 Phosphate concentrations in the epipelagic zone of six seamounts, the off-mount stations and two subtropical convergence transects.

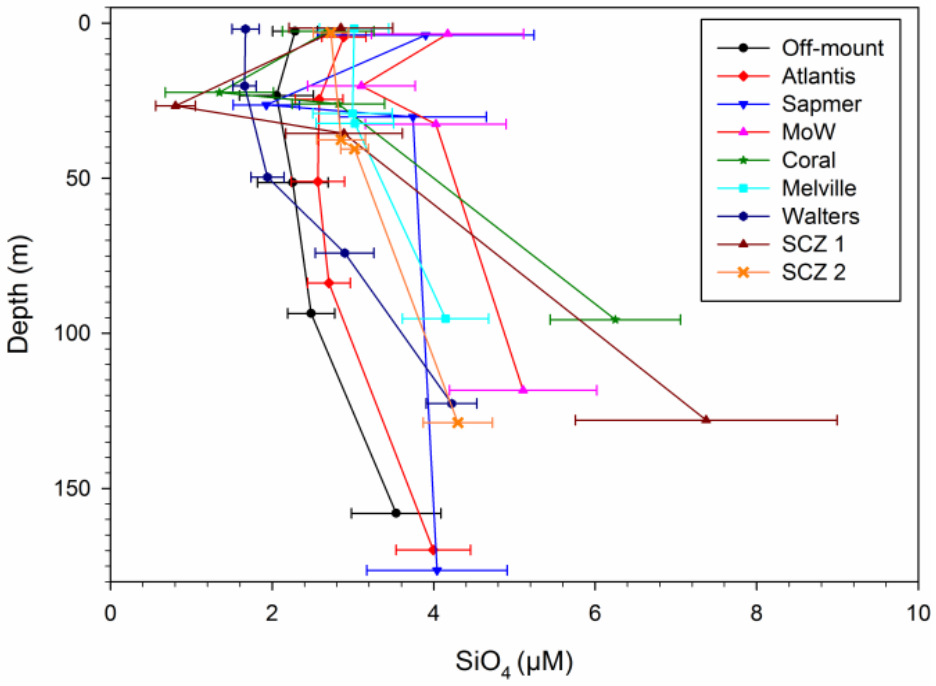

Fig. 6.8 Silicate concentrations in the epipelagic zone of six seamounts, the off-mount stations and two subtropical convergence transects.

Phosphate showed a gradient of increasing concentration with an increase in latitude, although no significant difference ($F = 10.74$; $p > 0.05$; $n = 304$) between adjacent seamounts were found (Fig. 6.7). At SCZ1 there was an elevated subsurface phosphate concentration, similar to nitrate. No significant differences ($F = 2.21$; $p > 0.05$; $n = 395$) were recorded in silicate concentrations between the study sites (Fig. 3d). Silicate concentrations decreased from the surface waters to ~30 m before increasing again in deeper waters. Nitrite showed a significant inverse correlation with depth overall (Table 6.2).

Table 6.2 Pearson correlation analysis with pairwise deletion of the environmental variables of the Agulhas Return Current. Significant correlations are indicated as follows: *** $p < 0.001$, ** $p < 0.01$, * $p < <0.05$.

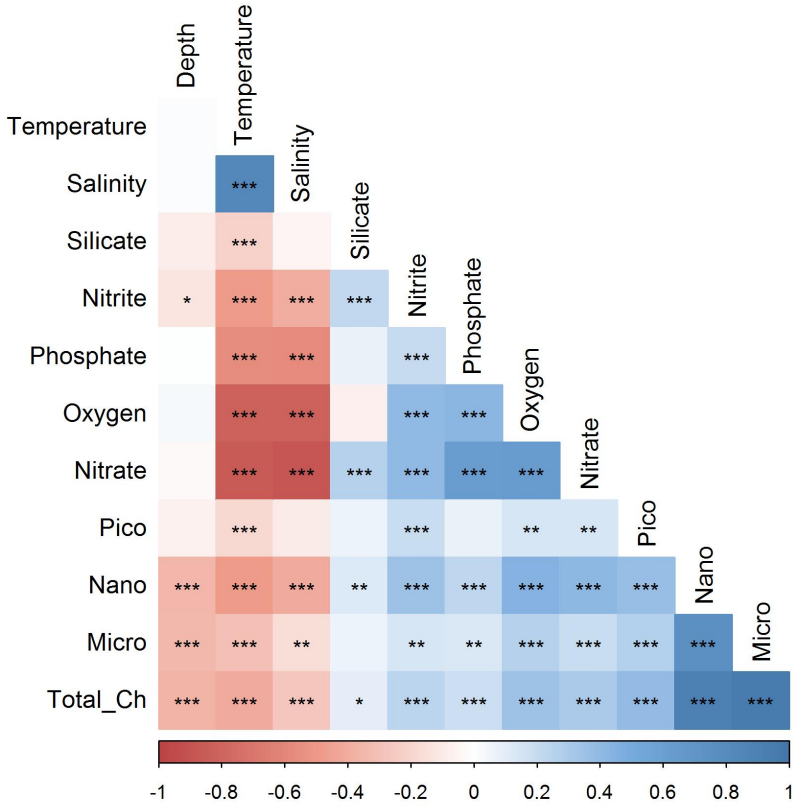

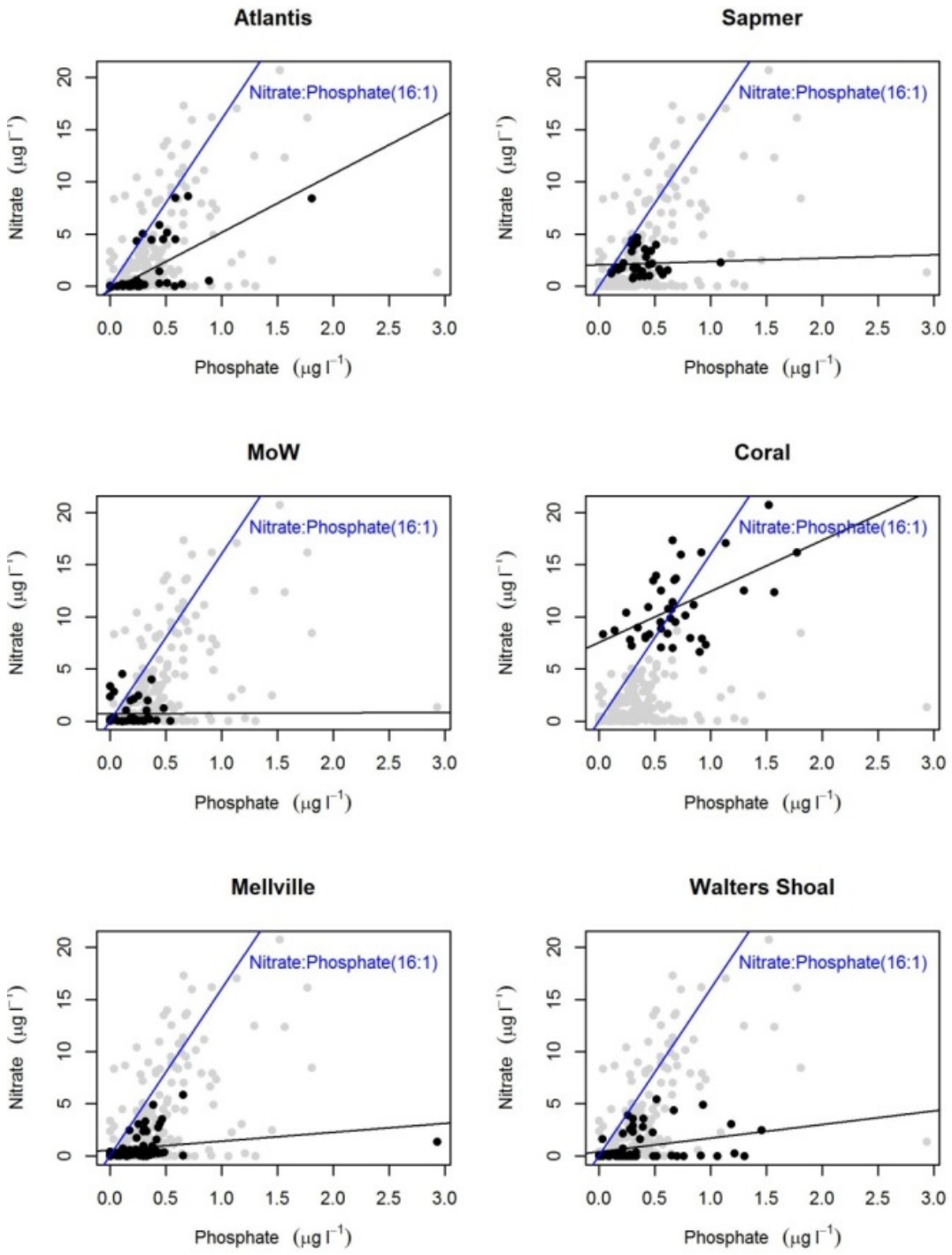

Fig. 6.9 Concentrations of nitrate versus phosphate in the epipelagic zone of the Agulhas Return Current. The black line is the regression line for the data and the blue line represents the Redfield Ratio (N:P = 16:1). Grey dots are all stations whereas the black dots represent the samples for the specific seamount.

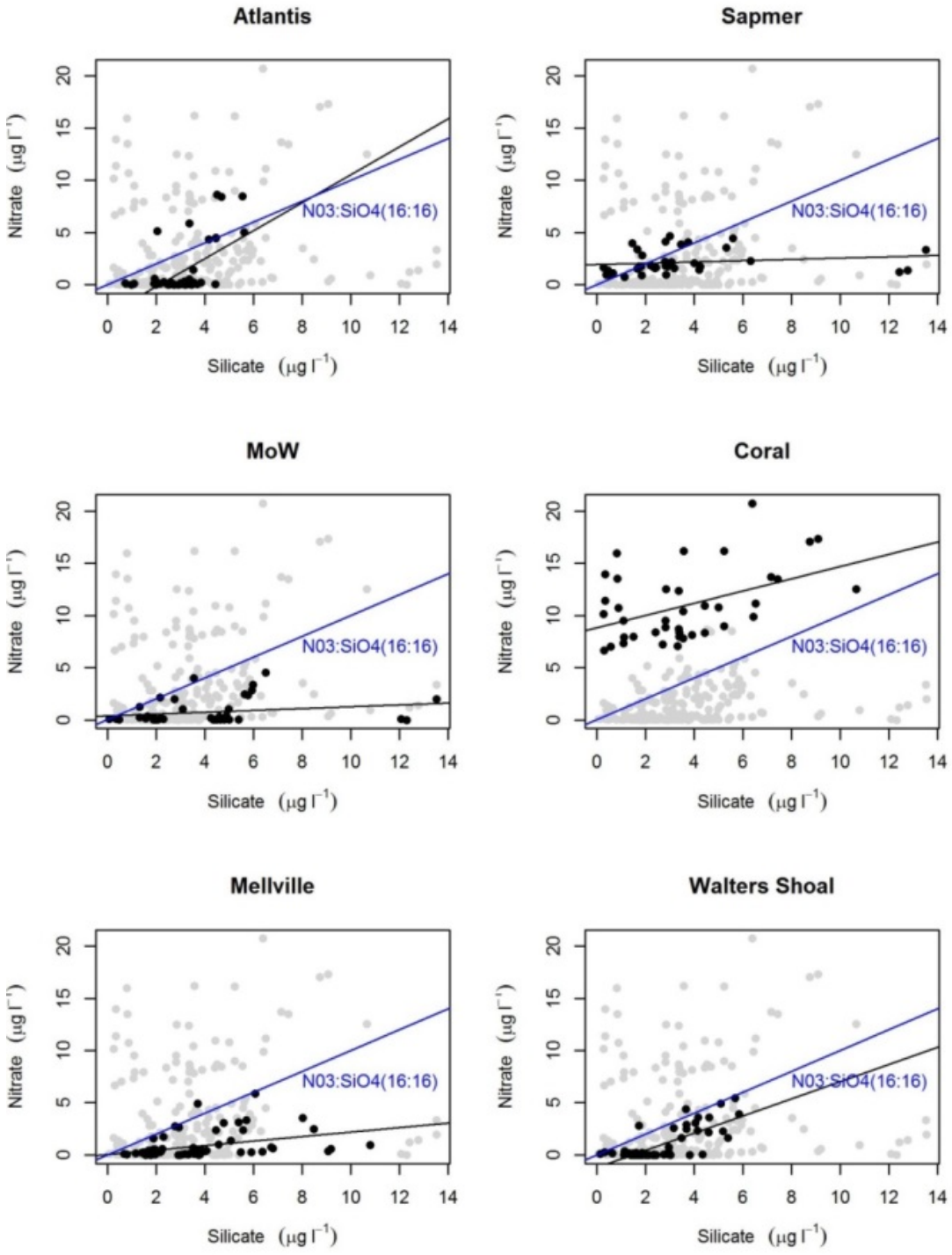

Fig. 6.10 Concentrations of nitrate versus silica in the epipelagic zone of the Agulhas Return Current. The black line is the regression line for the data and the blue line represents the Redfield Ratio (N:Si = 1:1).

The ratio of nitrate versus phosphate concentration at low concentrations indicates nitrate limitation at MoW (1:1), Sapmer (2:1) and Melville (2:1) (Fig. 6.9). The N:P ratio at Coral (12.5:1) was the closest to the 16:1 Redfield ratio (Fig. 6.9). The concentration of N:P at Atlantis was 5:1 (Fig. 6.9). Atlantis and Walters had a N:Si of 15:16 and 12:16 respectively indicating nitrogen limitation (Fig. 6.10). The water column above Coral had a nitrogen to Silicate ratio above 1 (18:16) indicating that Si was the limiting nutrient at the time of sampling (Fig. 6.10). Sapmer (4:16), MoW (4:16) and Melville (5:16) were nitrogen limited (Fig. 6.10).

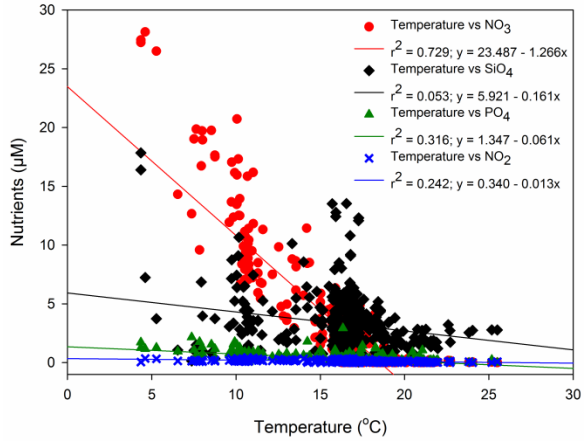

Fig. 6.11 Concentrations of nutrients (NO_3^-, SiO_4^{4-}; PO_4^{3-} and NO_2^-) versus temperature for all the euphotic zone stations of the Agulhas Return Current (n = 408).

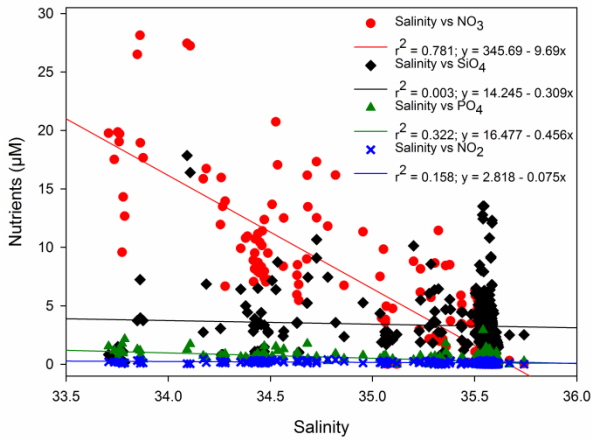

Fig. 6.12 Concentrations of nutrients (NO_3^-, SiO_4^{4-}; PO_4^{3-} and NO_2^-) versus salinity for all the euphotic zone stations of the Agulhas Return Current (n = 408).

The four nutrients had a significant correlation with temperature (Table 6.2). Furthermore, all, except silicate, showed a significant correlation with salinity (Table 6.2). Plotting the nutrients against temperature (Fig. 6.11) and salinity (Fig. 6.12), the nutrients showed an inverse linear relationship with both - this splits their relationships into two groups. At temperatures below 17.5°C and salinity below 34.5, the euphotic zone is characterised by higher nutrient concentrations (particularly nitrate). Where temperatures were over 17.5°C and salinity over 34.7, waters had lower nutrient concentrations. Nitrate plotted against temperature shows that off-

mount waters, Walters and the surface water (top 50 m) of Atlantis differ from the water measured at the rest of the seamounts and the SCZ transects. The correlations between nitrate concentrations and salinity separated Coral and SCZ1 from the other study areas.

6.4.2 Spatial variability of phytoplankton

Phytoplankton biomass (measured as chlorophyll *a,* Fig. 6.13 to Fig. 6.16) increased with an increase in latitude from the subtropics to the SCZ. Off-mount, Atlantis and Walters had a DCM at 95 m, 85 m and 75 m respectively. The DCM at Walters had a significantly higher ($F = 15.01$; $p < 0.05$; $n = 48$) concentration of total chlorophyll *a* and nanophytoplankton chlorophyll *a* compared to Atlantis, but was still significantly lower ($F = 18.22$; $p < 0.05$; $n = 26$) than the maximum chlorophyll *a* concentration at Coral. The higher latitude seamounts and SCZ transects had their maximum chlorophyll *a* (of all size fractions) in the surface waters (<40 m). There was no significant difference ($F = 92.36$; $p > 0.05$; $n = 116$) in chlorophyll *a* of waters deeper than 100 m between the study sites. Picophytoplankton (Fig. 6.16) contributed the least to the total phytoplankton biomass (especially at the higher latitude study sites) and showed no significant difference ($F = 3.77$; $p < 0.05$; $n = 408$) in concentration between study sites or at depth. There was a significant difference ($F = 10.31$; $p < 0.05$; $n = 408$) in the overall contribution made by the different size classes (picophytoplankton mean: 0.144 ± 0.007 µg l^{-1}; range 0 – 2.08 µg l^{-1}; nanophytoplankton mean: 0.879 ± 0.042 µg l^{-1}; range: 0.004 – 5.42 µg l^{-1}; and microphytoplankton mean: 1.032 ± 0.068 µg l^{-1}; range 0.001 – 9.91 µg l^{-1}).

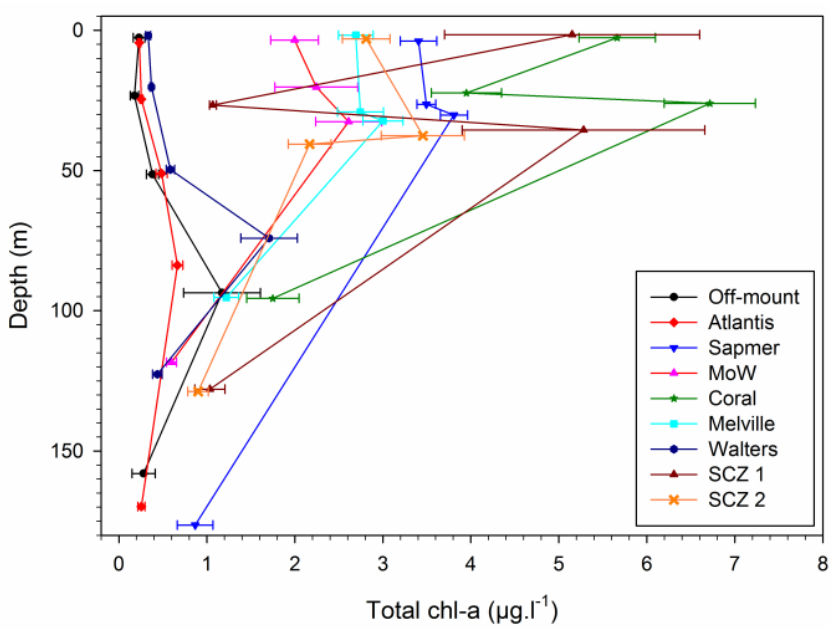

Fig. 6.13 Total chlorophyll *a* biomass in the epipelagic zone of six seamounts, the off-mount stations and two subtropical convergence transects.

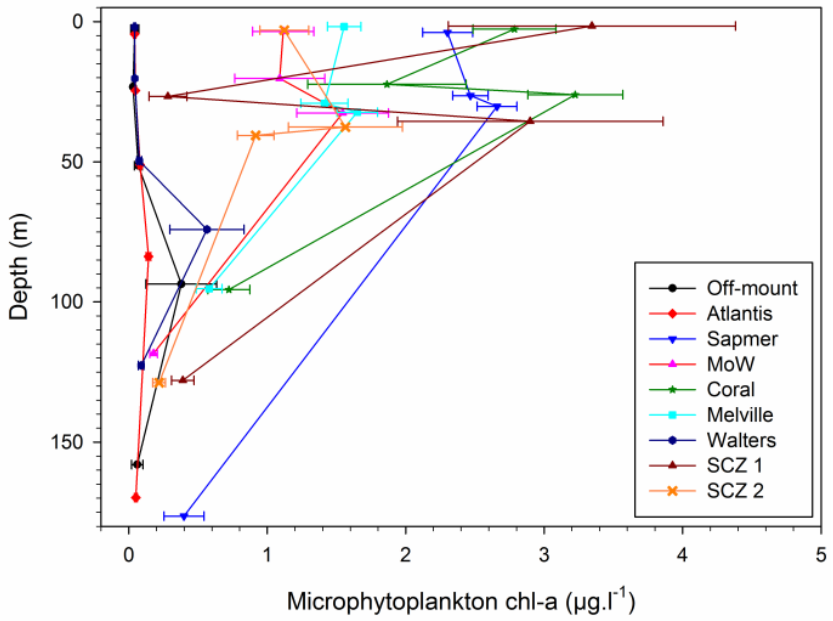

Fig. 6.14 Microphytoplankton chlorophyll *a* biomass in the epipelagic zone of six seamounts, the off-mount stations and two subtropical convergence transects.

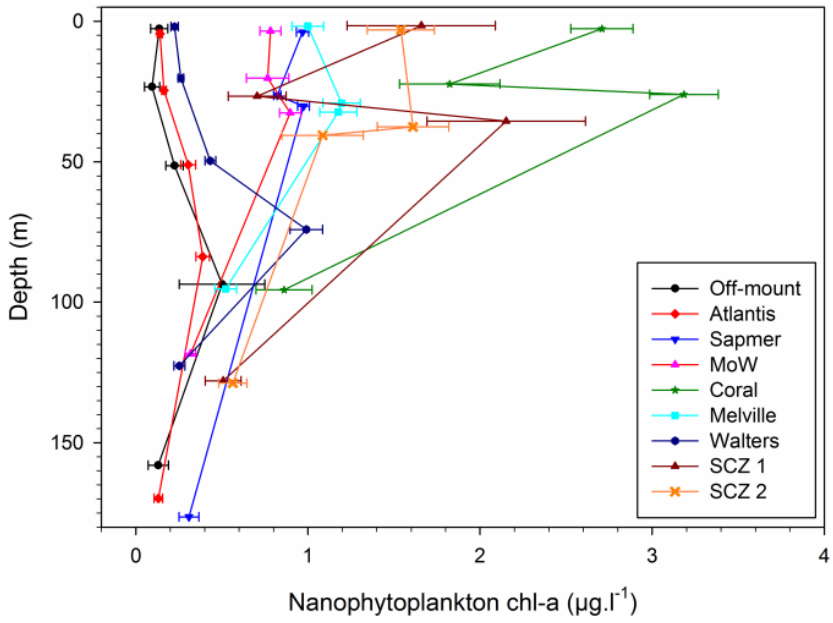

Fig. 6.15 Nanophytoplankton chlorophyll *a* biomass in the epipelagic zone of six seamounts, the off-mount stations and two subtropical convergence transects.

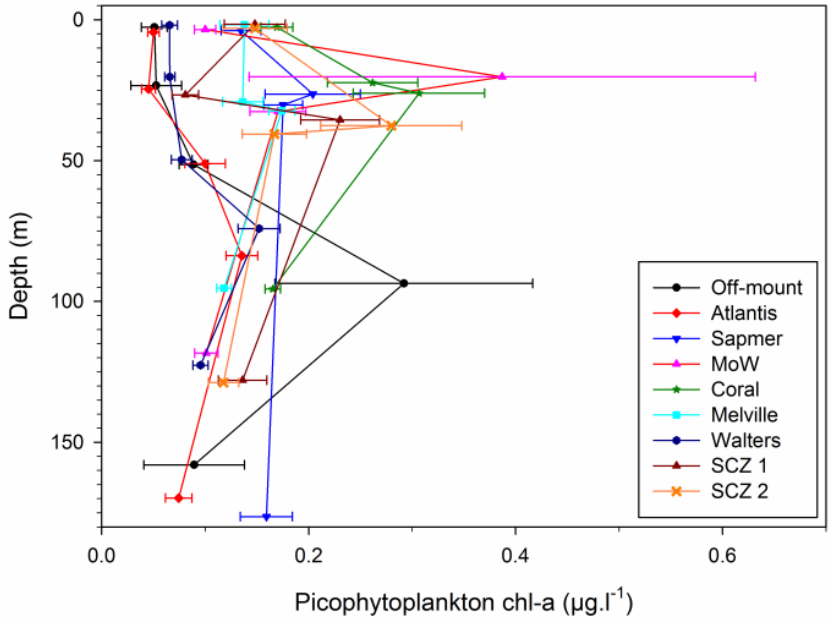

Fig. 6.16 Picophytoplankton chlorophyll *a* biomass in the epipelagic zone of six seamounts, the off-mount stations and two subtropical convergence transects.

Selected plots of the chlorophyll *a* concentration at depth and latitude in the euphotic zone illustrates the difference in phytoplankton biomass between the subtropics (Fig. 6.17) and the SCZ area (Fig. 6.18). It was only at the two shallowest seamounts (Coral: summit = 205 m; Fig. 6.18 and Melville Bank: summit = 108 m; Fig. 6.19 and Fig. 6.20) where evidence was found of a chlorophyll *a* response in the vicinity of the summit. The isothermal mixed-layer depth and the isopycnal mixed-layer depth (Appendix: Agulhas Retroflection; Fig. 9.6) were situated above the DCM (Fig. 6.17), forming a barrier to mixing. The isothermal mixed-layer depth and isopycnal mixed-layer depth were situated below the chlorophyll *a* maximum in Fig. 6.18 to Fig. 6.20 and more or less followed the 0.1 to 0.2 µg l^{-1} isoline of chlorophyll. The only area where the isothermal mixed-layer depth was situated 50 - 100 m below the summit was along the longitudinal transect over Melville Bank (Appendix: Agulhas Retroflection; Fig. 9.7). The deepening of the mixing layer from ca. 50 m in the subtropics to more than 100 m at the higher latitudes positively influences phytoplankton biomass.

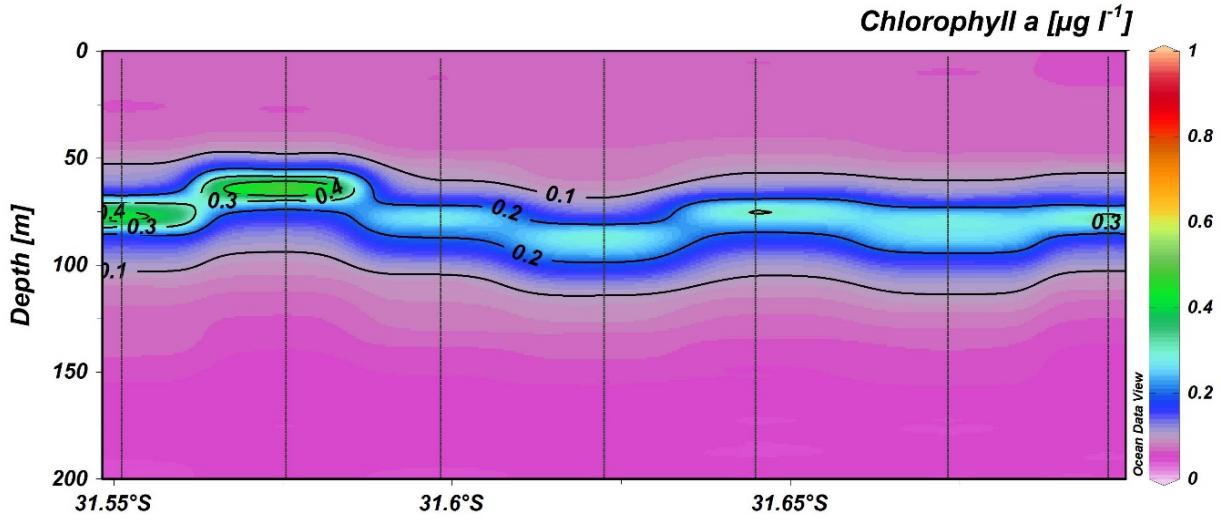

Fig. 6.17 Latitudinal depth transect of chlorophyll *a* (µg l^{-1}) concentrations for Walters Shoal. Vertical lines denote CTD positions.

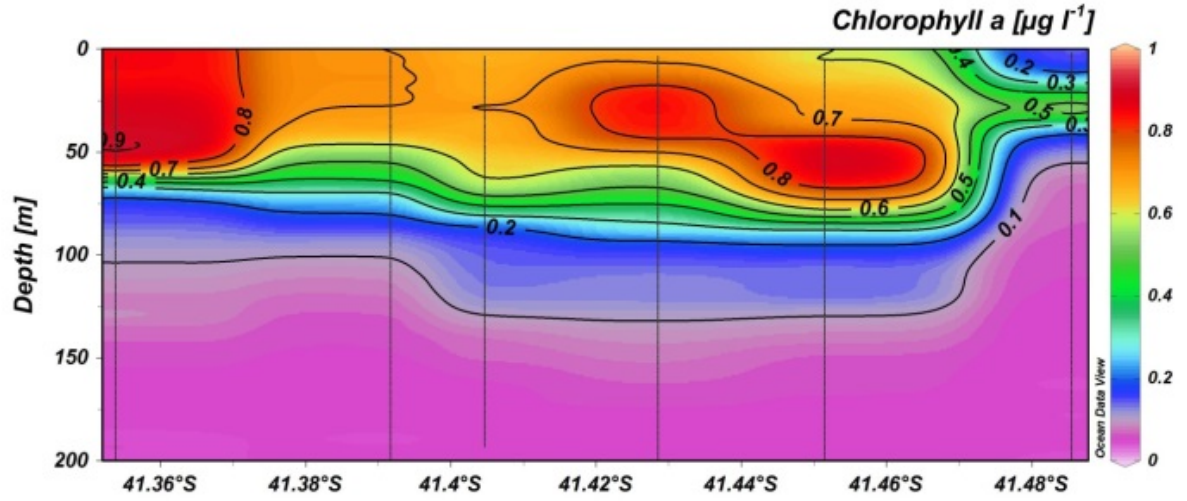

Fig. 6.18 Latitudinal depth transect of chlorophyll *a* (µg l^{-1}) concentrations for Coral Seamount. Vertical lines denote CTD positions.

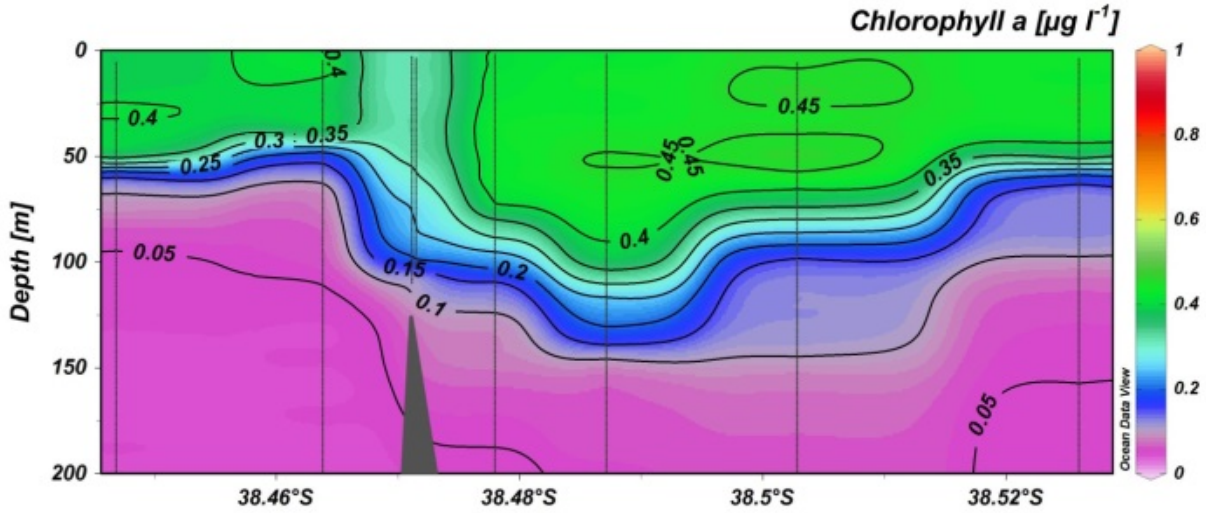

Fig. 6.19 Latitudinal depth transect of chlorophyll *a* (µg l^{-1}) concentrations for Melville Bank. Vertical lines denote CTD positions.

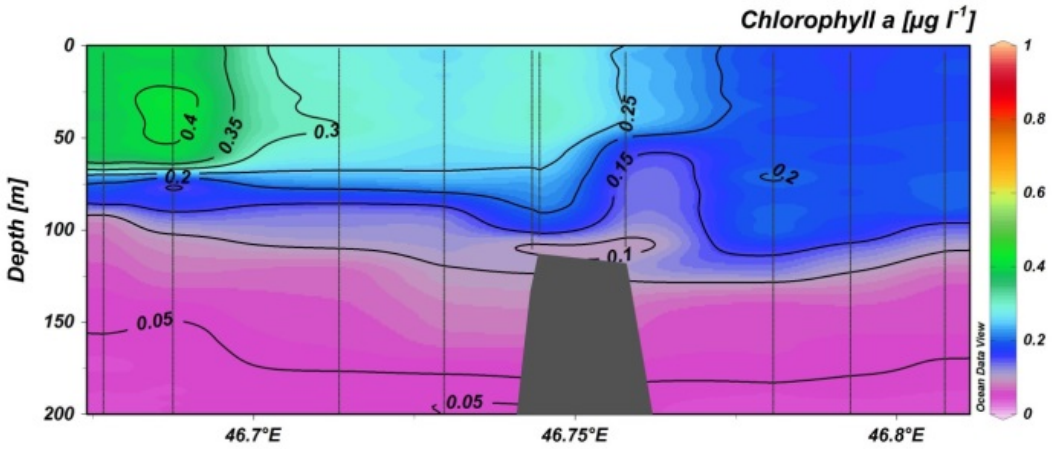

Fig. 6.20 Longitudinal depth transect of chlorophyll *a* (µg l^{-1}) concentrations for Melville Bank. Vertical lines denote CTD positions.

6.4.3 Phytoplankton composition

A total of 148 phytoplankton taxa were recorded during the survey: 74 diatom, 59 dinoflagellate, six silicoflagellate, four chlorophyte flagellate, three coccolithophore, and one prymnesiophyte. The dominant genera (>1 000 counts), in order of dominance were: *Pseudo-nitzschia* (diatom), *Alexandrium* (dinoflagellate), *Thalassiosira* (diatom), *Gymnodinium* (dinoflagellate), the Prymnesiophyte species; *Phaeocystis antarctica*; *Peridinium* spp. (dinoflagellate), *Navicula* spp. (diatom), *Oxytoxum* spp. (dinoflagellate), *Thalasionema* spp. (diatom) and *Chaetoceros* spp. (diatom).

The seamount with the highest phytoplankton diversity was Atlantis with 68 taxa in surface waters and 75 at the DCM (Fig. 6.21). Off-mount stations in subtropical waters had the second highest diversity (Fig. 6.21). Despite the high diversity, these stations, including Walters, had low phytoplankton biomass and were dominated by dinoflagellates. The other four seamounts and two SCZ transects had higher biomass although only Coral, SCZ1 and Sapmer had a significantly higher ($F = 15.23$; $p < 0.05$; $n = 121$) surface and DCM chlorophyll *a* concentration than the subtropical stations. Dominance also changed from dinoflagellates to diatoms and even the appearance of a bloom of *Pseudo-nitzschia* spp. (this genus contributed >75% of the total diatom cell count of the survey). The prymnesiophyte, *Phaeocystis antarctica* was abundant (3 064 cells in total) in the Subtropical Convergence Zone,

and in waters over Coral and Melville (Fig. 6.21). Coccolithophores were restricted to SCZ1, and the Coral and Atlantis seamount waters.

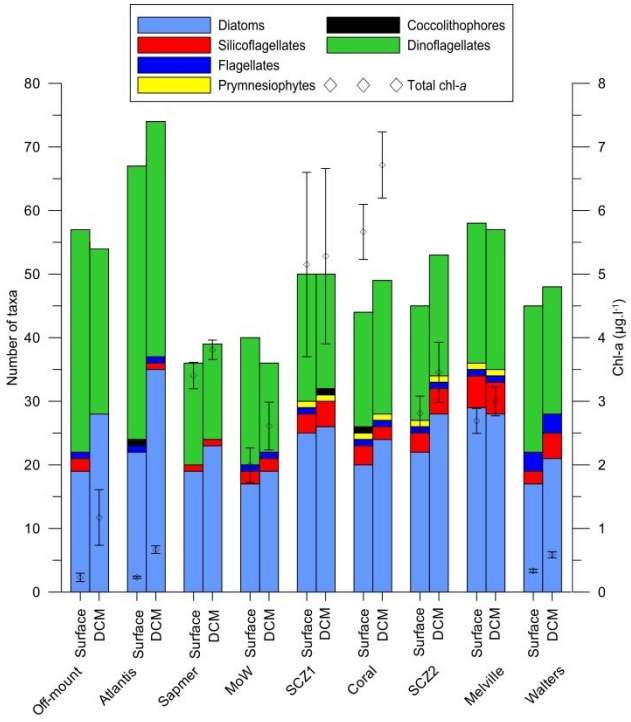

Fig. 6.21 Composition of phytoplankton from the surface and DCM layers of the nine study areas of the Agulhas Return Current. Mean total chlorophyll *a* concentrations are also provided for each site.

Multivariate analyses grouped the taxa into three communities (Fig. 6.22): subtropical phytoplankton (Atlantis, Walters and Off-mount); phytoplankton south of the ARC (Coral and SCZ1) and phytoplankton north of the ARC (Melville, Sapmer and MoW). The communities north and south of the ARC shared many species, especially the abundant *Pseudo-nitzschia* spp. The two SCZ transects shared species with most of the seamounts, although the southern waters of SCZ1 formed a community with Coral, south of the ARC, because of the dominance of *Phaeocystis antarctica*. The species associated with the off-mount stations were part of the subtropical community with *Alexandrium* cf. *carraun* responsible for the off-mount outlier (Fig. 6.22). The dominance of *Alexandrium* spp. at Walters and selected stations of SCZ2 explain the close grouping of these in ordination space. Cosmopolitan species characterised most of the stations sampled, but the change in

dominance and the appearance of local species was enough to split the samples into three distinct communities, representing different geographical areas.

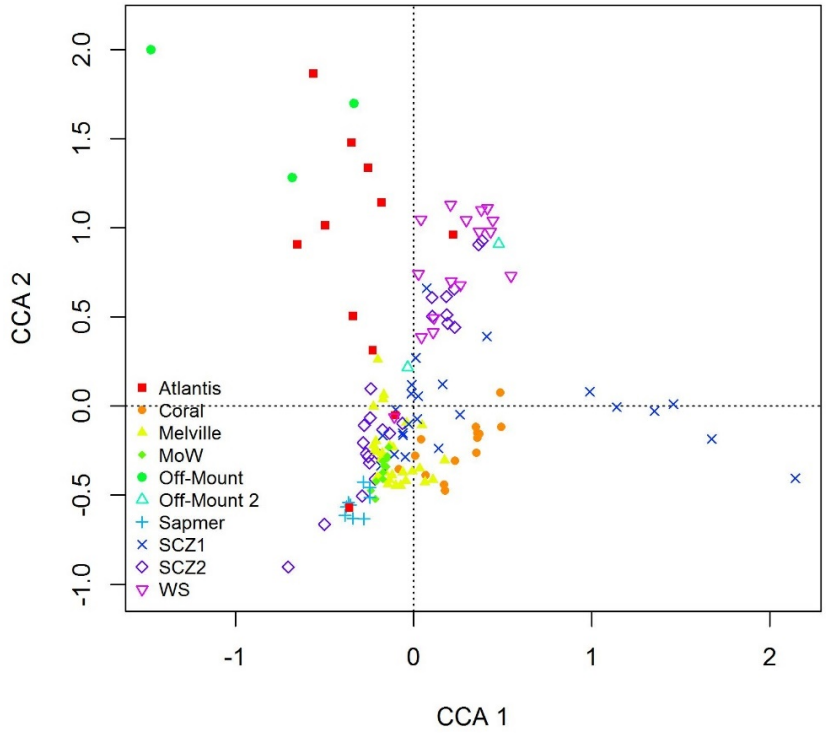

Fig. 6.22 Detrended Correspondence Analysis ordination of the phytoplankton of the nine study areas of the Agulhas Return Current.

6.4.4 Environmental drivers of phytoplankton variability

The first canonical axis (Fig. 6.23) accounted for 38% of the species–environment relation. The strongest correlations were with temperature (r = 0.71), nitrate (r = 0.89) and oxygen (r = 0.45). Adding the second canonical axis accounted for 68% of the cumulative variation and was positively correlated to temperature (r = 0.47; Fig. 6.23). These stations also had a higher than average phosphate concentration. The samples collected at Coral and the southern stations of SCZ1 had a higher than average nutrient and oxygen concentration and the lowest water temperatures. Waters north of the ARC, Melville, MoW and Sapmer were characterised by high silicate, low phosphate and nitrate concentrations, high salinity and shallower than

average bathymetry and a DCM. The spread of the SCZ1 and SCZ2 stations across the ordination is indicative of the spatial extent of the transects from the ARC through the STF and into the SAF.

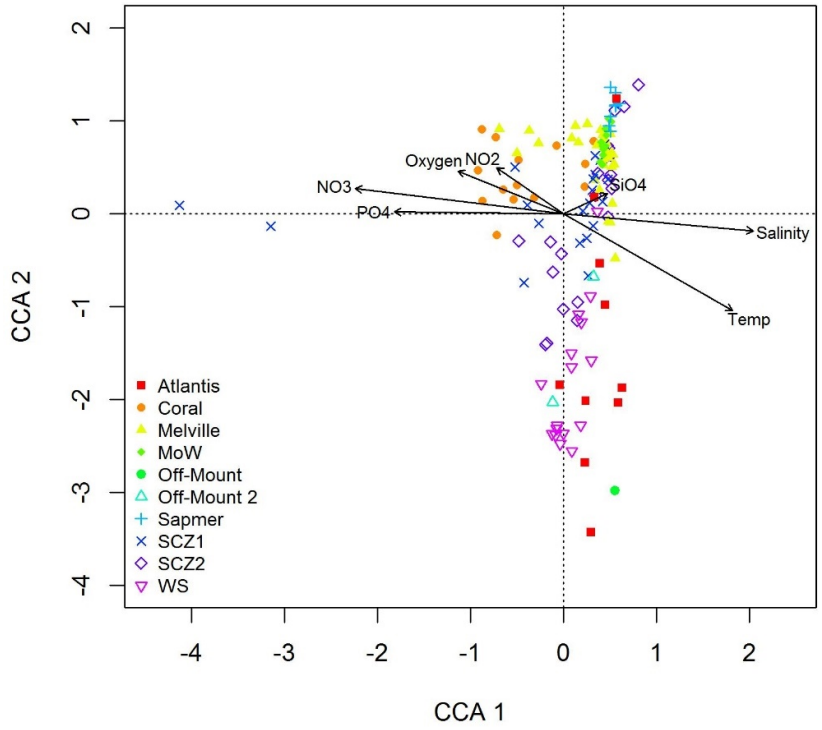

Fig. 6.23 Canonical Correspondence Analysis ordination of the phytoplankton of the nine study areas of the Agulhas Return Current constrained by environmental variables.

6.5 Discussion

6.5.1 Physical and chemical oceanography

The geographic spread of seamounts, off-mount stations and SCZ transects sampled during the survey in 2009 showed significant latitudinal differences in temperature, salinity and dissolved oxygen of the euphotic zone. Pollard and Read (2017) and Read and Pollard (2017) found that Coral was characterised by low

temperatures and salinity and high oxygen and density with a halocline situated at 70 to 100 m depth and a fresh surface layer. This study found similar results for both Coral and SCZ1 and an even bigger response in waters of the SCZ1 - probably because the transect extended deeper into the SAF (Pollard and Read, 2017; Read and Pollard, 2017). It was this relatively fresh, low temperature, high oxygen layer that had elevated concentrations of all the nutrients except silicate. This subsurface layer also had low concentrations of total chlorophyll *a*, but relatively high concentrations of picophytoplankton. The weak stratification of all physical and chemical parameters measured at Sapmer was as a result of an anticyclonic eddy that caused mixing to deeper than 400 m (Pollard and Read, 2017; Read and Pollard, 2017). Atlantis and Walters, although also influenced by eddies, showed near-surface stratification at the time of the survey (Pollard and Read, 2017; Read and Pollard, 2017). The lowest oxygen concentrations were measured at Walters and this is due to the southward flow of low oxygen water from the tropics (Pollard and Read, 2017). Oxygen concentrations peaked at the depth of maximal chlorophyll *a* concentration: at the DCM for the lower latitude stations and at the SCM for Coral and SCZ1. Isopycnals were shallowest at Coral and Atlantis because of the strong eastward flow of the ARC north of Coral and weak westward drift between Atlantis and the other seamounts (Pollard and Read, 2017).

Nitrogen and phosphorus are the main inorganic nutrients required for phytoplankton growth in marine ecosystems, although silicate could limit the growth of diatoms (Yool and Tyrrell, 2003; Crombet *et al.*, 2011; de Souza *et al.*, 2013). Nitrate, nitrite and phosphate showed a latitudinal increase in concentration from the oligotrophic subtropics to the mesotrophic STF. Nitrite and silicate showed a decrease in concentration with depth in the subsurface waters of the higher latitude seamounts that was mirrored by a decrease in total, micro and nanophytoplankton biomass and an increase in picophytoplankton biomass. The chlorophyll *a* maximum in the high latitude samples was situated between 30 and 40 m depth and was associated with an increased concentration of nitrite and silicate and a decreased concentration of nitrate and phosphate. The DCM in the subtropical stations was associated with increased concentrations of all the nutrients to form a nutricline, a boundary between the nutrient depleted surface waters and the light limited deeper ones (Cullen, 1982).

The high variability of the physical and chemical properties of the SCZ1 samples is due to the variability of the ARC, STF and SAF (Pollard and Read, 2017).

The N:P and N:Si ratios of the water control the phytoplankton community structure (Read *et al.*, 2000; Brauer *et al.*, 2012), that in turn determines the stoichiometry of the ocean (Mills and Arrigo, 2010; Weber and Deutsch, 2012; Martiny *et al.*, 2013). Ptacnik *et al.* (2010) is of the opinion that use of the relationships between major nutrients have limited applicability in understanding phytoplankton ecology and Anderson and Sarmiento (1994) reported that these ratios may not be applicable to the ocean waters shallower than 400 m. Redfield ratios are however useful in determining the utilisation of one nutrient relative to another. A near-to-origin intercept of nitrate versus phosphate indicates the competitive advantage of nitrogen-fixing phytoplankton groups at low ambient nitrate levels (Yool and Tyrrell, 2003; Mills and Arrigo, 2010). Nitrate was limiting at all the seamounts except Coral that had an N:P ratio of 12.5:1 - this is close to the average N:P ratio of marine phytoplankton (16:1), even more closely matched to the nutrient content of mean ocean waters (14.3:1) (Weber and Deutsch, 2012) and identical to that measured by Martiny *et al.* (2013) for cold nutrient-rich high-latitude areas in the Southern Ocean. From Weber and Deutsch (2012) it is evident that the area sampled during this survey extended from oceanic waters, with a N:P of <16, to more than 16 in the higher latitudes. Nitrogen fixing organisms are advantaged in nitrogen depleted waters, where N:P <16, but are out-competed where N is not limiting (N:P >16) due to the energy demand of fixing nitrogen (Tyrrel, 1999; Lenton and Klausmeier, 2006). Phosphorus is therefore the ultimate limiting nutrient in the ocean (Tyrrel, 1999). Nitrogen fixation is an important process, especially in the subtropics, keeping the ratio of N:P close to 16:1 (Lenton and Watson, 2000). Denitrification continuously removes nitrate from surface waters, thereby maintaining an N:P deficit and a population of nitrogen-fixing organisms (Lenton and Klausmeier, 2006).

All the seamounts, except Coral, had a N:Si ratio below 1, indicating that nitrogen was limiting. Coral on the other hand was silicate limited. The STF and the SAF had previously been found to be silicate limited (Read *et al.*, 2000; Mohan *et al.*, 2011). The proliferation of diatoms at Coral and in the STF and SAF are likely to have depleted silicate, similar to what Comeau *et al.* (1995) found on Cobb Seamount. If

the ratio remains below 1:1 then the proportion of diatoms in the phytoplankton community will decline and that will impact on the higher trophic level food web over the seamounts (Turner *et al.*, 1998). The deviation of N:Si from the Redfield ratio with depth is because biogenic silica dissolution is slower than the remineralisation processes of nitrate and phosphate (Tyrrel, 1999; Read *et al.*, 2000; Yool and Tyrrell, 2003).

Nutrients exhibited an inverse linear relationship with temperature and salinity, splitting the study area into three sectors defined by a temperature threshold of 17.5°C and a salinity threshold of 34.7. Higher nutrient concentrations can be expected where temperatures are less than 17.5°C and the salinity is less than 34.7. This splits the oligotrophic subtropical areas from the mesotrophic seamounts based on temperature and then further divides the seamounts into those north of the ARC and those situated south of it (Coral and SCZ1) based on salinity. de Souza *et al.* (2013) found a similar relationship where the upper euphotic zone grouped separately from the deeper water based on temperature and salinity.

6.5.2 Spatial variability of phytoplankton

Phytoplankton biomass showed the same latitudinal change as the nutrients and physical properties of the water. Chlorophyll *a* biomass increased with latitude and the DCM became shallower, from around 85 m in the subtropics to 35 m over the seamounts and long SCZ transects north and south of the ARC. Santos *et al.* (2013) found that the DCM varied significantly (from 15 m to 75 m) over the Condor Seamount between seasons and it may well be that the DCM depths recorded during this snapshot survey may vary during different times of the year. The mesotrophic nature of the ARC region could however sustain high chlorophyll *a* concentrations, a shallow DCM and nitricline (Estrada *et al.*, 1993). The mesoscale eddies associated with the ARC could be responsible for high chlorophyll *a* and nutrient variability through eddy-induced redistribution and spatially and temporally intermittent fluxes of nutrients into the euphotic zone, rather than a change in autochthonous growth (McGillicuddy Jr *et al.*, 1998; Levy *et al.*, 2001; Bibby and Moore, 2011; Chelton *et al.*, 2011; Drazen *et al.*, 2011). There was no significant

difference in biomass between the subtropics and the area under the influence of the ARC at depths deeper than 100 m.

Read *et al.* (2000) also found that the chlorophyll *a* peaked where the ARC, STF and SAF were in close proximity. However, during this survey the phytoplankton biomass measured on the SCZ1 transect was substantially higher (over 5 µg l^{-1}) than the maximum of 1.25 µg l^{-1} measured by Read *et al.* (2000). The maximum chlorophyll *a* concentration for this survey was 15.67 µg l^{-1}, measured in the SCM of the SAF along the SCZ1 transect (see Fig. 3 in (Pollard and Read, 2017). Sedwick *et al.* (2002) also recorded a maximum chlorophyll *a* concentration of less than 1 µg l^{-1} in the SAF/STF. This cannot really be attributed to season since both Read *et al.* (2000) and Sedwick *et al.* (2002) also sampled in summer (January and February). The main difference between their studies and this one is that they did not sample seamounts. With the exception of the subtropics, chlorophyll *a* concentrations were highly variable in the euphotic zone, highlighting the role of physical processes (upwelling and increased mixing) associated with frontal systems, eddies and shallow seamounts in local enhancement of primary production.

The mixed layer depth increased from around 50 m in the subtropics (with the DCM located below this layer) to as deep as 100 m in the higher latitudes. Most productivity occurred near the base of the surface mixed layer in the subtropics. Arrigo *et al.* (1999) found that the phytoplankton community structure varies as a function of the depth of the mixed layer. The latitudinal difference in seamounts studied and the variable influence of eddies on the vertical structure of the water column, made it difficult to detect any community differences associated with the depth of the mixed layer.

Micro- and nanophytoplankton made up most of the total chlorophyll *a* biomass in waters at the higher latitudes, whereas the subtropics had a more or less equal contribution of size fractions. The increase in picophytoplankton biomass in the subsurface waters at Coral and SCZ1 could be due to the presence of cyanobacteria. The smallest marine phytoplankton, collectively termed picophytoplankton, includes marine photosynthetic cyanobacteria such as *Prochlorococcus* and *Synechococcus* (Buitenhuis *et al.*, 2012). Fiala *et al.* (2003)

found that although *Pseudo-nitzschia* spp. were dominant in the STF of the Crozet Basin, pico- and nanophytoplankton had the highest biomass and cyanobacteria contributed the most to the picophytoplankton size fraction. However, cyanobacteria are only present in subtropical waters warmer than 12.5°C (Fiala *et al.*, 2003), which excludes them from the Coral seamount and SCZ1 waters. The sampling (0.7 µm filter paper instead of 0.2 µm) and preservation (2% Lugols) methods were found to be less than ideal for studying the picophytoplankton community. It would appear that the subsurface waters at Coral and SCZ1 were different to the rest of the profile and were in all likelihood Subantarctic Surface Water (Fig. 5f in Pollard and Read, 2017), as it was colder, less saline and more nutrient rich (although silicate depleted). The depletion of silicate, the high concentrations of nitrate and phosphate and the decreased biomass indicate that diatoms were silicate limited, which could explain their low numbers.

Phytoplankton biomass showed a positive response to the presence of a shallow (<200 m) seamount summit. Similar increases in chlorophyll *a* over the summit of seamounts have been found, however, no evidence of a persistent seamount effect on phytoplankton production have yet been recorded (Genin and Boehlert, 1985; Boehlert and Genin, 1987; Dower *et al.*, 1992; Comeau *et al.*, 1995; Odate and Furuya, 1998; Mourino *et al.*, 2001; Genin, 2004; Genin and Dower, 2007; White *et al.*, 2007; Arístegui *et al.*, 2009; Mohn *et al.*, 2009; Drazen *et al.*, 2011; Young *et al.*, 2011; Misic *et al.*, 2012). Even if there was an effect, it would have to be maintained over the seamount for several months to have a positive influence on the higher trophic level species resident on the seamount (Morato *et al.*, 2009; Clark *et al.*, 2010), unless the summit of the seamount was situated close to the DCM so that the benthic community directly benefitted from the phytoplankton (Cordeiro *et al.*, 2013). The export of phytoplankton biomass downstream of the seamounts (Genin and Dower, 2007; White *et al.*, 2007) was not found during this survey - possibly because the transects and stations were limited to the slopes and peak(s) of the seamounts.

The high concentration of nitrate and silicate in the water (ARC) flowing over Coral and Melville seamounts could have resulted in a positive phytoplankton response irrespective of a possible seamount effect. It is impossible to determine from the limited data which of the six possible physical processes (or combinations thereof)

described by White *et al.* (2007) was responsible for the enhanced biomass. Pollard and Read (2017) found that mesoscale eddies had the greatest influence on the circulation near each seamount and a shallow seamount will cause a flow disturbance that interacts with the euphotic zone (Beckmann and Mohn, 2002; Stevens *et al.*, 2014). At the time of sampling, Melville Bank was situated on the flank of a westward propagating cyclonic eddy that had pinched off the ARC (Pollard and Read, 2017). The current flow over Melville was the highest recorded during the survey (34 cm s^{-1}; Pollard and Read (2017)). The ARC meanders and on occasion Coral may lie within the ARC (Boebel *et al.*, 2003). Eddies play an important role in redistributing phytoplankton through horizontal advection and thereby sustaining new production within the euphotic zone (Woodward and Rees, 2001; Chelton *et al.*, 2011). Coral was located south of the ARC and on the boundary of the STF and the SAF and was subjected to an eastward circulation of 10 to 20 cm s^{-1} (Pollard and Read, 2017). The proximity of the frontal zones could be responsible for vertical mixing and the enhanced productivity recorded there (Read *et al.*, 2000; Clayton *et al.*, 2014). Perissinotto *et al.* (1990) and Comeau *et al.* (1995) found that increased vertical stability of the euphotic zone increased phytoplankton production. Such vertical stability is, however, unlikely to persist in this highly variable environment associated with the meandering ARC eddy field.

6.5.3 Phytoplankton composition

The phytoplankton community showed a latitudinal gradient with decreasing diversity as latitude increased. There was a concomitant change in dominance from dinoflagellates to diatoms. The other taxa made a substantially smaller contribution to the phytoplankton, but this could be an artefact of the preservation method used (Sonnekus *et al.* 2017). The Lugol's Iodine method was specifically developed to preserve diatoms (Parsons *et al.*, 1989; Karayanni *et al.*, 2004) and it could be that the chlorophyte flagellate cells were compromised using this method as the preservative is highly acidic. It is likely that the coccolithophores would have been underestimated using this preservative. The oligotrophic waters of the Indian Ocean are characterised by the smaller phytoplankton groups such as chlorophyte flagellates due to their ability to rapidly take up nutrients (Twomey *et al.*, 2007). Read

et al. (2000) found that diatoms were not dominant when the chlorophyll *a* was below 0.3 µg l^{-1}. For this study, this included the surface waters of the Off-mount stations and Atlantis. However, the high numbers of *Phaeocystis antarctica* indicate that the method did at least preserve soft-bodied cells.

The dominant diatom genus in the higher latitude stations was *Pseudo-nitzschia* that accounted for more than 50% of the cell counts from the entire survey. (Santos *et al.*, 2013) also found *Pseudo-nitzschia* to be the most abundant taxon on Condor Seamount. A large proportion of the taxa were cosmopolitan and recorded at all the stations. Despite this, the presence of a few dominant taxa was sufficient to group the phytoplankton into the three communities that corresponded with the waters that had a definable signature of nutrient concentration, salinity and temperature. The three communities were: subtropical, north of the ARC and south of the ARC. Although Atlantis, Walters and the Off-mount stations grouped together based on the physical, chemical and biomass data, it is interesting that the species composition was sufficiently similar to be considered a single community, despite the two seamounts being 15° of longitude apart (>800 nautical miles) and subjected to different oceanographic conditions. Pollard and Read (2017) recorded a slow (<20 cm s^{-1}) westward drift of mostly cyclonic eddies around Atlantis, whereas Walters is continuously subjected to fast-flowing cyclonic and anti-cyclonic eddies that originate from the East Madagascar Current and pass south of Madagascar to join the Agulhas Current.

The species composition at Coral and SCZ1 stations located in the SAF was unique enough to constitute their own community. Clayton *et al*. (2014) also recorded a clear distinction between subtropical and subpolar phytoplankton communities separated by a front. Turbulent hydrodynamics, as are found in the vicinity of frontal zones and eddies, favour diatoms such as species of *Chaetoceros*, *Pseudo-nitzschia*, *Thalassiosira* and *Thalassiothrix* (Bracher *et al.*, 1999; Santos *et al.*, 2013), all of which were abundant at Coral and in the SCZ transects. However, Coral also had a high abundance and diversity of dinoflagellates. Comeau *et al.* (1995) found that diatoms were dominant in the SCM over Cobb seamount and that dinoflagellates became dominant near the bottom of the euphotic zone. The assemblage of species associated with the STF and SAF in SCZ1 grouped those

stations with Coral, with *Phaeocystis antarctica* being the most dominant species. *Phaeocystis antarctica* requires nitrate and diatoms phosphate to attain maximum standing biomass (Arrigo *et al.*, 1999; Schoemann *et al.*, 2005), neither of which was limiting at Coral and SCZ1. It is understandable that the SCZ transects contained a variety of species associated with the eddies that flow from the ARC, the STF and the SAF.

The number of diatom genera occupying the DCM was almost always higher than in the surface water, especially in the subtropics. The ability of diatoms to grow at depth is commonly observed in other oligotrophic regions and often accompanied by large motile dinoflagellates (Cullen, 1982; Crombet *et al.*, 2011). Communities found on seamounts are variable over large spatial scales (Clark *et al.*, 2012) and the phytoplankton of the south-western Indian Ocean is no different. Bio-communication and material transfer (Lavelle and Mohn, 2010) between higher latitude seamounts is likely, considering the variability of mesoscale features and the extent of the ARC eddy field, explaining to some extent the large number of cosmopolitan species recorded at all the seamounts.

6.5.4 Environmental drivers of phytoplankton variability

The environmental drivers most responsible for the observed species distribution in the southern Indian Ocean were nitrate concentration and temperature. Similar results were found by Davidson *et al.* (2013) in they found that temporal changes in diatom and dinoflagellate communities were related to temperature and nitrate respectively. However, contrary to the findings of McGillicuddy Jr *et al.* (1998), there was no significant correlation between nitrate and standing phytoplankton biomass in this study.

Ordination (Fig. 6.23) showed a negative correlation between nitrate and silicate, indicating that either the one or the other was limiting at any given station. Despite constraining the ordination using environmental variables, the same three phytoplankton communities could be identified in the unconstrained analysis (Fig. 6.22), confirming the environmental control of the communities. Nutrient, temperature and salinity characteristics separated Coral and SCZ1 phytoplankton to be linked to low temperature and salinity waters. The separation of phytoplankton in

the subtropics from the other seamounts was not as strong and could only loosely be associated with low nitrate concentrations.

Current flow, an important possible physical driver of phytoplankton biomass, was not analysed in this study. It is however clear from Pollard and Read (2017) and Boebel *et al.* (2003) that the timescale of physical transport was shorter than what would be required for a phytoplankton response and the subsequent cascade up the trophic levels. Even if phytoplankton blooms developed, they decay so rapidly (Misic *et al.*, 2012) that it is difficult to study these events *in situ* in these remote parts of the ocean. Although impossible to determine from this snapshot survey, it is likely that the input of nutrients and biological material to the seamounts were allochthonous because the current flow past the seamounts was in the order of 30 to 50 cm s^{-1} and the circulation at each seamount was determined more by its proximity to an eddy than by the weak eastward water flow (Pollard and Read, 2017). However, Read *et al.* (2000) found that not all eddies associated with the ARC had elevated nutrient and chlorophyll *a* concentrations, and only by conducting a long-term survey would it be possible to determine if the production at any individual seamount is autochthonous or allochthonous. Individual seamounts in the southern Indian Ocean would in all likelihood also exhibit significant temporal variation (Mourino *et al.*, 2001; Carmo *et al.*, 2013).

6.6 Conclusions

Clear latitudinal differences were evident for all the variables measured during the survey despite the high variability associated with the mesoscale eddies. However, very few flagellates were recorded which can be ascribed to the preservation method used. The most limiting nutrient in the survey area, with the exception of Coral Seamount, was nitrogen. This would create conditions that advantage nitrogen-fixing species. The waters around Coral Seamount were silicon limited at the time of the study. It is doubtful that this would have a negative impact on diatom biomass because of the constant allochthonous introduction of inorganic nutrients through the ARC. The null hypothesis that there is no change in the phytoplankton community or depth of the chlorophyll maximum layer on and off a seamount could not be

completely rejected. Shallow seamounts that extend into the euphotic zone (<200 m) did have a positive influence on primary production, but unfortunately there were no comparative off-mount stations next to each seamount to compare species composition and depth of the DCM.

This study has contributed significantly to our knowledge of phytoplankton distribution and ecology and identified three distinct phytoplankton communities. This survey, however, only provided a snapshot and so could not resolve a number of processes that have timescales of longer than a day. The natural variability in processes influencing a seamount was compounded in this study by the fact that all six seamounts were located either within the Agulhas Current or ARC eddy field, making it difficult to confirm conclusions regarding the drivers and biological response on the seamounts.

7 The southern Agulhas Current Large Marine Ecosystem (sACLME)

7.1 Abstract

Four biogeographical regions were identified within the southern Agulhas Current Large Marnie Ecosystem (sACLME) and the composition of the phytoplankton communities and the associated physico-chemical variables in each were investigated. The phytoplankton community showed a longitudinal gradient with increasing diversity from west to east with a concomitant change in dominance from diatoms to dinoflagellates. Species diversity also showed a decrease from north to south. The other taxa made a substantially smaller contribution to the phytoplankton throughout the region. A total of 215 phytoplankton taxa were identified that were separated into two groups, the Agulhas Current group and the South West Indian Ocean Ridge group. The Agulhas Current group was further subdivided into the Agulhas Shelf, the Agulhas Bank and the Agulhas Retroflection

7.2 Introduction

The aim of this chapter is to present a large-scale view of the phytoplankton of the sACLME based on the results for each geographical region (presented in Chapters 3, 4, 5 and 6). Consideration is given to how global climate change may influence phytoplankton dynamics within the sACLME, as well as to make recommendations for further research.

The Agulhas Shelf (Chapter 3) was the most biodiverse region with 118 phytoplankton taxa recorded. It was characterised by low biomass in the north, increasing as the Agulhas Current forces upwelling (Lutjeharms, 2006; Goschen *et al.*, 2012; Goschen *et al.*, 2015) along its path southwards, transitioning from subtropical oligotrophic to cooler mesotrophic waters. The Agulhas Bank (Chapter 4) with its mesotrophic waters was the most productive area in terms of chlorophyll *a* biomass, but the increased productivity was associated with reduced diversity. As the Agulhas Current continued southwards on its trajectory, it enters the region known as the Agulhas Retroflection (Chapter 5), just south of the Agulhas Bank. The Retroflection was oceanographically dominated by the Agulhas Current that

dissected the sampling area with a clear boundary and physio-chemical gradients separating the Agulhas Current from the surrounding waters. These gradients also separated the phytoplankton into two distinct communities: the Agulhas Current and non-Agulhas Current group. The Agulhas Retroflection is where the Agulhas Current makes a 180° turn to flow eastwards as the ARC (Chapter 6). Although the ARC is by far the biggest geographical area within the sACLME, the study area was focussed towards its eastern end where it flows over the South West Indian Ocean Ridge. Forming a boundary between the ARC and the Southern Ocean is the SCZ that was characterised by steep environmental changes that are typical of frontal areas (Read *et al.*, 2000). Passing eddies and upwelling are sources of nutrients for the ARC (Read *et al.*, 2000). The variability of the ARC waters grouped its phytoplankton into three communities: subtropical seamount phytoplankton, phytoplankton of the waters north of the ARC, and phytoplankton south of the ARC (characterised by a bloom of *Phaeocystis antarctica*). The environmental drivers most strongly linked to these differences were nitrate concentrations and water temperature. These drivers displayed a clear latitudinal gradient unaffected by mesoscale variability of the ARC eddy field and allowed the three phytoplankton communities to persist. Pollard and Read (2017) suggested that some of the ARC near the Southwest Indian Ocean Ridge is deflected towards the equator and back to the origin of the Agulhas Current.

Phytoplankton forms the base of large marine ecosystem food webs and determines energy flow to higher trophic levels such as fish, shellfish, seabirds and marine mammals. In marine ecosystems, they play an important role in primary production, biochemical cycles and the regulating of the global carbon budgets of the oceans. Phytoplankton communities are dynamic and may vary between areas, as well as within the same water body. This high variability is a result of the complex hydrological features that drives them. Barlow *et al.* (2010) remarked that the phytoplankton communities are highly adaptable to changing environmental conditions and are able to change their physiological mechanisms accordingly. How will climate change, especially the warming (Rouault *et al.*, 2009) and broadening (Beal and Elipot, 2016) of the Agulhas Current affect phytoplankton communities and primary production?

In view of this question, the objective of this snapshot observation was to study the phytoplankton community structure of the sACLME by characterising species composition and chlorophyll *a*, and to evaluate them in relation to the prevailing physico-chemical variables. The information obtained from this study would be useful in contributing to our knowledge of the phytoplankton communities that occur within the sACLME. To determine whether the waters of sACLME have an influence on its phytoplankton community structure we developed the following hypotheses:

1. The distribution of phytoplankton changes from a low biomass, chlorophyte flagellate dominated community in the oligotrophic subtropical open waters on the northern Shelf and subtropical open waters, to an elevated chlorophyll *a* biomass and diatom dominated community in the cooler mesotrophic waters of the Agulhas Bank.
2. The sACLME can be divided into four biogeographic regions based on the phytoplankton community and the environmental drivers responsible for them.
3. Species richness decreases from the oligotrophic north to the mesotrophic southern region of the sACLME.
4. The main drivers determining the composition of the phytoplankton community in the sACLME are temperature and nitrate.

7.3 Study Area

The study was based on materials collected on several oceanographic surveys that were carried out over a period of 18 months from September 2009 to March 2011. Fifty-three transects with a total of 714 oceanographic and 314 biological stations were sampled. Sampling was conducted within the framework of ACEP II (African Coelacanth Ecosystem Program Phase II) and ASCLME (Agulhas Somali Current Large Marine Ecosystems Project). The study area covered the greater Agulhas Current system from 24°S to 42°S and 18°E to 58°E. The methodology and statistical analysis used in this study was identical to that presented in sections 3.3.2, 3.3.3, 3.3.4 and 3.3.5.

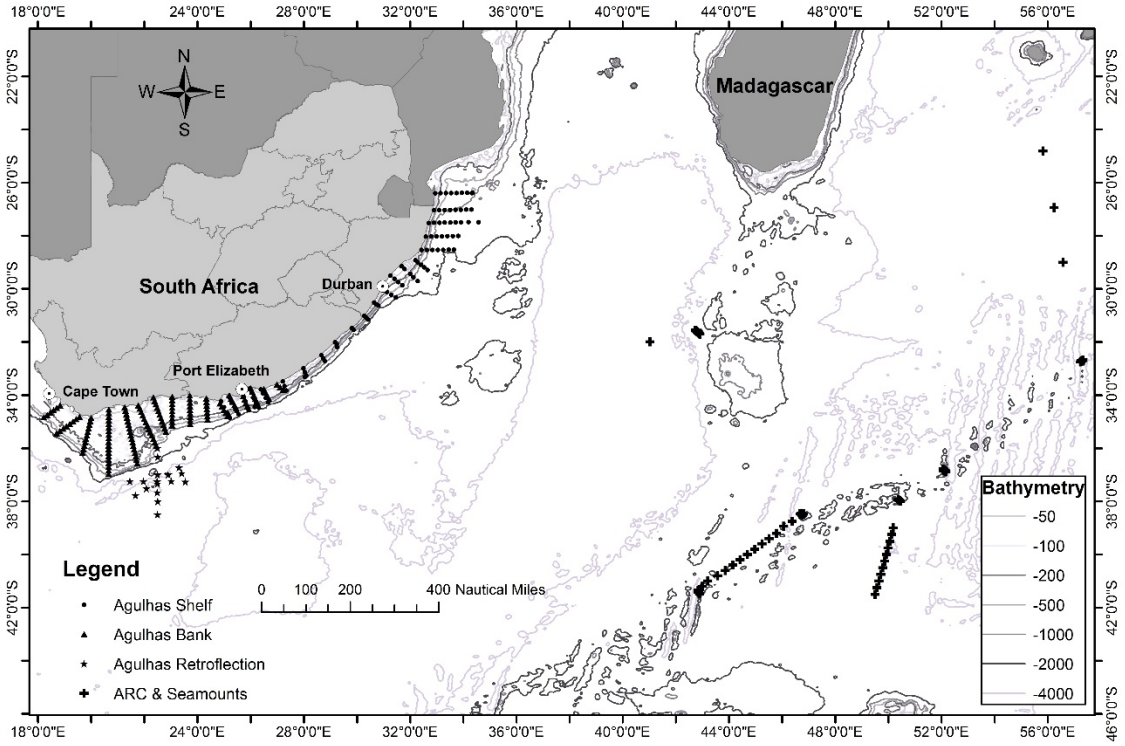

Fig. 7.1 Study site indicating the position of the environmental stations in the greater Agulhas Current system.

7.4 Statistical analyses

Main Effects Measures Analysis of Variance was used to determine significant differences among means. When a significant difference was found, a Pairwise Multiple Comparison Procedure was run to determine differences between individual means. All analyses were done using R version 3.5.0 (R Core Team, 2018) with packages *vegan* (Oksanen *et al.* 2018), *ggplot2* (Wickham *et al.* 2018) and *mvabund* (Wang et al. 2018). Detrended Correspondence Analysis (DCA) was used to identify patterns in the distribution of the species recorded at stations across the study area. CCA was used to obtain an ordination of species and stations as constrained by environmental variables. Monte Carlo permutation tests (999 unrestricted permutations; $p < 0.05$) were used to assess the significance of the relationship between the groups and selected environmental variables. Abundance and dominance were determined from the cell concentration data following the criteria proposed by Calijuri *et al.* (2002). Abundant species were those with values above the mean value of the community, and dominant species were those with values

surpassing 50% of the total number of cells counted. Species diversity and evenness indices were calculated using the *vegan* package from R (Oksanen *et al.*, 2018). A Generalized Linear Model (GLM) was also applied to further explore the relation between the environmental variables and phytoplankton abundance.

7.5 Results

7.5.1 Physical and chemical oceanographic conditions

A general comparison of the environmental features measured during the oceanographic surveys are summarised in Table 9.1 (Appendix: sACLME). Temperature varied from 21.76 ± 1.08°C for the northern Agulhas Shelf 15.74 ± 1.11°C for the western Agulhas Bank and to 10.55 ± 0.21°C for Coral Seamount, located in the Southern Ocean. Salinity exhibited an irregular pattern, with mean values lower for the subtropical convergence zone (SCZ) and Coral seamount waters. However, towards the Agulhas Retroflection, as well as in the SCZ, clear salinity gradients were observed. Surface waters of the Agulhas Bank were well oxygenated compared to the adjacent waters of the Shelf, the Retroflection and the ARC. At a depth of 10 and 20 m, the same pattern was observed but at lower concentrations. Oxygen showed a small but concomitant change with nutrients (Appendix sACLME: Table 9.1).

While nitrite concentration did not show a clear trend across the sACLME, nitrate and phosphate showed a gradient of increasing concentrations along the flow path of the Agulhas Current, peaking on the Agulhas Bank. Elevated levels of nutrients were found in regions of known upwelling throughout the sACLME. Nutrient concentrations remained relatively constant between the surface and the S/DCM but below the S/DCM, nutrient concentrations increased with depth. Silicate concentrations were relatively constant throughout the study area, but higher concentrations were found on the western Agulhas Bank as well as on the northern Agulhas Shelf.

The various correlations between the environmental variables are shown in Table 7.1. The distribution of chlorophyll *a* throughout the sACLME appears to be patchy,

and negatively correlated with temperature and nitrate and positively with oxygen. Temperature was also inversely correlated with phosphate (r = -0.45) but did not evince a relationship with chlorophyll *a*. Phosphate was also positively associated with nitrate (r = 0.56), silicate (r = 0.21) and nitrite (r = 0.19). Silicate had no significant correlation (t = -0.399; p = 0.69) with chlorophyll *a* concentration within the sACLME.

Table 7.1 Pearson correlation analysis with pairwise deletion of the environmental variables of the sACLME. Significant correlations are indicated as follows: *** p < 0.001, ** p < 0.01, * p << 0.05.

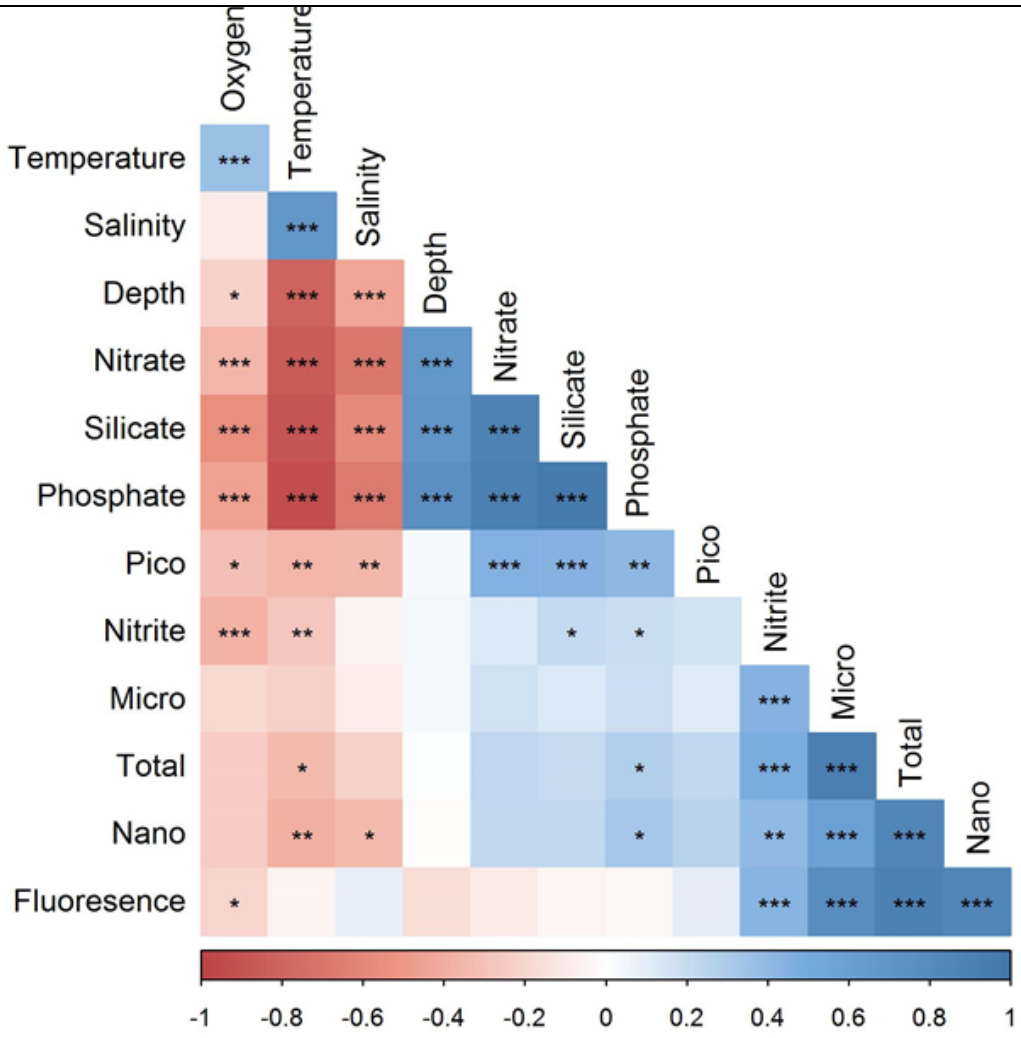

7.5.2 Spatial variability of phytoplankton

The highest chlorophyll *a* concentration was found along the coastal area of the sACLME and for the mesotrophic waters of the ARC. Chlorophyll *a* in the subtropical waters presented relative homogenous values, with values significantly lower in areas such as the Agulhas Shelf and Agulhas Bank. In general, the S/DCM for oligotrophic subtropical waters is located at greater depths when compared to the cooler mesotrophic waters of the sACLME.

Differences in size fractionated chlorophyll *a* were observed across the study area (Fig. 7.2). The northern and southern Agulhas Shelf waters had all three size classes of phytoplankton. The waters of the eastern and western Bank were dominated by microphytoplankton, due to the presence of large numbers of *Thalassiosira weissflogii.* As the Agulhas Current entered the Agulhas Retroflection Area the phytoplankton shifted towards nanophytoplankton. Along the ARC, picophytoplankton contributed little to the total chlorophyll *a*. The oligotrophic subtropical waters of the northern section of the Southwest Indian Ocean Ridge and the area around Walter's Shoal, especially the off-mount sites, were dominated by picophytoplankton.

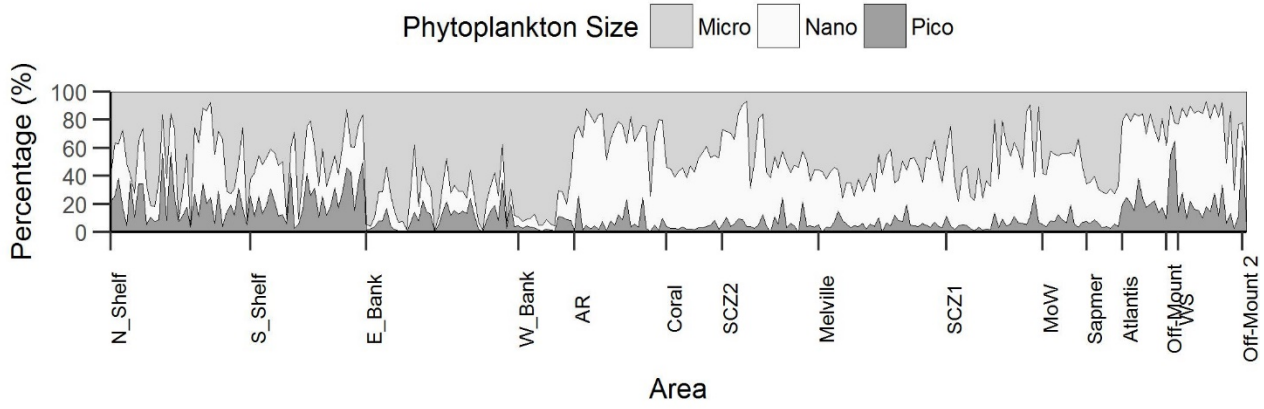

Fig. 7.2 Percentage contribution of size fractionated chlorophyll *a* to total chlorophyll *a* of the greater Agulhas Current.

7.5.3 Phytoplankton composition.

A total of 215 taxa were recorded throughout the study area, 72 of which were identified to species level. These taxa were grouped into six classes with 117 Bacillariophyceae (diatoms) and 81 Dinophyceae (dinoflagellates) taxa forming the dominant functional groups. Silicoflagellates (10), chlorophyte flagellates (4), prymnesiophytes (2) and coccolithophores (1) were also present. Only a few species were found to be numerically dominant with most species occurring at very low numbers. Three taxa contributed more than 50% of total cell counts: the pennate diatom *Pseudo-nitzschia* sp., the dinoflagellate, *Alexandrium* sp. and the centric diatom, *Thalassiosira* sp. (Fig. 7.3).

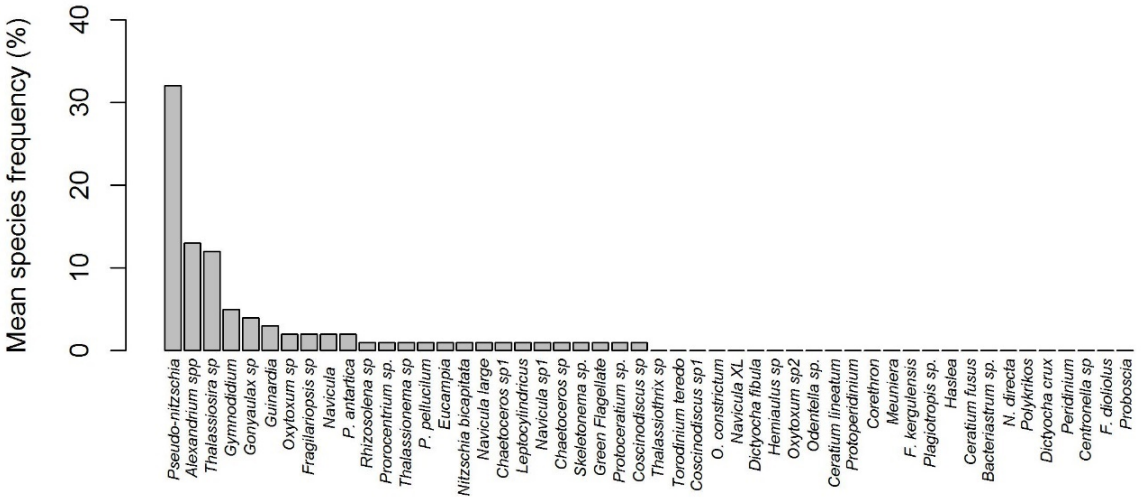

Fig. 7.3 Mean frequency (%) of the 50 most numerous species of the greater Agulhas Current.

While most taxa showed relative low abundance (<1% of total cells counted), those in the greatest abundance (Fig. 7.4) were found to be similar to the most widely distributed species (Fig. 7.5), with the first 6 taxa being identical. The highest mean relative abundances were for *Pseudo-nitzschia* sp. (32%), *Alexandrium* sp. (12%), *Thalassiosira* sp. (12%), *Gymnodinium* sp. (5%), *Gonyaulax* sp. (4%) and *Guinardia* sp. (3%). Twelve species occurred at more than 50% of the stations, with

Alexandrium sp. (98%); P*seudo-nitzschia* sp. (95%), and *Thalassiosira* sp. (95%) being the most widespread.

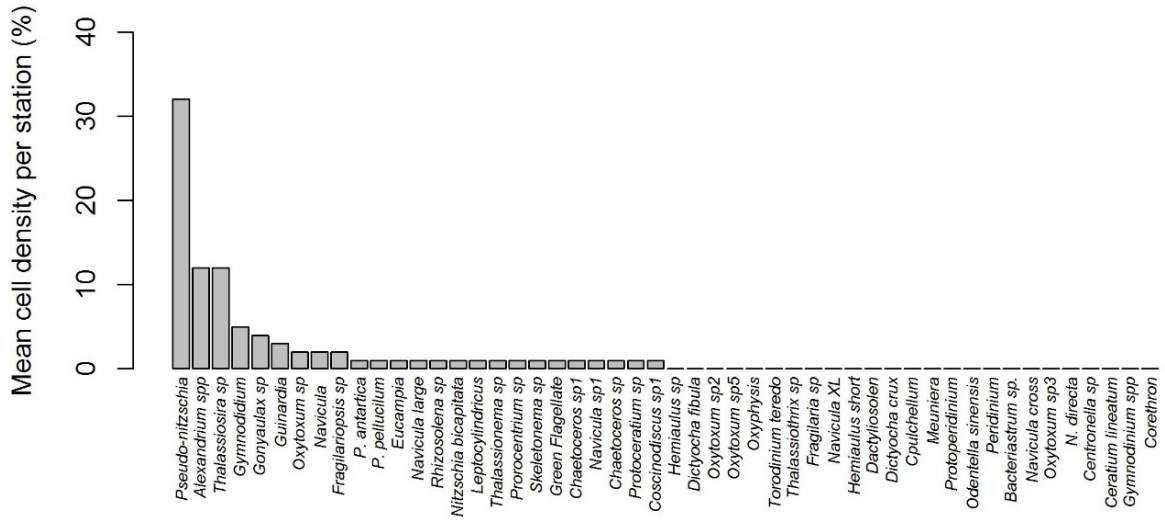

Fig. 7.4 Mean relative species contribution (%) to the phytoplankton of the 50 most numerous species of the greater Agulhas Current.

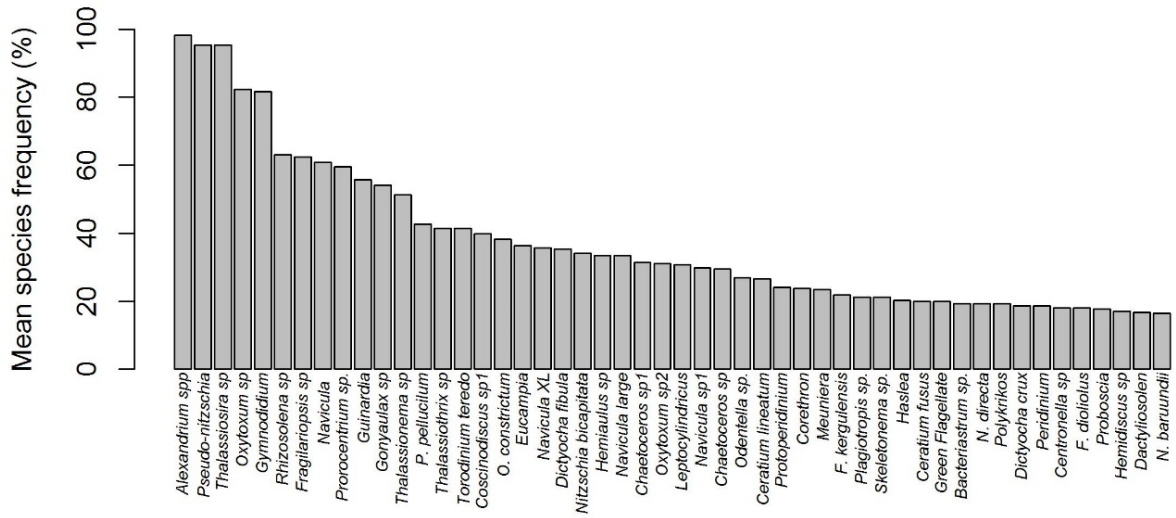

Fig. 7.5 Mean frequency of presence of the 50 most numerous species of the greater Agulhas Current.

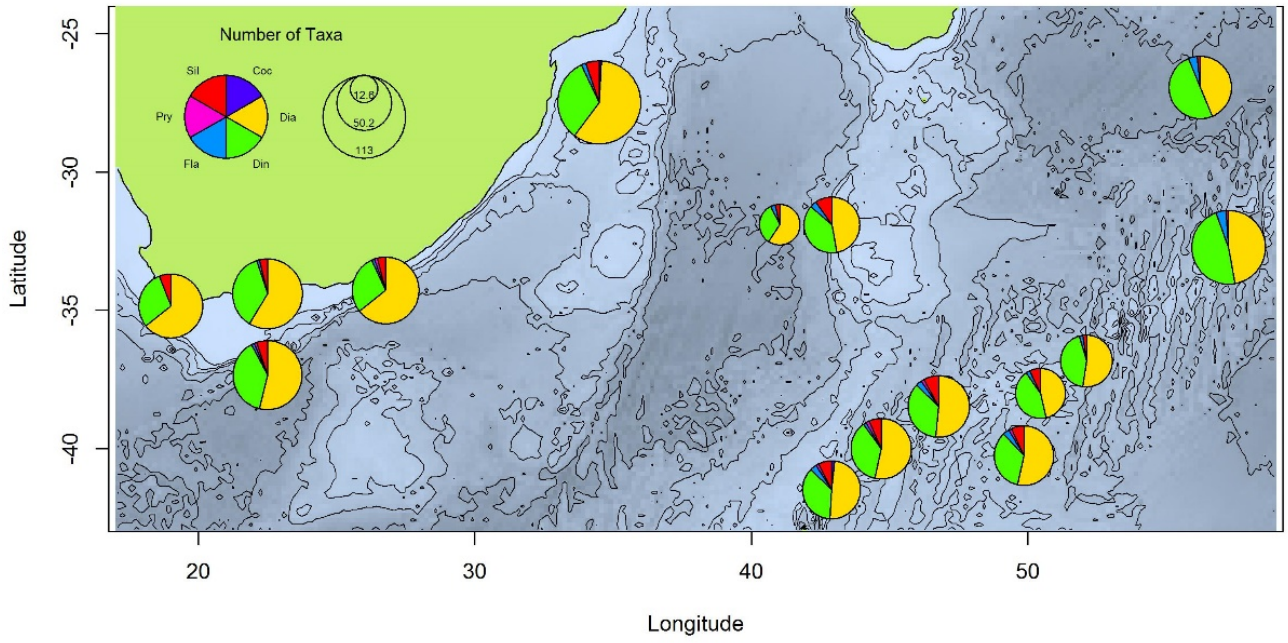

Fig. 7.6 The distribution of phytoplankton functional groups throughout the greater Agulhas Current.

Fig. 7.6 shows the distribution for the six functional groups and their contribution to the total number of phytoplankton taxa. The total number of taxa decreased southwards with the highest number of taxa observed along the northern Agulhas Shelf.

The number of taxa per station ranged between 4 (western Agulhas Bank) and 48 (northern Agulhas Shelf), with the Shannon-Weiner Index varying from 0.38 to 3.10 (Fig. 7.7). These parameters were higher and lower than the overall mean value for each (24 and 1.99 respectively). The Agulhas Current appears to be more species rich compared to the waters of the Southwest Indian Ocean Ridge, with Atlantis and the nearby Off-mount stations being the exception.

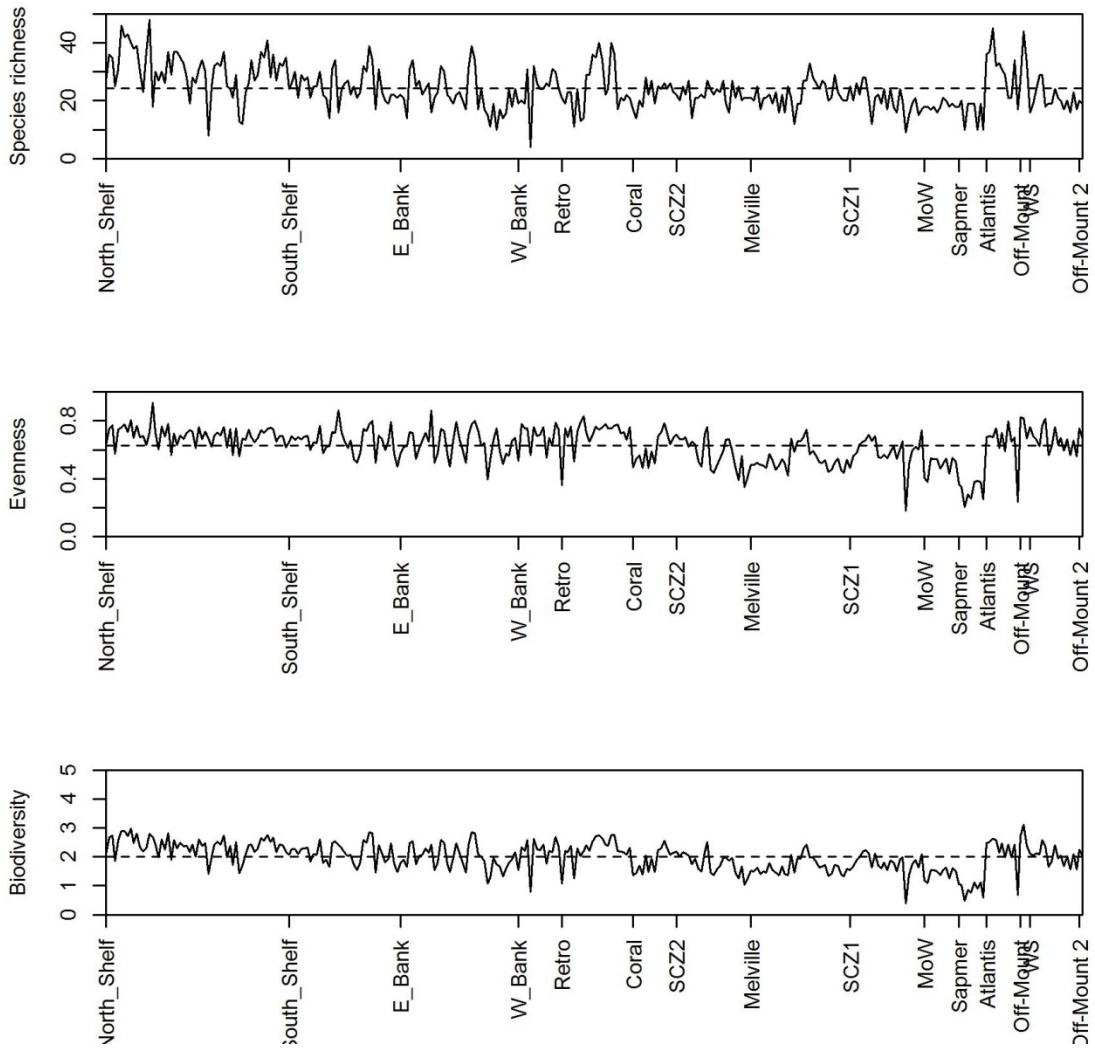

Fig. 7.7 Phytoplankton species richness (A), evenness (B) and Shannon–Wiener diversity (C) for all stations. The dashed line represents the overall mean.

Multivariate analyses grouped the 215 taxa into the following major groups (Fig. 7.8): Agulhas Current group and the Agulhas Return Current group. The Agulhas Bank, Retroflection and Shelf form smaller, overlapping communities in the Agulhas Current group.

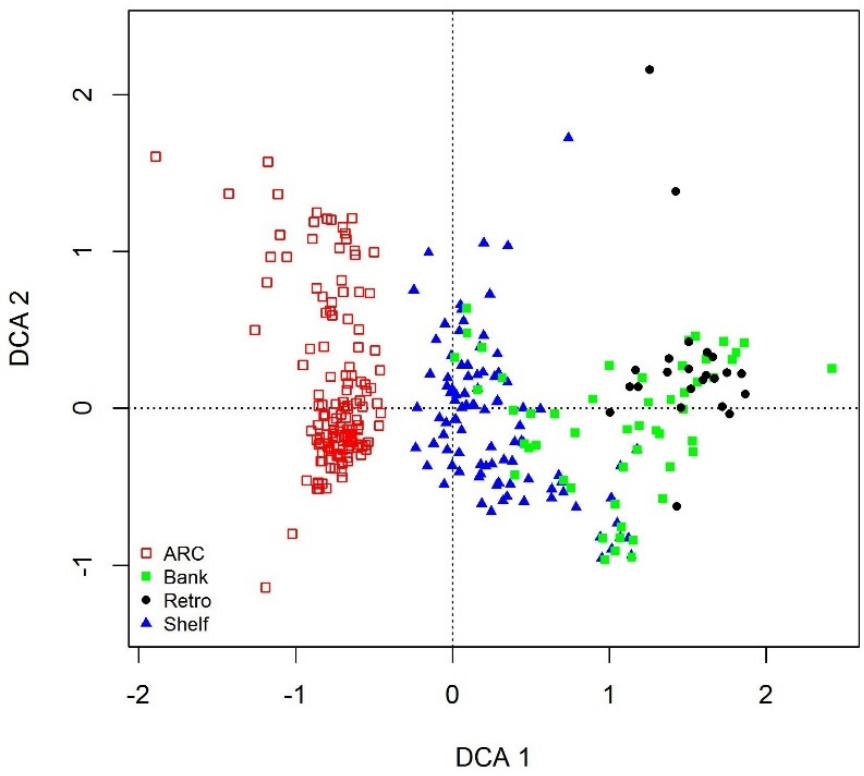

Fig. 7.8 Detrended Correspondence Analysis ordination of the samples taken across the greater Agulhas Current. The Agulhas Current samples are shown as solid symbols while the Agulhas Return Current (ARC) ones are shown as an open symbol.

7.5.4 Environmental drivers of phytoplankton variability

Statistical relationships between environmental variables and phytoplankton communities were explored using CCA (Fig. 5.17). The eigenvalues of the CCA1 was 0.24 and CCA2 was 0.07, explaining a cumulative 61% of the total variance of the species distribution. The explained variance of CCA1 was 47% and CCA2 was 14%. The Monte Carlo test confirmed the significance of the relationship model ($p < 0.01$). The first canonical axis was positively correlated to oxygen ($r = 0.78$) and nitrite ($r = 0.40$) but was negatively correlated with temperature ($r = -0.64$) and phosphate ($r = -0.20$). On the other hand, the second canonical axis had a negative relationship with nitrate ($r = -0.47$); phosphate ($r = -0.42$) and nitrite ($r = -0.14$) but

was positively correlated with temperature (*r* = 0.72) and salinity (r = 0.55). Temperature was positively correlated with salinity (r = 0.54) and temperature showed a negative correlation with nitrate (r = -0.57); phosphate (r = -0.34), nitrite (r = -0.39) and silicate (r = -0.10).

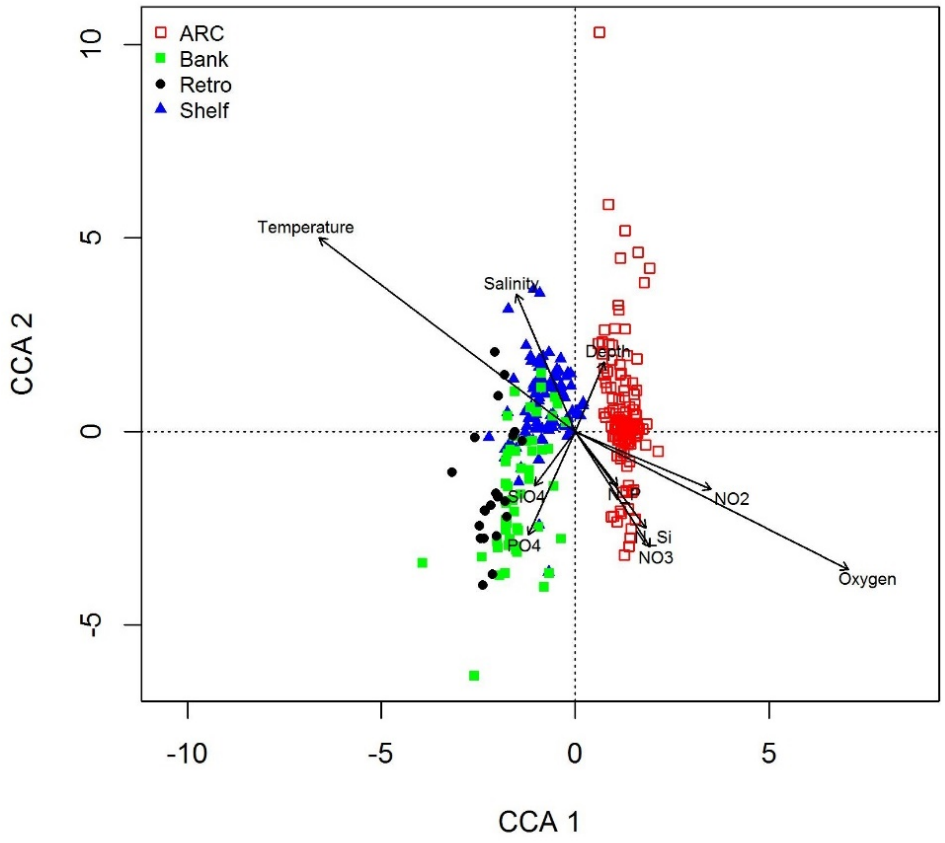

Fig. 7.9 Canonical correspondence analysis (CCA) ordination of the environmental variables measured at the sampling sites of the greater Agulhas Current. Environmental variables are temperature, salinity, concentrations of dissolved oxygen (oxygen), nitrite (NO_2^-), nitrate (NO_3^-); phosphate (PO_4^{3-}), silicate (SiO_4^{4-}) as well as the N:P ratio (N_P) and the N:Si Ratio (N_Si). Environmental variables are displayed as vectors. The Agulhas Current samples are shown as solid symbols while the Agulhas Return Current (ARC) ones are shown as an open symbol.

.

The relationships between the nutrient concentrations of the waters from the four biogeographical regions of the sACLME are illustrated in Fig. 7.10. Nutrient limitation for both the Bank and the Southwest Indian Ocean Ridge were highly variable, but less so for the Shelf and Retroflection. It is also evident from Fig. 7.10 that most of the sACLME is nitrogen limited.

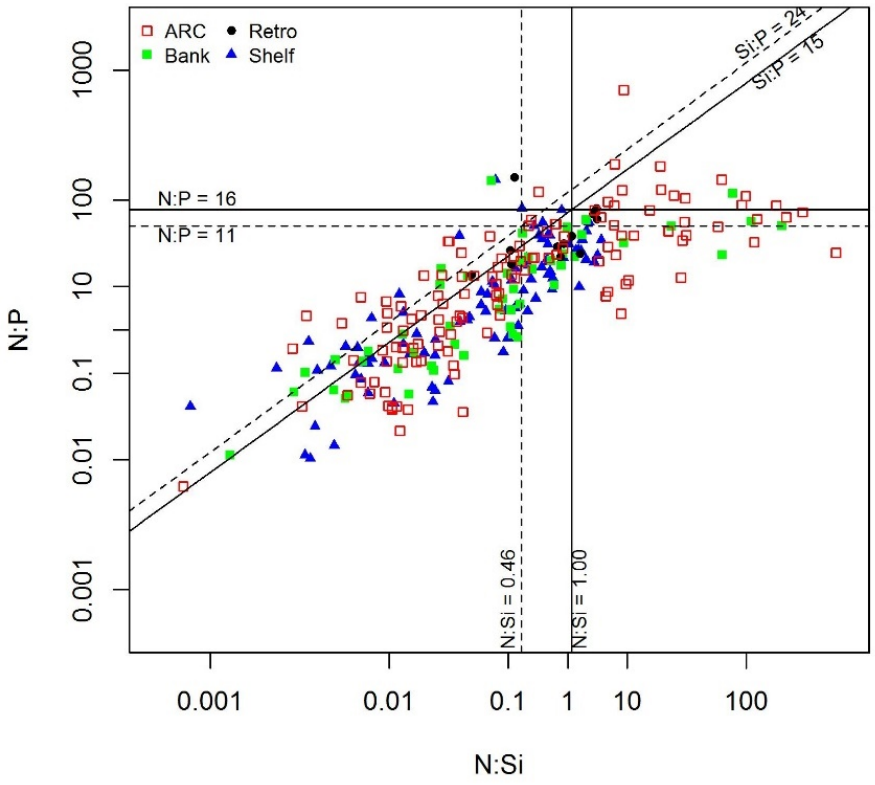

Fig. 7.10 Dissolved nutrient ratio relationships for the four major biogeographical areas of the greater Agulhas Current. Sampling sites are represented by different symbols. Solid lines indicate the Redfield ratios and dashed lines indicate the ratios following Jennings *et al.* (1984).

A generalised linear model was used to explore the environmental variables measured in the biogeographical areas. Results indicate that all the physio-chemical variables influenced the composition and distribution of phytoplankton in the

sACLME except for silicate that showed no significant influence on the distribution of the phytoplankton communities (Table 7.2).

Table 7.2 ANOVA results for the GLM model of the sACLME.

Environmental variable	Wald value	p
Intercept	18.68	0.033*
Biogeographical Area	37.55	0.031*
Temperature (°C)	27.28	0.033*
Salinity	15.68	0.032*
Oxygen (mg l^{-1})	20.80	0.033*
Nitrate (µM)	19.41	0.033*
Nitrite (µM)	20.24	0.031*
Phosphate (µM)	18.67	0.032*
Silicate (µM)	15.76	0.174
Test statistic	68.76	0.039*

Sigificance Codes: ***p < 0.001, ** p < 0.01, * p < 0.05

7.6 Discussion

7.6.1 Physical and chemical oceanography

The sACLME is comprised of the northern and southern Agulhas Shelf, the eastern and western Agulhas Bank, the Agulhas Retroflection as well as the Aguhas Return Current. The Subtropical Convergence is a frontal system that separates the sACLME from the subantarctic waters of the Southern Ocean. These two water masses differ in their biological as well as chemical and physical properties. The influence of the Agulhas Current on its immediate surroundings is well known and this is supported by the data set obtained in this study. During the eastern and western Bank survey, a Natal pulse was located off the eastern section of the

eastern Bank. Natal pulses are known to influence the dynamics, structure and biological properties of the coastal ocean (Lutjeharms, 2006; Goschen *et al.*, 2015).

Two regions of elevated nutrient concentration were observed within the sACLME: the combined region of the SCZ and the eddy field of the ARC, as well as the Agulhas Bank region. The SCZ, especially the proximity of the two frontal systems (Southern Ocean Front and STF), is known for its vertical stability and enhanced upwelling of nutrients (Read *et al.*, 2000). The leakage of nutrients across the fronts will enhance phytoplankton productivity in the immediate area, elevating chlorophyll *a* concentration. The eastern edge of the Agulhas Bank is also a known upwelling region that supplies it with nutrient-rich water, elevating phytoplankton productivity.

The geographic spread of the Agulhas Shelf, Agulhas Bank, Agulhas Retroflection and the Agulhas Return Current sampled during four oceanographic surveys between 2009 and 2011 showed significant latitudinal and longitudinal differences in temperature, salinity and dissolved oxygen of the epipelagic zone. Oxygen showed a small negtive correlation with nutrients, and this was expected since oxygen is consumed during the remineralisation of detritus and release of dissolved nutrients (Whitney *et al.*, 2013).

7.6.2 Spatial variability of phytoplankton

The distribution of chlorophyll *a* throughout the sACLME was patchy and showed significant differences between the various geographic areas. Chlorophyll *a* concentration is an important indicator of primary production and biomass (Henson *et al.*, 2010). Various authors emphasized the importance of the relationships between phytoplankton size classes and their distribution, structure and succession at both local and global scales. This in turn leads to a better understanding of how marine ecosystems function. The difference in distribution of phytoplankton size class can indicate whether the water mass is mesotrophic or oligotrophic. The former favouring the larger cell sizes of micro-and nanophytoplankton, and the latter picophytoplankton (Van de Poll *et al.*, 2013). McMurray *et al.* (1993) found that during summer and winter months, nanophytoplankton dominated over the western Agulhas Bank. During winter months, microflagellates (<15 µm) dominated the

nanophytoplankton, whereas during the summer months, diatoms, such as *Nitzschia delicatissma*, *Asterionella glacialis*, *Bacteriastrum delicatulum* and *Chaetoceros peruvianus* dominated. Froneman *et al.* (2001) reported that picophytoplankton dominated the waters of the ARC, but in our study, nano- and microphytoplankton where the main contributors to total chlorophyll *a* within the ARC. However, this study did not sample the ARC proper, which could explain the variation.

Seasonal variability can also occur within the Agulhus Current system. On the Agulhas Bank, a shift in phytoplankton size composition from a large microphytoplankton dominated community in summer to one dominated by small cells in winter has been observed (Froneman *et al.*, 1998). It is suggested that an increase in turbulence and the availability of light are contributing factors (Laubscher *et al.*, 1993).

7.6.3 Phytoplankton composition

In this study, the results showed a steady change in species richness along the "flow" of the greater Agulhas Current. As was expected, species richness decreased in regions of high productivity. The phytoplankton community also showed an increase in diversity with an increase in longitude. There was a concomitant change in dominance from diatoms to dinoflagellates (Fig. 5). The other taxa made a substantially smaller contribution to the phytoplankton throughout the region. Species diversity tends to decline towards the poles (Gaston, 2000) and this was also evident for the sACLME. The structure of the phytoplankton community was consistent throughout the sACLME. Hanson *et al.* (2007) made a similar observation for the Leeuwin Current off the Australian west coast. Another change in the structure of the phytoplankton community was the introduction of subantarctic species, such as *Phaeocystis antarctica*, across the subtropical convergence front into the ARC.

Gaines and Elabrachter (1987) and Taylor *et al.* (2008) suggested that approximately half of all dinoflagellate species are exclusively heterotrophic. Genera such as *Protoperidinium* sp., *Gymnodinium* sp., *Oxytoxum* sp., were common in the phytoplankton, similar to the findings from northern Australian waters (Hallegraeff

and Jeffrey, 1984) and the Leeuwin Current (Hanson *et al.*, 2007b). Hanson *et al.* (2007b) suggested that the presence of these heterotrophs is due to the abundance of pico- and nanophytoplankton as a food source for them.

Diatoms prefer new nitrogen and will therefore thrive in regions where upwelling occurs (Margalef, 1978; Furnas, 1990). The relatively large dinophysoids (*Dinophysis* spp.) were also recorded within the sACLME, where they preferred oligotrophic offshore and coastal waters. Three genera of silicoflagellates (Dictyochophyceae) were recorded: *Dictyocha* (six species), *Mesocena* (two species) and *Octactis* (one species). Silicoflagellates are good indicators for past and present changes within the water column due to their responsiveness to environmental signals that is retained within their skeletal remains (Takahashi, 1989). They are considered to be the most useful in describing productivity and sinking rates of siliceous phytoplankton (Pisias *et al.*, 1986). Takahashi (1989) found that species specific ratios of silicoflagellates are better productivity indicators than temperature and can show small but significant changes to the immediate environment. Silicoflagellates can also be used to indicate specific water masses (Takahashi and Blackwelder, 1992). Using a ratio of warm- to cold-water species it is possible to determine the origin of past and present water masses within the sACLME. It appears that silicoflagellates do not correlate to nutrient concentrations (Takahashi and Blackwelder, 1992), whereas diatoms do (Margalef, 1978; Furnas, 1990). For this reason, silicoflagellates are useful indictors of specific water bodies and can be used to predict past and present changes within the ARC.

The DCA (Fig. 7.8) displayed two distinct groups of phytoplankton communities, the Agulhas Current and Southwest Indian Ocean Ridge groups, but these partially overlap. As the Agulhas Current follows its course the Agulhas Current Group transitions into the Southwest Indian Ocean Group and this is evident throughout the SWIO with similar transitions within the Agulhas Current and SWIO Groups. “Transitions zones” are based on water temperature and the availability of nutrients. These transitions zone are normally associated with areas of upwelling and distinct oceanographic features such as fronts, etc. Changes in the strength and characteristics of the Agulhas Current will favour certain species above others.

7.6.4 Environmental drivers of phytoplankton variability

The CCA ordination yielded two main phytoplankton groups (Fig. 5.17), an Agulhas Current group and a Southwest Indian Ocean Ridge group. The Agulhas Current group consisted of three smaller groups: the Agulhas Shelf, the Agulhas Bank and the Agulhas Retroflection. The Southwest Indian Ocean Ridge group consisted of a more Subtropical Open Ocean group and an Agulhas Return Current group. The Agulhas Current group and Southwest Indian Ocean Ridge group are clearly divided by the Agulhas Current losing its characteristics (Lutjeharms and Ansorge, 2001).

Temperature is also important in regulating cellular processes within phytoplankton, which, in turn, has implications for co-limitation. Thus, temperature often works with or against other environmental variables. An elevation in temperature can shift a diatom dominated community to a nanophytoplankton dominated community (Hare *et al.*, 2007). This change can have severe consequences for the export of carbon to the deep ocean waters, with the smaller and less rapidly sinking nanophytoplankton species sequestering less carbon (Hare *et al.*, 2007).

At adequate light and temperature levels, phytoplankton growth can become limited by the availability of nutrients (Hecky and Kilham, 1988). Nutrients showed varied distribution throughout the sACLME. Nitrate was the most abundant source of nitrogen, especially in regions that were subject to the upwelling of cold nutrient-rich water, e.g. the SCZ (Read *et al.*, 2000), the eastern Agulhas Bank ((Lutjeharms *et al.*, 1996) and the western Agulhas Bank (Largier *et al.*, 1992). Phytoplankton communities are strongly influenced by the availability and the stoichiometry of the macronutrients of nitrogen, phosphorus and silicon. Redfield (1958) showed that phytoplankton take up nutrients from the water in a fixed ratio of C:N:P:Si of 106:16:1:15. Jennings *et al.* (1984) proposed a C:N:P:Si ratio of 62:11:1:24 for the Southern Ocean. Nutrient limitation and N:P ratio play an important role in determining the structure of phytoplankton communities and these variables vary considerably between regions (Read *et al.*, 2000; Lagus *et al.*, 2004; Brauer *et al.*, 2012). The low mean ratio of N:P of 5.51 is an indication that the sACLME is mainly nitrogen limited - this is typical of marine systems (Hecky and Kilham, 1988). Coral Seamount (31.74), Cape Recife (16.1) and Cape St Francis (16.45) were the only regions showing an excess of nitrogen. The Off-mount 2 and SCZ 1 were the only

areas near the N:P ratio of 11 (Appendix: 9.3 sACLME; Table 9.1) as suggested by Jennings et al. (1984) and a N:Si ratio of 1 and 0.45 as suggested by Redfield (1958) and Jennings et al. (1984). Regions of high N:Si corresponds well to the regions of higher chlorophyll a concentration, where nanophytoplankton was the major contributor to total chlorophyll a. A decline in Si:P ratios may cause a possible shift in the assemblage of the phytoplankton community towards a non-diatom community (Smayda, 1990) and a non-silicoflagellate community.

Diatoms and dinoflagellates are the most abundant functional groups of marine phytoplankton (Carter *et al.*, 2005) and this was also found to be true in the sACLME, where the dominance shifted from a dinoflagellate abundant assemblage in the east to a diatom abundant assemblage in the west (Fig. 7.6). Diatoms tend to prefer regions with high levels of nutrients, especially upwelling regions, that can support their rapid growth (Furnas, 1990) and provide vertical mixing to maintain their position in the euphotic zone (Smayda, 1970; Margalef, 1978). It was also evident from this study, e.g. southern Agulhas Current and Eastern Agulhas bank, that diatoms prefer regions where vertical mixing and upwelling occurs. Dinoflagellates on the other hand prefer more stratified waters where they can exploit the underlying nutrient-rich waters as well as the euphotic zone above (Margalef, 1978; Cullen, 1982). Small sized phytoplankton have a higher nutrient uptake efficiency and a greater surface area to volume ratio than their larger counterparts and can therefore exploit a nutrient-limited environment better. The significant correlation of nanophytoplankton to both the N:P ($r = 0.27$; $p < 0.01$) and N:Si ($r = 0.15$; $p < 0.01$) ratios showed that nanophytoplankton was able to better exploit the N-limitation within the sACLME. Picophytoplankton were found in low abundance throughout the sACLME, but this could be more of an artefact of using a 0.7 µm Whatman GFF filter and not a smaller 0.2 µm filter.

To assess phytoplankton communities and their ecological dynamics within marine food webs, understanding the spatial and temporal variability of phytoplankton is important. One dynamic of phytoplankton variability and an important driver in phytoplankton blooms is the mixed layer depth (Behrenfeld and Boss, 2014; Carvalho *et al.*, 2017). Behrenfeld and Boss (2014) refer to the various processes and limitations that may or may not enhance the formation of phytoplankton blooms

and drive species succession. These processes may change the understanding phytoplankton dynamics along the Agulhus System but will be better applied to study smaller and more specific regions within the Agulhas System.

The warming of the Agulhas Current (Rouault *et al.*, 2009) and the ACLME (Belkin (2009) through climate and global change will lead to a change in phytoplankton communities (Morán *et al.*, 2010) and productivity (O'Connor *et al.*, 2009; Boyce *et al.*, 2010; Thomas *et al.*, 2012). It is estimated that marine phytoplankton are responsible for ~ 50% of global primary productivity (Field *et al.*, 1998) and they have important roles in biogeochemical cycles and regulating the global carbon budgets in the world's oceans (Redfield, 1958; Falkowski *et al.*, 1998; Boyce *et al.*, 2010; Thomas *et al.*, 2012). Another consequence of ocean warming is an increase in metabolic rates of zoo- and phytoplankton. Phytoplankton biomass will decrease under increasing grazing pressure as heterotrophs and autotrophs respond differently due to their sensitivity to temperature (O'Connor *et al.*, 2009). The warming (Rouault *et al.*, 2009) and broadening (Beal and Elipot, 2016) of the Agulhas Current will have an impact on the phytoplankton communities within the sACLME. In its subtropical regions, the rise in ocean temperature will interrupt the supply of nutrients to the surface waters as a direct consequence of increased ocean stratification (Bopp *et al.*, 2005; Doney, 2006; Thomas *et al.*, 2012). On the other hand, the broadening of the Agulhas Current can lead to enhanced upwelling over the continental shelf (Beal and Elipot, 2016). An increase in upwelling frequency and strength will alter nutrient concentrations and ratios and is already been observed for the California Current System (Bograd *et al.*, 2015; Xiu *et al.*, 2018). An increase in frequency and strength of upwelling events will favour diatoms over the other functional groups (Anderson *et al.*, 2008). If this shift is in favour of the already dominant *Pseudo-nitzschia*, a neurotoxin (domoic acid) producing diatom, it can have devastating effects on the food web and can alter the abundance and community structure of zooplankton and ichthyoplankton. An increase in domoic acid production was observed under silicate or phosphate limitation for uni-algal batch cultures (Fehling *et al.*, 2004). Within the Santa Barbara Basin *Pseudo-nitzschia* blooms were linked to low Si:P and N:Si ratios (Anderson *et al.*, 2006; Anderson *et al.*, 2011). Altered biogeochemistry of upwelled source waters for the sACLME will

impact phytoplankton composition as well as the intensity and frequency of toxic *Pseudo-nitzschia* blooms. Regions of the Agulhas Shelf, Agulhas Bank and the ARC will be vulnerable to this. Frequent but weaker upwelling events along the coastal region of the sACLME accompanied by increase in temperature will favour dinoflagellates and harmful algal species, such as the subtropical dinoflagellate, *Lingulodinium polyedra* (F.Stein) J.D.Dodge (Whitfield *et al.*, 2016).

There will also be a progressive loss of phytoplankton biodiversity, up to one third of tropical species (Thomas *et al.*, 2012), with increasing water temperature and nutrient supply. If one third of the phytoplankton species is lost within the sACLME, ecosystem resilience as well as ecosystems services and functions will be impacted. The shift of tropical species southwards (Thomas *et al.*, 2012) within the sACLME could potentially bring non-blooming, “dormant” taxa into more favourable environmental conditions (e.g. elevated nutrients). This could result in massive algal blooms, species becoming invasive (Whitfield *et al.*, 2016) and negative socio-economic impacts for all the countries associated with the ACLME.

7.7 Conclusions

Clear latitudinal and longitudinal differences were evident for all the variables measured during the various cruises despite the high variability associated with mesoscale eddies and the Agulhas Current. The null hypothesis that the distribution of phytoplankton changes from a low, chlorophyte flagellate dominant community in the oligotrophic subtropical open waters of the east, to an elevated chlorophyll *a* biomass and diatom dominance in the cooler mesotrophic waters for the Agulhas Bank, could not be completely rejected. The oligotrophic subtropical open waters of the eastern sACLME and northern Agulhas Shelf had lower biomass, but consisted of a community largely made up of dinoflagellates and diatoms. Very few chlorophyte flagellates were recorded throughout the sACLME, which may be ascribed to the preservation method used. The Agulhas Bank, however, showed elevated levels of chlorophyll *a* and a phytoplankton community dominated by diatoms.

This study further demonstrates, albeit indirectly, that temperature forms an obvious environmental gradient that controls species distribution within the sACLME. The

ordination analysis provided a good understanding of the distribution of the various phytoplankton communities and the homogeneity, or in some instances, similarity, between communities. One major goal in biological oceanography is to mechanistically predict current and future phytoplankton distributions and rates of change and this study forms a baseline to compare with future changes. This study also contributed to our understanding of phytoplankton dynamics on a geographical scale. However, more studies are needed within the sACLME to address the forcing dynamics of water mass modifications, their impact on the transformation of upwelled water masses, and their effects on regional as well as large marine ecosystem processes. This study, however, only provided a snapshot and so could not resolve a number of processes that have timescales of longer than a day.

7.8 Future Research

The sampling was primarily conducted during spring and summer and it will therefore be advantageous to investigate the phytoplankton dynamics during autumn and winter to see how winter storms, shorter days and different oceanographic conditions (such as a stronger inshore counter current), will influence the phytoplankton community. As this study was only a snapshot of the phytoplankton community, long term monitoring of reference stations along the coast will be advantageous as to obtain a more detailed picture of the environmental drivers and their influence on the phytoplankton community. This in turn will also allow observation of specific changes in the phytoplankton community with regards to climate change.

8 References

Alves-de-Souza, C., Gonzalez, M.T., Iriarte, J.L., 2008. Functional groups in marine phytoplankton assemblages dominated by diatoms in fjords of southern Chile. Journal of Plankton Research 30, 1233-1243.

Anderson, C.R., Brzezinski, M.A., Washburn, L., Kudela, R., 2006. Circulation and environmental conditions during a toxigenic Pseudo-nitzschia australis bloom in the Santa Barbara Channel, California. Marine Ecology Progress Series 327, 119-133.

Anderson, C.R., Kudela, R.M., Benitez-Nelson, C., Sekula-Wood, E., Burrell, C.T., Chao, Y., Langlois, G., Goodman, J., Siegel, D.A., 2011. Detecting toxic diatom blooms from ocean color and a regional ocean model. Geophysical Research Letters 38, L04603.

Anderson, C.R., Siegel, D.A., Brzezinski, M.A., Guillocheau, N., 2008. Controls on temporal patterns in phytoplankton community structure in the Santa Barbara Channel, California. Journal of Geophysical Research: Oceans 113, C04038.

Anderson, G.C., 1969. Subsurface Chlorophyll Maximum in the Northeast Pacific Ocean. Limnology and Oceanography 14, 386-391.

Anderson, G.C., Parsons, T.R., Stephens, K., 1969. Nitrate distribution in the subarctic Northeast Pacific Ocean. Deep Sea Research and Oceanographic Abstracts 16, 329-334.

Anderson, L.A., Sarmiento, J.L., 1994. Redfield ratios of remineralization determined by nutrient data analysis. Global Biogeochemical Cycles 8, 65-80.

Arístegui, J., Mendonça, A., Vilas, J.C., Espino, M., Polo, I., Montero, M.F., Martins, A., 2009. Plankton metabolic balance at two North Atlantic seamounts. Deep Sea Research Part II: Topical Studies in Oceanography 56, 2646-2655.

Arrigo, K.R., Robinson, D.H., Worthen, D.L., Dunbar, R.B., DiTullio, G.R., VanWoert, M., Lizotte, M.P., 1999. Phytoplankton community structure and the drawdown of nutrients and CO2 in the Southern Ocean. Science 283, 365.

Baines, P.G., 2007. Internal tide generation by seamounts. Deep Sea Research Part I: Oceanographic Research Papers 54, 1486-1508.

Bang, N.D., 1970. Dynamic interpretations of a detailed surface temperature chart of the Agulhas Current retroflexion and fragmentation area. South African Geographical Journal 52, 67 - 76.

Banse, K., 1987. Clouds, deep chlorophyll maxima and the nutrient supply to the mixed layer of stratified water bodies. Journal of Plankton Research 9, 1031-1036.

Barlow, R., Kyewalyanga, M., Sessions, H., van den Berg, M., Morris, T., 2008. Phytoplankton pigments, functional types, and absorption properties in the Delagoa and Natal Bights of the Agulhas ecosystem. Estuarine, Coastal and Shelf Science 80, 201-211.

Barlow, R., Lamont, T., Kyewalyanga, M., Sessions, H., Morris, T., 2010. Phytoplankton production and physiological adaptation on the southeastern shelf of the Agulhas ecosystem. Continental Shelf Research 30, 1472-1486.

Barlow, R., Lamont, T., Morris, T., Sessions, H., van den Berg, M., 2014. Adaptation of phytoplankton communities to mesoscale eddies in the Mozambique Channel. Deep Sea Research Part II: Topical Studies in Oceanography 100, 106-118.

Barlow, R.G., Aiken, J., Holligan, P.M., Cummings, D.G., Maritorena, S., Hooker, S., 2002. Phytoplankton pigment and absorption characteristics along meridional transects in the Atlantic Ocean. Deep Sea Research Part I: Oceanographic Research Papers 49, 637-660.

Barlow, R.G., Aiken, J., Moore, G.F., Holligan, P.M., Lavender, S., 2004. Pigment adaptations in surface phytoplankton along the eastern boundary of the Atlantic Ocean. Marine Ecology Progress Series 281, 13-26.

Bathmann, U., Priddle, J., Treguer, P., Lucas, M., Hall, J., Parslow, J., 2000. Plankton ecology and biogeochemistry in the Southern Ocean: A review of the Southern Ocean JGOFS, in: Hanson, R.B., Ducklow, H.W., Field, J.G. (Eds.), The changing ocean carbon cycle : a midterm synthesis of the Joint Global Ocean Flux Study Cambridge University Press, New York, pp. 300-337.

Bathmann, U., Scharek, R., Klaas, C., Dubischar, C., Smetacek, V., 1997. Spring development of phytoplankton biomass and composition in major water masses of the Atlantic sector of the Southern Ocean. Deep Sea Research Part II: Topical Studies in Oceanography 44, 51-67.

Batiza, R., 1982. Abundances, distribution and sizes of volcanoes in the Pacific Ocean and implications for the origin of non-hotspot volcanoes. Earth and Planetary Science Letters 60, 195-206.

Beal, L.M., 2009. A Time Series of Agulhas Undercurrent Transport. Journal of Physical Oceanography 39, 2436-2450.

Beal, L.M., Bryden, H.L., 1999. The velocity and vorticity structure of the Agulhas Current at 32°S. Journal of Geophysical Research 104, 5151-5176.

Beal, L.M., De Ruijter, W.P.M., Biastoch, A., Zahn, R., 2011. On the role of the Agulhas system in ocean circulation and climate. Nature 472, 429-436.

Beal, L.M., Elipot, S., 2016. Broadening not strengthening of the Agulhas Current since the early 1990s. Nature 540, 570.

Beckley, L.E., 1998. The Agulhas Current Ecosystem with particular reference to dispersal of fish larvae, in: Sherman, K., Okemwa, E.N., Ntiba, M.J. (Eds.), Large Marine Ecosystems of the Indian Ocean: Assessment, sustainability, and management. Blackwell Science, Inc., Malden, p. 394.

Beckmann, A., 1995. Numerical modeling of timemean flow at isolated seamounts, in: Müller, P., Henderson, D. (Eds.), Topographic Effects in the Ocean., Honolulu, HI, pp. 57-66.

Beckmann, A., Mohn, C., 2002. The upper ocean circulation at Great Meteor Seamount. Ocean Dynamics 52, 194-204.

Behrenfeld, M.J., Boss, E.S., 2014. Resurrecting the Ecological Underpinnings of Ocean Plankton Blooms. Annual Review of Marine Science 6, 167-194.

Behrenfeld, M.J., Falkowski, P.G., 1997. A consumer's guide to phytoplankton primary productivity models. Limnology and Oceanography 42, 1479-1491.

Belkin, I.M., 2009. Rapid warming of Large Marine Ecosystems. Progress In Oceanography 81, 207-213.

Belkin, I.M., Cornillon, P.C., Sherman, K., 2009. Fronts in Large Marine Ecosystems. Progress In Oceanography 81, 223-236.

Belkin, I.M., Gordon, A.L., 1996. Southern Ocean fronts from the Greenwich meridian to Tasmania. Journal of Geophysical Research 101, 3675-3696.

Benitez-Nelson, C.R., Bidigare, R.R., Dickey, T.D., Landry, M.R., Leonard, C.L., Brown, S.L., Nencioli, F., Rii, Y.M., Maiti, K., Becker, J.W., Bibby, T.S., Black, W., Cai, W.-J., Carlson, C.A., Chen, F., Kuwahara, V.S., Mahaffey, C.,

McAndrew, P.M., Quay, P.D., Rappé, M.S., Selph, K.E., Simmons, M.P., Yang, E.J., 2007. Mesoscale Eddies Drive Increased Silica Export in the Subtropical Pacific Ocean. Science 316, 1017-1021.

Bibby, T.S., Moore, C.M., 2011. Silicate:nitrate ratios of upwelled waters control the phytoplankton community sustained by mesoscale eddies in sub-tropical North Atlantic and Pacific. Biogeosciences 8, 657-666.

Blain, S., Quéguiner, B., Armand, L., Belviso, S., Bombled, B., Bopp, L., Bowie, A., Brunet, C., Brussaard, C., Carlotti, F., Christaki, U., Corbière, A., Durand, I., Ebersbach, F., Fuda, J.-L., Garcia, N., Gerringa, L., Griffiths, B., Guigue, C., Wagener, T., 2007. Effect of natural iron fertilization on carbon sequestration in the Southern Ocean.

Blank, G.S., Robinson, D.H., Sullivan, C.W., 1986. Diatom mineralization of silicic acid. VIII. Metabolic requirements and the timing of protein synthesis. Journal of Phycology 22, 382-389.

Boden, B.P., Duncombe Rae, C.M., Lutjeharms, J.R.E., 1988. The distribution of diatoms of the south-west Indian Ocean surface waters between Cape Town and the Prince Edward Islands archipelago. South African Journal of Science 84, 811-818.

Boebel, O., Rossby, T., Lutjeharms, J., Zenk, W., Barron, C., 2003. Path and variability of the Agulhas Return Current. Deep Sea Research Part II: Topical Studies in Oceanography 50, 35-56.

Boehlert, G.W., Genin, A., 1987. A Review of the effects of seamounts on biological processes, in: Keating, B.H., Fryer, P., Batiza, R., Boehlert, G.W. (Eds.), Seamounts, Islands, and Atolls, pp. 319-334.

Bograd, S.J., Buil, M.P., Lorenzo, E.D., Castro, C.G., Schroeder, I.D., Goericke, R., Anderson, C.R., Benitez-Nelson, C., Whitney, F.A., 2015. Changes in source waters to the Southern California Bight. Deep Sea Research Part II: Topical Studies in Oceanography 112, 42-52.

Bollmann, J., Cortés, M.Y., Haidar, A.T., Brabec, B., Close, A., Hofmann, R., Palma, S., Tupas, L., Thierstein, H.R., 2002. Techniques for quantitative analyses of calcareous marine phytoplankton. Marine Micropaleontology 44, 163-185.

Bopp, L., Aumont, O., Cadule, P., Alvain, S., Gehlen, M., 2005. Response of diatoms distribution to global warming and potential implications: A global model study. Geophysical Research Letters 32.

Bouman, H., Platt, T., Sathyendranath, S., Stuart, V., 2005. Dependence of light-saturated photosynthesis on temperature and community structure. Deep Sea Research Part I: Oceanographic Research Papers 52, 1284-1299.

Bouman, H.A., Platt, T., Sathyendranath, S., Li, W.K.W., Stuart, V., Fuentes-Yaco, C., Maass, H., Horne, E.P.W., Ulloa, O., Lutz, V., Kyewalyanga, M., 2003. Temperature as indicator of optical properties and community structure of marine phytoplankton: implications for remote sensing. Marine Ecology Progress Series 258, 19-30.

Boyce, D.G., Lewis, M.R., Worm, B., 2010. Global phytoplankton decline over the past century. Nature 466, 591.

Bracher, A., Kroon, B.M.A., Lucas, M.I., 1999. Primary production, physiological state and composition of phytoplankton in the Atlantic sector ot the Southern Ocean. Marine Ecology Progress Series 190, 1-16.

Brauer, V., Stomp, M., Huisman, J., 2012. The nutrient-load hypothesis: patterns of resource limitation and community structure driven by competition for nutrients and light. The American Naturalist 179, 721-740.

Brink, K.H., 1983. The near-surface dynamics of coastal upwelling. Progress In Oceanography 12, 223-257.

Brink, K.H., 1995. Tidal and lower frequency currents above Fieberling Guyot. Journal of Geophysical Research 100, 10817-10832.

Brown, Z.W., Lowry, K.E., Palmer, M.A., van Dijken, G.L., Mills, M.M., Pickart, R.S., Arrigo, K.R., 2015. Characterizing the subsurface chlorophyll a maximum in the Chukchi Sea and Canada Basin. Deep Sea Research Part II: Topical Studies in Oceanography 118, 88-104.

Bryden, H., Beal, L., Duncan, L., 2005. Structure and transport of the Agulhas Current and its temporal variability. Journal of Oceanography 61, 479-492.

Brzezinski, M.A., 1985. The Si:C:N ratio of marine diatoms: Interspecific variability and the effect of some environmental variables. Journal of Phycology 21, 347-357.

Brzezinski, M.A., 1992. Cell-cycle effects on the kinetics of silicic acid uptake and resource competition among diatoms. Journal of Plankton Research 14, 1511-1539.

Brzezinski, M.A., Nelson, D.M., 1989. Seasonal changes in the silicon cycle with a Gulf Stream warm-core ring Deep Sea Research 36, 1009 - 1030.

Brzezinski, M.A., Olson, R.J., Chisholm, S.W., 1990. Silicon availability and cell-cycle progression in marine diatoms. Marine Ecology Progress Series 67, 83 - 96.

Buitenhuis, E.T., Li, W.K.W., Vaulot, D., Lomas, M.W., Landry, M.R., Partensky, F., Karl, D.M., Ulloa, O., Campbell, L., Jacquet, S., Lantoine, F., Chavez, F., Macias, D., Gosselin, M., McManus, G.B., 2012. Picophytoplankton biomass distribution in the global ocean. Earth System Science Data 4, 37-46.

Burchall, J., 1968a. An evaluation of primary productivity studies in the continental shelf region of the Agulhas current near Durban(1961–1966), Investigational Report. Oceanographic Research Institute, Durban, p. 44.

Burchall, J., 1968b. Primary production studies in the Agulhas current region off Natal-June 1965, Investigational Report,20. Oceanographic Research Institute, Durban, p. 16.

Button, D.K., 1985. Kinetics of nutrient-limited transport and microbial growth. Microbiological reviews 49, 270-297.

Calijuri, M.C., Dos Santos, A.C.A., Jati, S., 2002. Temporal changes in the phytoplankton community structure in a tropical and eutrophic reservoir (Barra Bonita, S.P.—Brazil). Journal of Plankton Research 24, 617-634.

Canale, R.P., Vogel, A.H., 1974. Effects of temperature on phytoplankton growth. Journal Environmental Engineering 100, 231-241.

Cardinale, B.J., Duffy, J.E., Gonzalez, A., Hooper, D.U., Perrings, C., Venail, P., Narwani, A., Mace, G.M., Tilman, D., Wardle, D.A., Kinzig, A.P., Daily, G.C., Loreau, M., Grace, J.B., Larigauderie, A., Srivastava, D.S., Naeem, S., 2012. Biodiversity loss and its impact on humanity. Nature 486, 59.

Cardinale, B.J., Matulich, K.L., Hooper, D.U., Byrnes, J.E., Duffy, E., Gamfeldt, L., Balvanera, P., O'Connor, M.I., Gonzalez, A., 2011. The functional role of producer diversity in ecosystems. American Journal of Botany 98, 572-592.

Carmo, V., Santos, M., Menezes, G.M., Loureiro, C.M., Lambardi, P., Martins, A., 2013. Variability of zooplankton communities at Condor seamount and surrounding areas, Azores (NE Atlantic). Deep Sea Research Part II: Topical Studies in Oceanography 98, 63-74.

Carrett, C., 2003. Internal tides and ocean mixing. Science 301, 1858-1859.

Carter, C.M., Ross, A.H., Schiel, D.R., Howard-Williams, C., Hayden, B., 2005. In situ microcosm experiments on the influence of nitrate and light on phytoplankton community composition. Journal of Experimental Marine Biology and Ecology 326, 1-13.

Carter, R.A., D'Aubrey, J., 1988. Inorganic nutrients in Natal continental shelf waters, in: Schumann, E.H. (Ed.), Coastal Ocean Studies of Natal, Lecture Notes on Coastal and Estuarine Studies. Springer, Berlin, pp. 131 - 151.

Carter, R.A., McMurray, H.F., Largier, J.L., 1987. Thermocline characteristics and phytoplankton dynamics in Agulhas Bank waters. South African Journal of Marine Science 5, 327-336.

Carter, R.A., Schleyer, M.H., 1988. Plankton distributions in Natal coastal waters, in: Schumann, E.H. (Ed.), Coastal Ocean Studies off Natal, South Africa, Lecture Notes on Coastal and Estuarine Studies. Springer-Verlag, Berlin, pp. 152 - 177.

Carvalho, F., Kohut, J., Oliver, M.J., Schofield, O., 2017. Defining the ecologically relevant mixed-layer depth for Antarctica's coastal seas. Geophysical Research Letters 44, 338-345.

Casal, T.G.D., Beal, L.M., Lumpkin, R., Johns, W.E., 2009. Structure and downstream evolution of the Agulhas Current system during a quasi-synoptic survey in February–March 2003. Journal of Geophysical Research: Oceans 114, n/a-n/a.

Castelao, R.M., Campos, E.J.D., Miller, J.L., 2004. A Modelling study of coastal upwelling driven by wind and meanders of the Brazil Current. Journal of Coastal Research, 662-671.

Chapman, P., Duncombe Rae, C.M., Allanson, B.R., 1987. Nutrients, chlorophyll and oxygen relationships in the surface layers at the Agulhas Retroflection. Deep Sea Research Part A. Oceanographic Research Papers 34, 1399-1416.

Chapman, P., Largier, J.L., 1989. On the origin of Agulhas Bank bottom water. South African Journal of Science 85, 515 - 519.

Chelton, D.B., Gaube, P., Schlax, M.G., Early, J.J., Samelson, R.M., 2011. The Influence of nonlinear mesoscale eddies on near-nurface oceanic chlorophyll. Science 334, 328.

Cheney, R.E., Richardson, P.L., Nagasaka, K., 1980. Tracking a Kuroshio cold ring with a free-drifting surface buoy. Deep Sea Research Part A. Oceanographic Research Papers 27, 641-654.

Christensen, M.S., 1980a. Sea-surface temperature charts for Southern Africa South of 26°S. 76, 541.

Christensen, M.S., 1980b. Sea-surface temperature charts for Southern Africa, south of 26°S. South African Journal of Science 76, 541-546.

Clark, M.R., Rowden, A.A., Schlacher, T., Williams, A., Consalvey, M., Stocks, K.I., Rogers, A.D., O'Hara, T.D., White, M., Shank, T.M., Hall-Spencer, J.M., 2010. The ecology of seamounts: structure, function, and human impacts. Annual Review of Marine Science 2, 253-278.

Clark, M.R., Schlacher, T.A., Rowden, A.A., Stocks, K.I., Consalvey, M., 2012. Science priorities for seamounts: Research links to conservation and management. PLOS ONE 7, e29232.

Clayton, S., Nagai, T., Follows, M.J., 2014. Fine scale phytoplankton community structure across the Kuroshio Front. Journal of Plankton Research 36, 1017-1030.

Codispoti, L.A., 1995. Is the ocean losing nitrate? Nature 376, 724-724.

Comeau, L.A., Vézina, A.F., Bourgeois, M., Juniper, S.K., 1995. Relationship between phytoplankton production and the physical structure of the water column near Cobb Seamount, northeast Pacific. Deep Sea Research Part I: Oceanographic Research Papers 42, 993-1005.

Condie, S.A., 1995. Interactions between western boundary currents and shelf waters: A mechanism for coastal upwelling. Journal of Geophysical Research: Oceans 100, 24811-24818.

Conley, D.J., Malone, T.C., 1992. Annual cycle of dissolved silicate in Chesapeake bay: implications for the production and fate of phytoplankton biomass. Marine Ecology Progress Series 81, 121 - 128.

Cordeiro, T.A., Brandini, F.P., Rosa, R.S., Sassi, R., 2013. Deep Chlorophyll Maximum in Western Equatorial Atlantic - How does it Interact with Islands Slopes and Seamounts? Marine Science 3, 30-37.

Crombet, Y., Leblanc, K., Quéguiner, B., Moutin, T., Rimmelin, P., Ras, J., Claustre, H., Leblond, N., Oriol, L., Pujo-Pay, M., 2011. Deep silicon maxima in the stratified oligotrophic Mediterranean Sea. Biogeosciences 8, 459-475.

Cullen, J.J., 1982. The deep chlorophyll maximum: Comparing vertical profiles of chlorophyll a. Canadian Journal of Fisheries and Aquatic Sciences 39, 791-803.

Cullen, J.J., 1991. Hypotheses to explain high-nutrient conditions in the open sea. Limnology and Oceanography 36, 1578 - 1599.

Cullen, J.J., 2015. Subsurface chlorophyll maximum layers: Enduring enigma or mystery solved? Annual Review of Marine Science 7, 207-239.

D'Addezio, J.M., Subrahmanyam, B., 2016. Sea surface salinity variability in the Agulhas Current region inferred from SMOS and Aquarius. Remote Sensing of Environment.

Darbyshire, J., 1972. The effect of bottom topography on the Agulhas Current. Pure and Applied Geophysics 101, 208 - 220.

Davidson, K., Gilpin, L.C., Pete, R., Brennan, D., McNeill, S., Moschonas, G., Sharples, J., 2013. Phytoplankton and bacterial distribution and productivity on and around Jones Bank in the Celtic Sea. Progress In Oceanography 117, 48-63.

De-Pauw, N., Naessens, F.E., 1991. Nutrient-induced competition between species of marine diatoms. Hydrobiologia Bulletin 25, 23-27.

de Baar, H.J.W., 1994. von Liebig's law of the minimum and plankton ecology (1899–1991). Progress In Oceanography 33, 347-386.

de Boyer Montégut, C., Madec, G., Fischer, A.S., Lazar, A., Iudicone, D., 2004. Mixed layer depth over the global ocean: An examination of profile data and a profile-based climatology. Journal of Geophysical Research: Oceans 109.

de Ruijter, W.P.M., Ridderinkhof, H., Lutjeharms, J.R.E., Schouten, M.W., Veth, C., 2002. Observations of the flow in the Mozambique Channel. Geophysical Research Letters 29, 140-141-140-143.

de Ruijter, W.P.M., van Leeuwen, P.J., Lutjeharms, J.R.E., 1999. Generation and evolution of Natal Pulses: Solitary meanders in the Agulhas Current. Journal of Physical Oceanography 29, 3043-3055.

de Souza, C.S., da Luz, J.A., Macedo, S., Montes, M.d.J.F., Mafalda, P., 2013. Chlorophyll a and nutrient distribution around seamounts and islands of the tropical south-western Atlantic. Marine and Freshwater Research 64, 168-184.

Demarcq, H., Barlow, R.G., Shillington, F.A., 2003. Climatology and Variability of Sea Surface Temperature and Surface Chlorophyll in the Benguela and Agulhas Ecosystems As Observed by Satellite Imagery. African Journal of Marine Science 25, 363-372.

Dencausse, G., Arhan, M., Speich, S., 2010. Spatio-temporal characteristics of the Agulhas Current retroflection. Deep Sea Research Part I: Oceanographic Research Papers 57, 1392-1405.

Deutsch, C.A., Tewksbury, J.J., Huey, R.B., Sheldon, K.S., Ghalambor, C.K., Haak, D.C., Martin, P.R., 2008. Impacts of climate warming on terrestrial ectotherms across latitude. Proceedings of the National Academy of Sciences 105, 6668.

DiTullio, G.R., Hutchins, D.A., Bruland, K.W., 1993. Interaction of iron and major nutrients controls phytoplankton growth and species composition in the tropical North Pacific Ocean. Limnology and Oceanography 38, 495-508.

Djurhuus, A., Read, J.F., Rogers, A.D., 2017. The spatial distribution of particulate organic carbon and microorganisms on seamounts of the South West Indian Ridge. Deep Sea Research Part II: Topical Studies in Oceanography 136, 73-84.

Dodson, A.N., Thomas, W.H., 1978. Reverse filtration, in: Sournia, A. (Ed.), Phytoplankton Manual-Monographs on oceanographic methodology. UNESCO, Paris, p. 190.

Doney, S.C., 2006. Plankton in a warmer world. Nature 444, 695.

Dower, J., Freeland, H., Juniper, K., 1992. A strong biological response to oceanic flow past Cobb Seamount. Deep Sea Research Part A. Oceanographic Research Papers 39, 1139-1145.

Drazen, J.C., De Forest, L.G., Domokos, R., 2011. Micronekton abundance and biomass in Hawaiian waters as influenced by seamounts, eddies, and the moon. Deep Sea Research Part I: Oceanographic Research Papers 58, 557-566.

Dugdale, R.C., 1985. The effects of varying nutrient concentration on biological production in upwelling regions, CalCOFI Report, pp. 93 - 96.

Dugdale, R.C., Goering, J.J., 1967. Uptake of new and regenerated forms of nitrogen in primary productivity. Limnology and Oceanography 12, 196-206.

Dugdale, R.C., Wilkerson, F.P., 1989. New production in the upwelling center at Point Conception, California: temporal and spatial patterns. Deep Sea Research Part A. Oceanographic Research Papers 36, 985-1007.

Dugdale, R.C., Wilkerson, F.P., Minas, H.J., 1995. The role of a silicate pump in driving new production. Deep Sea Research Part I: Oceanographic Research Papers 42, 697-719.

Duncan, C.P., 1970. The Agulhas Current, Oceanography. University of Hawaii, p. 76.

Duncan, C.P., Schladow, S.G., 1981. World surface currents from ship's drift observations. International Hydrographic Review 58, 101 - 112.

Eagle, G.A., Orren, M.J., 1985a. A seasonal investigation of the nutrients and dissolved oxygen in the water column along two lines of stations south and west of South Africa. Council for Scientific and Industrial Research, p. 178.

Eagle, G.A., Orren, M.J., 1985b. A seasonal investigation of the nutrients and dissolved oxygen in the water column along two lines of stations south and west of South Africa. , Research Report. Council for Scientific and Industrial Research, Stellenbosch, South Africa., p. 52.

Eide, L.I., 1979. Evidence of a topographically trapped vortex on the Norwegian continental shelf. Deep Sea Research Part A. Oceanographic Research Papers 26, 601-621.

Eppley, R.W., Rogers, J.N., McCarthy, J.J., 1969. Half-saturation constants for uptake of nitrate andammonium by marine phytoplankton. Limnology and Oceanography 14, 912-920.

Eriksen, C.C., 1998. Internal wave reflection and mixing at Fieberling Guyot. Journal of Geophysical Research 103, 2977-2994.

Estrada, M., Marrasé, C., Latasa, M., Berdalet, E., Delgado, M., Riera, T., 0., 1993. Variability of deep chlorophyll maximum characteristics in the Northwestern Mediterranean. Marine Ecology Progress Series 92, 289-300.

Evans, J.H., 1972. A modified sedimentation system for counting algae with an inverted microscope. Hydrobiologia 40, 247-250.

Falkowski, P.G., Barber, R.T., Smetacek, V., 1998. Biogeochemical Controls and Feedbacks on Ocean Primary Production. Science 281, 200.

Fasham, M.J.R., Platt, T., Irwin, B., Jones, K., 1985. Factors affecting the spatial pattern of the deep chlorophyll maximum in the region of the Azores front. Progress In Oceanography 14, 129-165.

Fehling, J., Davidson, K., Bolch, C.J., Bates, S.S., 2004. Growth and domoic acid production by Pseudo-nitzschia seriata (Bacillariophyceae) under phosphate and silicate limitation. Journal of Phycology 40, 674-683.

Fiala, M., Delille, B., Dubreuil, C., Kopczynska, E., Leblanc, K., Morvan, J., Quéguiner, B., Blain, S., Cailliau, C., Conan, P., Corvaisier, R., Denis, M., Frankignoulle, M., Oriol, L., Roy, S., 2003. Mesoscale surface distribution of biogeochemical characteristics in the Crozet Basin frontal zones (South Indian Ocean). Marine Ecology Progress Series 249, 1-14.

Field, C.B., Behrenfeld, M.J., Randerson, J.T., Falkowski, P., 1998. Primary production of the biosphere: Integrating terrestrial and oceanic components. Science 281, 237.

Fornari, D.J., Perfit, M.R., Allan, J.F., Batiza, R., Haymon, R., Barone, A., Ryan, W.B.F., Smith, T., Simkin, T., Luckman, M.A., 1988. Geochemical and structural studies of the Lamont seamounts: seamounts as indicators of mantle processes. Earth and Planetary Science Letters 89, 63-67, 70-83.

Franks, P.J.S., Walstad, L.J., 1997. Phytoplankton patches at fronts: A model of formation and response to wind events. Journal of Marine Research 55, 1-29.

Froneman, P.W., Ansorge, I.J., Richoux, N., Blake, J., Daly, R., Sterley, J., Mostert, B., Heyns, E., Sheppard, J., Kuyper, B., Hart, N., George, C., Howard, J., Mustafa, E., Pey, F., Lutjeharms, J.R.E., 2007. Physical and biological processes at the Subtropical Convergence in the South-west Indian Ocean. South African Journal of Science 103, 193 - 195.

Froneman, P.W., D. McQuaid, C., Perissinotto, R., 1995. Biogeographic structure of the microphytoplankton assemblages of the south Atlantic and Southern Ocean during austral summer. Journal of Plankton Research 17, 1791-1802.

Froneman, P.W., Laubscher, R.K., McQuaid, C.D., 2001. Size-fractionated Primary Production in the South Atlantic and Atlantic Sectors of the Southern Ocean. Journal of Plankton Research 23, 611-622.

Froneman, P.W., McQuaid, C.D., Laubscher, R.K., 1999. Size-fractionated primary production studies in the vicinity of the Subtropical Front and an adjacent warm-core eddy south of Africa in austral winter. Journal of Plankton Research 21, 2019-2035.

Froneman, P.W., Pakhomov, E., Meaton, V., 1998. Surface distribution of microphytoplankton of the south-west Indian Ocean along a repeat transect between Cape Town and the Prince Edward Islands. South African Journal of Science 94, 124-129.

Froneman, P.W., Pakhomov, E.A., 2000. Spatial and temporal variability in chlorophyll-a and diatom distribution in the south-east Indian Ocean. Vie et milieu 50, 275-288.

Froneman, P.W., Pakhomov, E.A., Balarin, M.G., 2004. Size-fractionated phytoplankton biomass, production and biogenic carbon flux in the eastern Atlantic sector of the Southern Ocean in late austral summer 1997–1998. Deep Sea Research Part II 54, 2715-2719.

Fryer, P., 1992. Mud volcanoes of the Marianas. Scientific American 266, 46-52.

Furnas, M.J., 1990. In situ growth rates of marine phytoplankton: approaches to measurement, community and species growth rates. Journal of Plankton Research 12, 1117-1151.

Gaines, G., Elabrachter, M., 1987. Heterotrophic nutrition, in: Taylor, F.J.R. (Ed.), The Biology of Dinoflagellates. Blackwell Scientific Publications, Oxford, pp. 224-268.

García, N., López-Elías, J.A., Miranda, A., Nolberta Huerta, M.M.-P., García, A., 2012. Effect of salinity on growth and chemical composition of the diatom Thalassiosira weissflogii at three culture phases. Latin American Journal of Aquatic Research 40, 435-440.

Garcia, S.M., Cohen, H., Freestone, D., Martinez, C., Oral, N., Rogers, A.D., Verlaan, P.A., Vousden, D., 2013. An ecosystem approach to management of seamounts in the Southern Indian Ocean. Volume 4 - A road map towards

sustainable use and conservation of biodiversity in the Southern Indian Ocean., Gland, Switzerland: IUCN. , p. 40.

Genin, A., 2004. Bio-physical coupling in the formation of zooplankton and fish aggregations over abrupt topographies. Journal of Marine Systems 50, 3-20.

Genin, A., Boehlert, G.W., 1985. Dynamics of temperature and chlorophyll structures above a seamount: An oceanic experiment. Journal of Marine Research 43, 907-924.

Genin, A., Dower, J.F., 2007. Seamount plankton dymanics, in: Pitcher, T.J., Morato, T., Hart, P.J.B., Clark, M.R., Haggan, N., Santos, R.S. (Eds.), Seamounts: Ecology, Fisheries and Conservation. Blackwell Publishing, , Oxford. , pp. 85-100.

Gieskes, W.W.C., Kraay, G.W., Tijssen, S.B., 1978. Chlorophylls and their degradation products in the deep pigment maximum layer of the tropical North Atlantic. Netherlands Journal of Sea Research 12, 195-204.

Gill, A.E., Schumann, E.H., 1979. Topographically induced changes in the structure of an inertial coastal jet: Application to the Agulhas Current. Journal of Physical Oceanography 9, 975-991.

Gordon, A.L., 1985. Indian-atlantic transfer of thermocline water at the Agulhas Retroflection. Science 227, 1030 - 1033.

Gordon, A.L., Lutjeharms, J.R.E., Gründlingh, M.L., 1987. Stratification and circulation at the Agulhas Retroflection. Deep Sea Research Part A. Oceanographic Research Papers 34, 565-599.

Goschen, W.S., Bornman, T.G., Deyzel, S.H.P., Schumann, E.H., 2015. Coastal upwelling on the far eastern Agulhas Bank associated with large meanders in the Agulhas Current. Continental Shelf Research 101, 34-46.

Goschen, W.S., Schumann, E.H., 1988. Ocean current and temperature structures in Algoa Bay and beyond in November 1986. South African Journal of Marine Science 7, 101-116.

Goschen, W.S., Schumann, E.H., 1990. Agulhas current variability and inshore structures off the Cape Province, South Africa. Journal of Geophysical Research: Oceans 95, 667-678.

Goschen, W.S., Schumann, E.H., Bernard, K.S., Bailey, S.E., Deyzel, S.H.P., 2012. Upwelling and ocean structures off Algoa Bay and the south-east coast of South Africa. African Journal of Marine Science 34, 525-536.

Gould, W.J., Hendry, R., Huppert, H.E., 1981. An abyssal topographic experiment. Deep Sea Research Part A. Oceanographic Research Papers 28, 409-440.

Grundlingh, M.L., 1983. On the course of the Agulhas Current. South African Geographical Journal 65, 49 - 57.

Hallegraeff, G.M., Jeffrey, S.W., 1984. Tropical phytoplankton species and pigments of continental shelf waters of North and North-West Australia. Marine Ecology Progress Series 20, 59-74.

Hansen, C., Kvaleberg, E., Samuelsen, A., 2010. Anticyclonic eddies in the Norwegian Sea; their generation, evolution and impact on primary production. Deep Sea Research Part I: Oceanographic Research Papers 57, 1079-1091.

Hanson, C.E., Pesant, S., Waite, A.M., Pattiaratchi, C.B., 2007a. Assessing the magnitude and significance of deep chlorophyll maxima of the coastal eastern Indian Ocean. Deep Sea Research Part II: Topical Studies in Oceanography 54, 884-901.

Hanson, C.E., Waite, A.M., Thompson, P.A., Pattiaratchi, C.B., 2007b. Phytoplankton community structure and nitrogen nutrition in Leeuwin Current and coastal waters off the Gascoyne region of Western Australia. Deep Sea Research Part II: Topical Studies in Oceanography 54, 902-924.

Hare, C.E., Leblanc, K., DiTullio, G.R., Kudela, R.M., Zhang, Y., Lee, P.A., Riseman, S., Hutchins, D.A., 2007. Consequences of increased temperature and CO2 for phytoplankton community structure in the Bering Sea. Marine Ecology Progress Series 352, 9-16.

Harris, T.F.W., van Foreest, D., 1978. The Agulhas Current in March 1969. Deep Sea Research 25, 549-561.

Hasle, G.R., 1978. The inverted-microscope method, in: Sournia, A. (Ed.), Phytoplankton Manual-Monographs on oceanographic methodology. UNESCO, Paris, p. 190.

Hayward, T.L., Venrick, E.L., McGowan, J.A., 1983. Environmental heterogeneity and plankton community structure in the central North Pacific. Journal of Marine Research 41, 711-729.

Hecky, R.E., Kilham, P., 1988. Nutrient limitation of phytoplankton in freshwater and marine environments: A review of recent evidence on the effects of enrichment1. Limnology and Oceanography 33, 796-822.

Heileman, S., Lutjeharms, J.R.E., Scott, L.E.P., 2008. Agulhas Current LME, in: Sherman, K., Hempel, G. (Eds.), The UNEP Large Marine Ecosystem Report: A perspective on changing conditions in LMEs of the world's Regional Seas. UNEP Regional Seas Report and Studies No. 182. . United Nations Environment Programme, Nairobi, Kenya.

Henry, A.E., 1975. Hydrology and nutrients salts of the South-east Atlantic and South-west Indian Oceans in 1968. , Investigational Report. Division of Sea Fisheries, South Africa, pp. 1-66.

Henson, S.A., Sarmiento, J.L., Dunne, J.P., Bopp, L., Lima, I., Doney, S.C., John, J., Beaulieu, C., 2010. Detection of anthropogenic climate change in satellite records of ocean chlorophyll and productivity. Biogeosciences 7, 621-640.

Hogg, N.G., 1973. On the stratified Taylor column. Journal of Fluid Mechanics 58, 517-537.

Holloway, P.E., Merrifield, M.A., 1999. Internal tide generation by seamounts, ridges, and islands. Journal of Geophysical Research 104, 25937-25951.

Howarth, R.W., 1988. Nutrient limitation of net primary production in marine ecosystems. Annual Review in Ecological Systematics 19, 89 - 110.

Hulburt, E.M., Rodman, J., 1963. Distribution of Phytoplankton species with respect to salinity between the coast of Southern New England and Bermuda. Limnology and Oceanography 8, 263-269.

Huppert, H.E., 1975. Some remarks on the initiation of inertial Taylor columns. Journal of Fluid Mechanics 67, 397-412.

Huppert, H.E., Bryan, K., 1976. Topographically generated eddies. Deep Sea Research and Oceanographic Abstracts 23, 655-679.

Hutchings, L., 1994. The Agulhas Bank: a synthesis of available information and a brief comparison with other east-coast shelf regions. Academy of Science of South Africa, pp. 179-185.

Iida, T., Odate, T., 2014. Seasonal variability of phytoplankton biomass and composition in the major water masses of the Indian Ocean sector of the Southern Ocean. Polar Science 8, 283-297.

Irigoien, X., Huisman, J., Harris, R.P., 2004. Global biodiversity patterns of marine phytoplankton and zooplankton. Nature 429, 863.

Jackson, J.M., Rainville, L., Roberts, M.J., McQuaid, C.D., Lutjeharms, J.R.E., 2012. Mesoscale bio-physical interactions between the Agulhas Current and the Agulhas Bank, South Africa. Continental Shelf Research 49, 10-24.

Jamart, B.M., Winter, D.F., Banse, K., 1979. Sensitivity analysis of a mathematical model of phytoplankton growth and nutrient distribution in the Pacific Ocean off the northwestern U.S. coast. Journal of Plankton Research 1, 267-290.

Jaroslow, G.E., Smith, D.K., Tucholke, B.E., 2000. Record of seamount production and off-axis evolution in the western North Atlantic Ocean, 25°25′–27°10′N. Journal of Geophysical Research 105, 2721-2736.

Jeffrey, S.W., Hallegraeff, G.M., 1990. Phytoplankton ecology of Australasian waters, in: Clayton, M.N., King, R.J. (Eds.). Longman Cheshire Pty Ltd., pp. 310-348.

Jennings, J.C.J., Gordon, L.I., Nelson, D.M., 1984. Nutrient depletion indicates high primary productivity in the Weddell Sea. Nature 309, 51.

Jones, B.H., Atkinson, L.P., Blasco, D., Brink, K.H., Smith, S.L., 1988. The asymmetric distribution of chlorophyll associated with a coastal upwelling center. Continental Shelf Research 8, 1155 - 1170.

Kaneko, A., Honji, H., Kawatate, K., Mizuno, S., Masuda, A., Miita, T., 1986. A note on internal wavetrains and the associated undulation of the sea surface observed upstream of seamounts Journal of the Oceanographical Society of Japan 42, 75 - 82.

Karayanni, H., Christaki, U., Van Wambeke, F., Dalby, A.P., 2004. Evaluation of double formalin--Lugol's fixation in assessing number and biomass of ciliates: an example of estimations at mesoscale in NE Atlantic. Journal of Microbiological Methods 56, 349-358.

Karl, D.M., 1999. A Sea of Change: Biogeochemical variability in the North Pacific Subtropical Gyre. Ecosystems 2, 181-214.

Kirk, J.T.O., 1994. Light and Photosynthesis in Aquatic Ecosystems, Second Ed. Cambridge University Press, Cambridge.

Krug, M., Tournadre, J., Dufois, F., 2014. Interactions between the Agulhas Current and the eastern margin of the Agulhas Bank. Continental Shelf Research 81, 67-79.

Kunze, E., Llewellyn Smith, S.G., 2004. The role of small-scale topography in turbulent mixing of the global ocean. Oceanography 17, 55-64.

Lagus, A., Suomela, J., Weithoff, G., Heikkilä, K., Helminen, H., Sipura, J., 2004. Species-specific differences in phytoplankton responses to N and P enrichments and the N:P ratio in the Archipelago Sea, northern Baltic Sea. Journal of Plankton Research 26, 779-798.

Lamont, T., Barlow, R.G., Morris, T., van den Berg, M.A., 2014. Characterisation of mesoscale features and phytoplankton variability in the Mozambique Channel. Deep Sea Research Part II: Topical Studies in Oceanography 100, 94-105.

Largier, J.L., 1990. Deep surface mixed layers on the continental shelf. Continental Shelf Research 10, 759-776.

Largier, J.L., Chapman, P., Peterson, W.T., Swart, V.P., 1992. The western Agulhas Bank: circulation, stratification and ecology. South African Journal of Marine Science 12, 319-339.

Largier, J.L., Swart, V.P., 1987. East-west variation in thermocline breakdown on the Agulhas Bank. South African Journal of Marine Science 5, 263-272.

Laubscher, R., Perissinotto, R., McQuaid, C., 1993. Phytoplankton production and biomass at frontal zones in the Atlantic sector of the Southern Ocean. Polar Biology 13, 471-481.

Lavelle, J.W., 2006. Flow, hydrography, turbulent mixing, and dissipation at Fieberling Guyot examined with a primitive equation model. Journal of Geophysical Research 111, C07014.

Lavelle, J.W., Mohn, C., 2010. Motion, commotion, and biophysical connections at deep ocean seamounts. Oceanography 23, 90-103.

Lenton, T.M., Klausmeier, C.A., 2006. Co-evolution of phytoplankton C:N:P stoichiometry and the deep ocean N:P ratio. Biogeosciences Discussions 3, 1023-1047.

Lenton, T.M., Watson, A.J., 2000. Redfield revisited: 1. Regulation of nitrate, phosphate, and oxygen in the ocean. Global Biogeochemical Cycles 14, 225-248.

Lentz, S.J., 1992. The surface boundary layer in coastal upwelling regions. Journal of Physical Oceanography 22, 1517-1539.

Lévy, M., 2008. The modulation of biological production by oceanic mesoscale turbulence, in: Weiss, J.B., Provenzale, A. (Eds.), Transport and Mixing in Geophysical Flows: Creators of Modern Physics. Springer Berlin Heidelberg, Berlin, Heidelberg, pp. 219-261.

Levy, M., Klein, P., Treuguier, A.-M., 2001. Impact of sub-mesoscale physics on production and subduction of phytoplankton in an oligotrophic regime. Journal of Marine Research 59, 535-565.

Lewin, J.C., 1962. Silicification, in: Lewin, R.E. (Ed.), Physiology and biochemistry of the algae. Academic Press, pp. 445 - 455.

Loftus, M.E., Seliger, H.H., 1975. Some limitations of the in vivo fluorescence technique. Coastal and Estuarine Research Federation 16, 79 - 92

Longhurst, A.R., 2007. Biogeographic partition of the ocean, Ecological Geography of the Sea (Second Edition). Academic Press, Burlington, pp. 19-34.

Longhurst, A.R., Harrison, G.W., 1989. The biological pump: Profiles of plankton production and consumption in the upper ocean. Progress In Oceanography 22, 47-123.

Lonsdale, P., 1983. Laccoliths(?) and small volcanoes on the flank of the East Pacific Rise. Geology 11, 706-709.

Lueck, R.G., Mudge, T.D., 1997. Topographically induced mixing around a shallow seamount. Science 276, 1831 - 1833.

Lund, J.W.G., Kipling, C., Cren, E.D., 1958. The inverted microscope method of estimating algal numbers and the statistical basis of estimations by counting. Hydrobiologia 11, 143-170.

Lutjeharms, J.R.E., 1981. Spatial scales and intensities of circulation in the ocean areas adjacent to South Africa. Deep Sea Research Part A. Oceanographic Research Papers 28, 1289-1302.

Lutjeharms, J.R.E., 1985. Location of frontal systems between Africa and Antarctica: some preliminary results. Deep Sea Research Part A. Oceanographic Research Papers 32, 1499-1509.

Lutjeharms, J.R.E., 1991. The temperature/salinity relationships of the South West Indian Ocean. South African Geographer 18, 15-31.

Lutjeharms, J.R.E., 2006. The Agulhas Current Springer, Berlin.

Lutjeharms, J.R.E., 2007. Three decades of research on the greater Agulhas Current. Ocean Science 3, 129-147.

Lutjeharms, J.R.E., Ansorge, I.J., 2001. The Agulhas Return Current. Journal of Marine Systems 30, 115-138.

Lutjeharms, J.R.E., Bang, N.D., Duncan, C.P., 1981. Characteristics of the currents east and south of Madagascar. Deep Sea Research Part A. Oceanographic Research Papers 28, 879-899.

Lutjeharms, J.R.E., Boebel, O., Rossby, H.T., 2003. Agulhas cyclones. Deep Sea Research Part II: Topical Studies in Oceanography 50, 13-34.

Lutjeharms, J.R.E., Bornman, T.G., 2010. The importance of the greater Agulhas Current is increasingly being recognised. . South African Journal of Science 106, 1 - 4.

Lutjeharms, J.R.E., Catzel, R., Valentine, H.R., 1989a. Eddies and other boundary phenomena of the Agulhas Current. Continental Shelf Research 9, 597-616.

Lutjeharms, J.R.E., Cooper, J., Roberts, M., 2000a. Upwelling at the inshore edge of the Agulhas Current. Continental Shelf Research 20, 737-761.

Lutjeharms, J.R.E., de Ruijter, W.P.M., Peterson, R.G., 1992. Interbasin exchange and the Agulhas retroflection; the development of some oceanographic concepts. Deep Sea Research Part A. Oceanographic Research Papers 39, 1791-1807.

Lutjeharms, J.R.E., Gordon, A.L., 1987. Shedding of an Agulhas ring observed at sea. Nature 325, 138-140.

Lutjeharms, J.R.E., Gründlingh, M.L., Carter, R.A., 1989b. Topographically induced upwelling in the Natal Bight. South African Journal of Science 85, 310-316.

Lutjeharms, J.R.E., Meyer, A.A., Ansorge, I.J., Eagle, G.A., Orren, M.J., 1996. The nutrient characteristics of the Agulhas Bank. South African Journal of Marine Science 17, 253-274.

Lutjeharms, J.R.E., Roberts, H.R., 1988. The Natal Pulse: An extreme transient on the Agulhas Current. Journal of Geophysical Research 93, 631 - 645.

Lutjeharms, J.R.E., Stockton, P.L., 1987. Kinematics of the upwelling front off southern Africa. South African Journal of Marine Science 5, 35-49.

Lutjeharms, J.R.E., Valentine, H.R., 1984. Southern ocean thermal fronts south of Africa. Deep Sea Research Part A. Oceanographic Research Papers 31, 1461-1475.

Lutjeharms, J.R.E., Valentine, H.R., Van Ballegooyen, R.C., 1993. On the Subtropical Convergence in the South Atlantic Ocean. South African Journal of Marine Science 89, 552-559.

Lutjeharms, J.R.E., Valentine, H.R., Van Ballegooyen, R.C., 2000b. The hydrography and water masses of the Natal Bight, South Africa. Continental Shelf Research 20, 1907-1939.

Lutjeharms, J.R.E., van Ballegooyen, R.C., 1984. Topographic control in the Agulhas Current system. Deep Sea Research Part A. Oceanographic Research Papers 31, 1321-1337.

Lutjeharms, J.R.E., Van Ballegooyen, R.C., 1988. The Retroflection of the Agulhas Current. Journal of Physical Oceanography 18, 1570-1583.

Margalef, R., 1978. Life-forms of phytoplankton as survival alternatives in an unstable environment. Oceanologica Acta 1, 493-509.

Martin, J.H., Fitzwater, S.E., 1988. Iron deficiency limits phytoplankton growth in the north-east Pacific subarctic. Nature 331, 341-343.

Martin, J.H., Fitzwater, S.E., Gordon, R.M., 1990. Iron deficiency limits phytoplankton growth in Antarctic waters. Global Biogeochemical Cycles 4, 5-12.

Martiny, A.C., Pham, C.T.A., Primeau, F.W., Vrugt, J.A., Moore, J.K., Levin, S.A., Lomas, M.W., 2013. Strong latitudinal patterns in the elemental ratios of marine plankton and organic matter. Nature Geoscience 6, 279.

Mcclain, C.R., Pietrafesa, L.J., Yoder, J.A., 1984. Observations of Gulf Stream-induced and wind-driven upwelling in the Georgia Bight using ocean color and infrared imagery. Journal of Geophysical Research: Oceans 89, 3705-3723.

McGillicuddy Jr, D.J., Robinson, A.R., Siegel, D.A., Jannasch, H.W., Johnson, R., Dickey, T.D., McNeil, J., Michaels, A.F., Knap, A.H., 1998. Influence of mesoscale eddies on new production in the Sargasso Sea. Nature 394, 263.

McMurray, H.F., Carter, R.A., Lucas, M.I., 1993. Size-fractionated phytoplankton production in western Agulhas Bank continental shelf waters. Continental Shelf Research 13, 307-329.

Meincke, J., 1971. Observation of an Anticyclonic Vortex Trapped above a Seamount. Journal of Geophysical Research 76, 7432-7440.

Menard, H.W., 1964. Marine geology of the Pacific. McGraw-Hill, New York.

Meyer, A.A., 1992. The nutrient chemistry of three oceanic regimes around southern Africa., Department of Oceanography. University of Cape Town, Cape Town, p. 126.

Meyer, A.A., Lutjeharms, J.R.E., de Villiers, S., 2002. The nutrient characteristics of the Natal Bight, South Africa. Journal of Marine Systems 35, 11-37.

Mills, M.M., Arrigo, K.R., 2010. Magnitude of oceanic nitrogen fixation influenced by the nutrient uptake ratio of phytoplankton. Nature Geoscience 3, 412.

Minas, H.J., Minas, M., Packard, T.T., 1986. Productivity in upwelling areas deduced from hydrographic and chemical fields. Limnology and Oceanography 31, 1182 - 1206.

Misic, C., Bavestrello, G., Bo, M., Borghini, M., Castellano, M., Covazzi Harriague, A., Massa, F., Spotorno, F., Povero, P., 2012. The “seamount effect” as revealed by organic matter dynamics around a shallow seamount in the Tyrrhenian Sea (Vercelli Seamount, western Mediterranean). Deep Sea Research Part I: Oceanographic Research Papers 67, 1-11.

Mitchell-Innes, B.A., 1967. Primary production studies in the south-west Indian Ocean 1961–1963, Investigational Report. Oceanographic Research Institute, Durban, p. 20.

Mitchell-Innes, B.A., Richardson, A.J., Painting, S.J., 1999. Seasonal changes in phytoplankton biomass on the western Agulhas Bank, South Africa. South African Journal of Marine Science 21, 217-233.

Mohan, R., Quarshi, A.A., Meloth, T., Sudhakar, M., 2011. Diatoms from the surface waters of the Southern Ocean during the austral summer of 2004. Current Science 100, 1323 - 1327.

Mohan, R., Shanvas, S., Thamban, M., Sudhakar, M., 2006. Spatial distribution of diatoms in surface sediments from the Indian sector of Southern Ocean. Current Science 91, 1495 - 1502.

Mohn, C., White, M., Bashmachnikov, I., Jose, F., Pelegrí, J.L., 2009. Dynamics at an elongated, intermediate depth seamount in the North Atlantic (Sedlo

Seamount, 40°20′N, 26°40′W). Deep Sea Research Part II: Topical Studies in Oceanography 56, 2582-2592.

Morán, X.A.G., López-Urrutia, Á., Calvo-Díaz, A., Li, W.K.W., 2010. Increasing importance of small phytoplankton in a warmer ocean. Global Change Biology 16, 1137-1144.

Morato, T., Bulman, C., Pitcher, T.J., 2009. Modelled effects of primary and secondary production enhancement by seamounts on local fish stocks. Deep Sea Research Part II: Topical Studies in Oceanography 56, 2713-2719.

Morgan, W.J., 1971. Convection plumes in the lower mantle. Nature 230, 42-43.

Mourino, B., Fernandes, E., Serret, P., Harbour, D., Sinha, B., Pingree, R., 2001. Varilbility and seasonality of physical and biological fields at the Great Meteor Tablemount. Oceanologica Acta 24, 1-20.

Mysak, L.A., Magaard, L., 1983. Rossby wave driven eulerian mean flows along non-zonal barriers, with application to the Hawaiian Ridge. Journal of Physical Oceanography 13, 1716-1725.

Nelson, D.M., Ahern, J.A., Herlihy, L.J., 1991. Cycling of biogenic silica within the upper water column of the Ross Sea. Marine Chemistry 35 461 - 476.

Nishikawa, T., Tarutani, K., Yamamoto, T., 2010. Nitrate and phosphate uptake kinetics of the harmful diatom Coscinodiscus wailesii, a causative organism in the bleaching of aquacultured Porphyra thalli. Harmful Algae 9, 563-567.

Noble, M., Mullineaux, L.S., 1989. Internal tidal currents over the summit of cross seamount. Deep Sea Research Part A. Oceanographic Research Papers 36, 1791-1802.

Nordli, E., 1953. Salinity and temperature as controlling factors for distribution and mass occurrence of Ceratia. Blyttia 11, 16-18.

O'Connor, M.I., Piehler, M.F., Leech, D.M., Anton, A., Bruno, J.F., 2009. Warming and Resource Availability Shift Food Web Structure and Metabolism. PLOS Biology 7, e1000178.

Odate, T., Furuya, K., 1998. Well-developed subsurface chlorophyll maximum near Komahashi No. 2 seamount in the summer of 1991. Deep Sea Research Part I: Oceanographic Research Papers 45, 1595-1607.

Oksanen, J., Blanchet, F.G., Kindt, R., Legendre, P., Minchin, P.R., O'Hara, R.B., Simpson, G.L., Solymos, P., Stevens, M.H.H., Wagner, H., 2018, vegan:

Community Ecology Package, R package version 2.5-2, https://CRAN.R-project.org/package=vegan

Olsen, S., Paasche, E., 1986. Variable kinetics of silicon-limited growth in Thalassiosira pseudonana (Bacillariophyceae) in response to changed chemical composition of the growth medium. British Phycological Journal 21, 183-190.

Olson, D.B., Evans, R.H., 1986. Rings of the Agulhas Current. Deep Sea Research Part A. Oceanographic Research Papers 33, 27-42.

Owens, W.B., Hogg, N.G., 1980. Oceanic observations of stratified Taylor columns near a bump. Deep Sea Research Part A. Oceanographic Research Papers 27, 1029-1045.

Paldor, N., Lutjeharms, J.R.E., 2009. Why is the stability of the Agulhas Current geographically bi-modal? Geophysical Research Letters 36, L14604.

Park, Y.-H., Gamberoni, L., Charriaud, E., 1993. Frontal structure, water masses, and circulation in the Crozet Basin. Journal of Geophysical Research 98, 12361 - 12385.

Park, Y.-H., Gambéroni, L., Charriaud, E., 1991. Frontal structure and transport of the Antarctic Circumpolar Current in the south Indian Ocean sector, 40–80°E. Marine Chemistry 35, 45-62.

Parsons, T.R., Maite, Y., Lalli, C.M., 1989. A manual of chemical and biological methods for seawater analysis. Pergamon Press, Toronto.

Paxinos, R., Mitchell, J.G., 2000. A rapid Utermohl method for estimating algal numbers. Journal of Plankton Research 22, 2255-2262.

Pearce, A.F., 1977a. The shelf circulation o! the coast of South Africa, CSIR Research Report, p. 220.

Pearce, A.F., 1977b. Some features of the upper 500 m of the Agulhas Current. Journal of Marine Research 35, 731-753.

Pearce, A.F., Gründlingh, M.L., 1982. Is there a seasonal variation in the Agulhas Current? Journal of Marine Research 40, 177-184.

Perissinotto, R., Duncombe Rae, C.M., Boden, B.P., Allanson, B.R., 1990. Vertical stability as a controlling factor of the marine phytoplankton production at the Prince Edward Archipelago (Southern Ocean) Marine Ecology Progress Series 60, 205 - 209.

Pisias, N.G., Murray, D.W., Roelofs, A.K., 1986. Radiolarian and silicoflagellate response to oceanographic changes associated with the 1983 El Niño. Nature 320, 259.

Platt, T., Bouman, H., Devred, E., Fuentes-Yaco, C., Sathyendranath, S., 2005. Physical forcing and phytoplankton distributions. Scientia Marina 69, 55-73.

Platt, T., Rao, D.V.S., Irwin, B., 1983. Photosynthesis of picoplankton in the oligotrophic ocean. Nature 301, 702.

Pollard, R., Read, J., 2017. Circulation, stratification and seamounts in the Southwest Indian Ocean. Deep Sea Research Part II: Topical Studies in Oceanography 136, 36-43.

Pondaven, P., Fravalo, C., Ruiz-Pino, D., Tréguer, P., Quéguiner, B., Jeandel, C., 1998. Modelling the silica pump in the Permanently Open Ocean Zone of the Southern Ocean. Journal of Marine Systems 17, 587-619.

Poulton, A.J., Holligan, P.M., Hickman, A., Kim, Y.-N., Adey, T.R., Stinchcombe, M.C., Holeton, C., Root, S., Woodward, E.M.S., 2006. Phytoplankton carbon fixation, chlorophyll-biomass and diagnostic pigments in the Atlantic Ocean. Deep Sea Research Part II: Topical Studies in Oceanography 53, 1593-1610.

Powell, T.M., Cloern, J.E., Huzzey, L.M., 1989. Spatial and temporal variability in South San Francisco Bay (USA). I. Horizontal distributions of salinity, suspended sediments, and phytoplankton biomass and productivity. Estuarine, Coastal and Shelf Science 28, 583-597.

Priede, I.G., Froese, R., 2013. Colonization of the deep sea by fishes. Journal of Fish Biology 83, 1528-1550.

Probyn, T.A., Mitchell-Innes, B.A., Brown, P.C., Hutchings, L., Carter, R.A., 1994. Review of primary production and related processes on the Agulhas-Bank. South African Journal of Science 90, 166 - 173.

Probyn, T.A., Mitchell-Innes, B.A., Searson, S., 1995. Primary productivity and nitrogen uptake in the subsurface chlorophyll maximum on the Eastern Agulhas Bank. Continental Shelf Research 15, 1903-1920.

Ptacnik, R., Andersen, T., Tamminen, T., 2010. Performance of the Redfield Ratio and a family of nutrient limitation I\indicators as thresholds for phytoplankton N vs. P Limitation. Ecosystems 13, 1201-1214.

R Core Team, 2018, R: A Language and Environment for Statistical Computing, R Foundation for Statistical Computing, Vienna, Austria, https://www.R-project.org/

Read, J., Pollard, R., 2017. An introduction to the physical oceanography of six seamounts in the southwest Indian Ocean. Deep Sea Research Part II: Topical Studies in Oceanography 136, 44-58.

Read, J.F., Lucas, M.I., Holley, S.E., Pollard, R.T., 2000. Phytoplankton, nutrients and hydrography in the frontal zone between the Southwest Indian Subtropical gyre and the Southern Ocean. Deep Sea Research Part I: Oceanographic Research Papers 47, 2341-2367.

Read, J.F., Pollard, R.T., 1993. Structure and transport of the Antarctic Circumpolar Current and Agulhas Return Current at 40°E. Journal of Geophysical Research: Oceans 98, 12281-12295.

Redfield, A.C., 1958. The biological control of chemical factors in the environment. American Scientist 46, 205-221.

Reid, F.M.H., 1983. Biomass estimation of components of the marine nanoplankton and picoplankton by the Utermohl settling technique. Journal of Plankton Research 5, 235-252.

Rhee, G.-Y., Gotham, I.J., 1981. The effect of environmental factors on phytoplankton growth: Temperature and the interactions of temperature with nutrient limitation. Limnology and Oceanography 26, 635-648.

Rhodes, L., Burke, B., 1996. Morphology and growth characteristics of Chrysochromulina species (Haptophyceae = Prymnesiophyceae) isolated from New Zealand coastal waters. New Zealand Journal of Marine and Freshwater Research 30, 91-103.

Richardson, P.L., 1980. Anticyclonic eddies generated near the Corner Rise seamounts. Journal of Marine Research 38, 673-686.

Roberts, M.J., 2005. Chokka squid (Loligo vulgaris reynaudii) abundance linked to changes in South Africa's Agulhas Bank ecosystem during spawning and the early life cycle. ICES Journal of Marine Science 62, 33-55.

Roberts, M.J., 2010. Coastal currents and temperatures along the eastern region of Algoa Bay, South Africa, with implications for transport and shelf–bay water exchange. African Journal of Marine Science 32, 145-161.

Roberts, M.J., van den Berg, M., 2005. Currents along the Tsitsikamma coast, South Africa, and potential transport of squid paralarvae and ichthyoplankton. African Journal of Marine Science 27, 375-388.

Rogers, A.D., 2004. The Biology, Ecology and Vulnerability of Seamount Communities. IUCN, Gland, Switzerland.

Rogers, A.D., Blaxter, J.H.S., Southward, A.J., 1994. The Biology of Seamounts, Advances in Marine Biology. Academic Press, pp. 305-350.

Rouault, M., Penven, P., Pohl, B., 2009. Warming in the Agulhas Current system since the 1980's. Geophys. Res. Lett. 36.

Rouault, M.J., Penven, P., 2011. New perspectives on Natal Pulses from satellite observations. Journal of Geophysical Research: Oceans 116.

Royer, T.C., 1978. Ocean eddies generated by seamounts in the North Pacific. Science 199, 1063-1064.

Rykaczewski, R.R., Dunne, J.P., 2010. Enhanced nutrient supply to the California Current Ecosystem with global warming and increased stratification in an earth system model. Geophysical Research Letters 37.

Ryther, J.H., Dunstan, W.M., 1971. Nitrogen, phosphorus, and eutrophication in the coastal marine environment. Science 171, 1008-1013.

Ryther, J.H., Hall, J.R., Pease, A.K., Bakun, A., Jones, M.M., 1966. Primary organic production in relation to the chemistry and hydrography of the western Indian Ocean. Limnology and Oceanography 11, 371 - 380.

Sá, C., Leal, M.C., Silva, A., Nordez, S., André, E., Paula, J., Brotas, V., 2013. Variation of phytoplankton assemblages along the Mozambique coast as revealed by HPLC and microscopy. Journal of Sea Research 79, 1-11.

Sætre, R., Da Silva, A.J., 1984. The circulation of the Mozambique channel. Deep Sea Research Part A. Oceanographic Research Papers 31, 485-508.

Sakshaug, E., Slagstad, D., Holm-Hansen, O., 1991. Factors controlling the development of phytoplankton blooms in the Antarctic Ocean-a mathematical model. Marine Chemistry 35, 259 - 271.

Santos, M., Moita, M.T., Bashmachnikov, I., Menezes, G.M., Carmo, V., Loureiro, C.M., Mendonça, A., Silva, A.F., Martins, A., 2013. Phytoplankton variability and oceanographic conditions at Condor seamount, Azores (NE Atlantic). Deep Sea Research Part II: Topical Studies in Oceanography 98, 52-62.

Schabhüttl, S., Hingsamer, P., Weigelhofer, G., Hein, T., Weigert, A., Striebel, M., 2013. Temperature and species richness effects in phytoplankton communities. Oecologia 171, 527-536.

Scharler, U.M., Ayers, M.J., de Lecea, A.M., Pretorius, M., Fennessy, S.T., Huggett, J.A., MacKay, C.F., Muir, D., 2016. Riverine influence determines nearshore heterogeneity of nutrient (C, N, P) content and stoichiometry in the KwaZulu-Natal Bight, South Africa. African Journal of Marine Science 38, S193-S203.

Schidt, R., Schminke, H.U., 2000. Seamounts and island building, in: Sigurdsson, H., Houghton, B.F. (Eds.), Encyclopedia of volcanoes. Academic Press, San Diego, p. 1417.

Schoemann, V., Becquevort, S., Stefels, J., Rousseau, V., Lancelot, C., 2005. Phaeocystis blooms in the global ocean and their controlling mechanisms: a review. Journal of Sea Research 53, 43-66.

Schumann, E.H., 1999. Wind-driven mixed layer and coastal upwelling processes off the south coast of South Africa. Journal of Marine Research 57, 671-691.

Schumann, E.H., Li van Heerden, I., 1988. Observations of Agulhas Current frontal features south of Africa, October 1983. Deep Sea Research Part A. Oceanographic Research Papers 35, 1355-1362.

Schumann, E.H., Martin, J.A., 1991. Climatological aspects of the coastal wind field at Cape Town, Port Elizabeth and Durban. South African Geographical Journal 73, 48-51.

Schumann, E.H., Perrins, L.A., Hunter, I.T., 1982. Upwelling along the south coast of the Cape Province, South Africa. South African Journal of Science 78, 238 – 242.

Schumann, E.H., Ross, A.B., Goschen, W.S., 1988. Cold water events in Algoa Bay and along the Cape south coast, South Africa, in March/April 1987. South African Journal of Science 84, 579–584.

Sedwick, P.N., Blain, S., Quéguiner, B., Griffiths, F.B., Fiala, M., Bucciarelli, E., Denis, M., 2002. Resource limitation of phytoplankton growth in the Crozet Basin, Subantarctic Southern Ocean. Deep Sea Research Part II: Topical Studies in Oceanography 49, 3327-3349.

Shannon, L.V., Hutchings, L., Bailey, G.W., Shelton, P.A., 1984. Spatial and temporal distribution of chlorophyll in southern African waters as deduced from

ship and satellite measurements and their implications for pelagic fisheries. South African Journal of Marine Science 2, 109-130.

Sherman, K., Okemwa, E.N., Ntiba, M.J., 1998. Large Marine Ecosystems of the Indian Ocean: Assessment, sustainability, and management. Blackwell Science, Inc., Malden, p. 394.

Sieburth, J.M., 1979. Sea Microbes. . Oxford University Press, New York.

Smayda, T.J., 1958. Biogeographical Studies of Marine Phytoplankton. Oikos 9, 158-191.

Smayda, T.J., 1970. The suspension and sinking of phytoplankton in the sea. Oceanography and Marine Biology - An Annual Review 8, 353-414.

Smith, D.K., Cann, J.R., 1990. Hundreds of small volcanoes on the median valley floor of the Mid-Atlantic Ridge at 24-30°N. Nature 348, 152-155.

Smith, S.V., 1984. Phosphorus versus nitrogen limitation in the marine environment. Limnology and Oceanography 29, 1149 - 1160.

Sommer, U., 1994. Are marine diatoms favoured by high Si:N ratios? Marine Ecology Progress Series 115, 309-315.

Sonnekus, M.J., Bornman, T.G., Campbell, E.E., 2017. Phytoplankton and nutrient dynamics of six South West Indian Ocean seamounts. Deep Sea Research Part II: Topical Studies in Oceanography 136, 59-72.

Staudigel, H., Clague, D.A., 2010. The geological history of deep-sea volcanoes: biosphere, hydrosphere, and lithosphere interactions. Oceanography 23, 58 - 71.

Stevens, C.L., Consalvey, M., Devine, J.A., Clark, M.R., 2014. Mixing and transport near the shallow-crested Rumble III seamount and the implications for plankton distribution. New Zealand Journal of Marine and Freshwater Research 48, 194-215.

Stramma, L., Lutjeharms, J.R.E., 1997a. The flow field of the subtropical gyre of the South Indian Ocean. J. Geophys. Res. 102, 5513-5530.

Stramma, L., Lutjeharms, J.R.E., 1997b. The flow field of the subtropical gyre of the South Indian Ocean. Journal of Geophysical Research: Oceans 102, 5513-5530.

Stramma, L., Peterson, R.G., 1990. The South Atlantic Current. Journal of Physical Oceanography 20, 846 - 859.

Sultan, E., Mercier, H., Pollard, R.T., 2007. An inverse model of the large scale circulation in the South Indian Ocean. Progress In Oceanography 74, 71-94.

Swart, V.P., Largier, J.L., 1987. Thermal structure of Agulhas Bank water. South African Journal of Marine Science 5, 243-252.

Takahashi, K., 1989. Silicoflagellates as productivity indicators: Evidence from long temporal and spatial flux variability responding to hydrography in the northeastern Pacific. Global Biogeochemical Cycles 3, 43-61.

Takahashi, K., Blackwelder, P.L., 1992. The spatial distribution of silicoflagellates in the region of the Gulf Stream warm-core ring 82B: application to water mass tracer studies. Deep Sea Research Part A. Oceanographic Research Papers 39, S327-S346.

Taylor, F.J.R., 1966. Phytoplankton of the Southwestern Indian Ocean. Nova Hedwigia 12, 433-476.

Taylor, F.J.R., Hoppenrath, M., Saldarriaga, J.F., 2008. Dinoflagellate diversity and distribution. Biodiversity and Conservation 17, 407-418.

Thomas, M.K., Kremer, C.T., Klausmeier, C.A., Litchman, E., 2012. A Global Pattern of Thermal Adaptation in Marine Phytoplankton. Science 338, 1085.

Thorrington-Smith, M., 1969. Phytoplankton studies in the Agulhas Current region off the Natal Coast, Investigational Report No. 23. Oceanographic Research Institute South Africa.

Throndsen, J., 1978. Centrifugation, in: Sournia, A. (Ed.), Phytoplankton Manual-Monographs on oceanographic methodology. UNESCO, Paris, p. 190.

Toole, J.M., Schmitt, R.W., Polzin, K.L., Kunze, E., 1997. Near-boundary mixing above the flanks of a midlatitude seamount. Journal of Geophysical Research: Oceans 102, 947-959.

Tuchman, M.L., Theriot, E., Stoermer, E.F., 1984. Effects of low level salinity concentrations on the growth of Cyclotella meneghiniana Kütz. (Bacillariophyta). Archiv fur Protistenkunde 128, 319-326.

Turner, R.E., Qureshi, N., Rabalais, N.N., Dortch, Q., Justic, D., Shaw, R.F., Cope, J., 1998. Fluctuating silicate:nitrate ratios and coastal plankton food webs. Proceedings of the National Academy of Sciences 95, 13048.

Twomey, L.J., Waite, A.M., Pez, V., Pattiaratchi, C.B., 2007. Variability in nitrogen uptake and fixation in the oligotrophic waters off the south west coast of Australia. Deep Sea Research Part II: Topical Studies in Oceanography 54, 925-942.

Tyrrel, T., 1999. The relative influence of nitrogen and phosphorous on oceanic primary production. Nature 400, 525-527.

Utermöhl, H., 1958. Zur Vervollkommnung der quantitativen Phytoplankton-Methodik. Mitteilungen der Internationalen Vereinigung für Theoretische und Angewandte Limnologie 9, 1-38.

Valentine, H.R., Lutjeharms, J.R.E., Brundrit, G.B., 1993. The water masses and volumetry of the southern Agulhas Current region. Deep Sea Research Part I: Oceanographic Research Papers 40, 1285-1305.

van Aken, H.M., Lutjeharms, J.R.E., Rouault, M., Whittle, C., de Ruijter, W.P.M., 2013. Observations of an early Agulhas Current Retroflection event in 2001: A temporary cessation of inter-ocean exchange south of Africa? Deep Sea Research Part I: Oceanographic Research Papers 72, 1-8.

Van de Poll, W.H., Kulk, G., Timmermans, K.R., Brussaard, C.P.D., van der Woerd, H.J., Kehoe, M.J., Mojica, K.D.A., Visser, R.J.W., Rozema, P.D., Buma, A.G.J., 2013. Phytoplankton chlorophyll a biomass, composition, and productivity along a temperature and stratification gradient in the northeast Atlantic Ocean. Biogeosciences 10, 4227-4240.

van der Vaart, P.C.F., de Ruijter, W.P.M., 2001. Stability of Western Boundary Currents with an Application to Pulselike Behavior of the Agulhas Current. Journal of Physical Oceanography 31, 2625-2644.

van Leeuwen, P.J., de Ruijter, W.P.M., Lutjeharms, J.R.E., 2000. Natal pulses and the formation of Agulhas rings. Journal of Geophysical Research: Oceans 105, 6425-6436.

Vandevelde, T., Legendre, L., Therriault, J.C., Demers, S., Bah, A., 1987. Subsurface chlorophyll maximum and hydrodynamics of the water column. Journal of Marine Research 45, 377-396.

Vastano, A.C., Warren, B.A., 1976. Perturbations to the Gulf Stream by Atlantis II Seamount. Deep Sea Research and Oceanographic Abstracts 23, 681-694.

Venrick, E.L., Mcgowan, J.A., Mantyla, A.W., 1973. Deep chlorophyll maximum of photosynthetic chlorophyll in the Pacific Ocean. Fisheries Bulletin 71, 41-52.

Vincent, W.F., 1979. Mechanisms of rapid photosynthetic adaptation in natural phytoplankton communities. I Redistribution of excitation energy between photosystems I and II. Journal of Phycology 15, 429-434.

Vousden, D., Scott, L.E.P., Sauer, W., Bornman, T.G., Ngoile, M., Stapley, J., Lutjeharms, J.R.E., 2008. Establishing a basis for ecosystem management in the western Indian Ocean. South African Journal of Science 104, 417-420.

Vrieling, E., Poort, L., Beelen, T., Gieskes, W.W.C., 1999. Growth and silica content of the diatoms Thalassiosira weissflogii and Navicula salinarum at different salinities and enrichments with aluminium. European Journal of Phycology 34, 307-316.

Weber, T., Deutsch, C., 2012. Oceanic nitrogen reservoir regulated by plankton diversity and ocean circulation. Nature 489, 419.

Wessel, P., 2007. Seamount characteristics, in: Pitcher, T.J., Morato, T., Hart, P.J.B., Clark, M.R., Haggan, N., Santos, R.S. (Eds.), Seamounts: Ecology, Fisheries & Conservation. Blackwell Publishing Oxford, p. 527.

Wessel, P., Sandwell, D.T., Kim, S.-S., 2010. The Global Seamount Census. Oceanography 23, 23 - 33.

White, M., Bashmachnikov, I., Arístegui, J., Martins, A., 2007. Physical processes and seamount productivity, in: Pitcher, T.J., Morato, T., Hart, P.J.B., Clark, M.R., Haggan, N., Santos, R.S. (Eds.), Seamounts: Ecology, Fisheries and Conservation. Blackwell Publishing, Oxford, pp. 65-84.

White, W.B., Walker, A.E., 1985. The influence of the Hawaiian Archipelago upon the wind-driven subtropical gyre in the western north Pacific. Journal of Geophysical Research 90, 7061-7074.

Whitfield, A.K., James, N.C., Lamberth, S.J., Adams, J.B., Perissinotto, R., Rajkaran, A., Bornman, T.G., 2016. The role of pioneers as indicators of biogeographic range expansion caused by global change in southern African coastal waters. Estuarine, Coastal and Shelf Science 172, 138-153.

Willén, E., 1976. A simplified method of phytoplankton counting. British Phycological Journal 11, 265 - 278.

Wilson, J.T., 1963. A possible origin of the Hawaiian islands. Canadian Journal of Physics 41, 863-870.

Woodward, E.M.S., Rees, A.P., 2001. Nutrient distributions in an anticyclonic eddy in the northeast Atlantic Ocean, with reference to nanomolar ammonium concentrations. Deep Sea Research Part II: Topical Studies in Oceanography 48, 775-793.

Xiu, P., Chai, F., Curchitser, E.N., Castruccio, F.S., 2018. Future changes in coastal upwelling ecosystems with global warming: The case of the California Current System. Scientific Reports 8, 2866.

Yentsch, C.S., 1965. Distribution of chlorophyll and phaeophytin in the open ocean. Deep Sea Research and Oceanographic Abstracts 12, 653-666.

Yesson, C., Clark, M.R., Taylor, M.L., Rogers, A.D., 2011. The global distribution of seamounts based on 30 arc seconds bathymetry data. Deep Sea Research Part I: Oceanographic Research Papers 58, 442-453.

Yool, A., Tyrrell, T., 2003. Role of diatoms in regulating the ocean's silicon cycle. Global Biogeochemical Cycles 17, 1103-1122.

Young, J.W., Hobday, A.J., Campbell, R.A., Kloser, R.J., Bonham, P.I., Clementson, L.A., Lansdell, M.J., 2011. The biological oceanography of the East Australian Current and surrounding waters in relation to tuna and billfish catches off eastern Australia. Deep Sea Research Part II: Topical Studies in Oceanography 58, 720-733.

Zubkov, M.V., Sleigh, M.A., Tarran, G.A., Burkill, P.H., Leakey, R.J.G., 1998. Picoplanktonic community structure on an Atlantic transect from 50°N to 50°S. Deep Sea Research Part I: Oceanographic Research Papers 45, 1339-1355.

9 Appendices and supplementary material

9.1 Agulhas Bank

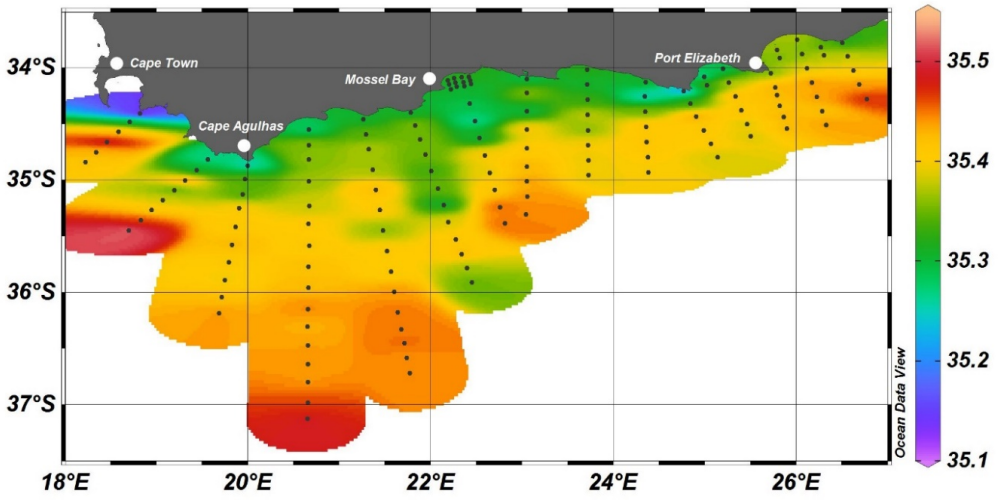

Fig. 9.1 Sea surface plot of salinity measured on the Agulhas Bank.

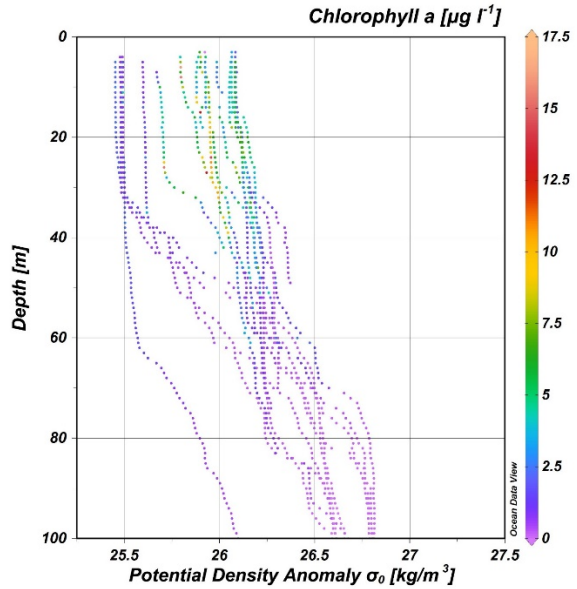

Fig. 9.2 A vertical station plot of potential density anomaly or sigma-theta with a chlorophyll *a* overlay to indicate the SCM for Transect 11.

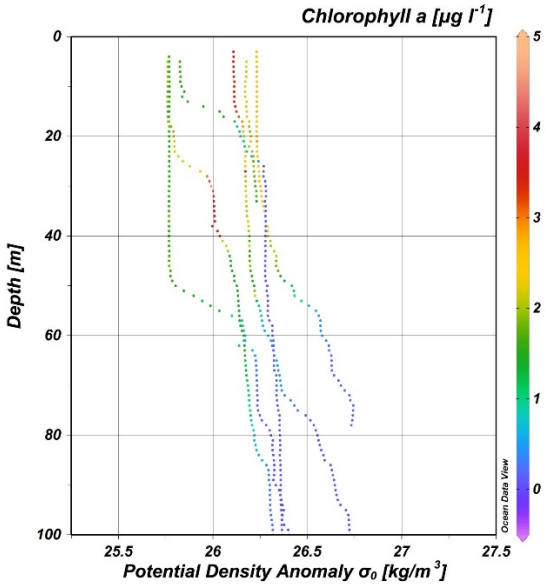

Fig. 9.3 A vertical station plot of potential density anomaly or sigma-theta with a chlorophyll *a* overlay to indicate the SCM for Transect 15.

Nitrate

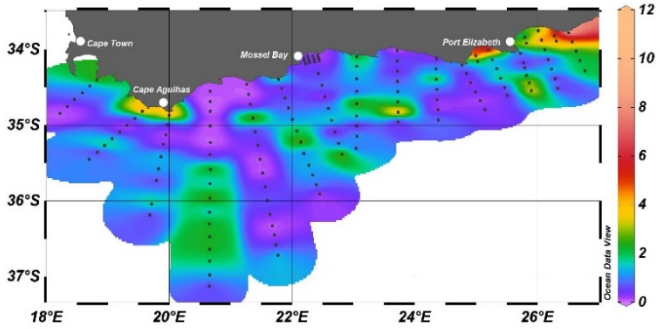

Nitrite

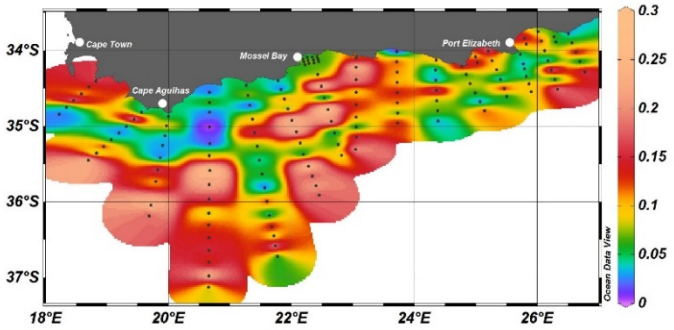

Phosphate

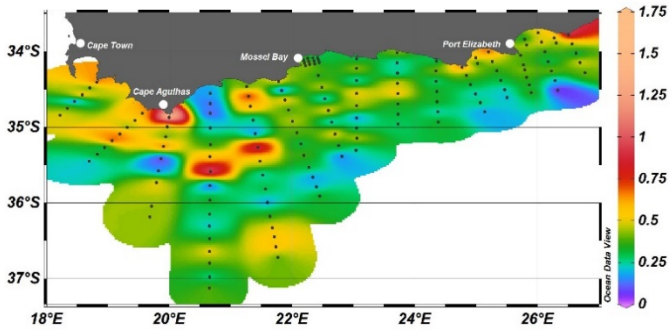

Silicate

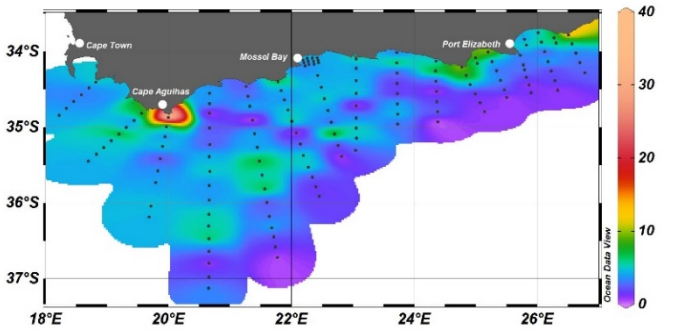

Fig. 9.4 Surface plots of nitrate, nitrite, phosphate and silicate concentrations of the Agulhas Bank.

9.2 Agulhas Retroflection

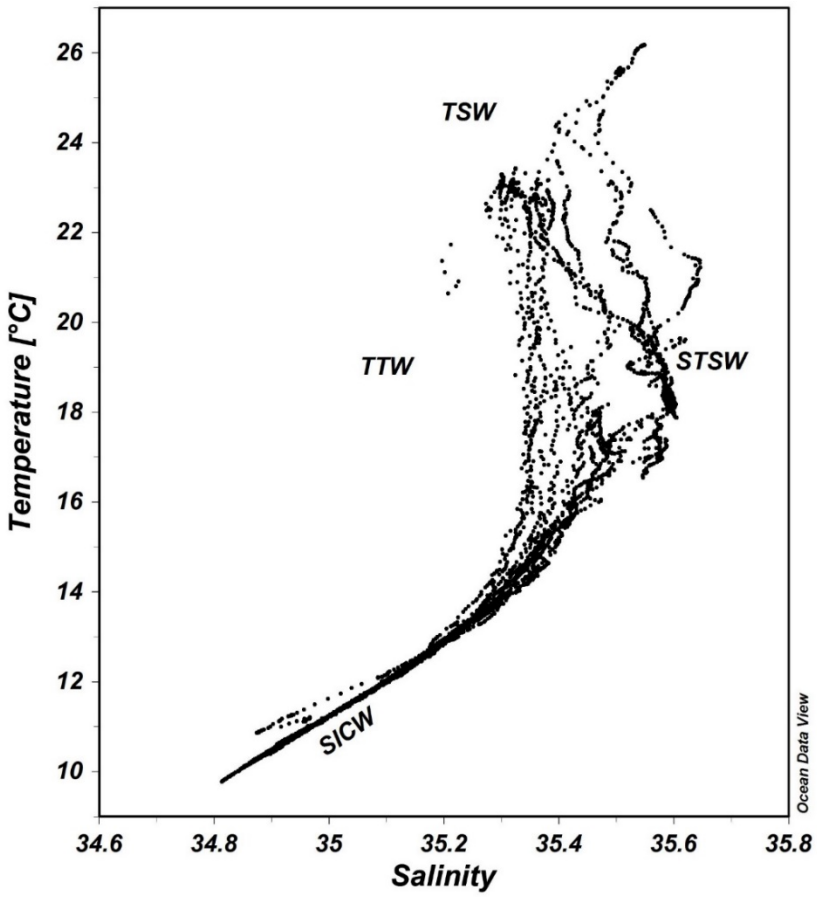

Fig. 9.5 Temperature – salinity plots of the Agulhas Retroflection epipelagic to compare water mass characteristics. Water masses identified are: Subtropical Surface Water (STSW), Tropical Surface Water (TSW), Tropical thermocline Water and South Indian Central Water.

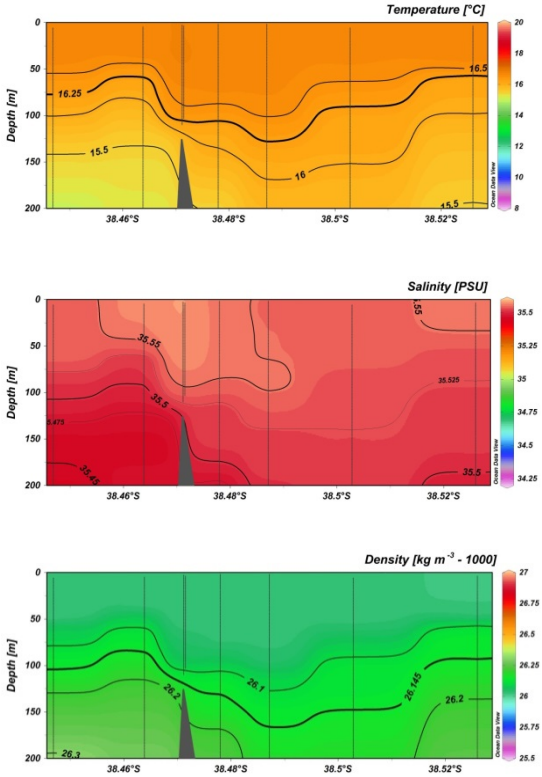

Fig. 9.6 Latitudinal transect showing the euphotic zone temperatures, salinity and density for Melville Bank. Vertical lines indicate the position of the CTD casts, whereas the bold contour line indicates either the MLD_T for temperature or the MLD_D for density.

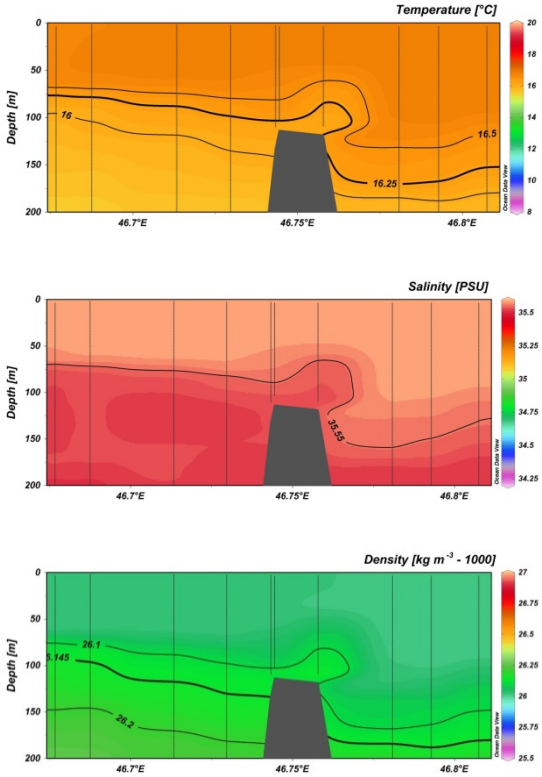

Fig. 9.7 Longitudinal transect showing the euphotic zone temperatures, salinity and density for Melville Bank. Vertical lines indicate the position of the CTD casts, whereas the bold contour line indicates either the MLD_T for temperature or the MLD_D for density.

9.3 sACLME

Table 9.1 Mean ± standard deviation (top row), minimum and maximum (bottom row) values of abiotic variables and chlorophyll *a* for the entire sACLME

Area	Salinity	Temperature (°C)	Oxygen (mg l^{-1})	Chlorophyll *a* (µg l^{-1})	NO_2^- (µM)	NO_3^- (µM)	SiO_4^{4-} (µM)	PO_4^{3-} (µM)	N:P	N:Si
Off-Mount	35.45 ± 0.12	21.34 ± 3.59	4.95 ± 0.19	0.09 ± 0.08	0.10 ± 0.09	0.21 ± 0.19	2.10 ± 0.56	0.07 ± 0.06	2.88 ± 2.65	0.17 ± 0.16
	35.32 - 35.56	17.26 - 24.04	4.79 - 5.16	0.04 - 0.18	0.00 - 0.17	0.04 - 0.42	1.74 - 2.74	0.00 - 0.11	0.00 - 5.22	0.02 - 0.33
Atlantis	35.55 ± 0.02	17.62 ± 1.05	5.30 ± 0.11	0.15 ± 0.11	0.06 ± 0.04	0.37 ± 0.58	3.12 ± 0.72	0.25 ± 0.11	2.06 ± 3.63	0.14 ± 0.18
	35.52 - 35.61	16.03 - 19.03	5.17 - 5.52	0.05 - 0.42	0.00 - 0.12	0.00 - 1.62	1.94 - 4.45	0.14 - 0.50	0.03 - 12.67	0.00 - 0.54
Sapmer	35.55 ± 0.00	15.90 ± 0.07	5.54 ± 0.02	0.36 ± 0.08	0.18 ± 0.09	1.39 ± 0.37	1.56 ± 1.06	0.36 ± 0.14	5.51 ± 3.68	1.89 ± 1.95
	35.54 - 35.55	15.82 - 16.04	5.52 - 5.57	0.16 - 0.46	0.09 - 0.34	0.94 - 1.84	0.27 - 2.84	0.17 - 0.57	2.18 - 11.49	0.39 - 6.69
SCZ #1	34.76 ± 0.78	12.69 ± 4.07	6.41 ± 1.54	0.55 ± 0.42	0.16 ± 0.10	8.45 ± 8.69	2.80 ± 2.12	0.67 ± 0.52	11.03 ± 11.30	9.91 ± 20.67
	33.71 - 35.59	5.28 - 17.29	5.33 - 11.18	0.09 - 1.39	0.01 - 0.45	0.02 - 26.50	0.14 - 8.56	0.00 - 2.16	0.00 - 43.46	0.05 - 90.74
Coral	34.41 ± 0.07	10.55 ± 0.21	6.46 ± 0.08	0.68 ± 0.21	0.19 ± 0.07	9.57 ± 2.46	2.58 ± 2.35	0.70 ± 0.19	31.74 ± 64.50	11.43 ± 12.59
	34.26 - 34.48	10.05 - 10.76	6.36 - 6.62	0.14 - 1.02	0.10 - 0.32	6.67 - 15.97	0.26 - 6.51	0.34 - 0.96	7.55 - 255.06	1.57 - 39.33
SCZ #2	35.33 ± 0.37	15.41 ± 2.27	5.55 ± 0.39	0.31 ± 0.15	0.15 ± 0.10	2.25 ± 2.56	2.79 ± 0.87	0.24 ± 0.27	5.33 ± 9.61	1.22 ± 1.81
	34.63 - 35.59	11.30 - 17.34	5.19 - 6.25	0.16 - 0.63	0.00 - 0.33	0.08 - 8.50	0.99 - 4.58	0.00 - 1.00	0.00 - 46.08	0.04 - 7.12
MoW	35.58 ± 0.01	17.08 ± 0.34	5.44 ± 0.05	0.27 ± 0.08	0.09 ± 0.07	0.05 ± 0.05	4.52 ± 4.13	0.19 ± 0.12	0.82 ± 0.77	0.05 ± 0.04
	35.55 - 35.59	16.31 - 17.30	5.39 - 5.57	0.20 - 0.44	0.00 - 0.21	0.00 - 0.14	0.36 - 12.31	0.00 - 0.42	0.00 - 2.12	0.01 - 0.17
Melville Bank	35.57 ± 0.03	16.69 ± 0.14	5.39 ± 0.20	0.31 ± 0.11	0.12 ± 0.06	0.25 ± 0.21	2.98 ± 2.15	0.19 ± 0.16	1.81 ± 2.15	0.14 ± 0.09
	35.44 - 35.59	16.04 - 16.81	5.29 - 6.44	0.10 - 0.47	0.01 - 0.26	0.00 - 0.72	0.68 - 9.20	0.00 - 0.65	0.00 - 8.72	0.02 - 0.32
Walters Shoal	35.58 ± 0.03	19.74 ± 1.42	4.94 ± 0.15	0.13 ± 0.08	0.12 ± 0.07	0.46 ± 0.80	2.42 ± 1.19	0.42 ± 0.37	1.87 ± 3.04	0.17 ± 0.18
	35.55 - 35.62	17.91 - 21.97	4.60 - 5.11	0.05 - 0.29	0.02 - 0.30	0.00 - 2.26	1.11 - 5.18	0.00 - 1.30	0.00 - 11.07	0.05 - 0.55

Table 9.1 Mean ± standard deviation (top row), minimum and maximum (bottom row) values of abiotic variables and chlorophyll *a* for the entire sACLME

Area	Salinity	Temperature (°C)	Oxygen (mg l^{-1})	Chlorophyll *a* (µg l^{-1})	NO_2^- (µM)	NO_3^- (µM)	SiO_4^{4-} (µM)	PO_4^{3-} (µM)	N:P	N:Si
Off-Mount 2	35.58 ± 0.01	20.24 ± 2.09	4.94 ± 0.01	0.18 ± 0.12	0.10 ± 0.04	0.67 ± 0.95	2.14 ± 0.36	0.15 ± 0.13	12.21 ± 16.85	0.33 ± 0.41
	35.57 - 35.59	18.77 - 21.72	4.93 - 4.95	0.10 - 0.27	0.07 - 0.13	0.00 - 1.34	1.88 - 2.39	0.06 - 0.24	0.30 - 24.13	0.04 - 0.61
Northern Agulhas Shelf	35.39 ± 0.05	21.76 ± 1.08	4.60 ± 0.19	1.25 ± 1.56	0.11 ± 0.11	1.00 ± 1.51	4.23 ± 6.07	0.36 ± 0.27	3.50 ± 5.50	0.32 ± 0.39
	35.21 - 35.50	18.71 - 23.93	4.17 - 5.27	0.05 - 8.23	0.00 - 0.61	0.00 - 8.23	1.01 - 45.28	0.00 - 1.66	0.00 - 32.00	0.00 - 1.65
Southern Agulhas Shelf	35.38 ± 0.08	18.73 ± 2.17	4.90 ± 0.49	2.54 ± 1.99	0.08 ± 0.07	2.92 ± 3.13	3.26 ± 1.75	0.62 ± 0.30	3.96 ± 3.04	0.71 ± 0.49
	35.15 - 35.49	14.83 - 21.85	4.07 - 6.24	0.26 - 8.66	0.00 - 0.28	0.05 - 12.50	1.04 - 8.85	0.22 - 1.50	0.18 - 12.12	0.05 - 1.76
Eastern Agulhas Bank	35.40 ± 0.06	18.07 ± 1.84	5.11 ± 0.28	1.94 ± 1.15	0.09 ± 0.07	1.24 ± 1.50	3.20 ± 3.22	0.40 ± 0.16	4.09 ± 5.15	2.84 ± 7.31
	35.18 - 35.47	14.23 - 22.01	4.66 - 5.84	0.51 - 5.96	0.01 - 0.26	0.01 - 6.04	0.11 - 11.93	0.06 - 0.81	0.06 - 23.31	0.00 - 36.45
Western Agulhas Bank	35.34 ± 0.12	15.74 ± 1.11	5.18 ± 0.32	2.15 ± 0.79	0.14 ± 0.09	1.56 ± 1.40	8.65 ± 12.10	0.58 ± 0.40	4.46 ± 7.94	0.29 ± 0.19
	35.12 - 35.49	14.45 - 17.58	4.51 - 5.56	0.99 - 3.51	0.01 - 0.27	0.08 - 4.39	2.61 - 37.86	0.00 - 1.56	0.00 - 31.33	0.02 - 0.55
Agulhas Retroflection	35.40 ± 0.10	21.10 ± 3.18	4.42 ± 0.35	0.91 ± 1.10	0.03 ± 0.06	1.51 ± 2.21	1.60 ± 1.42	0.17 ± 0.19	5.85 ± 7.98	0.52 ± 0.58
	35.30 - 35.61	15.68 - 26.16	3.62 - 4.80	0.00 - 4.11	0.00 - 0.23	0.00 - 7.04	0.00 - 4.45	0.00 - 0.56	0.00 - 34.00	0.00 - 1.63